Universidade de Lisboa

Faculdade de Ciências de Lisboa

Departamento de Biologia Animal

Molecular analysis of anterior endoderm during *Xenopus* development: A funtional and genomic approach.

Ana Cristina Guerra Matos Ferreira da Silva

Doutoramento em Biologia

(Biologia do Desenvolvimento)

2008

Universidade de Lisboa

Faculdade de Ciências de Lisboa

Departamento de Biologia Animal

Molecular analysis of anterior endoderm during *Xenopus* development: A funtional and genomic approach.

Ana Cristina Guerra Matos Ferreira da Silva

Tese orientada por:

Professor Doutor José António Belo

e Professora Doutora Sólveig Thorsteinsdóttir

Doutoramento em Biologia

(Biologia do Desenvolvimento)

2008

Aos meus Pais

1) Para a elaboração da presente tese de doutoramento foram usados integralmente como capítulos vários artigos científicos publicados, ou em preparação para posterior publicação, em revistas científicas internacionais indexadas. Uma vez que estes trabalhos foram realizados em colaboração com outros investigadores, e de acordo com o disposto no nº 1 do Artigo 41º do Regulamento de Estudos Pós-Graduados da Universidade de Lisboa, publicado no Diário da República - n.º 209, II Série de 30 de Outubro de 2006, esclareço que participei integralmente na concepção e execução do trabalho experimental, na interpretação dos resultados e na redacção dos manuscritos. Excepcionalmente, no artigo apresentado no Capítulo II.3.2.1 desta tese, "Comparative expression of mouse and chicken Shisa homologues during early development" (Dev Dyn, 235:2567-2573, 2006), os resultados referentes ao padrão de expressão do gene Shisa em ratinho foram integralmente obtidos por L. Gonçalves e M. Filipe, sob a orientação do Prof. Doutor José António Belo.

2) O facto de esta tese integrar vários artigos científicos levou a que a redacção dos vários capítulos tenha sido feita de acordo com as normas de cada revista, variando, portanto, ao longo desta tese. Os artigos referentes aos Capítulo II.2 e II.4, ainda em preparação, foram escritos de acordo com as regras exigidas pela revista Developmental Dynamics. O Capítulo II.3.1 consta de um artigo em preparação e encontra-se formatado de acordo com as regras exigidas pela revista Gene Expression Patterns. Por último, o Capítulo II.5 encontra-se formatado de acordo com as regras exigidas pela revista Development.

Em primeiro lugar gostaria de agradecer ao meu orientador, o Prof. Doutor José António Belo (ou apenas ZéTó), por toda a orientação, apoio e amizade prestados no decorrer destes últimos cinco anos.

I would like to express my gratitude to my co-supervisor Prof. Herbert Steinbeisser, not only for having me in his lab, but also for being a great supervisor and a good friend. Thank you for all the discussions and advices about diverse topics. It was a pleasure to be in your lab and I greatly thank you to give me that opportunity. Thank you as well to Dr Sarah Cramton, Karl and Martha for welcoming me in their home and for all the friendliness.

Gostava de agradecer à Prof. Doutora Sólveig Thorsteinsdóttir por ter aceite ser co-orientadora da minha tese. Obrigada por toda a sua ajuda durante o meu doutoramento, e especialmente durante a última fase de elaboração da tese.

Gostaria de agradecer à Fundação para a Ciência e Tecnologia pelo apoio financeiro sem o qual não teria sido possível realizar este trabalho.

À Faculdade de Ciências da Universidade de Lisboa gostaria de agradecer o voto de confiança ao aceitarem-me como estudante de doutoramento.

Ao instituto Gulbenkian de Ciência, ao Instituto de Genética Humana da Universidade de Heidelberg e ao Centro de Biomedicina Molecular e Estrutural da Universidade do Algarve agradeço as excelentes condições de trabalho.

Muito obrigada ao Joaquín Leon e à Maria Mota por terem aceite fazer parte do meu comité de tese, pelos conselhos e ajuda.

Aos actuais e antigos membros do grupo da Gastrulação (Ana, Bety, Cristina, Ester, Judite, Lisa, Margaret, Mário, Marisa, Marta, Neusa, Sara, Sofia, Vera) muito obrigada pelas discussões, sugestões, ajuda e amizade dentro e fora do laboratório. Um

obrigada especial ao Mário com quem aprendi grande parte do que sei sobre biologia molecular e banda desenhada. Muito obrigada por toda ajuda e apoio nos momentos mais difíceis. Obrigada pelas noitadas em que ficaste a ajudar-me a fazer explantes. Um obrigada especial também para a Sara por estar sempre disponível para me ajudar e aconselhar. Obrigada por me teres aberto a porta da tua casa e me teres alojado sempre que precisei de ir ao Algarve. Obrigada pela música que ao longo destes anos tem sido uma constante no laboratório.

Agradeço também a todas as pessoas no IGC que me aconselharam e ajudaram sempre que precisei, nomeadamente Sérgio, Nuno Afonso, Leonor, Jacinto, Susana, Célia, Cláudia e Lara.

I would like to thank all the current and former members of the Steinbeisser Lab for providing a friendly atmosphere and making me feel at home. I would like to thank Kirsten Linsmeier and Inge Bender for all the help, technical support and friendship. Thanks to Araceli Medina, Corinna Berger, Isabelle Köster, Klaus-Michael Kürner, Katja Heß, for all the help in and outside the lab, the stimulating discussions and for their friendship. Thank you all for making my time in Germany as pleasant as it ever was.

I would like to thanks Prof. Dr. Christof Niehrs for allowing me to use his frogs when our frogs were not cooperating. I would also like to thank everyone in his lab for all the help and friendliness, especially to Guillermo Barreto, Sónia Pinho, Emil Karaulanov and Suresh Swaminathan.

Gostaria de agradecer ao Dr. Raul Oliveira por me ter ajudado a recuperar rapidamente da cirurgia ao ombro de modo a que pudesse voltar à escrita desta tese.

Ao Paulo Gonçalves um MUITO OBRIGADA por me ter ajudado a recuperar grande parte dos dados contidos no disco rígido do meu portátil. Sem eles ter-me ia sido muito difícil escrever esta tese. (Um conselho a todos, façam cópias dos vossos trabalhos, especialmente da tese)

À Catarina, Liana, Margarida, Marta, Mónica e Vânia por estarem sempre disponíveis quando precisei.

Aos meus amigos e família que me aturam nos bons e maus momentos. Ao meu primo Rui que está sempre disponível para me ajudar.

A very special thanks to Rajeeb, there are not enough words to express how important your support was. Thank you for all the scientific discussions, help in the experimental work and critical review of this thesis. Thank you as well for all the patience, understanding and all the good times we shared during all these years. Without you this thesis wouldn't be the same.

Obrigada do fundo do coração, aos meus pais, por estarem sempre comigo, por toda a paciência, apoio incondicional e por todo o incentivo. Sem vocês nada disto teria sido possível.

Ao Ricardo, obrigada pela força, apoio, paciência, amizade e carinho incondicionais. Sem ti esta última parte teria sido muito mais difícil... desculpa algumas injustiças!

As experiências clássicas de embriologia experimental efectuadas por Spemann e Mangold demonstraram que o lábio dorsal do blastóporo (organizador) de embriões de anfíbios tem a capacidade de recrutar as células vizinhas e organizá-las de modo a alterar o seu destino e induzir a formação de um eixo secundário. De igual modo, Spemann e Mangold mostraram que as propriedades inductivas do organizador nos anfíbios vão sendo alteradas ao longo do tempo, sendo que o organizador de um embrião no início de gastrula tem a capacidade de induzir a formação de um eixo secundário completo quando transplantado para a região ventral de outro embrião. Contudo, se o transplante fosse efectuado usando um organizador de um embrião no fim do estadio de gastrula, havia apenas a indução de estruturas do tronco e cauda. Estas observações conduziram ao aparecimento do conceito de que em anfíbios o organizador pode ser subdividido em duas regiões com propriedades inductivas da cabeça (organizador da cabeça) e do tronco (organizador do tronco-cauda). A caracterização molecular dos genes expressos no organizador de Spemann tem demonstrado que também estas moléculas possuem diferentes propriedades de padronização: algumas moléculas como Cerberus, Dickkopf-1(Dkk-1) ou Frzb (Frizzled-related protein) têm a capacidade de induzir a formação de estruturas neurais anteriores, enquanto outras, tais como Chordin ou Noggin, são apenas capazes de induzir a formação de estruturas mais caudais. Em *Xenopus laevis*, foi observado que tanto *cerberus* como *dkk-1* são expressos durante a gastrulação, nas células da camada mais interna da mesendoderme anterior do organizador de Spemann, não sujeitas à involução. Por outro lado, em ratinho, estes genes são expressos na estrutura topologicamente equivalente à endoderme anterior dorsal (ADE) de *Xenopus*, a endoderme visceral anterior (AVE). Estudos realizados em embriões vertebrados, nomeadamente em ratinho, mostraram que vários factores de transcrição implicados na especificação do prosencéfalo são expressos na AVE. Foi de igual modo observado que a sua expressão na AVE era necessária para que a indução neural anterior se desencadeasse na ectoderme sobrejacente. Com base nestes estudos e em estudos semelhantes, foi proposto que a AVE, e as estruturas topologicamente equivalentes em outros vertebrados, seja o centro organizador da cabeça. No entanto, alguns estudos recentes têm contestado o papel da endoderme anterior na formação da cabeça e atribuido

esta função à mesoderme precordal. O principal objectivo desta tese foi a caracterização das propriedades inductivas deste organizador. Pretendíamos ainda esclarecer melhor a funcção endógena de Cerberus, um antagonista extracelular de Wnts, Nodals e BMPs com propriedades neuro-inductoras e identificar e caracterizar a função de novos genes expressos na ADE, em *Xenopus*.

Com o intuito de aprofundar a caracterização dos mecanismos moleculares responsáveis pela indução das estruturas anteriores do embrião, propusémo-nos a analisar o papel da ADE durante este processo através do estudo da função de genes expressos na ADE. Numa primeira fase, analisámos, em *Xenopus laevis*, a função endógena de *cerberus* na formação da cabeça. Para tal, efectuaram-se ensaios de perda de função, nos quais foi utilizado um morfólino desenhado contra a região não transcrita de *cerberus* (XcerMo). Neste estudo, demonstrámos que embora a microinjecção de XcerMo em embriões de *Xenopus* não tenha perturbado a formação da cabeça, a utilização de um sistema sensibilizado no qual *BMP-4*, *Xwnt-8* e *Xnr-1* foram expressos especificamente na ADE, permitiu que fosse revelada a necessidade da presença de Cerberus na formação da cabeça. Deste modo, fomos também capazes de mostrar *in vivo* que Cerberus inibe Xnr-1, XBMP-4 e Xwnt-8. O envolvimento de XCer na formação ou padronização do telencéfalo foi ainda averiguado em estudos com conjugados endoderme anterior/ectoderme dorsal. Os resultados obtidos permitiram concluir que Cerberus é necessário na ADE para que a padronização da neuroectoderme possa ocorrer correctamente. Paralelamente, procurámos identificar os elementos responsáveis pela expressão do *cerberus-like* de ratinho na AVE. Para tal, caracterizámos um fragmento de 4kb a montante desta região genómica, utilizando o Lacz como gene reporter. A injecção deste fragmento, ou de outras construções com várias delecções deste fragmento, em embriões de *Xenopus* permitiu a identificação de potenciais elementos regulatórios responsáveis pela sua expressão na ADE, o equivalente topologico da AVE de ratinho. Esta análise permitiu-nos demonstrar que a regulação transcripcional da expressão de *cerberus* em *Xenopus* e em ratinho está conservada.

Numa segunda fase desta tese, procuramos identificar e caracterizar funcionalmente novos genes expressos na ADE de *Xenopus*. Estes genes são os ortólogos de novos genes expressos na AVE de ratinho, recentemente identificados neste laboratório como resultado de uma abordagem genómica. Os padrões de expressão de potenciais ortólogos em *Xenopus* dos novos genes expressos na AVE de ratinho foram analisados,

por hibridação *in situ*, em diferentes estadios de desenvolvimento. Curiosamente, três dos cinco genes de rã analisados são expressos na ADE.

O *Shisa* de *Xenopus laevis* (*XShisa-1*) é um gene recentemente caracterizado como sendo um inibidor da via de sinalização de FGFs e Wnts. Neste estudo, demonstraram que no reticulo endoplasmático o Shisa se liga à forma imatura dos receptores de FGF e Wnt, impedindo a sua maturação e subsequente translocação para a superfície celular onde exercem a sua função. No presente estudo analisámos o padrão de expressão durante o desenvolvimento embrionário do *Shisa* de ratinho e de galinha bem como do *Shisa-2* de *Xenopus* (*XShisa-2*). Verificámos que o *Shisa* de ratinho e galinha são expressos predominantemente na AVE (hipoblasto em galinha), dobras encefálicas, sómitos, prosencéfalo, vesícula auditiva e nos primórdios dos membros. Ao contrário do que foi observado para *XShisa-1*, o *XShisa-2* não é expresso na ADE mas sim na mesoderme pré-somítica e mais tarde nos sómitos. No entanto, decidimos averiguar a função do *XShisa-2* durante o desenvolvimento embrionário utilizando um morfólino especifico contra *XShisa-2* (Shisa2Mo). A ausência da proteína XShisa-2 nos embriões de *Xenopus* leva a formação de sómitos mais estreitos e no deslocamento rostral de marcadores da mesoderme pré-somítica posterior. A ausência de XShisa-2 causa, de igual modo, a formação de olhos e placódios auditivos com tamanhos reduzidos. Estes resultados demostram que XShisa-2 é necessário durante a formação dos placódios auditivos, do olho e dos sómitos.

Na última parte deste trabalho, concentrámo-nos no estudo de uma nova família de genes expressos no organizador durante os estadios de gastrulação. Em *Xenopus laevis* foram identificados dois membros desta família, *XADTK1* e *XADTK2* (ADTK - Anterior Distal Tyrosine Kinase), os quais codificam para proteínas contendo um domínio catalítico de cinase. Verificou-se que tanto o *XADTK1* como o XADTK2 são pouco expressos maternamente. Durante os estadios de gastrulação a expressão de *XADTK1* pode ser observada na ADE. Mais tarde no desenvolvimento, os transcriptos de *XADTK1* podem ser detectados nas dobras neurais, placódios auditivos, primórdios do olho e notocorda. À semelhança com o que foi observado para o *XADTK1*, também o *XADTK2* é expresso na ADE. Em adição, é ainda possível detectar os transcriptos de *XADTK2* nas células do lábio dorsal do blastóporo. Em estadios larvares o *XADTK2* é expresso não só no sistema digestivo anterior mas também na região da cabeça e notochorda. Em experiências de perda de função foi demonstrado que o gene *XADTK1* é necessário

durante a formação do tubo neural em *Xenopus*. Inactivação da proteína XADTK1 provoca defeitos no fecho do tubo neural. Análise molecular de embriões injectados com um morfólino contra o *XADTK1* (XADTK1Mo) sugere que este gene poderá estar envolvido na formação das cristas neurais.

Palavras-chave: Organizador de Spemann, endoderme anterior dorsal, indução da cabeça, *Xenopus laevis*, Cerberus, gastrulação

The classical transplantation experiments conducted by Spemann and Mangold showed that the dorsal blastopore lip (organizer) of amphibian embryos has the remarkable property of recruiting and organizing the neighboring cells into a secondary body axis. They also established that the amphibian organizer could be subdivided into head and trunk inducing regions. The molecular characterization of genes expressed in the Spemann's organizer has shown that these molecules also exhibit different patterning properties. In order to further characterize the molecular mechanisms involved in the induction of anterior structures, we focused on the functional characterization of *cerberus*, a gene with head inducing properties. We found that Cerberus is required in the anterior dorsal endoderm (ADE) for proper patterning of the neurectoderm. In an attempt to identify the regulatory elements responsible for mouse *cerberus-like* gene in the anterior visceral endoderm (AVE), we characterized a 4kb upstream region of this gene using Lacz reporter assays. Injection of this fragment or various deletion constructs into *Xenopus* embryos identified potential regulatory elements that are responsible for its expression in the ADE, which is the topological equivalent of mouse AVE.

In a second part of this thesis we have identified and characterized novel genes expressed in the *Xenopus* ADE. These genes are the orthologs of genes differentially expressed in mouse AVE, which were identified in the lab by genomic approaches.

Xenopus Shisa-1 has been shown to inhibit both FGF and Wnt signaling by regulating the maturation of their receptors. We characterized the function of Shisa-2 and found that it is required for otic placode, eye and somite formation during *Xenopus* development.

In the last part of this work I have studied the role of *XADTK1* during embryogenesis. Knock-down of this gene, which belongs to a novel kinase-family, results in neural tube closure defects and impairment in neural crest formation.

Keywords: Spemann's organizer, anterior dorsal endoderm, head induction, *Xenopus laevis*, Cerberus, gastrulation.

Ad	**A**nterior **d**istal
ADE	**A**nterior **d**orsal **e**ndoderm
ADTK	**A**ntero**D**istal **T**yrosine **K**inase
AER	**A**pical **e**ctodermal **r**idge
AP	**A**ntero**p**osterior
ATP	**A**denosine **tri**phosphate
AVE	**A**nterior **v**isceral **e**ndoderm
Bambi	**B**MP and **A**ctivin **m**embrane-**b**ound **i**nhibitor
BCIP	5-**b**romo-4-**c**hloro-3-**i**ndolyl-**p**hosphate
BCNE	**B**lastula **C**hordin- and **N**oggin- Expressing center
bHLH	**B**asic **H**elix-**L**oop-**H**elix
BMP	**B**one **m**orphogenetic **p**rotein
bp	**b**ase **p**airs
BSA	**B**ovine **s**erum **a**lbumin
cAMP	**c**yclic **a**denosine **m**ono**p**hosphate
cDNA	**c**omplementary **DNA**
CDS	**Co**ding **s**equence
CE	**C**onvergent **e**xtension
Cer-s	**Cer**berus-**s**hort
CMV	**C**yto**m**egalo**v**irus
CNS	**C**entral **n**ervous **s**ystem
CoMo	**C**ontrol **m**orpholino **o**ligonucleotide
CRD	**C**ystein-**R**ich **D**omain
C-terminal	**C**arboxy-**terminal**
CV-2	**C**ross**v**einless-**2**
Cyp26	**C**ytochrome **P**450, family **26**
DE	**D**orsal **E**ctoderm
DIG	**Dig**oxygenin
Dkk-1	**D**ic**k**kopf-**1**
DMZ	**D**orsal **m**arginal **z**one

DNA	**D**esoxyribo**n**ucleic **a**cid
Dsh	**Dish**evelled
DV	**D**orso**v**entral
E(n)	**E**mbryonic day (number)
ECRs	**E**volutionary **c**onserved **s**equences
EDTA	**E**thylene**d**iamine**t**etra**a**cetic **a**cid
EGFP	**E**nhanced **g**reen **f**luorescent **p**rotein
EGTA	**E**thylene**g**lycol**t**etra**a**cetic **a**cid
En2	**En**grailed**2**
ER	**E**ndoplasmic **r**eticulum
EST	**E**xpressed **s**equence **t**ags
FGF	**F**ibroblast **g**rowth **f**actor
FGFR	**F**ibroblast **g**rowth **f**actor **r**eceptor
Fox	**F**orkhead b**ox**
Frzb	**Fr**i**z**zled-related protein
Fz	Frizzled
GBP	**G**SK3β **b**inding **p**rotein
Gsc	**G**oose**c**oid
GSK3β	**G**lycogen **s**ynthase **k**inase-**3 β**
HH	**H**amburger **H**amilton
Hh	**H**edge**h**og
IDME	**I**nvoluting **d**orsal **m**es**e**ndoderm
IMZ	**I**nvoluting **m**arginal **z**one
INT/BCIP	2-(4-**i**odophenyl)-5-(4-**n**itrophenyl)-3-phenyl**t**etrazolium chloride / 5-**b**romo-4-**c**hloro-3-**i**ndolyl-**p**hosphate
LiCl	**Li**thium **chl**oride
LR	**L**eft–**r**ight
LRP	**L**ow**d**ensity lipoprotein **r**eceptor-related **p**rotein family
MAPK	**M**itogen-**a**ctivated **p**rotein **k**inase
MBP	**M**yelin **b**asic **p**rotein
MBS-H	**M**odified **B**arth's **S**olution-**H**EPES
MBT	**M**id-**b**lastula **t**ransition
mcer	**m**ouse *cerberus-like*

xxvi

MEMFA	**M**OPS **E**GTA **M**gSO4 **f**orm**a**ldehyde solution
mesp	**mes**oderm **p**osterior
Mo	**M**orpholino **o**ligonucleotide
mRNA	**M**essenger **R**ibonucleic **A**cid
MyoD	**Myo**genic **d**ifferentiation
NBT	4-**N**itro **b**lue **t**etrazolium chloride
NC	**N**eural **c**rest
Ncam	**N**eural **c**ell **a**dhesion **m**olecule
N-terminal	ami**n**o-**terminal**
ODC	**O**rnithine **d**e**c**arboxylase
ON	**O**ver**n**ight
ORF	**O**pen **r**eading **f**rame
Otx2	**O**r**t**hodenticle homeobo**x** homolog **2**
PAGE	**P**oly**a**crylamide **g**el **e**lectrophoresis
PAPC	**P**ar**a**xial **p**roto**c**adherin
Pax6	**Pa**ired bo**x** homeodomain protein **6**
PBS	**P**hosphate-**b**uffered **s**aline
PCP	**P**lanar **c**ell **p**olarity
PCR	**P**olymerase **c**hain **r**eaction
pH	**p**ower **H**ydrogen
PSM	**P**re**s**omitic **m**esoderm
RA	**R**etinoic **a**cid
RNA	**R**ibo**n**ucleic **a**cid
RT	**R**oom **t**emperature
RT-PCR	**R**everse **t**ranscription **p**olymerase **c**hain **r**eaction
SDS	**S**odium **d**odecyl **s**ulfate
sFRP	**s**ecreted **F**rizzled-**r**elated **p**rotein
Shh	**S**onic **h**edge**h**og
Sox2	**S**ex determining region Y (SRY)-b**ox** containing protein **2**
STYKc	**S**erine/**T**hreonine/**Ty**rosine protein **k**inase **c**atalytic domain
TBD	**T**ail**b**ud **d**omain
TGF-β	**T**ransforming **g**rowth **f**actor **β**
Thy2	**Th**y**lacine2**

Tsg	**T**wisted **g**astrulation
UTR	**U**ntranslated **r**egion
UV	**U**ltra **v**iolet
VMZ	**V**entral **m**arginal **z**one
WISH	**W**hole **m**ount *in situ* **h**ybridization
Wnt	**W**ingless / **In**tegrated family members
Xcer	*Xenopus **cer**berus*
Xlr	**X**olloid-**r**elated
Xnr	*Xenopus **n**odal **r**elated*
YSL	**Y**olk **s**yncytial **l**ayer
ZPA	**Z**one of **p**olarizing **a**ctivity

Chapter I
Introduction

Amphibian embryos, like the ones of frogs and newts, have been widely used in developmental biology. Among them, the frog *Xenopus laevis* is the best characterized amphibian system. *Xenopus laevis* offers several advantages over other animals as an experimental animal, making them excellent model organisms for studying the mechanisms of early embryonic development in vertebrates: 1) embryos are easy to obtain in large numbers; 2) their embryonic development from fertilized egg to the tadpole stage can be easily followed because it takes place outside the maternal body; 3) the egg and the young embryo are large enough (1–2 mm in diameter) to be easily visualized. These features make the *Xenopus* embryo an excellent model system to perform microsurgery and manipulate the embryos experimentally under a stereomicroscope in ways that are not as easy performed in other vertebrate embryos.

I.1 Early *Xenopus laevis* development

All vertebrates share a conserved body plan, and their body plans can be described by three different axes — anterior–posterior (AP), dorsal–ventral (DV) and left-right (LR). During embryonic development the embryos form the head, trunk and tail along the AP axis and the backbone and belly of the animal along in the DV axis. The unfertilized *Xenopus* egg is polarized along the animal to vegetal axis before fertilization, as shown by a highly pigmented animal hemisphere and a lightly pigmented vegetal hemisphere (Moon and Kimelman, 1998). In the *Xenopus* embryo the DV axis is the first axis being determined and is defined, during fertilization, by the sperm-entry point (Fig. 1B). The dorsal side of the embryos is always formed on the side opposite to the sperm entry point. The sperm entry the oocyte, which can occur in any point in the animal hemisphere (Weaver and Kimelman, 2004), causes, during the first cell cycle which lasts about 90 minutes, the loosening of the outer layer of the egg, the cortex, from the dense yolky core cytoplasm. The cortex then begins to rotate relative to the core cytoplasm resulting in a 30º displacement of the cortex away from the sperm entry point in a process designated by cortical rotation (reviewed by Gerhart *et al.,* 1989). Cortical rotation is driven by an array of microtubules and coincides with the translocation of maternal components in the same direction as the cortical rotation (Fig. 1B). Dorsal determination seems to be associated with the translocation of maternal components with dorsalizing activity located in membrane vesicles in the vegetal pole of the embryo towards the prospective dorsal side of the embryo by cortical microtubules (reviewed by De Robertis

et al., 2000; Weaver and Kimelman, 2004). Both cortical rotation and the translocation of the dorsal determinants are essential for the establishment of the DV axis and depend on a proper formation of the microtubule array. If the microtubule polymerization is impaired or blocked during the first cell cycle, either by irradiating the fertilized egg at the vegetal pole with ultraviolet light, or by treatment with nocodazole, or by subjecting the embryos to low temperatures, cortical rotation is impaired and the dorsal determinant components remain in the vegetal pole of the embryo. This leads to the formation of a completely ventralized embryo lacking all dorsoanterior structures, referred to as a "belly piece" (reviewed by De Robertis *et al.*, 2000; Weaver and Kimelman, 2004). Microinjection of certain synthetic mRNAs that encode for Wnts and several downstream effectors of its pathway, such as β-catenin or Axin; Nodal-related factors; or even BMP antagonists, such as Noggin and Chordin are able to completely rescue the ventralized phenotype obtained by the above mentioned treatment of the embryos (reviewed by De Robertis *et al.*, 2000; Weaver and Kimelman, 2004).
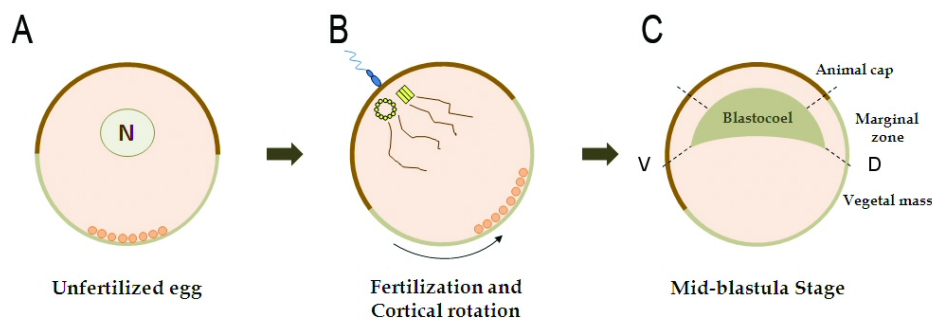
Figure 1- Dorsal side determination during *Xenopus laevis* early development. (A) In the unfertilized egg *VegT* mRNA and a dorsal determinant are translocated to the vegetal pole. The dorsal determinant is located in small membrane vesicles (orange dots). (B) Fertilization. Sperm entry induces microtubule polymerization which initiates a rotation of the cytoplasm relative to the cortex. The microtubules that extend from the centriole towards the dorsal side are responsible for the transportation of the dorsal determinant containing membrane vesicles to the prospective dorsal side. (C) At the mid-blastula stage the embryo is divided into three different regions: the animal cap, the marginal zone and the vegetal mass.

Several studies have suggested that the dorsal determinants are components of the canonical Wnt signaling pathway. Depletion of maternal β-catenin using antisense oligonucleotides results in embryos lacking all dorsal structures (Heasman *et al.*, 1994; Heasman *et al.*, 2000). However, transplantation of the subcortical vegetal cytoplasm of β-catenin depleted embryos to the ventral side of a normal embryo is still able to induce a secondary axis, suggesting that the dorsal determinant consists of an upstream factor of the Wnt canonical pathway that by moving to the dorsal side of the embryo leads to the stabilization and nuclear translocation of β-catenin on the dorsal side of the *Xenopus*

blastula (Marikawa and Elinson, 1999). Maternal *Wnt11* mRNA which was shown to be located in the vegetal cortex during oogenesis (Ku and Melton, 1993) seems to be both necessary and sufficient for the determination of the embryonic DV axis, as was shown by loss-of-function experiments (Tao *et al.,* 2005). In addition, UV treatment causes a reduction in the amount of *Wnt11* mRNA (Schroeder *et al.,* 1999). Other components of the Wnt signaling pathway, such as Disheveled and the GSK3-binding protein, were also shown to move from the vegetal pole to the dorsal side (Miller *et al.,* 1999; Weaver *et al.,* 2003). Vg1 might also be important for dorsal determination since it is localized and enriched in the dorsal side of morula embryo and involved in early patterning of the embryo (Birsoy *et al.,* 2006).

Once the first cell cycle is complete a series of eleven rapid cell divisions (20-30 min each) follow during which the level of transcription and signaling is very low. By the end of the twelfth cell cycle the embryo resembles a small sphere containing 4000 cells with a small intercellular cavity, the blastocoel and is composed of three different regions: the animal cap, the marginal zone and the vegetal mass (Fig. 1C). At this point in development, designated the mid-blastula transition (MBT), the cell cycle lengthens and zygotic transcription begins.

I.2 Mesoderm induction and Organizer formation

In the *Xenopus* embryo, mesoderm is specified during cleavage stages. The first experiments that demonstrated the process of mesoderm induction were performed by Peter Nieuwkoop. In his experiments he explanted both the animal caps and the vegetal cap of the embryo and cultured them either alone or together. When animal caps were cultured alone they developed into epidermis while the vegetal explants either did not develop into recognizable tissues or acquired some endodermal character, thereby showing that neither of the explants was able to develop mesodermal derivates when cultured alone. However, when he combined both the animal cap and the vegetal explants they developed a substantial amount of endoderm- and mesoderm-derived tissues such as notochord, prechordal plate, neural tube, somites, pharyngeal endoderm and tail parts (Nieuwkoop, 1969a,b). Using lineage tracing and 3H-thymidine labeling, Nieuwkoop showed that the mesoderm and pharyngeal endoderm developed exclusively from the animal cap tissue which was induced by the vegetal explants (Nieuwkoop and Ubbels, 1972). In subsequent experiments, when dorsal vegetal cells were cultured together with

the animal cap they were able to induce dorsal-type mesoderm such as notochord, skeletal muscle and head endoderm. In contrast, when ventral vegetal cells were used, they were only able to induce ventral-type mesoderm such as blood and somites (Boterenbrood and Nieuwkoop, 1973). Later on, experiments where the dorsal blastomeres at the 32-64 cell stage were transplanted into the ventral side of a normal embryo, axis duplication was obtained, and when dorsal blastomeres were transplanted into a ventralized embryo dorsal axis formation was rescued (Gimlich and Gerhart, 1984). Furthermore, this axis-inducing ability was found to be maximal at late blastula stages (Boterenbrood and Nieuwkoop, 1973; Jones and Woodland, 1987). These results supported the existence of a vegetal dorsalizing center that was named the Nieuwkoop center and was defined as the group of cells that are able to induce the animal hemisphere cells to form the organizer (Gerhart *et al.,* 1989).

Intense investigations have been made in order to understand how this inductive activity that leads to mesoderm formation is achieved at the molecular level. Work preformed in *Xenopus* embryonic cell lines showed that, both the fibroblast growth factor (FGF) as well as some members of the transforming growth factor-β (TGF-β) superfamily could act as potent mesoderm inducers. The use of dominant-negative receptors showed that FGF is necessary for the formation of the posterior mesoderm while TGF-βs are important for all mesoderm formation (Amaya *et al.,* 1991; Hemmati-Brivanlou and Melton, 1992). In addition, TGF-βs are able to induce anterior mesoderm without FGF signaling, while induction of posterior mesoderm by TGF-βs can only occur if the FGF pathway is active (Cornell and Kimelman, 1994; LaBonne and Whitman, 1994). More recently, loss of function studies have shown that depletion of FGF results in reduced somites and notochord as well as convergent extension defects (Conlon *et al.,* 1996; Fisher *et al.,* 2002). Although FGFs have been shown to be potent mesoderm inducing factors and are required for posterior mesoderm formation, their function *in vivo* is also necessary for the maintenance of the mesodermal fate.

At blastula stages, *Xenopus nodal related* genes (*Xnr*s), encoding members of the TGF-β superfamily were shown to be expressed in the vegetal region of the embryo in a dorsal to ventral gradient and were also reported to play important functions in mesoderm formation. When Nieuwkoop's mesoderm-induction experiments, where the animal and vegetal explants were combined, were repeated using Cerberus-short (Cer-s), a molecule that specifically inhibits Xnrs, the induction of both dorsal and ventral

mesoderm was blocked (Agius *et al.,* 2000). In addition, both Xnr-1 and Xnr-2 were shown to be able to completely rescue UV treated embryos (Jones *et al.,* 1995). The gradient of *Xnr* expression is thought to be activated by three maternally inherited proteins: VegT, Vg1 and β-Catenin.

VegT which is a T-box transcription factor is localized in the vegetal pole of the *Xenopus* oocyte (Lustig *et al.,* 1996; Stennard *et al.,* 1996; Zhang and King, 1996) as mentioned above and was shown to be a potent mesoderm inducer. Maternal depletion of *VegT* maternal mRNA using antisense oligonucleotides resulted in embryos with a severe impairment in meso- and endoderm induction (Kofron *et al.,* 1999; Zhang *et al.,* 1998). In VegT depleted embryos, reintroduction of *Xnrs* mRNAs, but not of *FGF* or even *activin* mRNAs, is able to rescue most endodermal and mesodermal gene expression (Kofron *et al.,* 1999; Xanthos *et al.,* 2001), suggesting that Xnr proteins are crucial players in mesoderm and endoderm formation.

Vg1 is another member of the TGF-β superfamily that has been implicated in mesoderm formation. In Vg1 depleted embryos, dorsal genes like *cerberus*, *chordin* and *noggin* are severely depleted while general endodermal markers are less affected. In addition, the activated form of Vg1 is able to induce dorsal mesoderm in animal cap explants and, when microinjected in the ventral side of the embryo, is able to induce a complete secondary body axis. However, Vg1 is not able to induce ventral mesoderm derivates, consistent with the dorsal enrichment of *Vg1* mRNA (Kessler and Melton, 1995).

An additional signaling pathway that has been implicated in mesoderm formation is the canonical Wnt signaling pathway. When maternal *β-catenin* is depleted from *Xenopus* oocytes, the embryos develop lacking dorsal structures, resembling the most severe phenotypes of the ventralized UV treated embryos (Heasman *et al.,* 1994). In wild type embryos, microinjection of both *VegT* and *Vg1* causes only low levels of *Xnr* transcription. However if β-catenin is also provided, it cooperates with VegT and Vg1 and high levels of *Xnr* expression are achieved, resulting in the induction of the organizer. Christian *et al.* (1992) thereby showed that the canonical Wnt pathway does not induce mesoderm directly, but acts synergistically with other signaling pathways in order to regulate organizer formation.

Taken together, during cleavage stages and after cortical rotation, *VegT* transcripts are localized in the vegetal hemisphere while *Vg1* transcripts are dorsally enriched

(Fig. 2). In addition, a member of the canonical Wnt pathway upstream of β-catenin, possibly *Wnt11*, is also dorsally enriched which results in the stabilization of β-catenin in the prospective dorsal side where it persists until the mid-blastula transition (Fig. 2). At this point in development, characterized by a burst in gene transcription activity, a number of mesoderm-specific genes are activated in the marginal zone. VegT activates the zygotic expression of *Xnrs* (*Xnr-1, -2, -4, -5*, and *-6*), *Activin* and *Derrière*, in the vegetal hemisphere, all having mesoderm inducing activity (Agius *et al.*, 2000; Clements *et al.*, 1999; Dale *et al.*, 1989; Kessler and Melton, 1995; Kofron *et al.*, 1999; Sun *et al.*, 1999; Zhang *et al.*, 1998). As a result of the activation of Wnt signaling in the dorsal side, the expression of *Xnrs* is higher in the dorsal side than in the ventral side of the embryo (Fig. 2). Thus, the region in the dorsal side of the blastula where the TGF-β and canonical Wnt signaling pathways intersect, forms the Nieuwkoop center (Fig. 2). In parallel, β-catenin also activates the transcription of additional targets that include *siamois* and *Xtwin*. Consequently, in the ventral marginal zone low levels of Xnrs induce ventral mesoderm. Simultaneously, in the dorsal side, high levels of Xnrs together with molecules like *siamois* trigger transcription of the organizer-specific genes, such as *cerberus* (Crease *et al.*, 1998; Cui *et al.*, 1996; Nishita *et al.*, 2000; Watabe *et al.*, 1995; Zorn *et al.*, 1999) and thereby induce the organizer (the most dorsal mesoderm), in the overlying cells (Fig. 2). The Nieuwkoop center cells will give rise to the anterior endoderm.
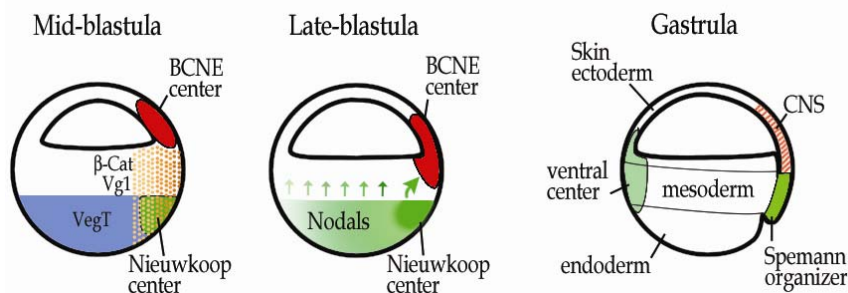
Figure 2- Mesoderm induction and organizer formation. At mid-blastula stages, high levels of β-catenin on the dorsal side (orange dots), together with vegetally localized transcription factor VegT (blue) and the dorsally enriched maternal TGF-β-family growth factor Vg1, generate a gradient of Xnr (green) molecules in the endoderm. In parallel, β-catenin on the dorsal side of the embryo induces the formation of a second signaling center, the BCNE center in the dorsal animal cells. The Xnr gradient in the endoderm induces the formation of mesoderm in the overlying tissue: low doses of Xnrs induce the formation of ventral mesoderm, while high doses lead to the establishment of Spemann's organizer in the dorsal mesoderm of gastrula embryos. The BCNE center is involved in the formation of neural tissue (CNS). (Adapted from De Robertis and Kuroda, 2004)

I.3 Mesoderm induction in other vertebrates

Since the experiments performed by Nieuwkoop, where for the first time it was elucidated how mesoderm and the organizer are induced in the animal hemisphere of the amphibian embryo, numerous studies have been done in order to better understand the molecular mechanisms behind mesoderm formation, not only in amphibians but also in other vertebrates. Recent studies have shown that in fish the processes by which the mesoderm and organizer are formed are very similar to the ones occurring in the amphibian embryo. Experiments have demonstrated that the yolk syncytial layer (YSL) is a source of mesoderm- and endoderm-inducing signals (Mizuno *et al.*, 1996; Rodaway *et al.*, 1999). In addition, experiments where RNAs present in the YSL were specifically eliminated using a mixture of RNAses, revealed that transcripts in the YSL are necessary for the formation of all endoderm and ventrolateral mesoderm as well as for the induction of the nodal related genes, *squint* and *cyclops*, in the ventrolateral marginal blastomeres (Chen and Kimelman, 2000). Both *squint* and *cyclops* show overlapping expression patterns and, in the absence of either *squint* and *cyclops*, cyclopic embryos will develop. However, when both gene products are removed, only mesoderm in the ventral part of the embryo (which later gives rise to the tail mesoderm) forms (Feldman *et al.*, 1998). These results demonstrated that in fish, as previously demonstrated in the frog, Nodal signaling is necessary for proper mesoderm induction. The nature of the initial factor present in the YSL that acts upstream of Nodal signaling is still unknown. In embryos where the YSL transcripts have been depleted, the dorsal-most mesoderm is still formed. This has been attributed to the stabilization of β-catenin signal in the dorsal-most blastomeres, which results in specific activation of genes such as *bozozok*. In the dorsal-most blastomeres, the combination of β-catenin signals, together with the unknown factor present in the YSL responsible for *squint* and *cyclops* expression, leads to the induction of the fish organizer.

In the chicken embryo, the mesoderm is formed in the posterior region of the epiblast. Transplantation experiments have shown that only the posterior part of the marginal zone is able to induce a complete secondary axis when transplanted to the anterior portion of the marginal zone of a host embryo (Eyal-Giladi and Khaner, 1989; Khaner and Eyal-Giladi, 1989). These results, together with grafting and fate mapping experiments, suggested that the posterior marginal zone of the pre-primitive streak stage embryo is the avian equivalent of the amphibian Nieuwkoop center (Bachvarova *et al.*,

1998). The two signaling pathways acting in the amphibian Nieuwkoop center, the TGF-β and canonical Wnt signaling pathways, have also been shown to be active in the chicken embryo posterior marginal zone (Hume and Dodd, 1993; Roeser *et al.*, 1999; Seleiro *et al.*, 1996; Shah *et al.*, 1997). As in other vertebrates, chicken Nodal (cNodal) seems to also play a role in mesoderm formation since its expression pattern, in the posterior marginal zone, overlaps with the early mesoderm territory (Lawson *et al.*, 2001). It has been demonstrated that cVg1, the homologue of *Xenopus* Vg1, regulates *Nodal* expression. Like c*Nodal*, c*Vg1* is also expressed in the posterior marginal zone and when misexpressed in other regions of the marginal zone, c*Vg1* is able to induce ectopic expression of c*Nodal* in the epiblast (Seleiro *et al.*, 1996; Shah *et al.*, 1997; Skromne and Stern, 2001). Expression of c*Vg1* in other regions of the embryo besides the marginal zone does not lead to axis induction. In addition, when c*Vg1* is misexpressed in the anterior marginal zone along with Wnt antagonists, axis induction is inhibited, emphasizing the requirement of both TGF-β and Wnt canonical signaling pathways for axis induction (Skromne and Stern, 2001). Chicken *Wnt8c* is expressed throughout the marginal zone in a gradient fashion with highest expression in the posterior side. It has been shown to be necessary for Vg1 to induce *Nodal* expression (Hume and Dodd, 1993; Skromne and Stern, 2001). Therefore, in the chicken embryo, evidence show that mesoderm is formed in the posterior region of the epiblast as a consequence of nodal signaling. c*Nodal* expression is in turn activated by cVg1 in combination with canonical Wnt signaling. Then, Nodal signaling together with Wnt8c induce the formation of the primitive streak which induces organizer genes in its most anterior end. During early stages of gastrulation, as the primitive streak elongates towards the anterior side of the embryo, it keeps emitting mesoderm inducing factors that will be responsible for continuous formation and patterning the mesoderm (Lawson *et al.*, 2001; Stern *et al.*, 1995).

Unlike what has been reported for other vertebrates, in the case of the mouse embryo no region similar to the Nieuwkoop center has been identified. However, different studies performed in mice have shown that loss of Nodal signaling results in embryos where most mesoderm fails to form and thus support the idea that in the mouse, as in other vertebrates, Nodal also plays an important role in mesoderm formation (for review see Kimelman and Bjornson, 2004). However, the signals upstream of Nodal are still unknown. Unlike the role of Vg1 in both amphibian and chick mesoderm induction, removal of *gdf-1*, a mouse gene closely related to *Vg1*, results in embryos showing

left/right asymmetry defects while mesoderm formation appears seems unaffected (Wall *et al.*, 2000). At 5.5 dpc, *Nodal* is expressed throughout the entire epiblast. As the anterior visceral endoderm (AVE) forms, it starts to secrete Nodal antagonists such as *cerberus-like* and *lefty-1* and, as the AVE migrates towards the anterior region of the embryo, Nodal signaling becomes restricted to the posterior region of the embryo, the region where mesoderm is formed (Perea-Gomez *et al.*, 2002). It is thought that in the mouse embryo, other signaling pathways, like BMP and Wnt signaling, may be involved in mesoderm formation in the mouse. Mutant mice for components of the BMP signaling pathway such as BMPRI and BMP-4 fail to form any mesoderm which demonstrates that BMP signaling is crucial for all mesoderm induction (Mishina *et al.*, 1995; Winnier *et al.*, 1995). Transgenic mouse embryos overexpressing c*Wnt8c* or embryos null for the Wnt inhibitor, *Axin*, have multiple primitive streaks (Popperl *et al.*, 1997; Zeng *et al.*, 1997). In addition, knockout mice for the *Wnt3a* gene do not express *Nodal* at 7.5dpc and do not form mesoderm (Liu *et al.*, 1999). Furthermore, inactivation of *β-catenin* in mouse embryos leads a failure in mesoderm formation (Haegel *et al.*, 1995), evidencing the fundamental role of the canonical Wnt signaling in mesoderm formation in the mouse.

I.4 Chordin- and Noggin-expressing (BCNE) center

Recent studies have shown that, unlike what was previously thought, in *Xenopus* blastula embryos, two signaling centers located in the dorsal side of the embryo are involved in patterning the embryo (Fig. 3). One is the Nieuwkoop center (see Section I.2) and the other is the Blastula Chordin- and Noggin- Expressing (BCNE) center, which is located in the dorsal animal cells and contain cells that will become neuroectoderm and organizer precursor cells. The cells that constitute the BCNE center later give rise to a large part of the brain, the retina as well as the floor plate and notochord. In 2001, Wessely *et al.* have shown that, at blastula stages, the dorsal animal cap as well as the dorsal marginal zone express BMP antagonists such as *chordin* and *noggin* as well as *Xnr-3*. In addition, they saw that embryos lacking all mesoderm, due to injection of *Cer-s* mRNA, were still able to develop a central nervous system (CNS) containing a cyclopic eye and brain tissues. This region of *chordin* and *noggin*'s expression was initially designated as the pre-organizer and shown to be exclusively dependent on a β-catenin signal (Wessely *et al.*, 2001). Later on, during gastrulation, expression of *chordin* and *noggin* in the Spemann organizer endomesoderm also requires Nodal-related signals (Wessely *et al.*, 2001). More

recently, it was shown that dorsal animal cap explants that had not yet contacted with mesoderm were able to differentiate into CNS tissue (Kuroda *et al.,* 2004). However, it was also shown by transplantation experiments that this pre-organizer region, when transplanted to the ventral side of the embryo, was not able to induce CNS in neighboring cells (Kuroda *et al.,* 2004). Thus this region lacks any organizer-inducing activity. As a result, the so-called pre-organizer was renamed the BCNE center.
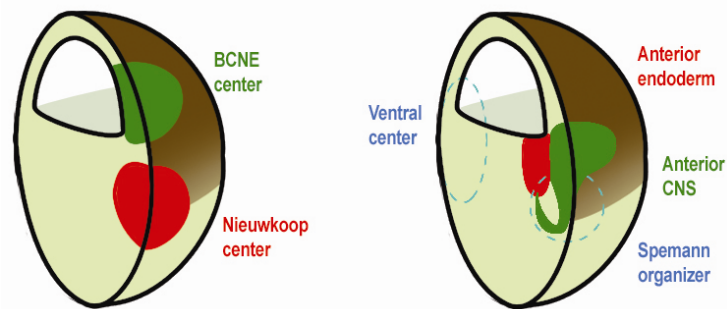
Figure 3 – Localization of the blastula and gastrula signaling centers in *Xenopus* embryos. The BCNE (green) center is located in the dorsal animal animal cap region and gives rise to the prospective brain and floor plate and notochord. The other signaling center present at blastula stages is the Nieuwkoop center (red), which will become anterior endoderm at gastrula stages. At gastrula stages, Spemann organizer is form in the dorsal most mesoderm. In the opposite direction, the ventral signaling center is formed. (Adapted from De Robertis and Kuroda, 2004)

In summary, at the mid-blastula transition, as soon as zygotic transcription starts, β-catenin signal on the dorsal side of the embryo induces either on its own or together with vegetally located mRNAs, the formation of the BCNE center in the dorsal animal cells and the Nieuwkoop center in the dorsal vegetal cells, respectively. The BCNE center then expresses in addition to *chordin* and *noggin*, genes like s*iamois*, *pintallavis*, and *Xnr-3*, and will be involved in neural specification while the Nieuwkoop center, that expresses *Xnr*s and *cerberus*, will be involved in endoderm development.

I.5 Spemann's organizer in amphibians

In 1924, Hans Spemann and his student Hilde Mangold performed one of the most famous experiments in experimental embryology. They transplanted tissues from a gastrulating newt embryo and placed it into different locations in a different host newt embryo of the same age. In this experiment they observed that the only piece of tissue in the early gastrula capable of maintaining its original fate was the dorsal lip of the blastopore. Interestingly, transplantation of the dorsal lip of the blastopore to the ventral side of the host embryo, a region that would normally become epidermis, lead to the formation of a secondary axis, with neural tube, notochord and somites (reprinted as

Spemann and Mangold, 2001). When they repeated this experiment using a pigmented donor and an albino host, they were able to observe that the graft tissue had differentiated into notochord and sometimes also into floor plate of the neural tube, with a minor contribution to somites and gut roof. On the other hand, remarkably, the major portion of the secondary axis was derived from cells of the host embryo. This included most of the neural tube and sometimes even the floorplate, the pronefrons, most of the somites and the gut. Thus apart from maintaining its own fate in a new location, the dorsal lip of the blastopore changed the fate of neighboring host cells, "organizing" them into a secondary axis. These experiments constituted the first evidence of the existence of an organizing center that was able to recruit, in a non-cell-autonomous way, other cells to acquire different fate than the one they were committed to and was responsible for the establishment of the embryonic body plan, which then Spemann referred as the "organizer" (later dubbed the Spemann's organizer). Spemann's experiments have been performed using *Xenopus laevis* embryos and by use of lineage tracing techniques it was possible to precisely document the contributions of both the donor and the host grafts to the secondary axis (Gimlich and Cooke, 1983; Smith and Slack, 1983).

In current times, the Spemann's organizer that consists of a small group of cells located above the dorsal blastopore lip, is thought to dorsalize ventral mesoderm and recruit non-organizer cells to form paraxial structures. The direct descendants of the organizer give rise to the embryonic axial structures (pharyngeal endoderm, head mesoderm and notochord), promote gastrulation movements and induce neural fates within the ectoderm.

I.6 Organizer in other vertebrates

Following the experiments performed by Spemann and Mangold, which led to the concept of an organizing center, structures that would be functionally equivalent to the amphibian organizer were identified in other vertebrates based on their ability to induce secondary axis when transplanted to a different region of a young gastrula embryo (Fig. 4). By performing grafting experiments in chicken embryos, Waddington found that grafts containing the anterior half of the primitive streak were able to induce ectopic neural tissue in the host embryo upon transplantation (reviewed in Stern, 2000). In addition, when he grafted duck primitive streaks into a chicken host that led to the formation of ectopic neural folds, he confirmed that the effects observed in the host

13

embryo were due to an induction process that had maximal activity when the graft included the most anterior end of the primitive streak known as the Hensen's node. These findings lead him to conclude that in birds the equivalent structure to the amphibian organizer is the Hensen's node (reviewed in Joubin and Stern, 2001). Similarly, Oppenheimer demonstrated, using vital dyes and transplantation experiments that a population of cells with organizer-like activity was located in the dorsal marginal zone of a teleost embryo, in the dorsal embryonic shield (reviewed in Joubin and Stern, 2001). In more recent years, it was demonstrated that when the node of a mouse embryo, located in the anterior tip of the primitive streak, was grafted into posterolateral locations of a host mouse embryo it could induce the formation of a secondary axis (Beddington, 1994). Furthermore, when inter-species organizer grafts were performed using chicken, rabbit, fish, amphibians and mouse embryos it was demonstrated that with all different combinations it could be possible to induce the formation of neural tissue in the host tissue (see Joubin and Stern, 2001). These results indicated that the main properties of the organizer are conserved among different species.
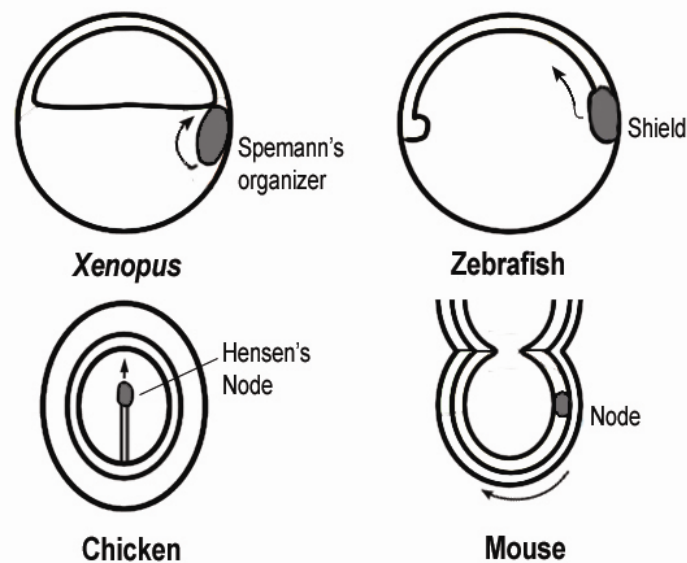
Figure 4 - The organizer structure in different vertebrate embryos. The organizer is represented as a grey oval region and the direction of migration of the organizer cells during gastrula stages is indicated by black arrows.

I.7 Regional specification of the organizer

From later work performed by Spemann, came the first evidence that the organizer could be divided into different parts and each of these partial organizers could induce a partial axis (Spemann, 1931; Fig. 5). In his experiment, Spemann found that by grafting an early gastrula lip, which consisted of presumptive prechordal mesendoderm,

into the blastocoel of a host embryo, secondary head structures were formed. By contrast, when he grafted late gastrula lips, which consisted of presumptive chordamesoderm, only secondary trunks formed. During gastrulation, the prechordal mesendoderm is one of the first organizer cells to gastrulate and transplantation experiments have shown that these cells show the most potent head-inducing activity. Then, the chordamesodermal cells are the next to involute and have trunk- and tail-inducing activity. Thereby, based on their different inducing abilities, the organizer can be divided into head trunk and tail organizers. Like in the frog, distinct head trunk and tail organizers were also identified in other vertebrates. The existence of these different organizers arises from the fact that Spemann's organizer is a dynamic structure composed of distinct cell populations. As cells migrate, they acquire different fates, inducing properties and emitting different factors that generate signaling gradients that locally pattern the AP axis of the embryo.
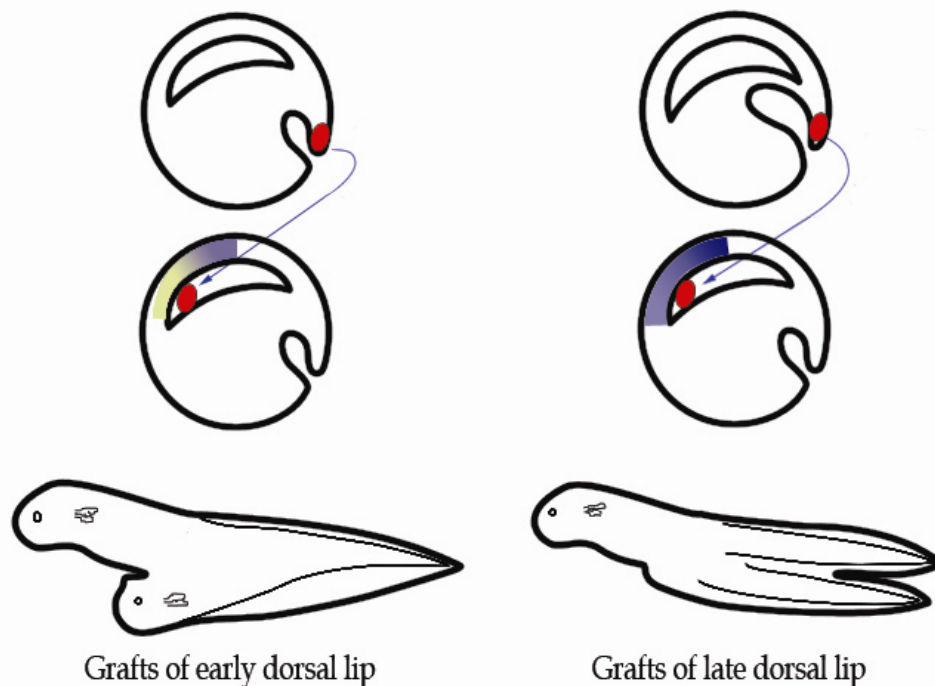
Figure 5 - Spemann dorsal lip transplantation experiments that gave rise to the notion of head and tail organizers in the amphibian embryo. (A) When an early dorsal blastopore lip (red) is grafted to the ventral side of a host embryo, a complete secondary axis forms. (B) When a late dorsal blastopore lip (red) is grafted, only caudal structures develop. (Adapted from Foley and Stern, 2001)

From the work performed in *Xenopus laevis* embryos, it was demonstrated that a secondary head structure could be formed when either the BMP and Wnt or the BMP and Nodal signaling pathways were inhibited simultaneously (Glinka *et al.,* 1997). In addition, overexpressing any of these signaling cascades would result in head defects. These results, together with the study of Cerberus, a multifunctional antagonist that binds and

inhibits BMPs, Wnts and Nodals, and is able to induce ectopic head-like structures when injected into the ventral side of a frog embryo, led to the suggestion that head induction would require triple inhibition of all three signaling pathways (Bouwmeester *et al.*, 1996; Piccolo *et al.*, 1999).

The prechordal mesendoderm expresses BMP antagonists (*noggin* and follistatin), Wnt antagonists (*dkk-1*, *Frzb-1* and *Crescent*) and Nodal antagonists (*Antivin/lefty*). *In vivo* requirement for BMP signaling in head development has been demonstrated in compound mutant mice for *chordin$^{-/-}$noggin$^{-/-}$* and *dkk1$^{+/-}$noggin$^{+/-}$* by showing head defects. However, *in vivo* requirements for Nodal in head formation has not been proven, as neither *lefty/cerberus-like* mouse double mutants nor antivin-morphant zebrafish embryos exhibit any head defects (Niehrs, 2004). Instead, anti-Nodals function as negative feedback regulators for mesoderm formation. Thereby, Nodals which are potent mesoderm and endoderm inducers may affect neural induction and patterning in indirect ways through mesoderm and endoderm.

In *Xenopus* embryos, when BMP signaling is blocked in the ventral side of the embryo either by overexpressing a dominant negative form of BMP receptor or a BMP inhibitor, secondary trunks are induced. This finding led to the suggestion that trunk formation requires BMP inhibition. Indeed, the prospective chordamesoderm, the region considered to be the trunk organizer expresses various BMP antagonists (De Robertis *et al.*, 2000). Studies performed in zebrafish embryos have shown that BMP signaling is both necessary and sufficient for trunk formation (Gonzalez *et al.*, 2000). On the other hand, Wnt antagonists are expressed in much lower levels in the trunk organizer than in the head organizer which is consistent with the fact that Wnt signaling is required for the expression of trunk mesodermal marker such as *Xbra* and *XmyoD* (Niehrs, 2004). Nevertheless, Wnt inhibition is necessary for notochord formation and overexpression of anti-BMPs results in secondary axis that lack notochord. Double inhibition of Wnt and BMP is able to induce a notochord. Nodal signaling has an important role in mesoderm induction and thereby is necessary for proper trunk formation. In summary, the trunk organizer requires Wnt and Nodal signaling to be active while BMP signaling needs to be inhibited.

I.7.1 AVE/Hypoblast/Anterior Endoderm and head induction

Unlike what was found in the frog embryo where the head and trunk-tail organizers are contiguous tissues, in higher vertebrates like mouse and chicken that is not the case (Fig. 6). Various embryological, genetic and molecular studies indicate that the mouse AVE is involved in early anterior neuroectoderm specification and is thereby the mouse head organizer. The mouse AVE and the chicken anterior hypoblast are considered to be the topological equivalents of the amphibian anterior endoderm and shown to be essential for anterior neural induction.
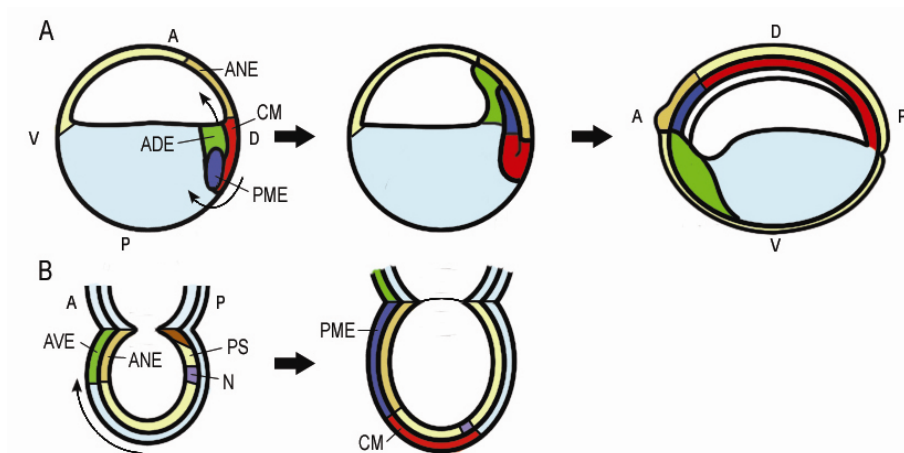
Figure 6 - Comparative schemes of *Xenopus* and gastrulae. (A) The Spemann organizer comprises the chordamesoderm (CM, red), prospective prechordal plate (PME, dark blue) and anterior endoderm (ADE, green). As gastrulation proceeds, the anterior endoderm and the prechordal endomesoderm migrate toward the anterior and pattern the overlying anterior neural plate (ANE, orange). (B) At early gastrula mouse embryo, the anterior visceral endoderm (AVE, green) is in contact with the prospective anterior neural plate. The primitive streak (PS, yellow) and the node (N, mouse organizer, purple) form in the posterior end of the embryo. The PS and the node contain the precursors of the PME and the CM. As gastrulation proceeds, the AVE is displaced anteriorly and the PME comes in contact with the anterior neural ectoderm. Topological equivalent structures in both mouse and *Xenopus* embryos are shown with the same color. (Adapter from Foley and Niehrs, 2000; and Niehrs, 2004)

Experiments with Cerberus and Dickkopf-1 (Dkk-1), secreted proteins with strong head inducing activities when ectopically expressed in the ventral side of the *Xenopus* embryo, provided the first molecular evidence for the existence of a specific anterior neural inducing activity (Bouwmeester *et al.*, 1996; Glinka *et al.*, 1998). During gastrulation, the mouse AVE is displaced anteriorly by the prechordal mesoderm, and both express secreted molecules such as Cerberus-like or Dkk-1 that are thought to influence the adjacent neuroectoderm (Beddington and Robertson, 1999). Several embryological, genetic and molecular studies have indicated that the AVE is involved in early anterior neuroectoderm specification.

17

The role for the AVE as an anterior neural inducing center was first proposed based on lineage tracing and ablation experiments. When either the AVE or the prechordal mesoderm are removed from early gastrulating embryos, the expression of forebrain markers is inhibited. While the prechordal mesoderm is a potent anterior neural inducer, as demonstrated in frog, chick and fish embryos, transplanted AVEs show little inductive activity in most vertebrates. Grafts of pre-streak rabbit and chick hypoblasts were only able to transiently induce anterior neural markers in the area opaca of chick hosts (Foley *et al.*, 2000; Knoetgen *et al.*, 1999). Similarly, the corresponding structure in *Xenopus laevis*, the non-involuting anterior dorsal endoderm, is able to impart anterior character to the neuroectoderm, as indicated by explant recombination experiments (Jones *et al.*, 1999; Lupo *et al.*, 2002). These results suggested that although the AVE has an important function in the early anteriorization of the prospective neuroectoderm, additional signals may be necessary for the maintenance and fine patterning of the rostral neural structures.

Several orthologs of known anterior neural inducers in *Xenopus* were found to be expressed in the AVE. Such was the case for Cer-1 (Belo *et al.*, 1997; Biben *et al.*, 1998; Shawlot *et al.*, 1998), Dkk-1 (Glinka *et al.*, 1998), Lefty-1 (Oulad-Abdelghani *et al.*, 1998) and Sfrp5 (Finley *et al.*, 2003). In addition, transcription factors with known roles in forebrain specification, like Otx2 (Acampora *et al.*, 1995; Ang *et al.*, 1994), Lim-1, Gsc (Belo *et al.*, 1997; Biben *et al.*, 1998), Foxa2 (Perea-Gomez *et al.*, 1999), Hex (Thomas *et al.*, 1998) and Hesx1 (Thomas and Beddington, 1996), were also found to be expressed in the AVE before anterior mesendoderm formation.

Surgical removal of Hesx1-expressing AVE results in the loss of Hesx1 activity in the prospective forebrain tissue and a smaller cephalic neural plate (Thomas and Beddington, 1996). However, knockout mice for several AVE genes like *cer-1*, *gsc* and *lefty-1* developed with no anterior development phenotype (Belo *et al.*, 1997,1998; Meno *et al.*, 1998; Rivera-Perez *et al.*, 1995; Shawlot *et al.*, 1999). For other AVE genes like *dkk-1*, *Hesx1* and *Hex*, mild deficiencies in the rostral-most region of the forebrain are observed (Martinez-Barbera and Beddington, 2001; Martinez-Barbera *et al.*, 2000a; Martinez Barbera *et al.*, 2000b; Mukhopadhyay *et al.*, 2001). Analysis of chimeric embryos revealed that Otx2, Lim-f1 and Foxa2 activities are required in the AVE for the primary induction of the anterior neural plate (Acampora *et al.*, 1998; Dufort *et al.*, 1998; Rhinn *et al.*, 1998; Shawlot *et al.*, 1999; Varlet *et al.*, 1997) while conditional gene inactivation of *Smad2* activity in the

AVE demonstrated its requirement for the initial specification of rostral neuroectoderm (Vincent *et al.,* 2003). In *cer-1/lefty-1* compound mutants an expansion of the anterior primitive streak markers is observed, and in some cases an ectopic primitive streak develops (Perea-Gomez *et al.,* 2002). In contrast, *cripto* mutant embryos, which fail to form embryonic mesoderm and endoderm and in which the AVE is not displaced anteriorly, express anterior neural markers but at a distal position (Ding *et al.,* 1998). Observations in chick embryos showed that the hypoblast directs cell movements in the epiblast so as to keep the prospective forebrain region away from the anterior end of the primitive streak (Foley *et al.,* 2000). The mouse AVE has also been shown to suppress the expression of posterior markers (Kimura *et al.,* 2000).

Thus, the AVE and its equivalent structures in other vertebrates are thought to function either by exerting a shielding capability over the prospective anterior neural plate, keeping it away from the caudalizing influence of the primitive streak-derived organizer (and thereby promoting anterior positional identity) or, rather than exerting a major role during neural induction, acting by preventing ectopic organizer formation (Foley *et al.,* 2000; Kimura *et al.,* 2000; Perea-Gomez *et al.,* 2001a; Perea-Gomez *et al.,* 2001b; Perea-Gomez *et al.,* 2002).

I.8 Molecules involved in gastrulation

In more recent years, a high amount of genes expressed in the organizer have been isolated and these have helped in understanding the molecular mechanisms underlying the inductive properties of the organizer. Some of these genes encode for transcription factors while others encode for secreted proteins. Among the transcription factors expressed in the organizer are Siamois, Goosecoid (the first molecule expressed in the organizer to be isolated), Pintallavis, Xotx2, Xlim-1, Xbra, Xanf-1/HNF3-β, Xtwin and Xnot2 proteins. While some, like Goosecoid and Siamois are exclusively expressed in the organizer, others such as Xnot2 and Xbra are initially expressed throughout the entire marginal zone and later on, as a result of cell-cell signaling, become restricted to the organizer. These transcription factors function in the organizer by regulating the expression of the secreted factors that will then pattern the nearby cells (for review see De Robertis *et al.,* 2000; Harland and Gerhart, 1997). Among the secreted factors are Chordin, Noggin, Follistatin, ADMP, Xnr-1,-2,-3,-4, Cerberus, Antivin/Lefty, Frzb-1, sFRP2, Crescent, Dkk1 and eFGF, some of which will be discussed below (De Robertis *et al.,* 2000;

Fig. 8). With the isolation of these organizer genes, and by studying their function during gastrulation and the mechanism by which they exert their functions, it was possible to demonstrate that one of the main roles of the organizer is to secrete molecules that function as antagonists for three classes of growth factors (BMPs, Wnts and Nodals). In general, these antagonists act by interacting directly with the growth factors or with their receptors (Fig. 7). This binding inhibits them and "frees" the organizer from these factors that otherwise would inhibit its activity. The expression of both the growth factors as well as of its antagonists generates a signaling gradient that is responsible for patterning the embryonic axes (for review see Niehrs, 2004).
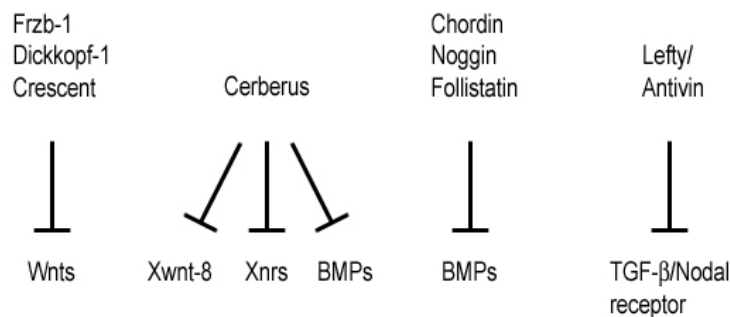
Figure 7 – Spemann's organizer secreted molecules. The organizer is a source of secreted proteins that are able to bind to different growth factors in the extracellular space and block their signaling. Crescent, Frzb-1 and Dickkopf-1 are Wnt antagonists. Cerberus is able to inhibit both Xwnt-8, Xnrs and BMPs. Chordin, Noggin and Follistatin are BMPs inhibitors. Lefty/Antivin bind to the TGF-β/Nodal receptor and inhibit Nodal signaling.

I.8.1 Nodal antagonists

The Antivin/Lefty is an Activin/Nodal antagonist expressed in the organizer in zebrafish, *Xenopus* and mouse that functions by binding to the EGF-CFC co-receptors blocking their interaction with Nodal and Activin receptors. In addition, because the transcription of *Antivin/lefty* is induced by Nodal itself, *Antivin/lefty* acts as a feedback inhibitor that limits the Nodal signal in time and space (Cheng *et al.*, 2000; Meno *et al.*, 1999). The generated gradient in Nodal signaling is crucial for the patterning of the DV axis, and exists by the fine tuning of both the growth factors as well as their antagonists. Experiments have shown that low Nodal signaling induces growth factors, such as BMP-4 in zebrafish and Wnt8 in both zebrafish and frog (Agathon *et al.*, 2003; Agius *et al.*, 2000), whereas increasingly high doses of Nodal signaling induce growth factors antagonists, like Chordin, Dkk-1 and Cerberus (Wessely *et al.*, 2001). In mice it was shown that Cerberus-like and Lefty-1 have redundant roles in restricting Nodal signaling to the epiblast (Perea-Gomez *et al.*, 2002).

I.8.2 BMP antagonists

Chordin and Noggin are BMP antagonists expressed in the Spemann organizer during gastrula stages and in the notochord and prechordal plate at later stages (Sasai *et al.*, 1994; Smith and Harland, 1992). They function by binding, directly, to the BMPs, in the extracellular space, and blocking their binding to BMP receptors (BMPR; Piccolo *et al.*, 1996; Zimmerman *et al.*, 1996). In the frog, when Chordin expression is knocked-down using antisense morpholino oligonucleotides, the embryos develop with a phenotype similar to the one observed in the zebrafish mutant *chordino*, showing a reduction in the size of the neural plate and CNS tissue as well as expansion of the ventral mesoderm (Oelgeschlager *et al.*, 2003; Schulte-Merker *et al.*, 1997). In the mouse, most *chordin*$^{-/-}$ mutants exhibit a normal CNS and the *noggin*$^{-/-}$ mutants do not show any phenotype during gastrulation or neural plate formation. However, when both genes are knocked out simultaneously, the embryos lack anterior notochord and the prosencephalic vesicle and exhibit L/R asymmetry defects later on. This indicates that *chordin* and *noggin* have redundant functions and are required for the formation of all embryonic axes in the mouse (Bachiller *et al.*, 2000; McMahon *et al.*, 1998).

Follistatin is another BMP antagonist expressed in the organizer during gastrulation (Hemmati-Brivanlou *et al.*, 1994; Iemura *et al.*, 1998). Follistatin also binds directly to the BMP ligands but, unlike Chordin and Noggin, the Follistatin/BMP complex is still able to bind to the BMPR but is unable to signal (Iemura *et al.*, 1998).

Xnr3 encodes for a Nodal-related protein that lacks mesoderm inducing activity and instead behaves as a BMP antagonist. In animal cap assays, overexpression of *Xnr-3* is able to induce neural differentiation (Hansen *et al.*, 1997). Recently, a work performed in *Xenopus tropicalis* showed that Xnr3 is able to antagonize BMP signaling through its aminoterminal proregion (Haramoto *et al.*, 2004).

I.8.3 Wnt antagonists

Among the Wnt inhibitors that can be found in Spemann's organizer are Dkk-1, Frzb-1/sFRP-3, sFRP-2 and Crescent. Frzb-1, sFRP-2 and Crescent belong to the same family of secreted proteins designated secreted Frizzled-related proteins (sFRPs). They contain a domain similar to the Wnt binding domain present in the Frizzled (Fz) Wnt receptors and function in the extracellular space by binding to Wnts and antagonizing

their activity (Kawano and Kypta, 2003; Leyns *et al.,* 1997). *Frzb-1* is specifically expressed in the dorsal mesendoderm. In *Xenopus* embryos, microinjection of *Frzb-1* mRNA is able to rescue the effects of ectopic *Xwnt8* expression (Leyns *et al.,* 1997; Wang *et al.,* 1997). In addition, overexpression of *Frzb-1* in the dorsal side causes an expansion of the organizer, resulting in a moderately dorsalized embryo (Leyns *et al.,* 1997). It was shown that the endogenous function of Frzb-1 is to antagonize the ventralizing activity of the ventrally expressed Xwnt8 (Leyns *et al.,* 1997).

In contrast to *Frzb-1*, *sFRP-2* is expressed in the prospective neural plate in addition to its organizer domain (Pera and De Robertis, 2000). *Crescent*, on the other hand, is initially expressed in the anterior dorsal endoderm and then in the dorsal lip. Afterwards it can also be detected in the prechordal plate and pharyngeal endoderm (Pera and De Robertis, 2000). sFRP-2 and Crescent are thought to function as non-canonical Wnt inhibitors and regulate convergent extension movements during gastrulation (Pera and De Robertis, 2000). In addition, in ventral mesodermal explants, *crescent* mRNA is able to induce cardiac tissue differentiation (Schneider and Mercola, 2001). In a very recent study, mouse sFRP2 was also shown to function as a BMP inhibitor (Reversade and De Robertis, 2005).

Dkk-1 (Dickkopf-1) belongs to a different class of Wnt inhibitors. *Dkk-1* is expressed in the anterior endoderm and in the prechordal plate and has been shown to be a very potent head-inducing activity (Glinka *et al.,* 1998). Dkk-1 functions by binding a Wnt coreceptor LRP-5/6 (LDL receptor-related protein-5/6; Mao *et al.,* 2001) and another transmembrane protein, Kremen forming a ternary complex on the cell surface (Mao *et al.,* 2002). This complex is then removed from the cell surface by endocytosis. Thereby, Dkk-1 inhibits Wnt signaling by removing the co-receptor from the cell surface. Embryos microinjected with *Xdkk-1* mRNA develop with enlarged heads and shortened trunks (Glinka *et al.,* 1998). In addition, in *Xenopus* embryos microinjection of *Xdkk-1* neutralizing antibodies inhibits head and prechordal plate formation (Glinka *et al.,* 1998; Kazanskaya *et al.,* 2000). In mouse, *dkk-1* mutants lack CNS structures more rostral to the midbrain and *dkk-1* and *noggin* compound mutants display severe head defects (del Barco Barrantes *et al.,* 2003; Mukhopadhyay *et al.,* 2001).

Similarly to what happens with BMP signaling, the interaction between Wnts and their antagonists also generates a Wnt signaling gradient that is necessary for the proper patterning of the AP axis.

22

I.8.5 Cerberus

Cerberus was the first secreted head-inducing factor isolated in *Xenopus* and is the founding member of a still growing family of cell-cell signaling regulators, designated as the Cerberus/Dan family (Bouwmeester *et al.,* 1996). *Cerberus* encodes for a 260 aminoacid protein containing a signal peptide at the N-terminal and a Cystein-Rich Domain (CRD) containing 9 cysteines at the C-terminal region, which is expressed in the anterior most region of the non-involuting endoderm (Piccolo *et al.,* 1999). When microinjected into the ventral side of *Xenopus* embryos, it leads to the formation of ectopic head-like structures which include fore- and midbrain, optic vesicles, cement gland and olfactory placodes, without the induction of more posterior structures (Bouwmeester *et al.,* 1996). Biochemical analysis has shown that Cerberus is a multivalent antagonist that binds to Xnrs, Xwnt-8 and BMP-4 in the extracellular space (Piccolo *et al.,* 1999). These three signaling pathways are necessary for trunk development and their inhibition is necessary for head formation. Thus, the secretion of Cerberus to the extracellular space in the anterior endoderm serves to generate and maintain a trunk-free region in the anterior region of the embryo so that the head can be formed (Piccolo *et al.,* 1999).

Since the isolation of *Xenopus* Cerberus (XCer) other Cerberus-related molecules have been identified in other vertebrate species (Table I): mouse Cerberus-like (mCer-1; Belo *et al.,* 1997; Biben *et al.,* 1998; Shawlot *et al.,* 1998), chicken Cerberus (cCer; Rodriguez Esteban *et al.,* 1999; Yokouchi *et al.,* 1999; Zhu *et al.,* 1999), *Xenopus* Coco (Bell *et al.,* 2003), zebrafish Charon (Hashimoto *et al.,* 2004) and mouse Cerberus-like-2 (mCer-2; Marques *et al.,* 2004). *Xenopus* cer, chicken *cer* and mouse *cer-1* are syntenic genes (www.metazome.net) and, at peri-gastrulation stages, are expressed in topologically equivalent embryonic structures, such as the anterior endoderm, hypoblast and anterior visceral endoderm, respectively (Belo *et al.,* 1997; Bouwmeester *et al.,* 1996; Foley *et al.,* 2000). By early neurulation stages, *mcer-1* and *ccer* transcripts are also detected in the anterior definitive mesendoderm (Belo *et al.,* 1997; Rodriguez Esteban *et al.,* 1999). But at later stages, namely during somitogenesis, Cerberus-related genes display very distinct expression patterns: *Xcer* expression is no longer observed; *mcer-1* transcripts are found in the rostral half of the two most recently formed somites (somites I and II) and rostral presomitic mesoderm; *ccer* is expressed in the left paraxial and lateral plate mesoderm; zebrafish *charon* and *mcer-2* are both expressed around the node region, but with a

23

remarkable difference between their expression patterns: *charon* is expressed symmetrically in the node, while *mcer-2* is strongly expressed on the right side (Belo *et al.,* 1997; Bouwmeester *et al.,* 1996; Hashimoto *et al.,* 2004; Marques *et al.,* 2004; Rodriguez Esteban *et al.,* 1999).

Table 1 – Summary of the expression pattern of *cerberus* family members.

Gene	Peri-Gastrulation	Post-Gastrulation	References
Xcer			Bouwmeester et. al, 1996 Piccolo et. al, 1999 Silva et. al, 2003 Kuroda et. al, 2004
mcer-1			Belo et. al, 1997 Belo et. al, 2000 Perea-Gomez et. al, 2002 Yamamoto et. al, 2004
ccer			Rodriguez-Esteban et. al, 1999 Bertocchini and Stern, 2002 Tavares et. al, 2007
Xcoco			Bell et. al, 2003 Vonica and Brivanlou, 2007
zcharon			Hashimoto et. al, 2004
mcer-2			Marques et. al, 2004

An artificial construct consisting of the carboxy-terminal cysteine knot domain of Cerberus was shown to bind only to Nodal. This construct was designated Cerberus-short (Cer-s) and when injected in embryos is able to inhibit Nodal signaling but not Activin, Vg1 or Derrière signals (Agius *et al.,* 2000; Piccolo *et al.,* 1999). In animal cap explants, microinjection of *Xcer* mRNA induces anterior CNS markers such as *Xotx2* but not more posterior ones like *Engrailed-2* (*En2*). Endodermal (*endodermin*) and cardiac markers

(*Nkx-2.5*) were also upregulated in these animal cap experiments (Agius *et al.,* 2000; Piccolo *et al.,* 1999). In addition, it was demonstrated that *mcer-1* was able to induce the same markers as *Xcer* (Belo *et al.,* 1997; Biben *et al.,* 1998), however *mcer-1* is not able to induce ectopic head-like structures when microinjection in the ventral blastomeres (Belo *et al.,* 1997). Unlike XCer, mCer-1 was shown to bind and inhibit both BMP and Nodal signals, but was not able to bind to Wnt proteins (Belo *et al.,* 2000). In the mouse, knockout mutant mice for *mcer-1* lack gastrulation phenotypes (Belo *et al.,* 1997; Biben *et al.,* 1998; Shawlot *et al.,* 1998). However, when *mcer-1⁻/⁻*; *lefty-1⁻/⁻* double mutants are generated, development of the anterior region of the embryo was impaired (Perea-Gomez *et al.,* 2002; Yamamoto *et al.,* 2004). In chicken, cCer was shown to be necessary for head formation, by preventing the formation of the trunk mesoderm in the prospective head neuroectoderm through its anti-Nodal activity (Bertocchini and Stern, 2002). On the other hand, XCoco, zCharon and mCer–2 were shown to be essential later in development, more precisely in the establishment of the L/R asymmetry (Vonica *et al.,* 2007; Hashimoto *et al.,* 2004; Marques *et al.,* 2004).

I.9 Ventral signaling center

In recent years, increasing evidence has been emerging supporting the existence of a ventral signaling center, during gastrula stages (for review see De Robertis and Kuroda, 2004; (Fig. 8)). Several genes encoding secreted or cell surface proteins are expressed in the region opposite the Spemann organizer. Their expression pattern places these genes in the BMP-4 synexpression group. Among the molecules expressed in this ventral signaling center are BMP-2, -4 and -7, CV-2 (Crossveinless-2), Sizzled, Tsg (Twisted Gastrulation), Xlr (Xolloid-Related) and Bambi (BMP and Activin membrane-bound inhibitor).

CV-2 protein contains five CR domains similar to the BMP-binding modules present in Chordin (Coffinier *et al.,* 2002; Conley *et al.,* 2000). *CV-2* is expressed in the ventral mesoderm and ectoderm in both *Xenopus* and mouse and, when overexpressed, *CV-2* acts like a BMP antagonist (Binnerts *et al.,* 2004; Coffinier *et al.,* 2002; Moser *et al.,* 2003). However, *CV-2* is upregulated by BMP-4 in the embryo.

Ventral center		Spemann organizer
BMP-4 Bambi CV-2 Sizzled Xlr Tsg	ectoderm CNS mesoderm endoderm	Antivin/Lefty Cerberus Chordin Crescent Dkk-1 Follistatin Frzb-1Noggin sFRP2 Shh Xnrs
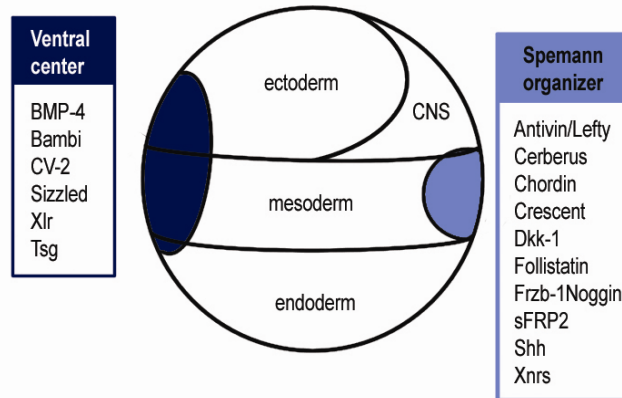
Figure 8 – Dorsal (Spemann organizer) and ventral signaling centers secreted proteins. (Adapted from De Robertis and Kuroda, 2004).

Sizzled encodes for a SFRP-like protein that functions as a BMP inhibitor (Collavin and Kirschner, 2003; Salic *et al.,* 1997; Yabe *et al.,* 2003). Sizzled binds to the metalloproteinases responsible for the degradation of Chordin (Lee *et al.,* 2006). Loss of function experiments using morpholino oligos against *sizzled* showed that microinjection of *sizzled* morpholinos causes ventralization of the embryo (Collavin and Kirschner, 2003).

Xlr is a Tolloid-like zinc metalloprotease that is expressed in the ventral marginal zone of gastrula *Xenopus* embryos. Xlr expression was shown to be regulated by BMP signaling. When microinjected in *Xenopus* embryos, *Xlr* mRNA generates a weak ventralized phenotype with reduced heads, enlarged tails and ventral mesoderm and in some cases with no notochord, similar to the phenotypes observed when low dosages of *BMP-4* mRNA is injected (Dale *et al.,* 1992; Goodman *et al.,* 1998). Biochemical studies have shown that Xlr increases the activity of BMP-4 by proteolytic degradating Chordin, *in vitro* (Piccolo *et al.,* 1997; Wardle *et al.,* 1999).

Tsg binds both to BMP and Chordin, forming a ternary complex. It is thought that Tsg functions both as a BMP agonist and antagonist. The effects of Tsg overexpression are highly dependent on the amount of Xolloid present. When high levels of Xolloid are present, Tsg enhances BMP signaling by promoting the proteolytic cleavage of Chordin by Xolloid. On the other hand, when Xolloid levels are low, Tsg inhibits BMP signaling (reviewed in De Robertis *et al.,* 2000).

Bambi is a transmembrane protein similar to the BMP receptor type I that lacks the catalytic intracellular kinase domain and in that way functions as a cell surface inhibitor of BMP signaling (Onichtchouk *et al.,* 1999). Bambi stably associates with the TGF-β

receptors and inhibits TGF-β signaling. Evidence show that the inhibitory effects of BAMBI are mediated by its intracellular domain (Onichtchouk *et al.,* 1999).

In summary, BMPs are expressed throughout the embryo during gastrula stages and BMP antagonists are expressed in the Spemann organizer. The ventral marginal zone is the region of highest levels of BMP signaling while the dorsal marginal zone marks the region of lowest BMP signaling. This gradient of BMPs along the DV axis is necessary for the patterning of all layers. For example, in *Xenopus* mesoderm while no BMP is necessary for notochord, low dosage of BMP signaling is required for muscle and even higher BMP signaling is necessary for lateral plate and blood formation.

I.10 Gastrulation movements

Gastrulation is a highly dynamic process by which the three germ layers that are initially located on, or close to, the surface of the embryo are rearranged in order to achieve their final positions in the embryo: the mesoderm placed between the external layer, the ectoderm, and the internal layer, the endoderm. This rearrangement of the germ layers is achieved by different types of cell movements, which differs among different organisms. In *Xenopus* embryos, gastrulation movements include involution, epiboly and convergence extension and are accompanied by changes in cell adhesion and cell shape (reviewed in Keller *et al.,* 2003). During late blastula stages, as a response to the TGF-β signaling, cells from the dorsal marginal zone change their shape, by apical constriction, acquire a "bottle" shape and start to move inwards (Kurth, 2005; Fig. 9A,B). As a result of this invagination, the bottle cells start to form dorsally a slit-like structure, the blastopore, the first external sign of gastrulation. At the same time, cells from the vegetal mass undergo an active movement, the vegetal rotation, pushing the mesendodermal cells towards the animal pole and causing the blastocoel floor area to increase (reviewed in Heasman, 2006; Fig. 9A,B and Fig. 10). This movement generated by the vegetal mass causes the involution of the involuting marginal zone (IMZ). Studies have shown that the main driving force responsible for the involution of the IMZ is the vegetal rotation and not the invagination of the bottle cells. Bottle cells are thought to be necessary for the initiation of involution, but if removed after their formation, gastrulation proceeds normally (Keller, 2005). Involution begins in the dorsal side and as the gastrulation process proceeds, it expands laterally and ventrally. Once involuted, the IMZ turns inward, back on itself and subsequently moves across the blastcoel roof (Fig. 9B-D). This

migration of the IMZ depends on an integrin-mediated cell interaction with the fibronectin-containing extracellular matrix of the blastocoel roof (Keller *et al.*, 2003; Fig. 9E). Meanwhile, as involution is occurring, the ectodermal precursors expand and spread vegetally (small arrows in Fig. 9A,B). This movement involves cell division coupled with intercalation of several layers of cells into one (radial intercalation).
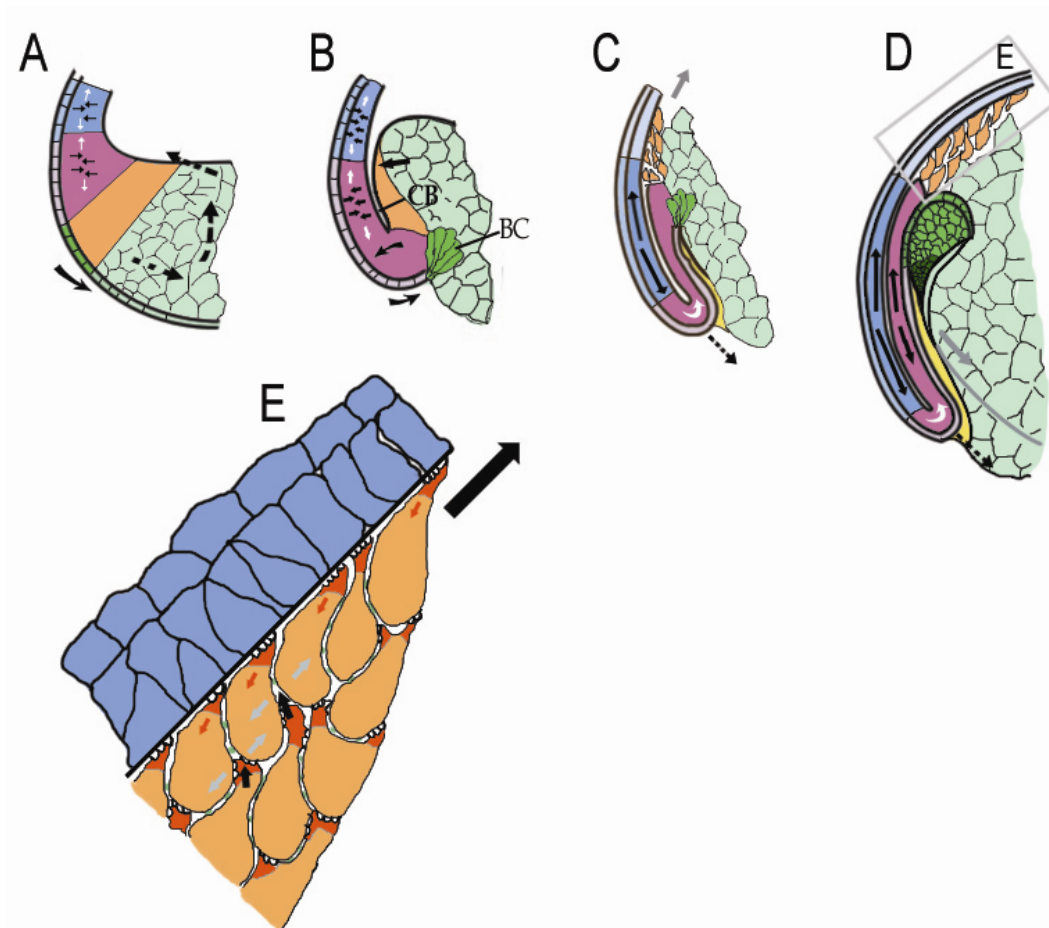
Figure 9 – Gastrulation movements in Xenopus embryos. (A-D,E is an enlargement of box in D)The movements of the tissues and cells are indicated by arrows. Axial mesoderm (magenta), bottle cells (BC, green), cleft of Brachet (CB), fibronectin-containing matrix layer (black line in E), IMZ (orange and magenta), IMZ deep layer (magenta), mesoderm (orange), posterior neural tissue (blue), vegetal endodermal cells (light green). (Adapted from Keller and Shook, 2004)

As gastrulation proceeds, the prospective axial and paraxial mesoderm and the overlying posterior neural plate narrow along the mediolateral axis (convergence) and lengthen along the AP axis (extension) (black arrows in Fig. 9C,D; Fig. 11). During convergent extension (CE), dorsal mesodermal cells become polarized mediolaterally and make stable contacts with neighboring cells, generating tension in the mediolateral axis. These convergent extension movements predominate in the embryo from midgastrula

and last through neurulation. They are responsible for simultaneously narrowing and elongating the body axis and contribute to involution and blastopore closure.
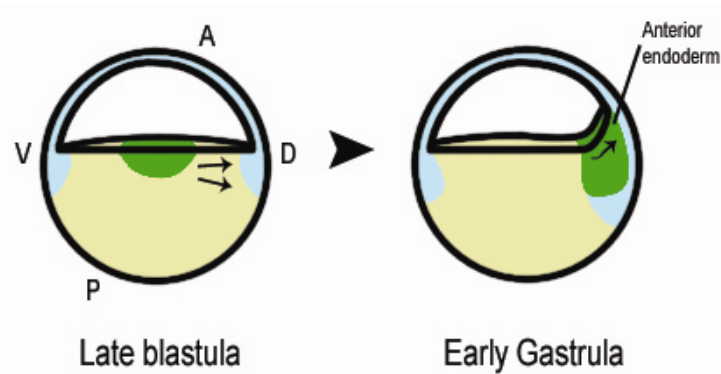
Figure 10 – Vegetal rotation. In the late blastula stage *Xenopus* embryo, vegetal rotation pushes the mesendodermal cells towards the animal pole. (Adapted from Foley and Niehrs, 2000)

Different signaling pathways have been shown to be involved in CE movements during gastrulation. Among them are the non-canonical Wnt, the FGF, the Nodal and BMP signaling pathways. Throughout several recent studies it has been established that the non-canonical Wnt signaling pathway is a crucial mediator of CE movements. In vertebrates, the non-canonical Wnt signaling pathway involves the Wnt5a class of ligands (which include Wnt5a, Wnt4, Wnt 11) that bind to the transmembrane protein receptors Frizzled (Fz), signal through Dishevelled (Dsh), activate the small GTPases of the Rho family, Rho kinase and JNK, and have been shown to be involved in regulating cell polarity, cell adhesion and cell migration (for review see Pandur *et al.*, 2002). In *Xenopus* embryos, overexpression of either *Wnt5a* or *Wnt11* disrupts morphogenetic movements (Du *et al.*, 1995; Moon *et al.*, 1993). On the other hand, the canonical Wnt pathway has also been implicated in CE movements. Downregulation of the canonical Wnt downstream target Xnr3 causes both head and CE defects (Yokota *et al.*, 2003).

Figure 11 - Covergent extension movements.

I.11 Neural tube closure

Neurulation is the process by which the embryo forms a neural tube, which will later differentiate into the brain and spinal cord. The ectodermal cells fated to become

neural tissue undergo a cell shape change by becoming elongated while the cells fated to become epidermis become more flattened. This change in cell shape causes the prospective neural region to rise and form the neural plate. Later, the neural plate thickens and rises forming the neural folds, which then move towards the midline of the embryo and fuse. Beneath the epidermis the neural tube is formed and the dorsalmost portion of the neural tube will give rise to the neural crest.

The separation of the neural plate from the other ectodermal cells is a result of a process called neural induction. The dorsal mesodermal cells signal to the ectodermal cells above inducing them to develop into neural tissue. As mentioned above, at the molecular level, high BMP activity defines epidermis while absence of BMP signaling specifies the neural plate (for review see Stern, 2005). The BMPs that are expressed widely in the embryo during blastula/early gastrula stages act within the ectoderm in order to induce epidermis. However, the dorsal part of the animal ectoderm is subjected to a cocktail of secreted molecules such as FGFs and BMP inhibitors, from the BCNE center and the organizer in order to induce neural tissue. Low FGF signaling cooperates with the BMP inhibitors to inhibit Smad1 phosphorylation through the activation of MAPK signaling, repressing BMP transcription and inducing the expression of Chordin and Noggin (Stern, 2005, 2006).

During neural tube closure, while the cells of the epidermis migrate towards the midline, the neural plate undergoes convergent extension. Neurulation occurs as cells in the superficial neuroectoderm undergo apical constriction which leads to the formation of the neural groove. Continuous change in cell shape in the neural plate, notochord and somites causes the neural folds to rise and come together. When apical constriction does not occur as in the case of Shroom depletion, the neural tube does not close. On the other hand, when convergent extension fails neural tube closure is also impaired. Certain signaling pathways such as Hedgehog and non-canonical Wnt/Planar cell polarity (PCP) pathway have been shown to be involved in neural tube closure. Several studies have shown that, in vertebrate embryos, disruption of the PCP signaling pathway leads to severe caudal neural tube closure defects. Time-lapse studies in *Xenopus* embryos has revealed that PCP-dependent convergent extension was necessary to narrow the distance between the elevating neural folds, allowing them to come into contact and fuse (Wallingford and Harland, 2002).

Examination of mutant mice exhibiting anterior neural tube defects has revealed that the phenotypes observed resulted from defects during ciliogenesis which suggested that cilia might be necessary for anterior neural tube closure. At the molecular level, the open neural tube defects of these mutant mice resulted from a failure in the Hedgehog signaling pathway. Recent studies have also implicated the PCP pathway in cilliogenesis (Wallingford, 2006).

I.12 Somitogeneses

During neurulation, while the neural tube is being formed and patterned, other events are occurring in its proximity, such as somitogenesis. Somitogenesis is the process by which somites are formed. Somites are blocks of mesodermal cells located on both sides of the neural tube (Pourquie, 2001). These transient structures will give rise to bone, cartilage, tendons and dermis of the back of the animal and all the skeletal muscles of the body except those of the head (Brent and Tabin, 2002). In *Xenopus*, during gastrulation the dorsal mesodermal cells are already involved in muscle specification. The paraxial mesoderm arises from the deep layers of two symmetrical regions of the marginal zone located on either side of the Spemann organizer. As gastrulation proceeds the paraxial mesoderm extends towards the ventral side of the embryo, giving rise to the lateral and ventral muscles (Keller, 2000).

Several signaling pathways have been implicated in muscle specification. In the frog, *in vitro* treatment of animal cap cells with FGF can induce these cells to adopt a paraxial mesoderm fate (Fisher *et al.,* 2002). Overexpressing a dominant-negative FGF receptor impairs trunk and tail formation (Amaya *et al.,* 1991; Griffin *et al.,* 1995). Mutant mice for *fgf8* and *fgfr1* do not form paraxial mesoderm and axial mesoderm is enlarged, suggesting that paraxial mesoderm cells are converted to an axial fate (Deng *et al.,* 1994; Sun *et al.,* 1999; Yamaguchi *et al.,* 1994). These results indicate that FGF signaling is critical for paraxial mesoderm formation. FGF signaling has been shown to be necessary for the maintenance of *Xbra*'s expression and *vice versa* (Heasman, 2006). By mid-gastrula stages, myogenic markers like *Mespo*, *Myf5* or *MyoD* are expressed in an equatorial ring resembling *Xbra* and *fgf*'s expression. Depletion of FGF4, FGFR1 or Xbra results in the reduction of these myogenic markers (Conlon *et al.,* 1996; Fisher *et al.,* 2002; Yokota *et al.,* 2003). The canonical Wnt signaling pathway has also been implicated in the formation of the paraxial mesoderm. Microinjection of *Xwnt8* RNA in frog embryo causes an

enlargement of the paraxial mesoderm territory (Christian and Moon, 1993), while microinjection of a dominant-negative version of *Xwnt8* (Hoppler *et al.*, 1996) impairs proper paraxial mesoderm formation. In mice, mutation of *Wnt3a* results in the neutralization of cells normally fated to give rise to paraxial mesoderm (Yamaguchi *et al.*, 1999). In addition, studies have shown that triple depletion of *noggin*, *chordin* and *follistatin* eliminate muscle precursor gene expression suggesting that repressing BMP signaling seems also to be required for muscle specification during gastrula stages (Khokha *et al.*, 2005). In this way, specification of the paraxial mesoderm is achieved from the combined action of FGF, Wnt and BMP/TGF-β signaling.

The establishment of the paraxial mesoderm is dependent on the morphogenetic movements occurring during gastrulation. During gastrulation, the prospective paraxial mesoderm converges toward the blastopore, involutes and subsequently elongates along the AP axis to form the presomitic mesoderm (PSM). The PSM will then begin to segment into somites at its rostral extremity (Pourquie, 2001). Segments continue to form in a sequential fashion from anterior to posterior. In *Xenopus* embryos, somite formation involves a 90º rotation movement of the paraxial mesoderm cells (Hamilton, 1969; Fig. 12).
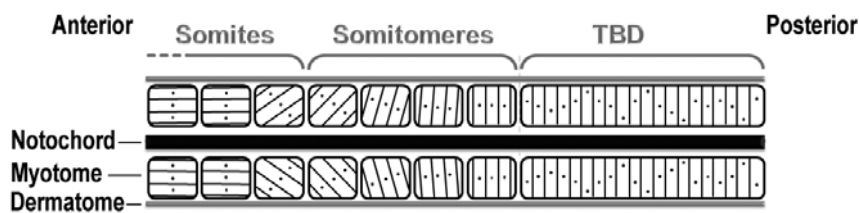
Figure 12 – Somitogenesis in *Xenopus laevis* embryos. In *Xenopus* the posterior part of the presomitic mesoderm is designated as Tailbud domain (TBD).The anterior region of the presomitic mesoderm is pre-patterned into somitomeres. A somite, consisting entirely of myotomal cells, is formed when a group of cells segregates, rotates 90º, and orients parallel to the notochord. (Adapted from Jen *et al.*, 1997)

The presomitic mesoderm can be subdivided into two regions, a caudal domain where somitic boundaries are not yet determined, and a rostral domain where these boundaries are being patterned. In the caudal domain, also known in *Xenopus* as the tail bud domain (TBD), genes like *fgf8*, *Xbra* and *Xwnt3* are expressed in a gradient fashion from posterior to anterior (Pourquie, 2003) and the limit between the two domains in the PSM, named the determination front, marks the place were segmentation will take place.

The molecular mechanism responsible for the position of the determination front was shown to involve both FGF and Wnt signaling pathways. Overexpression of FGF in the PSM causes an anterior expansion of the genes normally restricted to the

unsegmented portion of the PSM, which indicates that FGF signaling is necessary for maintaining the immature state of the caudal PSM. Increasing the local concentration of Fgf8 protein, in the PSM, results in the formation of smaller somites. On the other hand, inhibiting FGF signaling leads to the formation of bigger somites (Dubrulle *et al.,* 2001). Similar to what is observed for FGF8, increasing the amount of Wnt3a locally leads to the formation of smaller somites and shifts the segment boundary anteriorly, while downregulation of Wnt signaling by overexpressing *Axin2*, an inhibitor of the Wnt signaling cascade leads to the formation of larger somites (Aulehla *et al.,* 2003). Furthermore, the expression of *fgf8* in the PSM appears to be dependent on Wnt3a since its expression is strongly downregulated in the tail buds of embryos containing a hypomorphic mutation of Wnt3a (*vestigial tail*, *vt*; Aulehla *et al.,* 2003).

While the position in the PSM where segmentation will take place depends on the determination front, the rate at which somites are formed is dependent on the segmentation clock. Several genes exhibiting a cyclic expression pattern in the PSM have been identified in chicken, fish, frog and mouse embryos suggesting that the segmentation clock is conserved among vertebrates (reviewed in Pourquie, 2003). The cyclic expression of these genes in the PSM oscillates largely in synchrony and is regulated at the transcriptional level (Cole *et al.,* 2002; Morales *et al.,* 2002). Most of these genes were shown to be downstream of Notch signaling. However, Wnt signaling is also involved and appears to act upstream of the Notch-regulated cyclic genes (Aulehla *et al.,* 2003). Axin2, a Wnt inhibitor, is expressed in a graded manner along the PSM, peaking in the TBD. In *vestigial tail* mutant mice, Axin2 is strongly downregulated, which suggests that *Axin2* expression is controlled by Wnt3 (Aulehla and Herrmann, 2004). The oscillatory expression of *Axin2* and downstream targets of Notch are out of phase, i.e. when expression of *Axin2* is on, Notch targets are off and *vice versa*. In mutant mice were Notch signaling is impaired, like $Dll1^{-/-}$ embryos, Axin2 transcription is not affected. However, when Wnt signaling in the PSM is strongly downregulated or abolished, the oscillations of lunatic fringe (a modulator of the Notch signaling pathway) is abolished (Aulehla *et al.,* 2003). This data suggest that the oscillation of the genes downstream of Notch is dependent on Wnt3a. In summary, the Wnt signaling pathway plays a central role in somitogenesis by regulating both the segmentation clock and the morphogenetic gradient (Aulehla and Herrmann, 2004).

I.13 Aim of this Thesis

The identification of molecules expressed in the anterior endoderm of the gastrula *Xenopus* embryo having potent head-inducing abilities, such as Cerberus and Dkk-1, has suggested that this region, and the equivalent structures in other vertebrates, might function as a head organizing center (Bouwmeester *et al.,* 1996; Glinka *et al.,* 1998). Since then several studies have supported this hypothesis (de Souza and Niehrs, 2000). However, other studies have failed to show a role for these genes in head induction but rather play a role in heart formation (de Souza and Niehrs, 2000). Thus, the general aim of the present work was to further contribute to the understanding of the role of the anterior endoderm during embryonic development.

As a first approach we decided to focus on the role of *Xenopus cerberus* (Chapter II.1). So far only overexpression studies had been performed with *Xcer*, which showed that its head-inducing ability was achieved by binding and blocking the signaling activities of Xnr-1, XBMP-4 and Xwnt-8 (Piccolo *et al.,* 1999). We aimed therefore, to determine the endogenous role of *Xcer* and whether or not it was involved in head formation. For that, we used antisense oligonucleotides against *Xcer* and took advantage of constructs that allow specific activation of Xnr-1, BMP-4 and Wnt-8 under the control of mouse *cerberus-like* promoter region, thus restricting their expression to anterior endoderm.

Next, a preliminary characterization of a mouse *cerberus-like* 4kb fragment upstream of the ATG was performed (Chapter II.2). In a previous work, this mouse *cerberus-like* promoter fragment was shown to be specifically and exclusively activated in the AVE of mouse embryos. The observation that this promoter fragment was able to mimic the expression of endogenous *Xcer*, when microinjected into *Xenopus* embryos, enabled us to take advantage of this system in this study. The aim was to search for the *cis*-regulatory regions responsible for the expression of *mcer-1* in the AVE/Anterior endoderm and compare it with the factors that were shown to regulate *Xcer* expression.

The results presented in the following chapters (Chapters II.3 – II.5) had as a starting point a differential screening performed in the lab to search for novel AVE specific genes. Three of the novel mouse genes expressed in the mouse AVE (*mADTK1, mShisa, mAd4*) served as "templates" to search for their *Xenopus* orthologs. These novel *Xenopus* genes (*XADTK1, XADTK2, XShisa-1, XShisa-2, XAd4)* were isolated and their expression patterns analyzed. With that, we aimed to determine whether these novel

genes would also be expressed in the topological equivalent of the mouse AVE, namely the *Xenopus* anterior endoderm. *XADTK1* and *XShisa-2* were chosen for further studies (Chapters II.4 and II.5) and by using a loss of function approach we aimed to uncover the function of these novel genes during *Xenopus* development.

Chapter II

Results

II.1 Endogenous Cerberus activity is required for anterior head specification in *Xenopus*

Endogenous Cerberus activity is required for anterior head specification in *Xenopus*.

Ana Cristina Silva[1,5], Mário Filipe[1,5], Klaus-Michael Kuerner[2,4], Herbert Steinbeisser[2,4,6] and José António Belo[1,3,6]

[1]Instituto Gulbenkian de Ciência, Rua da Quinta Grande, 6, Apartado 14, 2781-901 Oeiras, Portugal; [2]Max-Planck-Institut fur Entwicklungsbiologie, AbtV, Spemannstr. 35, 72076 Tuebingen, Germany; [3]Faculdade de Engenharia de Recursos Naturais, Universidade do Algarve, Campus de Gambelas, 8000-010 Faro, Portugal; [4]Present address: Institute for Human Genetics, University of Heidelberg, Im Neuenheimer Feld 328, 69120 Heidelberg, Germany; [5]These authors contributed equally to this work; [6]Authors for correspondence: José A. Belo e-mail: jbelo@igc.gulbenkian.pt, Herbert Steinbeisser e-mail: herbert.steinbeisser@med.uni-heidelberg.de

Endogenous Cerberus activity is required for anterior head specification in *Xenopus*.

Ana Cristina Silva[1,5], Mário Filipe[1,5], Klaus-Michael Kuerner[2,4], Herbert Steinbeisser[2,4,6] and José António Belo[1,3,6]

[1]Instituto Gulbenkian de Ciência, Rua da Quinta Grande, 6, Apartado 14, 2781-901 Oeiras, Portugal; [2]Max-Planck-Institut fur Entwicklungsbiologie, AbtV, Spemannstr. 35, 72076 Tuebingen, Germany; [3]Faculdade de Engenharia de Recursos Naturais, Universidade do Algarve, Campus de Gambelas, 8000-010 Faro, Portugal; [4]Present address: Institute for Human Genetics, University of Heidelberg, Im Neuenheimer Feld 328, 69120 Heidelberg, Germany; [5]These authors contributed equally to this work; [6]Authors for correspondence: José A. Belo e-mail: jbelo@igc.gulbenkian.pt, Herbert Steinbeisser e-mail: herbert.steinbeisser@med.uni-heidelberg.de

Keywords: Cerberus; head induction; morpholino; targeted activation

Summary

We analyzed the endogenous requirement for Cerberus in *Xenopus* head development. "Knock-down" of Cerberus function by antisense morpholino oligonucleotides did not impair head formation in the embryo. In contrast, targeted increase of BMP, Nodal and Wnt signaling in the Anterior-Dorsal-Endoderm (ADE) resulted in synergistic loss of anterior head structures, without affecting more posterior axial ones. Remarkably, those head phenotypes were aggravated by simultaneous depletion of Cerberus. These experiments demonstrated for the first time that endogenous Cerberus protein can inhibit BMP, Nodal and Wnt factors *in vivo*. Conjugates of Dorsal Ectoderm (DE) and ADE explants in which Cerberus function was "knocked-down" revealed the requirement of Cerberus in the ADE for the proper induction of anterior neural markers and repression of more posterior ones. This data supports the view that Cerberus function is required in the leading edge of the ADE for correct induction and patterning of the neuroectoderm.

Introduction

In amphibians, the formation of the Anterior-Posterior (AP) axis is dependent on Spemann's organizer activity (Spemann and Mangold, 1924). Classical transplantation

43

experiments demonstrated that the inductive properties of the organizer change in the course of development. The early organizer can induce a complete secondary body axis including head, whereas the late organizer can only induce trunk-tail structures (Spemann, 1931). This led to the concept of two organizing centers: the head and the trunk-tail organizers. Recently, molecules which are expressed in the Spemann's organizer have been identified in *Xenopus* (reviewed in De Robertis *et al.,* 1997). When ectopically expressed in the ventral side of *Xenopus* embryos, some of these factors, like *goosecoid*, *noggin* or *chordin*, can induce secondary body axis (Cho *et al.,* 1991; Smith and Harland, 1992; Sasai *et al.,* 1994). In contrast to these axis inducing factors, secreted proteins such as Cerberus and Dickkopf-1 are only able to induce head-like structures (Bouwmeester *et al.,* 1996; Glinka *et al.,* 1997). In *Xenopus*, *cerberus* is expressed in the non-involuting Anterior Dorsal Endoderm (ADE), but not in the involuting mesoderm. The presence of the strong head inducing factor Cerberus in the ADE raised the possibility that this region could be the head organizing center in *Xenopus* (Bouwmeester *et al.,* 1996; Bouwmeester and Leyns, 1997).

Biochemical analysis in *Xenopus* showed that Cerberus can bind to Xnr-1, BMP-4 and Xwnt-8 and thereby blocks their function (Piccolo *et al.,* 1999). These inhibitory properties of Cerberus are considered essential for the head inducing activity of this secreted factor.

In the mouse, a gene homologous to *cerberus* was isolated (Belo *et al.,* 1997; Biben *et al.,* 1998; Shawlot *et al.,* 1998). The expression of mouse *cerberus-like (cer-1)* and other markers such as *Hesx1*, *lim-1* and *Otx2* in the Anterior Visceral Endoderm (AVE), led to the hypothesis that this region is the topological mouse equivalent of the ADE in *Xenopus* (Acampora *et al.,* 1995; Thomas and Beddington, 1996; Belo *et al.,* 1997; Bouwmeester and Leyns, 1997). Therefore the AVE was proposed to be the head organizer in the mouse. This view is supported by the finding that in chimeric mutant mouse embryos composed of AVE lacking either *Otx2*, *lim-1* or *HNF-3ß* and wild-type epiblast, the head is not properly induced (Rhinn *et al.,* 1998; Shawlot *et al.,* 1999; Dufort *et al.,* 1998). Surprisingly, in generated *cer-1* KO mouse lines no phenotypic head and axis defects were observed, arguing against a role of *cer-1* in early embryogenesis (Belo *et al.,* 2000; Shawlot *et al.,* 2000; Stanley *et al.,* 2000).

In *Xenopus*, the endogenous function of Cerberus in the ADE remains unclear due to the lack of loss-of-function data. In order to characterize the function of Cerberus in

head formation, a novel combination of strategies was employed. Endogenous Cerberus was "knocked-down" using an antisense morpholino oligonucleotide that specifically blocked the translation of the *cerberus* mRNA (CerMo). In addition, the relative levels of the signaling molecules BMP-4, Xnr-1 and Xwnt-8, which are antagonized by Cerberus, were raised in the ADE. This was achieved by driving their expression under the control of a mouse *cer-1* promoter fragment that is specifically activated in the ADE and closely resembles the spatio-temporal expression pattern of endogenous *cerberus*. Dorsal-vegetal injection of the CerMo does not cause visible head defects in the *Xenopus* embryo. In contrast, targeted increase of BMP, Nodal or Wnt activity in the ADE resulted specifically in the loss of head, but not trunk-tail structures. These factors synergistically inhibited head structures when simultaneously expressed in the ADE. Remarkably, these phenotypes caused by BMP, Nodal or Wnt were strongly enhanced when, in addition, Cerberus function in the ADE was blocked by the CerMo. The endogenous function of Cerberus in head formation, revealed in this sensitized system, could also be demonstrated in an explant recombination assay. ADE can induce forebrain markers when conjugated with Dorsal Ectoderm (DE) but not when Cerberus function was "knocked-down" by the morpholino oligo. Furthermore, we demonstrate that, concomitantly, the ADE represses the expression of more caudal neural markers through the activity of Cerberus.

Here we demonstrate that endogenous Cerberus can inhibit BMP, Nodal and Wnt *in vivo*, and that this activity is required in the ADE for proper head induction/patterning in *Xenopus*.

Materials and methods

Plasmid constructs and morpholino Oligonucleotide

An *Eco*RI genomic fragment containing the first exon of *cer-1* and 4 Kb of non coding upstream region was isolated from a mouse genomic library generated in Lambda Fix II (Stratagene) and subcloned in pBluescriptIIKS+ (Stratagene). The 4.0 Kb upstream region was subcloned in pBSIIKS+ and a *Nco* I site was introduced at the ATG translation start site by PCR-based mutagenesis, generating McerP. The plasmid McerP-LacZ was constructed by inserting a *Nco*I – *Bam*HI fragment, containing a ß-galactosidase CDS with a nuclear localization signal and the SV40 polyA signal, at the *cer-1* ATG site of McerP.

To obtain the misexpression constructs the CDS from *Xnr-1*, *XBMP-4* and *Xwnt-8* cDNAs were amplified by PCR with primers that introduced a *Nco* I site at the ATG translation start.

Primers used were the following:

Xnr1-F (5'-TTTACTAGTCCATGGCATTTCTGACAGCAGTCC-3') and *Xnr1*-R (5'-TTTGTCGACTTAACTGCACCCACATTCCTC-3'); *XBMP4*-F (5'-TTTACTAGTCCATGGGAATTCCTGGTAACCGAATGCTG-3') and *XBMP4*-R (5'-TTTGTCGACTCAACGGCACCCACACCCTTCC-3'); *Xwnt8*-F (5'-TTTACTAGTCCATGGGACAAAACACCACTTTGTTCATCC-3') and *Xwnt8*-R (5'-TTTGTCGACTCATCTCCGGTGGCCTCTG-3').

Each of these amplified CDSs was digested with *Nco* I and inserted at the ATG of McerP. A 263 bp *Xho*I-*Apa*I fragment containing the SV40 polyA signal from pCS2+ was inserted downstream of the each stop codon, generating McerP-Xnr1, McerP-BMP4 and McerP-Xwnt8. The plasmids CMV.Xnr1, CMV.BMP4 and CMV.Xwnt8 were constructed by cloning the respective CDS PCR fragments at the *Eco*RI (filled in)-*Xho*I sites of pCS2+.

The *cerberus* morpholino oligonucleotide, obtained from Gene Tools LLC, was designed to target the 5' UTR region between bases -35 and -11 upstream of the AUG (5'-CTAGACCCTGCAGTGTTTCTGAGCG-3'). To express the C-terminal HA tagged Cerberus protein in *Xenopus* embryos, a 1.4 kb *Eco*RI-*Xho*I fragment from pCDNA.*Xcer*HA (containing bases from –50 in the 5' UTR) was subcloned in pCS2+. The *Xcer*-HA rescue construct was generated by subcloning a 1.36 kb *Eco*RV-*Xho*I fragment from pCDNA.*Xcer*-HA, which only includes 11 bases upstream of the ATG, into the *Eco*RI site of pCS2+.

mRNA Synthesis and Microinjection

Capped sense mRNAs were synthesized using the Ambion mMessage mMachine kit. *Xenopus* eggs were obtained as described in Medina *et al.* (2000) and staged according to Nieuwkoop and Faber (1967). *In vitro* fertilization and microinjection of *X. laevis* embryos were performed as described previously (Bouwmeester *et al.,* 1996).

Conjugate assays

Dorsal ectoderm (DE) and anterior dorsal endoderm (ADE) were dissected from stage 10.5 embryos in 1xMBS-H. Conjugates were made by recombining the DE with the

ADE and were grown in 0.5xMBS-H until siblings reached late tailbud stage 30/31. The conjugates were assayed by RT-PCR for expression of the neural markers *eomes*, *Xemx1*, *XBF1*, *En2* and *Krox20*.

In situ hybridization and ß-galactosidase staining

Whole mount and hemi section in situ hybridization and anti-sense probe preparation was carried out as described in Belo *et al*. (1997). The plasmids containing *XBF1*, *Xotx2* and *Xshh* fragments were linearized using *Xba*I, *Eco*RI and *Kpn*I respectively, and transcribed using T3 RNA polymerase. Plasmids containing *lacZ*, *Xcer*, *Xhex*, *XKrox20* and *Xnot2* were cut with *Sal*I, *Eco*RI, *Not*I, *Eco*RI and *Eco*RI respectively, and transcribed using T7 RNA polymerase. Stained embryos (stage 21 and above) were bleached by illumination in 1% H_2O_2, 4% formamide and 0.5×SSC pH 7.0. For ß-galactosidase staining, embryos were fixed in MEMFA (RT, 1h), rinsed in PBS and stained by using X-gal (Steinbeisser *et al.,* 1989).

RT-PCR

Total RNA was prepared from embryos or conjugates with Trizol reagent (GibcoBRL) and treated with RNase-free DNase I (Promega). 1st strand cDNA primed by random hexamers was synthesized with AMV reverse transcriptase (Roche) and PCR was performed using standard conditions and the following sets of primers: *Engrailed2*-F (5'-ATGAGCAGAATAACAGGGAAGTGGA-3') and *Engrailed2*-R (5'-CCTCGGGGACATTGACTCGGTGGTG-3'), 28 cycles; *eomes*-F (5'-GCCTACGAAACAGACTACTCCT-3') and *eomes*-R (5'-TAATGGAGGGAGGGGTTTCTAC-3'), 28 cycles; *Krox20*-F (5'-AACCGCCCCAGTAAGACC-3') and *Krox20*-R (5'-GTGTCAGCCTGTCCTGTTAG-3'), 24 cycles; *Nkx2.1*-F (5'-CTGACATATTGAGTCCCCTGGAGG-3′) and *Nkx2.1*-R (5'-CCAGGTTTCCCAAATTGCCATTGC-3'), 30 cycles; *ODC*-F (5'-CAGCTAGCTGTGGTGTGG-3') and *ODC*-R (5'-CAACATGGAAACTCACACC-3'), 21 cycles; *Xag*-F (5'-CTGACTGTCCGATCAGAC-3') and *Xag*-R (5'-GAGTTGCTTCTCTGGCAT-3'), 23 cycles; *XBF1*-F (5'-AAAGTGGACGGCAAAGACGGTG-3') and *XBF1*-R (5'-CCAATGAACACATCGTCGCTGC-3'), 26 cycles; *Xemx1*-F

(5'-GCAGAAGCCTTTGTCAGTGG-3')   and   *Xemx1*-R

(5'-CCTCCAGTTTCTGCCTCTTG-3'), 31 cycles.

In vitro translation and Western Blot analysis

For *in vitro* transcription/translation the TNT®* Coupled Reticulocyte Lysate System (Promega) was used according to the manufacture's instructions. Protein extraction of embryos was carried out as described in Munchberg *et al.* (1999). Proteins were heated in sample buffer and separated by denaturating SDS-PAGE using a 13.5% polyacrylamide gel (Laemmli, 1970). Subsequent proteins were transferred to a nitrocellulose membrane (Townbin *et al.* 1979), detected with monoclonal rabbit anti-α-HA antibody (Santa Cruz) for Xcer-HA or monoclonal mouse anti-c-myc (Oncogene) for ΔN Moesin-myc and developed using a chemiluminescent substrate (Pierce).

Results

Antisense morpholino oligonucleotide inhibits Cerberus activity.

Antisense morpholino oligonucleotides are able to inhibit the translation of mRNAs in embryos (Heasman, 2002). To block the endogenous function of *Xenopus cerberus* in the ADE, we designed a morpholino oligonucleotide complementary to the 5′ UTR region between bases –35 and –11 of the *cerberus* mRNA (CerMo; Fig. 1A).

The sequence of the morpholino oligo was compared with all the available *Xcerberus* EST sequences present in the general publicly accessible Databases. In all the found entries for *Xcerberus*, the 5′ UTR sequence complementary to the oligo was present. This strongly indicates that in the frog embryo, no additional *cerberus* messages with a different 5′ UTR exist. We tested the ability and specificity of this CerMo to inhibit translation of *cerberus* mRNA in a cell free transcription-translation system and in *Xenopus* embryos. Western blot analysis for the HA-tagged Cerberus protein, demonstrated that only mRNAs containing the 5′ UTR sequences complementary to CerMo (5′ UTR cer-HA) were efficiently blocked in both systems (Fig. 1B,C). Standard control morpholino (CoMo) did not inhibit translation of *cerberus* mRNA. Neither CoMo nor CerMo interfered unspecifically with the translation of an unrelated control mRNA Δ*N Moesin-myc* (Fig. 1B,C).
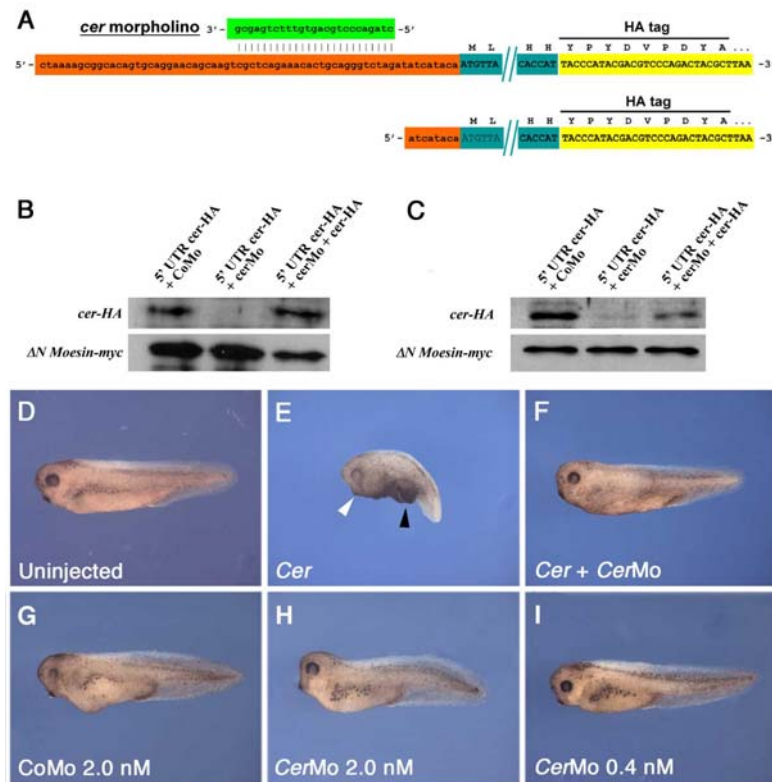
Figure 1. Cer morpholino inhibits translation of *Cerberus* mRNA. (A) Scheme of the HA-tagged Cerberus expression construct (5' UTR cer-HA; top), the HA-tagged Cer rescue construct (cer-HA; bottom) and the morpholino sequence targeting the *cerberus* 5' UTR sequences. (B-C) Western blot analysis of HA-tagged Cerberus and myc-tagged ΔN-moesin proteins. (B) *In vitro* transcription/translation of Cerberus protein in reticulocytes from 220 ng of plasmid was blocked by 20 pmol of the CerMo (lane 2) but not by control morpholino (CoMo) (lane 1). Transcription/translation from an equal amount of rescue plasmid was not blocked by the CerMo (lane3). (C) Four-cell stage embryos injected in the animal pole with a total of 120 pg of 5' UTR cer-HA construct were grown till stage 10.5 and one embryo equivalent protein extracts were used per lane in Western blots. Translation of 5' UTR cer-HA was blocked by coinjection with 1.6 pmol of CerMo (lane 2), but not with 2.0 pmol CoMo (lane 1). Coinjection of 80 pmol of the rescue construct was able to overcome the CerMo effect (lane 3). (D-F) Ectopic head-like structures induced by the injection of 700 pg of 5' UTR cer-HA capped mRNA in the ventral side of four-cell stage embryos (E) are suppressed by coinjection of 3.2 pmol of CerMo (F). White arrowhead indicates the cement gland of the primary axis while the black arrowhead points to the ectopic cement gland. (G-I) No significant anterior defects are visible in embryos microinjected in the two dorsal-vegetal blastomeres at four-to-eight cell stage either with a total of 16 pmol of CoMo (G) or with 16 pmol (H) and 3.2 pmol (I) of CerMo.

Morpholino "knock-down" of Cerberus in the ADE does not prevent head formation.

Synthetic *cerberus* mRNA can induce head-like structures when microinjected in the ventral side of *Xenopus* embryo (Fig. 1E; Bouwmeester et al, 1996). This induction was not observed when the 5' UTR *cerberus* mRNA and the CerMo were coinjected (Fig. 1F), demonstrating that the morpholino can efficiently inhibit Cerberus activity in the embryo. In order to assess the phenotypic effect of "knocking-down" endogenous Cerberus, four-to-eight-cell stage embryos were injected with CerMo in the two dorsal-vegetal blastomeres, whose clonal descendants include the ADE cells (Bauer et al, 1994). Despite

the ability of the CerMo to block Cerberus activity, we did not observe any visible phenotypes in embryos injected with 3.2 pmol of CerMo (Fig. 1I). Mild axis defects were observed when the maximal possible dose (16 pmol) of either CoMo or CerMo was injected (Fig. 1G,H). Using this morpholino mediated "knock-down" strategy, we conclude that reducing Cerberus activity in the ADE was not sufficient to impair head formation in the *Xenopus* embryo.

Gain of BMP, Nodal or Wnt function in the ADE perturbs head formation.

Cerberus protein can bind to and antagonize BMP-4, Xnr-1 and Xwnt-8 molecules (Piccolo et al, 1999). We reasoned that an alternative way to modulate Cerberus activity in the ADE would be by locally raising the levels of BMP, Nodal and Wnt proteins. This changes the balance between the agonists (BMP, Nodal and Wnt) and the antagonist Cerberus. Such a strategy requires that these factors be expressed strictly in the ADE, as their presence in the dorsal ecto-mesoderm strongly interferes with axis formation. Unfortunately, according to the available fate maps, the dorsal-vegetal blastomeres of the 8-cell stage embryo will give rise not only to the ADE, but also to ecto-mesodermal cells (Bauer et al, 1994). This compromises the usefulness of the injection of RNA or constitutive expression constructs in these blastomeres. Therefore, the precise targeting of gene expression to the ADE, can only be achieved through the use of a promoter, specific for that region.

A 4.0 KB mouse *cerberus-like* promoter fragment isolated from a genomic library, was found to be specifically activated in the AVE of transgenic mouse lines (M. Filipe, unpublished). This promoter fragment was fused to a NLS-*lacZ* reporter gene (generating McerP-LacZ; Fig. 2A) and microinjected into *Xenopus* embryos. Surprisingly the mouse *cer-1* promoter was only activated in the dorsal side of gastrula embryos and LacZ activity could only be detected in the ADE (Fig. 2B,C). In contrast, CMV driven *lacZ* expression could be detected in both dorsal and ventral tissues (Fig. 2D,E). The temporal and spatial specificity of this promoter was confirmed by in situ hybridization (Fig. 2F,F',G,G') and by RT-PCR (not shown). *Xenopus* embryos were injected dorsally at the four-to-eight cell stage with the McerP-LacZ construct and sagitally sectioned through the dorsal lip, at stage 10$^+$ and 11. The left halves of these embryos were hybridized with an antisense *lacZ* probe (Fig. 2F,G). The corresponding right halves were hybridized with a probe against *Xcer* (Fig. 2F',G'). The region of *lacZ* expression precisely matched the endogenous

cerberus expression domain, detected in the corresponding half embryos. This finding enabled us to use the mouse *cerberus-like* promoter as a tool to precisely target expression of BMP, Nodal and Wnt proteins to the ADE of *Xenopus* embryos. For that end, we fused the *cer-1* promoter to *BMP-4*, *Xnr-1* or *Xwnt-8* cDNAs generating McerP-BMP4, McerP-Xnr1 and McerP-Xwnt8, respectively. These constructs were injected in the two dorsal-vegetal blastomeres of eight-cell stage embryos. When 80 pg of either McerP-BMP4, McerP-Xnr1 or McerP-Xwnt8 were injected, head development was markedly affected in stage 35 embryos, whereas the trunk-tail structures appeared normal (Fig. 3D,G,J). In contrast, the injection of 80 pg of CMV- driven *BMP-4*, *Xnr-1* or *Xwnt-8* expression constructs resulted in severe axial defects (Fig. 3A,B,C), leading to either a complete ventralization (CMV.BMP4; Fig. 3B) or dorsalization (CMV.Xnr1; Fig. 3B) of the embryo. When McerP-LacZ was coinjected to monitor targeting efficiency, LacZ activity was only detected in the anterior gut/liver/heart region of the *Xenopus* embryos (Fig. 3E,H,K). Due to its stability, β-galactosidase protein can act as a lineage tracer for the cells where it was originally expressed. Its detection in the aforementioned tissues, which had already been shown to originate from the ADE (Bouwmeester et al, 1996), provides further evidence that the activation of M*cer-1* promoter in the ADE recapitulates the expression pattern of *cerberus*.
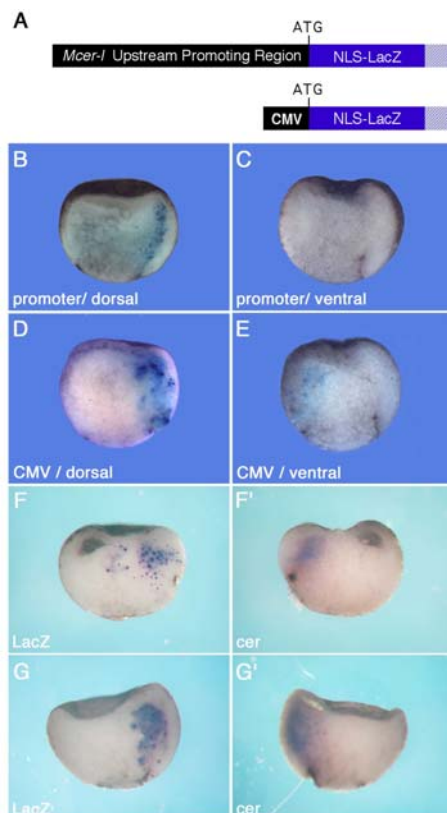
Figure 2. *lacZ* expression driven by the Mcer promoter mimics endogenous *cerberus* expression domain in the early frog embryo. (A) Scheme of the McerP-LacZ and CMV-LacZ constructs. (B-E) LacZ staining of embryos injected at the four-to-eight-cell stage either in the two dorsal-vegetal (B, D) or ventral-vegetal (C, E) blastomeres with McerP-LacZ or CMV-LacZ constructs. Embryos were injected at four-to-eight cell stage in both dorsal-vegetal blastomeres with McerP-LacZ, grown to stage 10+ (F-F') or 11 (G-G'), sagitally sectioned and each half was hybridized with a LacZ (F, G) or a Xcer (F', G') probe.

The severity of the induced head defects was dependent on the amount of McerP-Xnr1, -BMP4 or -Xwnt8 constructs injected (20, 40 and 80 pg/embryo). However, not all anterior structures were equally affected by the different constructs. Increasing dosages of McerP-Xnr1 caused the graded reduction of brain, eye and cement gland structures (Fig. 3I,H,G). McerP-BMP4 also caused the graded loss of brain and eye structures (Fig. 3F,E,D), but residual cement gland tissue was still visible at high dosage of BMP-4 (Fig. 3D). In contrast, the cement gland was the first structure to be lost in McerP-Xwnt8 injected embryos (Fig. 3L). A severe reduction of the head and a cyclopic eye were also observed in this case. A further increase in Xwnt8 dose completely eliminated the head (Fig. 3K,J). In summary, we observed that graded but distinct defects are obtained by the targeted increase of each of the signaling molecules in the ADE.
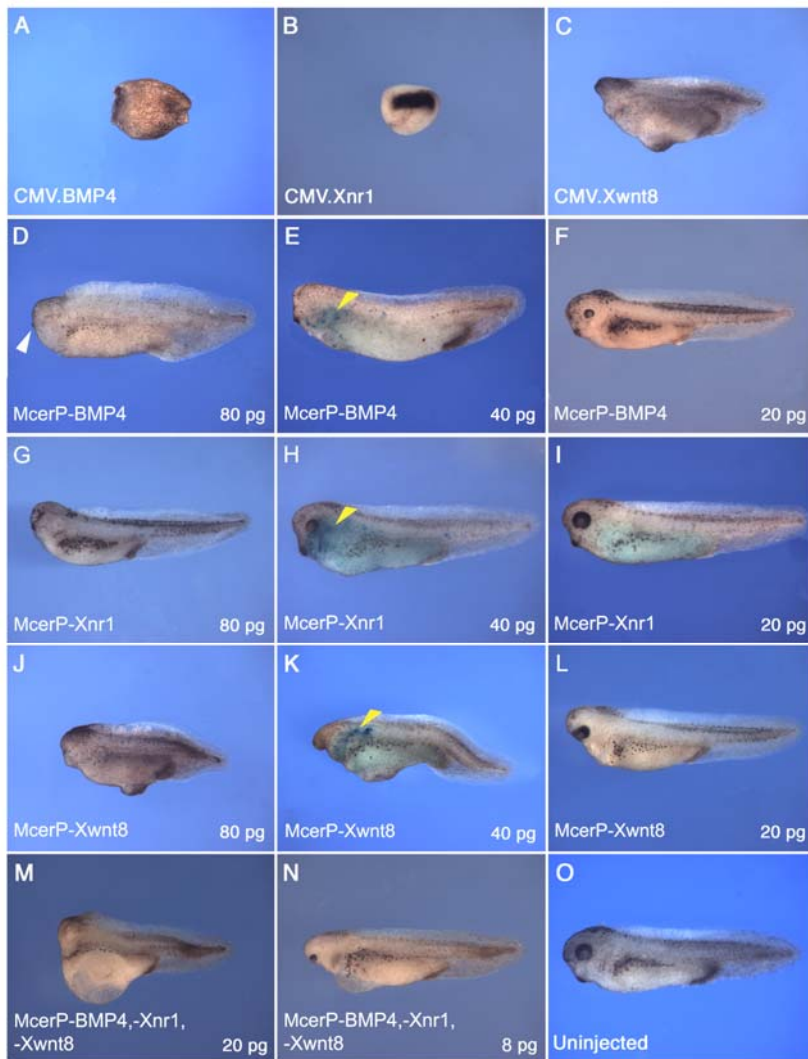
Figure 3. Head defects induced by McerP-BMP4, Xnr1 and Xwnt8 microinjection in the frog embryo. Embryos were injected at the four-to-eight-cell stage in the two dorsal-vegetal blastomeres. (A-C) Injection of 80 pg of CMV.BMP4 (A; 100%, n = 22), CMV.Xnr1(B; 94%, n = 17) and CMV.Xwnt8 (C; 20%, n = 25) led to very severe phenotypes. (D-F) Injection of 20 pg (F; 60%, n = 20), 40 pg (E; 62%, n = 34) and 80 pg (D; 50%, n = 24) of McerP-BMP4 showed a concentration dependent increase in head truncation. (G-I) A progressive head reduction and loss of eye were observed when 20 pg (I; 100%, n = 26), 40 pg (H; 24%, n = 21) and 80 pg (G; 59%, n = 34) of McerP-Xnr1. (J-L) Increasing the amount of McerP-Xwnt8 from 20 pg (L; 60%, n = 25) to 40 pg (K; 62%, n = 28) to 80 pg (J; 74%, n = 19) resulted in loss of cement gland and cyclopia and ultimately in complete truncation of the head. (M, N) Synergistic effect of McerP-BMP4, Xnr1 and Xwnt8 is shown by the coinjection of 8 pg (N; 65%, n = 23) and 20 pg (M; 63%, n = 46)of each construct which resulted in more severe defects than the ones observed in embryos injected with equal amounts of the individual constructs (F, I and L). 20 pg of McerP-LacZ was coinjected to access the correct targeting of the promoters to the ADE (yellow arrowheads in E, H and K).

BMP, Nodal and Wnt activities synergistically suppress head formation.

Independently raising the levels of Xnr-1, BMP-4 or Xwnt-8 in the ADE led to defects in head formation. In a following step, we tested whether those three factors could synergistically inhibit head structures. Simultaneous microinjection of the three *Mcer-1* promoter expression constructs, at a concentration of 8 pg each per embryo, resulted in loss of cement gland, reduction of the brain and a small cyclopic eye (Fig. 3N). In embryos injected with a combination of 20 pg of each construct, the rostral head, including eyes, was completely lost (Fig. 3M). These experiments clearly demonstrated that BMP, Nodal and Wnt activity in the ADE synergize to inhibit head formation.

Next we tested whether the local increase of BMP, Nodal and Wnt activity in the ADE, can affect the patterning of this tissue. Such patterning defects could be responsible for the head phenotypes observed in tadpoles. To address this issue, embryos were injected dorsally with a mixture of McerP-BMP4, McerP-Xnr1 and McerP-Xwnt8 (20 pg of each per embryo) and grown until stage 10$^+$ or 12. These embryos, and uninjected siblings, were then hemi-sectioned and analyzed by in situ hybridization for typical ADE markers (Fig. 4). At stage 10$^+$, the expression domains of *cerberus* and *Xhex* (Fig. 4A,A') were unaltered in injected embryos (Fig. 4C,C'). Also, no visible changes in *cerberus* and *Xhex* expression were observed in stage 12 embryos (Fig. 4B,B',D,D'). These results demonstrated that the ADE patterning is not perturbed by elevated levels of BMP, Nodal and Wnt signaling.
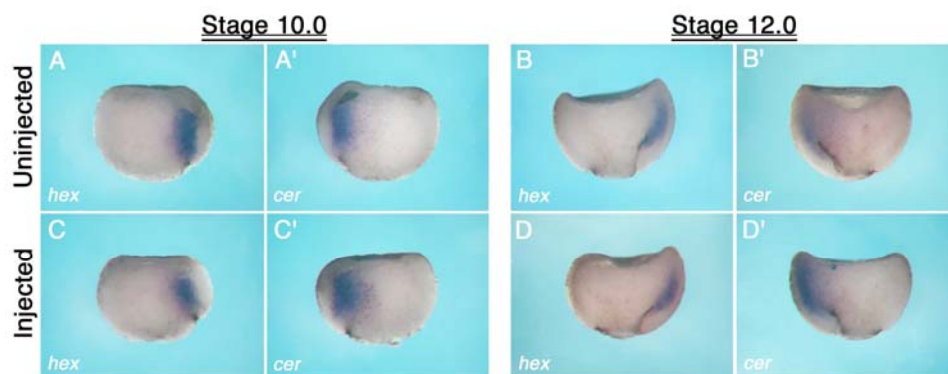
Figure 4. Misexpression of BMP-4, Xnr-1 and Xwnt-8 does not interfere with anterior endomesoderm patterning. (A-A' and C-C') Stage 10 and (B-B' and D-D') 12 embryos halves from uninjected (A-B') or injected twice dorsally at the four-to-eight cell stage embryos, with a mixture of 20 pg each of McerP-BMP4, McerP-Xnr1 and McerP-Xwnt8 (C-D'), were sagitally sectioned and each half was hybridized with a *Xhex* or a *Xcer* probe. The expression of these endomesodermal markers was unchanged in the injected embryos (C, C', D, D') when compared to the uninjected embryos (A, A', B, B').

Increased BMP, Nodal and Wnt signaling in the ADE inhibits the formation of anterior neural tissue.

In order to trace back the molecular events leading to the observed head phenotypes, we analyzed the expression of neural marker genes by RT-PCR, at different stages of development. This method allowed us to determine when, in embryogenesis, the perturbation of head development was initiated. Furthermore, we were able to establish at which level the AP axis of the neural tissue was affected. For this purpose, embryos were injected dorsally with a mixture of McerP-BMP4, McerP-Xnr1 and McerP-Xwnt8 (20 pg each/embryo). At stages 12, 13 and 15, RNA was extracted from pools of 5 randomly picked injected embryos or uninjected siblings. RT-PCR analysis showed that expression of the anterior neural markers *XBF1*, *Xemx1* and *Nkx2.1* (Bourguignon *et al.*, 1998; Pannese *et al.*, 1998; Hollemann and Pieler, 2000; Small *et al.*, 2000) was reduced in the injected embryos (Fig. 5A). Expression of *XBF1*, a pan telencephalic marker, was clearly reduced by stage 13. The same expression profile was observed for the ventral forebrain marker *Nkx2.1*. *Xemx1*, a marker for the dorsal telencephalon, was already downregulated by stage 12. In contrast, the expression of more posterior neural markers was not affected. Both *Engrailed-2* (Hemmati-Brivanlou *et al.*, 1991), a mid-hindbrain boundary marker, and *Krox20* (Bradley *et al.*, 1993), a marker for rhombomeres 3 and 5, were not reduced in the injected embryos (Fig. 5A). The cement gland marker *Xag* (Aberger *et al.*, 1998) was also downregulated. From this analysis we conclude that increased levels of BMP, Nodal and Wnt in the ADE, repress the expression of anterior neural markers down to the mid-hindbrain level, as early as stage 12.

We further extended the molecular characterization of the induced head phenotype by performing an in situ hybridization analysis for neural markers in stage 22/24 embryos. The anterior neural expression of *XBF1*, *Xotx2* and *Xnot2* (Bourguignon *et al.*, 1998; Blitz and Cho, 1995; Gont *et al.*, 1993) was absent in the injected embryos (Fig. 5B-G). Expression of *Xnot2* in the chordoneural hinge (Fig. 5G) and of *XBF1* in the olfactory placodes (Fig. 5C) was not affected. Similarly, the expression domain of *Krox20* was unchanged in injected embryos, despite the obvious loss of structures rostral to rhombomere 3 (Fig. 5H,I). *Xshh* (Stolow and Shi, 1995; Ekker *et al.*, 1995), a gene expressed in the ventral neural tube and notochord along the entire AP axis (Fig. 5J), was not detected in the rostral end of the injected embryo (Fig. 5K), while its expression in the remaining embryonic regions was identical to the uninjected controls. This *in situ*

hybridization analysis confirmed and extended the previous RT-PCR data, demonstrating that elevated levels of BMP, Nodal and Wnt signaling in the ADE specifically inhibit the formation of forebrain and midbrain structures.
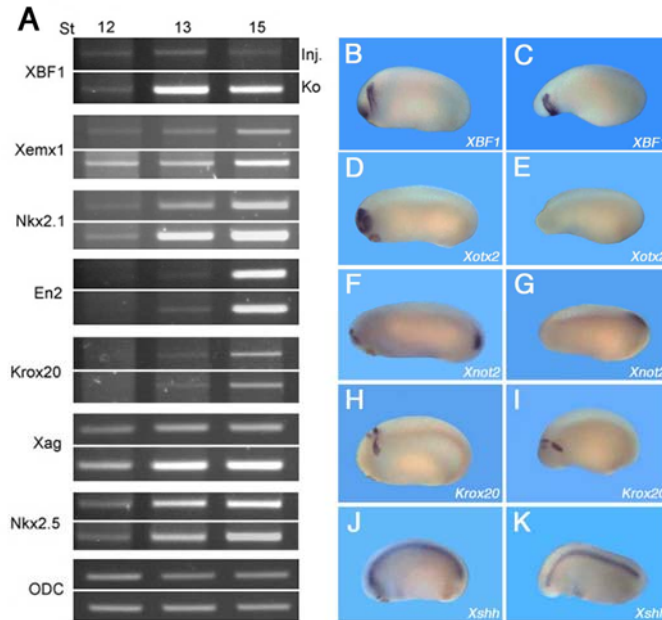
Figure 5. Molecular markers analysis after microinjection of McerP-BMP4, -Xnr1 and -Xwnt8 in frog embryos. (A) RT-PCR analysis at stages 12, 13 and 15 show that the cement gland and anterior neural markers *Xag*, *XBF1*, *Xemx1* and *Nkx2.1* are down-regulated in embryos coinjected with McerP-BMP4, McerP-Xnr1 and McerP-Xwnt8 (20 pg each), when compared with uninjected controls, while the levels of more posterior neural markers, like *En2* and *Krox20*, are not changed. *ODC* was used as a loading control. RNA extracts used for the RT-PCRs were made from pools of 5 randomly picked embryos. (B-K) In situ hybridization analysis for different molecular markers at stages 22/24. The injection of McerP-BMP4, McerP-Xnr1 and McerP-Xwnt8 (20 pg each) leads to the suppression of the anterior domains of expression of *XBF1* (B-C), *Xotx2* (D-E) and *Xnot2* (F-G). Expression of the hindbrain marker, *Krox20* (H-I), was not significally changed in the injected embryos as well as in the controls. (J-K) *Xshh* expression in injected embryos does not extend as anteriorly as it does with the uninjected sibling embryos.

Cerberus morpholino oligonucleotide specifically enhances the head defects induced by BMP, Nodal and Wnt.

Since CerMo by itself had no visible effect on head formation (Fig. 1H,I), we tested whether a possible function of Cerberus could be revealed in a sensitized experimental system. We simultaneously raised the levels of the agonists BMP, Nodal and Wnt up to a threshold level, sufficient to titrate their antagonists but without producing a severe phenotype. Hence, we analyzed whether this phenotype could be aggravated by simultaneously reducing Cerberus activity in the ADE. Dorsal injection of low doses (8 pg each) of a mixture of McerP-BMP4, McerP-Xnr1 and McerP-Xwnt8 caused a partial loss of the head (Fig. 6B and 3N). Remarkably, coinjection of CerMo strongly increased the head phenotype (Fig. 6C). The phenotype caused by CerMo was specific, since it could be

rescued by injection of a full-length Cerberus expression construct that cannot be blocked by the morpholino oligonucleotide (Fig. 6D).
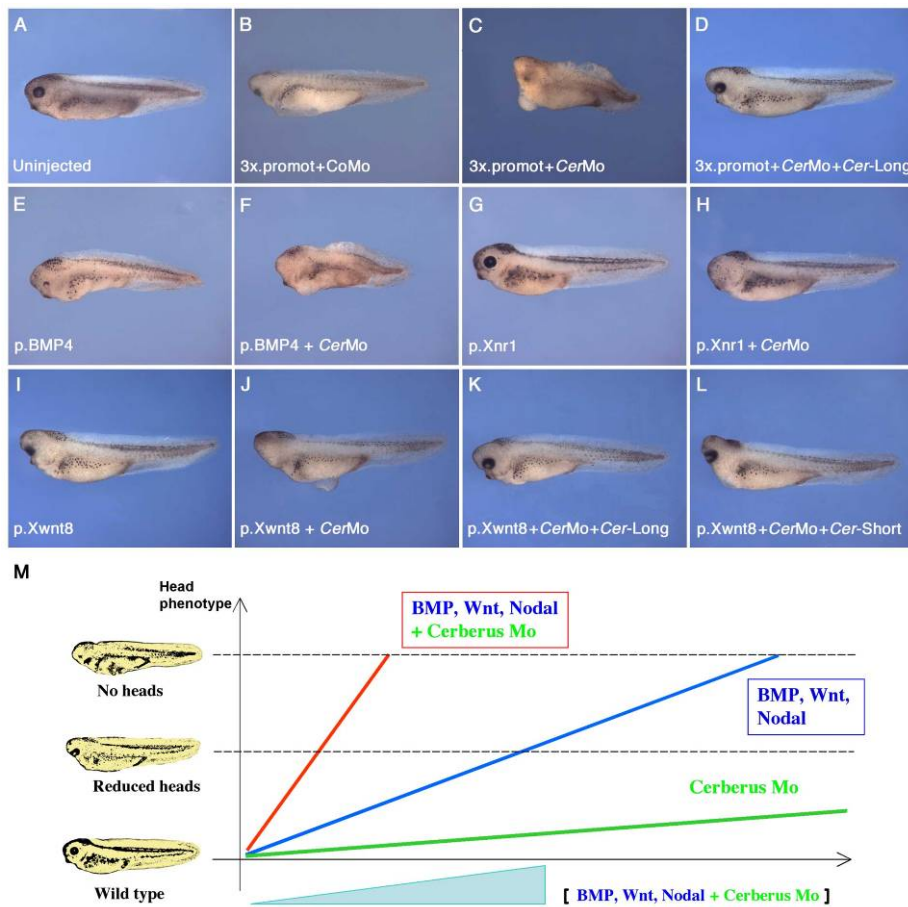
Figure 6. "Knock-Down" of endogenous Cerberus enhances the head phenotypes induced by microinjection of McerP-BMP4, -Xnr1 and -Xwnt8. (A-D) The head defects observed by the coinjection of McerP-BMP4, -Xnr1 and -Xwnt8 (8 pg each) together with the CoMo (B; 64%, n = 62) can be aggravated when endogenous *cerberus* is knock-down by 1.6 pmol of CerMo (C; 65%, n = 46). The specificity of this sensitization was verified by the coinjection of Cer-Long plasmid, which could rescue the phenotype (D; 58%, n = 42). (E-J) The mild phenotypes obtained by individually injecting McerP-BMP4 (E; 30%, n = 44), McerP-Xnr1 (G; 40%, n = 40) or McerP-Xwnt8 (I; 66%, n = 47) were also aggravated by the coinjection of 1.6 pmol CerMo (F; 25%, n = 41. H; 60%, n = 39. J; 58%, n = 44 respectively). (K-L) CerMo dependent aggravation of the McerP-Xwnt8 phenotype could be completely rescued by Cer-Long construct (K; 66%, n = 48), but only partially rescued if Cer-Short plasmid (L; 55%, n = 44) is used instead. These results were observed in two independent experiments. (M) Graphical representation of the range of phenotypes observed by increasing amounts of BMP, Wnt and Nodal misexpressed in the ADE, showing the requirement of lower amounts of these signals to generate the same phenotypes when endogenous Cerberus is depleted.

We next asked whether CerMo could also enhance the phenotypes caused by single injection of either McerP-BMP4, McerP-Xnr1 or McerP-Xwnt8. Microinjection of 20 pg of McerP-BMP4, McerP-Xnr1 or McerP-Xwnt8 led to the already described head defects (Fig. 6E,G,I). In all cases, coinjection of CerMo strongly enhanced these phenotypes (Fig. 6F,H,J). We also had shown that the cement gland was very sensitive to elevated Xwnt8 levels (Fig. 3L). Eyes and cement gland were absent in McerP-

56

Xwnt8/CerMo injected embryos, and both structures could be rescued by co-expression of full-length Cerberus protein (Fig. 6K). On the other hand Cerberus-Short, which only binds to Nodal, could partially rescue the eye phenotype, but not the cement gland (Fig. 6L). This last result also suggests an interplay between Wnt and Nodal signaling, which would explain why the Nodal inhibitor Cer-S could partially rescue the eye phenotype induced by Wnt misexpression in the ADE.

In conclusion, these results clearly demonstrate that endogenous Cerberus protein can inhibit BMP-4, Xnr-1 and Xwnt-8 activities *in vivo*.

Cerberus function in the ADE is required for the activation of forebrain markers.

The ADE when combined with stage 10.5 Dorsal Ectoderm (DE) explants induces dorsal telencephalic markers (Lupo et al, 2002). We have shown that in the embryo, modulating Cerberus activity in the ADE by raising BMP-4, Nodal and Xwnt8 levels represses the expression of forebrain markers, including *XBF1* and *Xemx1* (Fig. 5A). To test whether the Cerberus function in the ADE was required for the activation of dorsal telencephalic markers in the neuroectoderm, we used a modified explant recombination system (Fig. 7A). RT-PCR analysis of ADE/DE conjugates revealed that uninjected ADE induced expression of both a pan telecephalic marker, *XBF1*, as well as a dorsal telencephalic marker, *Xemx1* (Fig. 7B). In contrast, ADE explants in which Cerberus function had been "knocked-down" with CerMo failed to induce both telencephalic markers (Fig. 7B). The CerMo effect was specific because expression of *XBF1* and *Xemx1*could be rescued by coinjection of a *cerberus* DNA construct that can not be blocked by the CerMo.

Cerberus activity in the ADE also modulates the expression of posterior neural markers. DE explants express *Krox20*, a hindbrain marker, and *En2*, which demarcates the mid-hindbrain boundary (Fig. 7C, lane 2). In contrast to the more anterior neural markers, expression of *Krox20* was inhibited in the DE/ADE but not in the DE/ADE CerMo conjugates (Fig. 7C). These experiments demonstrate that Cerberus activity in the ADE is required for the induction of forebrain markers and for the simultaneous repression of more posterior ones, such as *Krox20*.
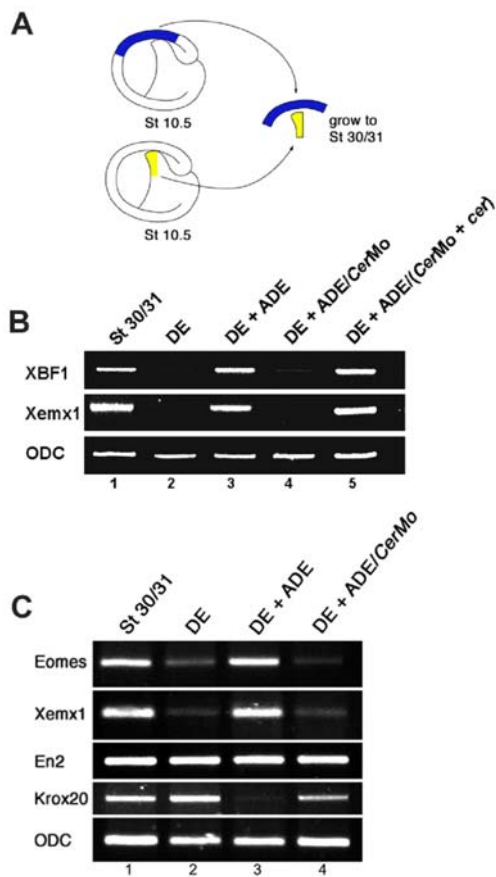
Figure 7. Endogenous Cerberus activity is required for correct expression of neural markers in a tissue recombination induction assay. (A) ADE (yellow) explanted from either stage 10.5 uninjected embryos or from ones injected dorsal-vegetally with 3.2 pmol of CerMo, were conjugated with isochronic dorsal ectoderms (blue). Conjugates were grown until sibling embryos reached stage 30/31. (B) RT-PCR analysis of telencephalic markers in DE/ADE conjugates at stage 30/31. DE explants show expression of *XBF1* and *Xemx1*. When DE is conjugated with control ADE, dorsal telencephalic markers are up-regulated (lane 3). CerMo injected ADEs are no longer able to up-regulate neither *XBF1* nor *Xemx1* in the DE/ADE conjugates (line 4). Cer-HA DNA construct, which lacks the 5'UTR sequences complementary to CerMo, con rescue the induction of both telencephalic markers in the DE/ADE CerMo conjugates. (C) RT-PCR analysis of neural markers from the DE/ADE conjugates at stage 30/31. DE show expression of *Xemx1* and *eomes* but, when conjugated with control ADE, marked up-regulation of these dorsal telencephalic markers (lane 3). ADE CerMo conjugated with dorsal ectoderm suppresses expression of *Xemx1* and *eomes* (line 4). Expression levels of the mid-hindbrain marker *En2* are unchanged both in unconjugated DE (lane 2) as well as in DE /ADE (lane 3) or DE/ADE CerMo conjugates (lane 4). *Krox20* is downregulated in the DE/ADE conjugates (lane 3) but its expression levels are partially rescued in DE conjugates with CerMo injected ADE (lane 4).

Discussion

Targeted increase of BMP, Nodal and Wnt activities in the ADE affects head formation.

The currently accepted model of head formation in the vertebrate embryo, postulates the existence of a head organizing center. The Anterior Dorsal Endoderm (ADE) in the amphibian, as well as the Anterior Visceral Endoderm (AVE) in the mouse embryo have been implicated as head organizers (reviewed in Beddington and Robertson, 1999). Simultaneous inhibition of BMP, Wnt and Nodal signaling in the ventral mesoderm of *Xenopus* embryos results in the formation of ectopic head-like structures (Bouwmeester *et al.*; 1996; Piccolo *et al.,* 1999; Glinka *et al.,* 1997 and 1998). The dorsal mesendoderm in *Xenopus* expresses secreted antagonists for BMP, Wnt and Nodal proteins such as Cerberus, Dickkopf, Frzb and Crescent (Bouwmeester *et al.,* 1996; Glinka *et al.,* 1998; Leyns *et al.,* 1997; Pera and de Robertis, 2000). According to this model, Cerberus would play an important role in the head organizer center. The presence of Cerberus, which can inhibit Xwnt-8, Xnr-1 and XBMP-4, in the ADE would generate a trunk-signaling free zone in the

anterior region of the embryo, therefore restricting the trunk territory to the opposite side of the embryo, the posterior part.

To test *in vivo* the requirement for this Cerberus mediated triple inhibition in the ADE, one cannot rely on dorsal microinjection of RNA or CMV-driven DNA constructs coding for either BMP-4, Xnr-1 or Xwnt-8 proteins. When those constructs are microinjected in the dorsal blastomeres, their activation in the ecto-mesodermal layers leads to strong axial defects, ranging from strong ventralization (in the case of *BMP-4* injection; Fig. 3A) to strong dorsalization (*Xnr-1* injection; Fig. 3B). Using a mouse *cer-1* promoter fragment we were able to drive the expression of these signaling molecules in the ADE of *Xenopus* embryos. Since the activation of this promoter closely resembles the spatial and temporal expression of the *Xcer* gene, one could use it to very precisely target the expression of a given molecule to the ADE. Targeted expression of increasing doses of BMP-4 led to head defects with progressive severity (Fig. 3D-F). Remarkably, neither the AP axis nor the cement gland were affected. Even at higher doses, 80 pg, cement gland tissue was present, although the head was severely reduced. This phenotype was very different from the one observed after injection of CMV.BMP4. When the ventralizing and anti-neural activities of BMP-4 (Fainsod *et al.* 1994; Wilson and Hemmati-Brivanlou *et al.* 1995) are spatially restricted to the ADE only head defects were observed, while the axial structures remained undisturbed. A similar phenotype had already been reported for the misexpression of BMP-4 in the anterior neural plate, driven by a *Pax-6* promoter fragment in transgenic frog embryos (Hartley *et al.,* 2001). After gastrulation, the expression of *BMP-4* in the *Pax-6* domain downregulated most anterior neural markers, leading to the suppression of anterior brain and eye formation. This revealed that the interplay between BMP signaling and localized inhibitors was necessary for the correct patterning of the anterior neural structures.

Injection of increasing amounts of McerP-Xnr1 resulted in gradual loss of the eye and reduction of anterior brain structures (Fig. 3G). This was surprising because the Nodal proteins are TGF-ß factors with strong dorsalizing activity. Ectopic Nodal signaling in the entire mesoderm results in expanded Spemann's organizer tissue and excess of dorso-anterior structures (Jones *et al.,* 1995; Smith *et al.,* 1995; Joseph and Melton, 1997) Similar results were obtained when the Nodal inhibitor Lefty1 was "knocked-down" in *Xenopus* by antisense morpholino oligos (Branford and Yost, 2002). This led to the increase of Nodal signaling in the marginal zone causing an upregulation of Nodal responsive

organizer genes. In contrast, expression of such genes in the ADE was unchanged, indicating that the level of Nodal signaling was not elevated there.

The *cer-1* promoter construct drove the expression of Xnr-1 in the ADE but not in the organizer, thereby eliminating the dorsalizing effect on the mesoderm and, instead, revealing the anti–head activity of this protein. This is in agreement with experiments in zebrafish, where overexpression of Nodal protein converted forebrain into more posterior neural or mesodermal tissue. Elevating the level of the Nodal inhibitor Antivin caused the loss of posterior ectoderm but did not influence forebrain and eye structures (Thisse *et al.*, 2000).

Microinjection of McerP-Xwnt8 resulted in severe head defects ranging from cyclopia (at 20 pg; Fig. 3L), to a severe truncation of the head when a higher dosage of this construct was used. Interestingly, in this case, and in contrast to the McerP-BMP4 injected embryos, the cement gland was the first structure to disappear (compare Fig. 3D,L). Kiecker and Niehrs, in 2001, have shown that a gradient of Wnt/ß-catenin signaling was involved in the anteroposterior neural patterning of *Xenopus* embryos. Wnt activity in the posterior neural plate is required for the differentiation of posterior neural cells. Our own results strongly indicate, however, that a targeted increase of Wnt activity in the ADE also prevented formation of anterior neural structures, but did not affect more posterior neural tissue. These observations are supported by genetic data from the zebrafish model. Increased Wnt signaling in the anterior head due to a mutation in the *axin* gene, a negative regulator of the Wnt signaling pathway, resulted in the loss of forebrain structures (Heisenberg *et al.*, 2001).

When the activity of the signaling molecules BMP-4, Xnr-1 and Xwnt-8 was simultaneously upregulated in the ADE driven by the McerP constructs, a strong synergistic defect in head structures could be observed (Fig. 3M,N). Interestingly, the targeted activation of these molecules in the ADE did not affect the normal patterning of locally expressed genes such as *Xhex* and even *cerberus* itself (Fig. 4). Although it has been shown that *Xnr-1 was* able to induce *cerberus* expression, that seems to occur in a specific time frame. In particular, *cerberus* was only induced by the injection of *Xnr-1* mRNA, and not by a *Xnr-1* DNA construct, which is only expressed after midblastula transition (Piccolo *et al.*, 1999). Interestingly, we observed that the adjacent anterior neuroectoderm was severely affected upon targeted expression of BMP-4, Xnr-1 and Xwnt-8 proteins in the ADE (Fig. 5). The anterior neural markers *XBF1*, *Xemx1* and *Nkx2.1* and the cement

gland marker *Xag* showed a marked decrease in the injected embryos, as shown by RT-PCR and in situ hybridization. However, more posterior markers like *En2*, expressed in the mid and hindbrain and *Krox20*, expressed in rhombomeres 3 and 5, were not affected by the gain of function of BMP-4, Xnr-1 and Xwnt-8 in the ADE. Nevertheless, these embryos display a severe truncation of the head region rostral to these structures. In conclusion, these results strongly indicate that the combined increase of BMP, Wnt and Nodal activities in the ADE severely compromised the head formation program, suggesting the need for a tight locally controlled inhibition of those activities.

Correct balance of agonists vs. antagonists in the ADE was essential for head formation.

In some cases, the requirement for a given gene during embryonic development can only be demonstrated by the use of sensitized or compound system approaches. The mouse *cerberus-like* gene has been inactivated in ES cells (Belo *et al.*, 2000; Shawlot *et al.*, 2000; Stanley *et al.*, 2000), failing to reveal a phenotype during mouse embryogenesis. Mutant mouse embryos lacking both Nodal inhibitors Cer-l and Lefty-1 (*cer-1^-/-^;lefty-1^-/-^*) displayed striking early embryonic phenotypes not observed in the single mutants (Perea-Gomez *et al.*, 2002). Furthermore, in this sensitized compound mutant background, removal of a single copy of *Nodal* can partially rescue the *cer-1^-/-^;lefty-1^-/-^* mutant phenotypes. Therefore, only using this genetic system, the requirement for the redundant activities of *cerberus-like* and *lefty-1* at the level of nodal inhibition could be assessed. In the *cer-1^-/-^;lefty-1^-/-^* mice, *nodal* signaling is enhanced in the entire embryo. This has profound consequences on the formation of the primitive streak. Similar results were obtained in chicken embryos where nodal activity was enhanced in the epiblast, and, simultaneously, the hypoblast expressing the *cerberus* homologue, *caronte,* was removed (Bertocchini and Stern, 2002). In our *cerberus-like* promoter based assay, nodal activity is only enhanced in the ADE and therefore the formation of the trunk is not affected. Both the mouse, chick and frog experiments demonstrate that Cerberus function *in vivo* can only be revealed in sensitized assay systems.

As in the mouse, suppression of *Xenopus* Cerberus does not impair head formation (Fig. 1H,I). Similar results were obtained when the ADE region was extirpated from DMZ explants (Schneider and Mercola, 1999) and such explants still developed partial head-like

structures. In order to reveal a putative role of Cerberus in head formation we established a novel sensitized assay system in the *Xenopus* embryo.

We tested the biological relevance of the Cerberus inhibitory activity in the ADE by simultaneously "knocking-down" Cerberus activity and elevating the levels of the agonists BMP-4, Xnr-1 and Xwnt-8. When mild dosages of these 3 proteins were targeted to the ADE the resulting weak head phenotype was strongly enhanced when Cerberus was "knocked-down" by coinjection of the CerMo (compare Fig. 6B,C). This indicated that the agonists (BMP, Wnt and Nodal) must reach a critical threshold level in order to inhibit head formation. This threshold level could be lowered through the suppression of the antagonist Cerberus by CerMo, resulting in an aggravation of the phenotype (Fig. 6M). When the relative balance of agonists *vs.* antagonists was restored by coinjection of a full-length *cerberus* construct that was not targeted by CerMo, the head phenotype was rescued almost completely. This novel approach clearly demonstrated that Cerberus is a functional inhibitor of BMP-4, Xnr-1 and Xwnt-8 activities *in vivo* (Fig. 6E-L) and that this biological activity in the ADE is required for the correct specification of the head.

Endogenous Cerberus activity and anterior neural patterning.

Cerberus was able to induce anterior neural markers including the dorsal telencephalic markers *eomes* and *Xemx1* in animal cap explants (Bouwmeester *et al.,* 1996; Lupo *et al.,* 2002). Similar results were obtained when the activities of the BMP inhibitor Chordin and the Cerberus truncated protein cer-ΔC1 were combined (Fetka *et al.,* 2000; Lupo *et al.,* 2002). This N-terminal fragment of Cerberus can inhibit Wnt activity (Fetka *et al.,* 2000) and retains a residual Nodal inhibiting activity (Lupo *et al.,* 2002). In contrast, the coinjection of *chd* and *cer-S* mRNA was unable to induce the same set of markers, pointing to the simultaneous requirement of the anti-BMP and anti-Wnt activities of Cerberus in this process. Induction of *XBF1*, *Xemx1* and *eomes* expression in dorsal ectoderm explants (DE) was also observed when they were conjugated with ADE, a tissue where endogenous *cerberus was* expressed (Lupo *et al.,* 2002).

"Knocking-down" Cerberus function in the ADE with a morpholino oligo, resulted in a loss of *XBF1*, *Xemx1* and *eomes* induction in ADE/DE conjugates (Fig. 7B,C). Furthermore, uninjected ADE repressed the expression of the more posterior neural marker *Krox20* in the explanted DE, but this marker was activated in conjugates of DE/ADE injected with CerMo (Fig. 7C, lane 4). In embryos injected with CerMo however,

eomes and *Xemx1* expression in the brain was not significantly changed (data not shown). This indicates that in the embryonic context other molecules may compensate for the reduced Cerberus activity. This could also explain the reportedly formation of head in the DMZ explants lacking Cerberus expressing ADE tissue (Schneider and Mercola, 1999). The completeness of these head structures however, was not demonstrated because strictly forebrain markers were not analyzed. Cerberus is the only known factor however expressed in the leading edge of the ADE with anti-BMP, -Nodal and -Wnt activity. Thus, the anterior neural patterning activity of Cerberus in ADE/DE conjugates could be revealed through CerMo mediated loss-of-function, since no other factors could compensate for it in this system. When the formation of the AP axis in *Xenopus* embryos is perturbed by interfering with gastrulation movements very often neural patterning defects were observed. It is tempting to speculate that these defects are due to the incorrect positioning of the ADE and that spatially altered Cerberus activity causes aberrant neural patterning.

In conclusion, in the ADE/DE explant system (Fig. 7) a dual novel role for the Anterior Dorsal Endoderm is described: not only ADE induces the expression of anterior neural markers but also represses the expression of more caudal ones through the activity of Cerberus. This clearly demonstrates that the endogenous Cerberus activity in the leading edge of the anterior dorsal endoderm is required for the correct induction and patterning of the brain.

Acknowledgments

References

Aberger, F., Weidinger, G., Grunz H. and Richter, K. (1998). Anterior specification of embryonic ectoderm: the role of the *Xenopus* cement gland-specific gene XAG-2. *Mech. Dev.* **72**, 115-130.

Acampora, D., Mazan, S., Lallemand, Y., Avantaggiato, V., Maury, M., Simeone, A. and Brulet, P. (1995). Forebrain and midbrain regions are deleted in Otx2-/- mutants due to a defective anterior neuroectoderm specification during gastrulation. *Development* **121**, 3279-3290.

Bauer, D. V., Huang, S. and Moody, S. A. (1994). The cleavage stage origin of Speman's Organizer: analysis of the movements of blastomere clones before and during gastrulation in *Xenopus*. *Development* **120**, 1179–1189.

Beddington, R. S. and Robertson, E. J. (1999). Axis development and early asymmetry in mammals. *Cell* **96**, 195–209.

Belo, J. A., Bouwmeester, T., Leyns, L., Kertesz, N., Gallo, M., Follettie, M. and De Robertis, E. M. (1997). Cerberus-like is a secreted factor with neutralizing activity expressed in the anterior primitive endoderm of the mouse gastrula. *Mech. Dev.* **68**, 45–57.

Belo, J. A., Bachiller, D., Agius, E., Kemp, C., Borges, A. C., Marques, S., Piccolo, S. and De Robertis, E. M. (2000). Cerberus-like is a secreted BMP and Nodal antagonist not essential for mouse development. *Genesis* **26**, 265–270.

Bertocchini, F. and Stern, C. D. (2002). The hypoblast of the chick embryo positions the primitive streak by antagonizing Nodal signaling. *Dev. Cell* **3**, 735-744.

Biben, C., Stanley, E., Fabri, L., Kotecha, S., Rhinn, M., Drinkwater, C., Lah, M., Wang, C. C., Nash, A., Hilton, D., Ang, S. L., Mohun, T. and Harvey, R. P. (1998). Murine cerberus homologue mCer-1: a candidate anterior patterning molecule. *Dev. Biol.* **194**, 135-151.

Blitz, I. L. and Cho, K. W. (1995). Anterior neurectoderm is progressively induced during gastrulation: the role of the *Xenopus* homeobox gene orthodenticle. *Development* **121**, 993-1004.

Bourguignon, C., Li, J. and Papalopulu, N. (1998). XBF-1, a winged helix transcription factor with dual activity, has a role in positioning neurogenesis in *Xenopus* competent ectoderm. *Development* **125**, 4889-4900.

Bouwmeester, T., Kim, S. H., Sasai, Y., Lu, B. and De Robertis, E. M. (1996). Cerberus, a head inducing secreted factor expressed in the anterior endoderm of Spemann's organizer. *Nature* **382**, 595–601.

Bouwmeester, T. and Leyns, L. (1997). Vertebrate head induction by anterior primitive endoderm. *Bioessays* **19**, 855-863.

Bradley, L. C., Snape, A., Bhatt, S. and Wilkinson, D. G. (1993). The structure and expression of the *Xenopus* Krox-20 gene: conserved and divergent patterns of expression in rhombomeres and neural crest. *Mech. Dev.* **40**, 73-84.

Branford, W. W. and Yost, H. J. (2002). Lefty-dependent inhibition of Nodal- and wnt-responsive organizer gene expression is essential for normal gastrulation. *Curr. Biol.* **12**, 2136-2141.

Cho, K. W., Blumberg, B., Steinbeisser, H. and De Robertis, E. M. (1991). Molecular nature of Spemann's organizer: the role of the *Xenopus* homeobox gene *goosecoid. Cell* **67**, 1111-1120.

De Robertis, E. M., Kim, S. H., Leyns, L., Piccolo, S., Bachiller, D., Agius, E., Belo, J. A., Yamamoto, A., Hainski-Brousseau, A., Brizuela, B., Wessely, O., Lu, B. and Bouwmeester, T. (1997). Patterning by genes expressed in Spemann's organizer. *Cold Spring Harb Symp Quant Biol.* **62**,169-175.

Dufort, D., Schwartz, L., Harpal, K. and Rossant, J. (1998). The transcription factor HNF3beta is required in visceral endoderm for normal primitive streak morphogenesis. *Development* **125**, 3015-3025.

Ekker, S. C., McGrew, L. L., Lai, C. J., Lee, J. J., von Kessler, D. P., Moon, R. T. and Beachy, P. A. (1995). Distinct expression and shared activities of members of the hedgehog gene family of *Xenopus* laevis. *Development* **121**, 2337-2347.

Fainsod, A., Steinbeisser, H. and De Robertis E. M. (1994). On the function of BMP-4 in patterning the marginal zone of the *Xenopus* embryo. *EMBO J.* **13**, 5015-5025.

Fetka, I., Doederlein, G. and Bouwmeester, T. (2000). Neuroectodermal specification and regionalization of the Spemann organizer in *Xenopus. Mech. Dev.* **93**, 49-58.

Glinka, A., Wu, W., Onichtchouk, D., Blumenstock, C. and Niehrs, C. (1997). Head induction by simultaneous repression of Bmp and Wnt signalling in *Xenopus. Nature* **89**, 517-519.

Glinka, A., Wu, W., Onichtchouk, D., Blumenstock, C. and Niehrs, C. (1998). Dickkopf-1 is a member of a new family of secreted proteins and functions in head induction. *Nature* **391**, 357-362.

Gont, L. K., Steinbeisser, H., Blumberg, B. and de Robertis, E. M. (1993). Tail formation as a continuation of gastrulation: the multiple cell populations of the *Xenopus* tailbud derive from the late blastopore lip. *Development* **119**, 991-1004.

Hartley, K. O., Hardcastle, Z., Friday, R. V., Amaya, E. and Papalopulu, N. (2001). Trangenic *Xenopus* embryos reveal that anterior neural development requires continued suppression of BMP signaling after gastrulation. *Dev. Biol.* **238**, 168-184.

Heasman, J. (2002). Morpholino oligos: making sense of antisense? *Dev. Biol.* **243**, 209–214.

Heisenberg, C., Houart, C., Take-Uchi, M., Rauch, G., Young, N., Coutinho, P., Masai, I., Caneparo, L., Concha, M., Geisler, R., Dale, T. C., Wilson, S. W. and Stemple, D. L. (2001). A mutation in the Gsk3-binding domain of zebrafish Masterblind/Axin1 leads to a fate transformation of telencephalon and eyes to diencephalons. *Genes Dev.* **15**, 1427-1434.

Hemmati-Brivanlou, A., de la Torre, J. R., Holt, C. and Harland, R. M. (1991). Cephalic expression and molecular characterization of *Xenopus* En-2. *Development* **111**, 715-724.

Hollemann, T. and Pieler, T. (2000). Xnkx-2.1: a homeobox gene expressed during early forebrain, lung and thyroid development in *Xenopus* laevis. *Dev. Genes Evol.* **210**, 579-581.

Jones, C. M., Kuehn, M. R., Hogan, B. L., Smith, J. C. and Wright, C. V. (1995). Nodal-related signals induce axial mesoderm and dorsalize mesoderm during gastrulation. *Development* **121**, 3651-3662.

Joseph, E. M. and Melton, D. A. (1997). Xnr4: a *Xenopus* Nodal-related gene expressed in the Spemann organizer. *Dev. Biol.* **184**, 367-372.

Kiecker, C. and Niehrs, C. (2001). A morphogen gradient of Wnt/beta-catenin signalling regulates anteroposterior neural patterning in Xenopus. *Development* **128**, 4189-4201.

Laemmli, U. K. (1970). Cleavage of structural proteins during assembly of the head of bacteriophage T4. *Nature* **227**, 680-689.

Leyns, L., Bouwmeester, T., Kim, S. -H., Piccolo, S. and de Robertis, E. M. (1997). Frzb-1 is a secreted antagonist of Wnt signaling expressed in the Spemann Organizer. *Cell* **88**, 747-756.

Lupo, G., Harris, W. A., Barsacchi, G. and Vignali, R. (2002). Induction and patterning of the telencephalon in *Xenopus* laevis. *Development* **129**, 5421-5436.

Medina, A., Reintsch, W. and Steinbeisser, H. (2000). *Xenopus* frizzled 7 can act in canonical and non-canonical Wnt signaling pathways: implications on early patterning and morphogenesis. *Mech. Dev.* **92**, 227-237.

Munchberg, S. R. and Steinbeisser, H. (1999). The *Xenopus* Ets transcription factor XER81 is a target of the FGF signaling pathway. *Mech. Dev.* **80**, 53-65.

Pannese, M., Lupo, G., Kablar, B., Boncinelli, E., Barsacchi, G. and Vignali, R. (1998). The *Xenopus* Emx genes identify presumptive dorsal telencephalon and are induced by head organizer signals. *Mech. Dev.* **73**, 73-83.

Pera, E. M. and de Robertis, E. M. (2000). A direct screen for secreted proteins in *Xenopus* embryos identifies distinct activities for the Wnt antagonists Crescent and Frzb-1. *Mech. Dev.* **96**, 183-195.

Perea-Gomez, A., Vella, F. D., Shawlot, W., Oulad-Abdelghani, M., Chazaud, C., Meno, C., Pfister, V., Chen, L., Robertson, E., Hamada, H., Behringer, R. R. and Ang, S. L. (2002). Nodal antagonists in the anterior visceral endoderm prevent the formation of multiple primitive streaks. *Dev. Cell* **3**, 745-756.

Piccolo, S., Agius, E., Leyns, L., Bhattacharyya, S., Grunz, H., Bouwmeester, T. and De Robertis, E. M. (1999). The head inducer Cerberus is a multifunctional antagonist of Nodal, BMPand Wnt signals. *Nature* **397**, 707–710.

Rhinn, M., Dierich, A., Shawlot, W., Behringer, R. R., Le Meur, M. and Ang, S. L.(1998). Sequential roles for Otx2 in visceral endoderm and neuroectoderm for forebrain and midbrain induction and specification. *Development* **125**, 845-856.

Sasai, Y., Lu, B., Steinbeisser, H., Geissert, D., Gont, L. K. and De Robertis, E. M. (1994). *Xenopus chordin*: a novel dorsalizing factor activated by organizer-specific homeobox genes. *Cell* **79**, 779–790.

Schneider, V. A. and Mercola, M. (1999) Spatially distinct head and heart inducers within the *Xenopus* organizer region. *Current Biology* **9**, 800-809.

Shawlot, W., Deng, J. M. and Behringer, R. R. (1998). Expression of the mouse *cerberus-related* gene, *Cerr1*, suggests a role in anterior neural induction and somitogenesis. *Proc. Natl. Acad. Sci.* **95**, 6198–6203.

Shawlot, W., Wakamiya, M., Kwan, K. M., Kania, A., Jessell, T. M. and Behringer, R. R. (1999). Lim1 is required in both primitive streak-derived tissues and visceral endoderm for head formation in the mouse. *Development* **126**, 4925-4932.

Shawlot, W., Min Deng, J., Wakamiya, M. and Behringer, R. R. (2000). The cerberus-related gene, Cerr1, is not essential for mouse head formation. *Genesis* **26**, 253-258.

Small, E. M., Vokes, S. A., Garriock, R. J., Li, D. and Krieg, P. A. (2000). Developmental expression of the *Xenopus* Nkx2-1 and Nkx2-4 genes. *Mech. Dev.* **96**, 259-262.

Smith, W. C. and Harland, R. M. (1992). Expression cloning of noggin, a new dorsalizing factor localized to the Spemann organizer in *Xenopus* embryos. *Cell* **70**, 829-840.

Smith, W. C., McKendry, R., Ribisi, S. Jr. and Harland, R. M. (1995). A Nodal-related gene defines a physical and functional domain within the Spemann organizer. *Cell* **82**, 37-46.

Spemann, H. and Mangold, H. (1924). Über Induktion von Embryonalanlagen durch Implantation Artfremder Organisatoren. *Rouxí Arch. Entw. Mech.* **100**, 599-638.

Spemann, H. (1931). Über den Anteil von Implantat und Wirtskeim an der Orientierung und Beschaffenheit der induzierten Embryonalanlage. *Rouxí Arch. Entw. Mech.* **123**, 389-517.

Stanley, E. G., Biben, C., Allison, J., Hartley, L., Wicks, I. P., Campbell, I. K., McKinley, M., Barnett, L., Koentgen, F., Robb, L. and Harvey, R. P. (2000). Targeted insertion of a lacZ reporter gene into the mouse Cer1 locus reveals complex and dynamic expression during embryogenesis. *Genesis* **26**, 259-264.

Steinbeisser, H., Alonso, A., Epperlein, H. -H. and Trendelenburg, M. F. (1989). Expression of mouse histone H1(0) promoter sequences following microinjection into *Xenopus* oocytes and developing embryos. *Int.J.Dev.Biol.* **33**, 361-368.

Stolow, M. A. and Shi, Y. B. (1995). *Xenopus* sonic hedgehog as a potential morphogen during embryogenesis and thyroid hormone-dependent metamorphosis. *Nucleic Acids Res*. **23**, 2555-2562.

Thisse, B., Wright, C. V. and Thisse, C. (2000). Activin- and Nodal-related factors control antero-posterior patterning of the zebrafish embryo. *Nature* **403**, 425-428.

Thomas, P. and Beddington, R. (1996). Anterior primitive endoderm may be responsible for patterning the anterior neural plate in the mouse embryo. *Curr. Biol.* **6**, 1487–1496.

Townbin, H., Staehlin, T. and Gordon, J. (1979). Electrophoretic transfer of protein from polyacrylamide gels to nitrocellulose sheets: procedure and some applications. *Proc.Natl.Acad.Sci.USA* **76**, 4350-4354.

Wilson, P. A. and Hemmati-Brivanlou, A. (1995). Induction of epidermis and inhibition of neural fate by Bmp-4. *Nature* **376**, 331-333.

II.2 Characterization of the *mcer-1 cis*-Regulatory Region During Early

Development of *Xenopus*

Characterization of the *mcer-1 cis*-Regulatory Region During Early Development of

Xenopus

Ana Cristina Silva[1,2], Mário Filipe[1], Herbert Steinbeisser[3], and José António Belo[1,2,4]

In preparation

[1]Instituto Gulbenkian de Ciência, Rua da Quinta Grande, 6, Apartado 14, 2781-901 Oeiras, Portugal; [2]Centro de Biomedicina Molecular e Estrutural, Universidade do Algarve, Campus de Gambelas, 8000-010 Faro, Portugal; [3]Institute of Human Genetics, University of Heidelberg, Im Neuenheimer Feld 366, 69120 Heidelberg, Germany; [4]Author for correspondence: José A. Belo, Tel: +351214407942, Fax: +351214407970, e-mail: jbelo@igc.gulbenkian.pt.

Characterization of the *mcer-1 cis*-regulatory region during early development of *Xenopus*

Ana Cristina Silva[1,2], Mário Filipe[1], Herbert Steinbeisser[3], and José António Belo[1,2,4]

[1]Instituto Gulbenkian de Ciência, Rua da Quinta Grande, 6, Apartado 14, 2781-901 Oeiras, Portugal; [2]Centro de Biomedicina Molecular e Estrutural, Universidade do Algarve, Campus de Gambelas, 8000-010 Faro, Portugal; [3]Institute of Human Genetics, University of Heidelberg, Im Neuenheimer Feld 366, 69120 Heidelberg, Germany; [4]Author for correspondence: José A. Belo, Tel: +351214407942, Fax: +351214407970, e-mail: jbelo@igc.gulbenkian.pt.

Abstract

Cerberus related molecules are well known Wnt, Nodal and BMP inhibitors that have been implicated in different processes including anterior-posterior patterning and left-right asymmetry. In both mouse and frog, two Cerberus related genes have been isolated, *mcer-1* and *mcerl-2*, and *Xcer* and *Xcoco*, respectively. Until now, little is known about the mechanisms involved in their transcriptional regulation. Here, we report a heterologous analysis of the mouse *cerberus-like* gene upstream regulatory regions, responsible for its expression in the visceral endodermal cells. Our analysis showed that the consensus sequences for a TATA, CAAT or GC boxes were absent but a TGTGG sequence was present at position -172 to -168 bp, relative to the ATG. Using a series of deletion constructs and transient expression in *Xenopus* embryos, we found that a fragment of 1.4 kb of *mcer-1* promoter sequence could reproduce the endogenous expression pattern of *Xenopus cerberus*. A 0.7 kb mcel upstream region was able to drive reporter expression to the involuting mesendodermal cells, while further deletions abolished reporter gene expression. These results suggest that the *cis*-regulatory sequences between mammals and amphibians were conserved.

Introduction

During vertebrate embryonic development, head and anterior tissues arise from events occurring in the developing gastrula embryo. Several studies in the mouse embryo have shown that the anterior visceral endoderm (AVE) has some head-organizing

properties and was therefore suggested to be the head organizer in the mouse. In *Xenopus* embryos, the anterior dorsal endoderm (ADE) was considered to be the topological and functional equivalent of the AVE. This idea was based not only in similar topology but also due to similarities in gene expression, including, *Hex* (Newman *et al.,* 1997; Thomas *et al.,* 1998), *lim-1*, *dickkopf-1* (*dkk-1*; Glinka *et al.,* 1998) and *cerberus* (Bouwmeester *et al.,* 1996; Belo *et al.,* 1997; Biben *et al.,* 1998).

Xenopus Cerberus (*Xcer*) was the first head inducing gene to be isolated. Cerberus is a potent Wnt, BMP and Nodal inhibitor that functions in the extracellular space by creating a region, free from trunk-signaling, in the anterior part of the embryo, thereby allowing head induction and patterning. It belongs to the Cerberus/Dan gene family that includes mouse *cerberus-like* gene (*mcer-1*; Belo *et al.,* 1997; Biben *et al.,* 1998; Shawlot *et al.,* 1998), chicken *cerberus* (*ccer*; Rodriguez Esteban *et al.,* 1999; Yokouchi *et al.,* 1999; Zhu *et al.,* 1999), *Xenopus coco* (Bell *et al.,* 2003), zebrafish *charon* (Hashimoto *et al.,* 2004) and mouse *cerberus-like-2* (*mcer–2*; Marques *et al.,* 2004). *Xcer* and mouse *mcer-1* genes are expressed, during peri gastrulation, in topological equivalent embryonic structures, such as the anterior endomesoderm and anterior visceral endoderm, respectively (Bouwmeester *et al.,* 1996; Belo *et al.,* 1997). While *Xcer* expression is restricted to the gastrulation stages, *mcer-1* can be also detected at later stages in the anterior definitive mesendoderm and, during somitogenesis, in the rostral half of the two newly formed somites and rostral presomitic mesoderm.

Recent studies have shown that Nodal and Wnt downstream target genes, *Xlim-1*, *Mix-1* and *Xotx2*, and *siamois*, respectively, regulate the expression of *Xcer* in the anterior endoderm (Yamamoto *et al.,* 2003). However, little is known about the transcriptional regulation of other Cerberus related genes. In this study, we decided to investigate the molecular mechanisms underlying the regulation of the mouse *cer-1* during gastrulation. We have shown that a 4kb fragment of 5′ upstream regulatory sequences of the mouse *cer-1* gene is able to drive reporter gene (EGFP) expression in the anterior visceral endoderm (Mesnard *et al.,* 2004). In this study, we show that injection of the *mcer-1* reporter constructs into *Xenopus* embryos results in similar expression pattern to that of *Xcer*, indicating an evolutionary conservation of *cerberus* regulation during gastrulation, between mouse and *Xenopus*. Furthermore, we have analyzed the murine upstream regulatory region in *Xenopus* embryos in order to determine the regulatory elements responsible for *mcer-1* expression in the frog's anterior endoderm.

Results

Expression of the mouse *cerberus-like* promoter driving LacZ in *Xenopus* embryos.

To investigate the role of mouse Anterior Visceral Endoderm (AVE) during embryonic axis formation a mouse *cerberus-like* (*mcer-1*) transgenic line had been generated, where a 4.0 kb *mcer-1* promoter fragment, isolated from a genomic library, drove the expression of a EGFP reporter gene (Mesnard *et al.*, 2004). Mouse *cerberus-like* is expressed in the AVE during pre- and early-streak stages. By late-streak stage *mcer-1* is also detected in the anterior definitive endoderm. Later in development, *mcer-1* could be detected in the newly formed somites (Belo *et al.*, 1997). In contrast, this *mcer-1* transgenic line drives expression of EGFP exclusively in the AVE. No fluorescent cells could be found either in the definitive endoderm arising from the node or in the somites and presomitic mesoderm (Mesnard *et al.*, 2004). Therefore, the EGFP expression pattern in these transgenic embryos reflects the first expression domain detected for *mcer-1*. This means that 4 kb upstream region of *mcer-1* contains only the regulatory elements for its correct spatiotemporal expression in the AVE. Regulatory elements necessary for the expression in the definitive endoderm and the presomitic mesoderm/somites are probably present futher upstream, in the intron or downstream of *mcer-1* gene.

A β-galactosidase (LacZ) reporter construct which consisted of the whole 4.0 kb *mcer-1* fragment upstream of transcription start site (-4040 to -2) fused to a *NLS-LacZ* reporter gene (which we will name here as mcer-1 4.0; Silva *et al.*, 2003) was then produced. In parallel, a LacZ reporter construct carrying a 6.0 kb *Xenopus laevis* DNA fragment upstream the ATG (Xcer 6.0) was also generated. These clones were then microinjected into the two dorsal blastomeres of 4-cell stage *Xenopus* embryos (200pg/embryo). In both injections, LacZ activity could only be detected in the cell population that endogenously expresses *Xcer*, the anterior dorsal endoderm of gastrula embryos (ADE; Fig. 1A,B; Silva *et al.*, 2003). In addition, in a small percentage of embryos, LacZ activity could also be detected in the involuting mesendoderm, a population of cells where *Xcer* is also expressed (Jones *et al.*, 1999; Brickman *et al.*, 2000). When the ventral-vegetal blastomeres were microinjected no expression was observed (data not shown; Silva *et al.*, 2003). In contrast, microinjection of the simian cytomegalovirus promoter reporter construct (CMV-LacZ) lead to LacZ ubiquitous expression (Fig. 1C).
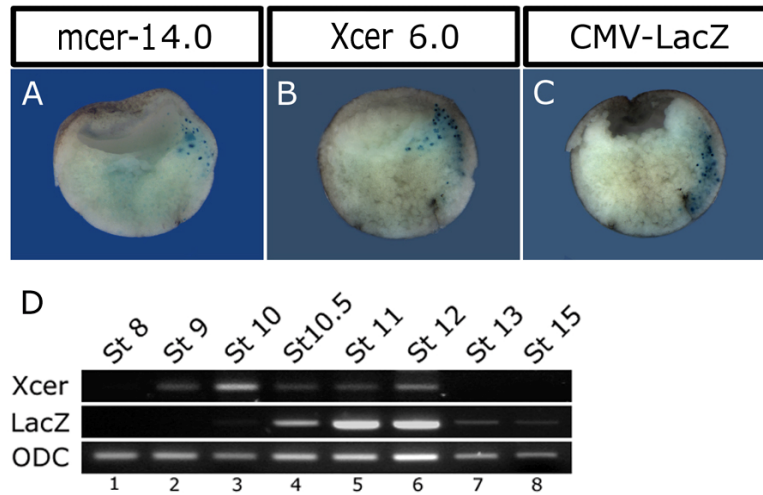
Fig. 1. Spatial and temporal expression of a *LacZ* reporter gene directed by a 4.0 kb *mcer-1* upstream promoter fragment. Comparison of LacZ expression pattern between gastrula embryos, injected with either a **(A)** 4.0 kb *mcer-1* upstream promoter driving expression of *LacZ* reporter construct (mcer-1 4.0), a **(B)** 6.0 kb Xcer upstream promoter driving expression of LacZ reporter construct (Xcer 6.0) or a **(C)** constitutively active LacZ reporter construct (CMV-LacZ). The expression pattern of mcer-1 4.0 and Xcer 6.0 are similar to that of the endogenous *Xcer* expression at gastrula stages. In all panels, the embryos are oriented with the dorsal side to the right. **D:** Time course of mcer-1 4.0 expression in *Xenopus* embryos compared with that of endogenous *Xcer*. ODC was used as a loading control.

In order to determine how faithfully *mcer-1* promoter activity is recapitulated in *Xenopus laevis* embryos, the temporal and spatial specificity of this promoter was confirmed by RT-PCR (Fig. 1D) and by *in situ* hybridization (Silva *et al.*, 2003). *Xenopus* embryos injected dorsally with the mcer-1 4.0 construct, sagitally sectioned through the dorsal lip at early gastrula stages, hybridized one half with an antisense *LacZ* probe, and the other with a antisense *Xcer* probe, showed that the region of *LacZ* expression precisely matched the endogenous expression domain of *Xcer* (Silva *et al.*, 2003). RT-PCR analysis revealed that *Xcer* starts to be expressed around stage 9, shows a peak of expression by stage 10, and is down regulated afterword (Fig. 1D). By comparison with *Xcer*, one can observe that mcer-1 4.0 shows a delay in activation and persists until very late, when *Xcer* transcripts are no longer detected (Fig. 1D). This lack of repression may be attributed to the increased stability of the *LacZ* RNA. In addition, although the reporter transcripts were no longer detected by RT-PCR in tailbud embryos, LacZ protein activity could still be detected by LacZ staining in the ADE descendent cells (data not shown). This phenomenon can be attributed to the high stability of the LacZ protein. To further elucidate on the specificity of the *mcer-1* upstream region in directing *LacZ* expression to the ADE of the *Xenopus* embryos, a dorsal blastomere from each tier of 32 cells embryos was injected either with mcer-1 4.0 or with CMV-LacZ (60 pg/embryo; Fig. 2). As shown in Fig. 2 microinjection of the CMV-LacZ construct into the A1 and B1 blastomeres

resulted in the staining of the ectoderm and involuting mesoderm, respectively, at stage 11 (Fig. 2A,A',C,C'). The observed staining is consistent with the fate map for these blastomeres at stage 11 (Fig. 2I, yellow and red staining; Moody, 1987b; Moody, 1987a; Bauer *et al.*, 1994). When either the A1 or B1 blastomeres were injected with mcer-1 4.0 reporter construct, no staining was observed at stage 11 (Fig. 2B,B',D,D'). Microinjection of C1 and D1 blastomeres with CMV-LacZ led to staining in the involuting mesoderm and anterior mesendoderm, and in the endoderm, respectively (Fig. 2E,G). Staining in the anterior endoderm was observed when either C1 or D1 blastomeres were injected with mcer-1 4.0 (Fig. 2F,H).
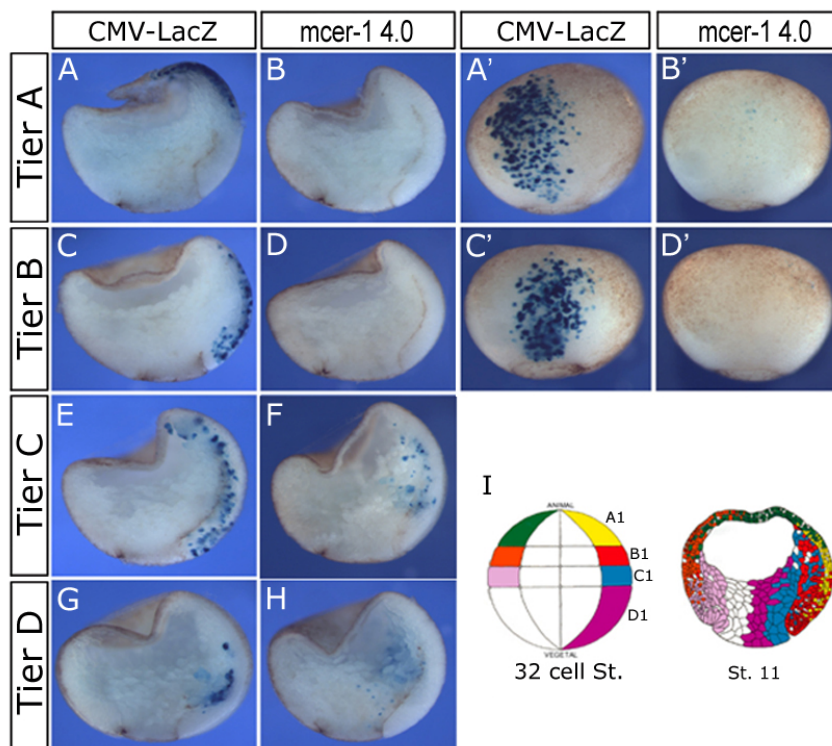
Fig. 2. Specificity of the mouse *cerberus-like* reporter construct. *Xenopus* embryos at were microinjected with 60 pg of either CMV-LacZ **(A,A',C,C',E,F)** or mcer-1 4.0 **(B,B',D,D',F,H)** reporter constructs in one dorsal blatomere at 32 cell stage. Embryos microinjected into **(A,A',B,B')** A1 blastomere, **(C,C',D,D')** B1 blastomere, **(E,F)** C1 blastomere and **(G,H)** D1 blastomere were scored for LacZ activity at stage 11. mcer-1 4.0 reported contruct was activated only when microinjected into the C1 or D1 blastomeres, that will give rise to the ADE and the involuting mesendoderm in the gastrula embryo. In contrast, CMV-LacZ was expressed in any of the injected blastomeres. The embryos are oriented with the dorsal side to the right except in **(A',B',C',D')** where dorsal is facing up. **I:** Fate map of the different blastomeres of the 32 cell embryo at stage 11 (from Bauer *et al.,* 1994).

In summary, the results observed by transiently expressing mcer-1 4.0 indicate that the 4 kb *cis*-regulatory fragment contains most of the elements necessary to mimic the correct spatiotemporal expression of *Xcer*.

Deletion study of the mouse *cerberus-like cis*-regulatory region in *Xenopus* embryos.

As a first step towards understanding the regulation of *mcer-1* in the AVE and determining if the regulation of its endodermal expression is evolutionarily conserved between mouse and *Xenopus*, we decided to transiently express constructs carrying deletions of the *mcer-1* 5′ regulatory region in *Xenopus* embryos (Fig. 3A). The different deletion reporter constructs were microinjected into the marginal zone of the dorsal blastomeres at 4 cell stage and LacZ activity was detected at gastrula stages. When sequences between -4043 bp and -1421 bp upstream from the transcription start site were deleted (corresponding to mcer-1 3.5 to mcer-1 1.4, and mcer-1 Δ-3.5/-1.4), no alteration of reporter gene expression was observed, during gastrulation (Fig. 3C-G). In all these cases LacZ expression was predominantly located in the ADE. However, in a small percentage of stained embryos (< 10%) LacZ staining was also detected in the involuting mesendoderm (IDME) in addition to the anterior endodermal domain (Fig. 3M). The expression analyses of further deletions between -1421 bp and -763 bp upstream from the start site (constructs mcer-1 0.7 and mcer-1 Δ-2.2/-0.7; Fig. 3A) revealed that the specificity of the reporter constructs was lost, resulting in an increase of the percentage of embryos showing exclusively prechordal plate staining and a drastic decrease in the percentage of embryos showing anterior endodermal staining (Fig. 3H-I',M). In contrast, when sequences between -647 bp and -181bp (constructs mcer-1 0.6, mcer-1 0.2 and mcer-1 Δ-0.7/-0.2; Fig. 3A) were deleted, expression was no longer detected or was very weak (Fig. 3J-M).

In summary, our deletion analysis showed that the 1421 bp promoter fragment is sufficient to drive reporter gene expression in the ADE of the *Xenopus* embryos, suggesting that the regulatory elements necessary for a proper expression are positioned within this region. In addition, further reduction of the promoter length to 763bp resulted in a statistically significant decrease of LacZ expression in the ADE. This indicated the presence of a regulatory region between positions -1421 and -647 responsible for the specificity of the *mcer-1* 5′ *cis*-regulatory region.
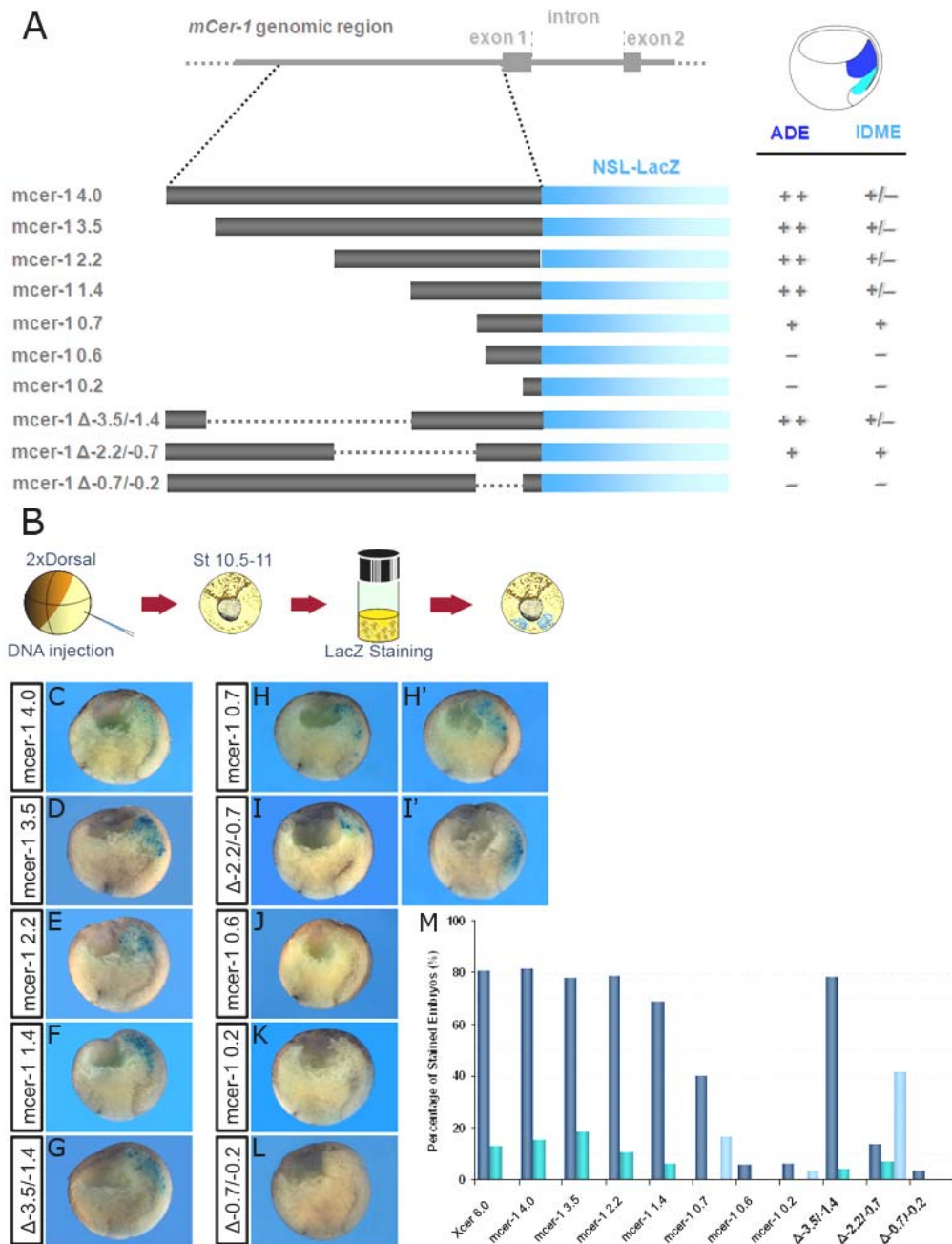
Fig. 3. Deletion analysis of *mcer-1 cis*-regulatory sequences. **A:** At the top is a map of 4.0 kb of upstream sequence, the two exons and the intron. Below are shown the promoter fragments tested. *mcer-1* upstream sequences (grey boxes) were fused to the reporter *NSL-LacZ* gene (blue boxes) to determine the activity of each DNA fragment. Positive (+) and lack (-) of LacZ expression in the anterior dorsal endoderm (ADE) and in the involuting dorsal mesendoderm (IDME) of gastrula stage *Xenopus* embryos is shown on the right. **B:** Scheme of the procedure used for the expression analysis of the *mcer-1* reporter constructs in *Xenopus* embryos. Four-cell stage *Xenopus* embryos were microinjected with the *mcer-1* reporter constructs (200 pg/embryo) and grown until gastrula stages. Embryos were then fixed, washed in PBS and the colour reaction to detect reporter gene expression was developed for 12 to 24 hours. For better visualization, embryos were hemisectioned. **(C-L)** Expression analysis of *mcer-1* deletions constructs. The embryos are oriented with the dorsal side to the right, in all panels. Constructs **C:** mcer-1 4.0 **D:** mcer-1 3.5 **E:** mcer-1 2.2 **F:** mcer-1 1.4 **G:** mcer-1 Δ-3.5/-1.4 **H,H′:** mcer-1 0.7 **I,I′:** mcer-1 Δ-2.2/-0.7 **J:** mcer-1 0.6 **K:** mcer-1 0.2 **L:** mcer-1 Δ-0.7/-0.2. **M:** Graphic representing the influence of different *mcer-1* promoter deletion constructs on its activity. The graphic shows the percentage of embryos with staining in the ADE (■), the IDME (■) or in both (■). Each experiment was repeated at least three times with 30 embryos each.

Conservation of cerberus *cis*-regulatory region across species.

In order to identify potential evolutionary conserved sequences (ECRs) that might control the expression of cerberus in different vertebrate species, we have compared the promoter sequences of mouse, *Xenopus*, human and rat *cerberus* (Fig. 4A). For this, we used VISTA tools (mVISTA; http://genome.lbl.gov/vista/index.shtml) which are useful instruments to detect conservation in large sequence fragments and compare sequences from multiple species.

Analysis and comparison of the 4-kb genomic fragment of *mcer-1* sequences to the 6-kb genomic fragment of *Xcer* did not reveal any apparent ECRs (Fig. 4A, upper lane). However, the 5′ genomic sequences of mouse, human and rat display 7 and 2 highly conserved regions (Fig. 4A, middle and lower lanes) with an overall homology of 74.2% and 82.2%, respectively (Table I).

Table I - Evolutionary conserved sequences between mouse and rat or human *cis*-regulatory regions.

mouse *vs*. rat			mouse *vs*. human		
start	end	homology	start	end	homology
-1	-392	86.8%	-87	-273	79.6%
-479	-2941	81.4%	-310	-419	71.8%
			-590	-797	73.9%
			-1522	-1634	79.8%
			-1683	-1830	69.6%
			-1914	-2079	72.9%
			-2811	-2713	70.0%

This analysis indicates that the *cerberus* promoter is highly conserved in higher vertebrates. Although *mcer-1* and his ortholog in *Xenopus*, Xcer, were expressed in topological equivalent structures no apparent sequence similarity was observed.
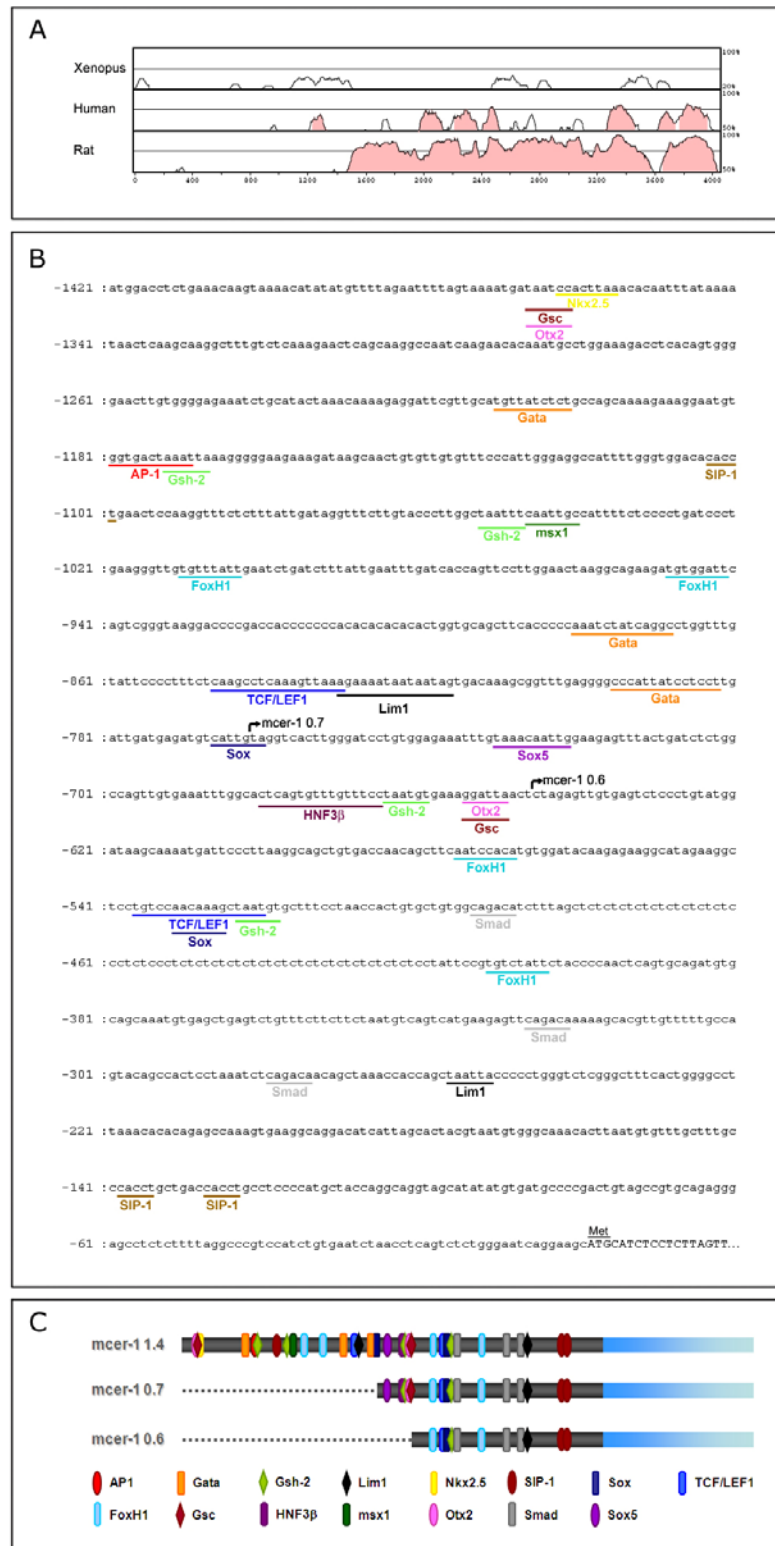
Fig. 4. Sequence analysis of the *mcer-1* upstream promoter region. **A:** Evolutionary conserved sequences between the 4.0 kb *mcer-1* upstream promoter region and the frog (upper panel), human (middle panel) and rat (lower panel) upstream promoter sequences. Intergenic conserved elements are represented in pink. **B:** Nucleotide sequence of 1421 bp upstream of the *mcer-1* ATG. The mcer-1 0.7 and mcer-1 0.6 deletion boundaries are indicated. Putative binding sites for known transcription factors are indicated. The translational start site (ATG) is outlined. **C:** Scheme of the location of potential binding sites for known transcription factors in three *mcer-1* deletion constructs.

Candidate transcription regulators for anterior endodermal specific expression of *mcer-1* in *Xenopus* embryos

To recognize possible binding sites for known transcription factors we have analyzed the *mcer-1* 1.4 kb genomic sequence using consensus detecting programs (TFSearch 1.3, and MatInspector Professional 5.2) as well as manual inspection. This analysis revealed neither the presence of the consensus sequence for a TATA box, an Inr (initiator; YYANWYY), nor a DPE (downstream core promoter element; DSWYVY). Nevertheless, a TGTGG sequence was present from position -172 to -168 and might function as a substitute TATA box sequence (Hen *et al.,* 1983; Saltzman and Weinmann, 1989).

This bioinformatics analysis showed several putative transcription factor-binding sites that may act as *cis*-regulatory elements. In Fig. 4B,C and in Table II, we highlight some of these binding sites that are present in the region between -1421 and -2 bp. This analysis revealed eight core motifs for the homeodomain factors (TAAT), including two binding sites for bicoid-type homeodomain proteins (GGATTA; Hanes and Brent, 1989; Simeone *et al.,* 1992). *Goosecoid* and *Otx2* are both bicoid related genes that are expressed, during gastrulation, both in the mouse AVE and the frog ADE superimposing with *cerberus* expressing domain (Cho *et al.,* 1991; Blum *et al.,* 1992; De Roberts *et al.,* 1992; Simeone *et al.,* 1992; Simeone *et al.,* 1993; Pannese *et al.,* 1995), which makes them good candidates for regulating *mcer-1* expression. Two binding core sites for Lim-1, which is also expressed in the head organizer (Taira *et al.,* 1992; Barnes *et al.,* 1994) and four binding core sites for Gsh-2 (CTAATKWS) were also detected. The mouse *cer-1* promoter contains two TCF/LEF1 binding sites (CTTTGWW) and an AP-1 binding site (RSTGACTMANN), downstream targets of the canonical and non-canonical Wnt signaling pathway, respectively. Both TCF/LEF1 binding sites overlap with other transcription factor binding sites and the AP-1 binding site partially overlaps with one Gsh-2 site. Sequence analyses revealed the presence of consensus binding sites for transcription factors that function as nuclear effectors of the Nodal signaling pathway, such as SMAD (GTCTAGAC) and FoxHI (AATXXACA).

Several other putative binding sites for transcription factors which are known to be expressed during gastrulation, in vertebrates, were also revealed within the regulatory region analyzed: three core binding sites for Sox (WWCAAWG), including a binding site for Sox-5 (NNAACAATNN), three GATA binding sites (RNSNNGATAANNGN,

MNAGATAANR and NNCWGATARNNNN), three SIP-1 (CACCT) consensus sequences and one HNF3β binding site (NAWTGTTTRTTT). In addition, binding sites for the transcription factors Nkx2.5 (CCACTTAA) and Msx-1 (CAATTGC) were also detected. Msx-1 which is expressed in animal pole and the ventral zone but not in the dorsal marginal zone during *Xenopus* gastrulation (Maeda *et al.,* 1997) may act as a repressor.

Table II - Putative transcription factor-binding sites present in the region between -1421 and -2 bp of the mouse cerl-1 promoter, their location and conservation in the human and rat promoter.

Transcrition factor	Location	Conserved	Transcrition factor	Location	Conserved
AP-1	-1181 to -1171		Msx1	-1048 to -1042	
FoxHI	-1012 to -1005	🐀	Nkx2.5	-1364 to -1357	
	-950 to -943	🐀	Otx2	-1368 to -1363	🐀
	-577 to -570			-656 to -651	🐀 🧍
	-413 to -406	🧍	SIP-1	-1105 to -1101	
GATA	-1212 to -1203			-140 to -136	🐀
	-882 to -870			-129 to -125	🐀 🧍
	-797 to -784		Smad	-495 to -490	🐀
Gsc	-1368 to -1363	🐀		-328 to -323	
	-656 to -651	🐀 🧍		-281 to -276	
Gsh-2	-1174 to -1169		Sox	-768 to -762	
	-1054 to -1049	🐀		-533 to -527	
	-666 to -661	🧍	Sox5	-732 to -723	🐀 🧍
	-525 to -520		TCF/LEF1	-538 to -522	
HNF3β	-682 to -667			-848 to -832	
Lim-1	-832 to -818	🐀			
	-258 to -253	🐀 🧍			

85

The sequence between -1421 bp and -763 bp was shown to be necessary for the proper spatial expression of the *mcer-1* promoter in the ADE of *Xenopus* embryos (Fig. 2). When we deleted this region, several binding sites were removed. These include binding elements for Nkx-2.5, GATAs, AP-1, Gsc/Otx2, Gsh-2, Msx-1, FoxH1, TCF/LEF-1, Lim-1 and Sox. In mcer-1 0.7 and mcer-1 Δ-2.2/-0.7 reporter constructs, which lack the above mentioned sequence, the majority of the injected embryos loose their LacZ expression in the ADE domain but not in the involution mesendodermal domain. These results showed that some of these transcription factors might be responsible for activating the reporter gene expression in the ADE. In addition, injection of mcer-1 0.6, mcer-1 0.2 or mcer-1 Δ-0.7/-0.2 reporter constructs, completely abolished LacZ expression. These regulatory sequences lack elements for Gsh-2, Gsc/Otx2, HNF3β and Sox5. Thus, some of these transcription factors might be essential for the regulation of m*cer-1*. In fact, when the promoter sequences of mouse, human and rat where compared for the presence of evolutionary conserved *cis*-regulatory elements one could observe that both Sox5 and Otx2/Gsc binding sites showed the highest degree of conservation (TableII).

Discussion

Study of Cerberus regulation during gastrulation using a cross species approach.

The expression of the mouse *cerberus-like* during embryonic development is initiated as early as E5.5 on the anterior side of the visceral endoderm, including the distal tip, as described previously (Belo *et al.,* 1997). As the primitive streak starts to form, *mcer-1* expression is restricted to the anterior side and, at late streak, E6.5-E7.0, a new domain of expression is detected in the definitive endoderm cells emerging from the node. At neural plate stages, the expression of m*cerl-1* is excluded from the node and by early headfold stage, E7.5, *mcer-1* transcripts are confined to the midline, including anterior gut endoderm and mesoderm from the prechordal and notochordal plates. During early somitogenesis, *mcer-1* expression starts to be downregulated in the anterior domain and appears in a new domain, comprising the last two somites formed and the more rostral portion of the presomitic mesoderm (Belo *et al.,* 1997). In contrast, *Xenopus* Cerberus is exclusively expressed during gastrula stages in two domains, the anterior dorsal endoderm (ADE) that is considered to be the topological and functional equivalent of the mouse embryo anterior visceral endoderm (AVE), and the involuting mesendoderm,

which will later become the pre-chordal plate (Bouwmeester *et al.,* 1996; Jones *et al.,* 1999; Brickman *et al.,* 2000).

Until recently, very little was known about the gene regulatory elements involved in regulating expression of vertebrate Cerberus related genes. In the last years, a study undertook a detailed analysis of the *cis*-regulatory region of *Xenopus cerberus* required for expression within ADE (Yamamoto *et al.,* 2003) and showed that *Xcer* is a direct target gene for Xlim-1, Mix-1, Xotx2, and Siamois. In previous work, a transgenic mouse line was generated in which EGFP was expressed in the AVE under the control of a 4.0 kb *cis*-regulatory fragment upstream of the *mcer-1* gene, with the purpose of isolating novel genes involved in forebrain induction and patterning (Mesnard *et al.,* 2004; Filipe *et al.,* unpublished). In this transgenic line, the EGFP expression was observed only in the AVE while no fluorescent cells could be found either in the definitive endoderm, somites or presomitic mesoderm. Thus, the 4.0 kb regulatory fragment could only mimic the first domain of expression of *mcer-1,* which indicated that it contained the regulatory elements for the AVE and that *mcer-1* expression requires at least two regulatory regions. The early expression of *mcer-1* in the AVE requires the 5′ regulatory elements of the gene, while the regulatory elements necessary for the expression in the definitive endoderm and the presomitic mesoderm/somites must lie further upstream, in the intron or downstream of the *mcer-1* coding sequence. We have already isolated the *mcer-1* intron and 3 kb of 3′ downstream region and subcloned in a beta-globin minimal promoter-LacZ construct. In the future, these constructs will be used to search for the regulatory elements necessary to drive expression in the definitive endoderm and in the somites/presomitic mesoderm.

The aim of this study was to identify the *mcer-1 cis*-regulatory elements responsible for driving its expression in the AVE. By determining how the expression of *mcer-1* is regulated, we hope to be able to better understand how endoderm is formed and patterned. To investigate the regulation of *mcer-1* expression in the AVE, we have performed a cross-species study where the regulation of the *mcer-1* gene was analyzed by transiently expressing a series of reporter deletion constructs in *Xenopus laevis* embryos. This approach led to a rapid identification of a region of the *mcer-1 cis*-regulatory region necessary for the expression of *mcer-1* in the ADE, the topological equivalent of the mouse AVE.

Our results showed that microinjection of a LacZ reporter construct, containing the 4.0 kb *mcer-1* upstream promoter fragment, into *Xenopus* embryos resulted in a specific

spatial and temporal activation of the reporter gene. Like endogenous *Xcer*, reporter gene expression was shown to be initially activated in the non-involuting anterior dorsal endoderm and in the involuting mesendoderm, and down-regulated after gastrulation. In addition, it was never expressed in the ventral side, even when injected in the ventral blastomeres. These results indicated that the *mcer-1* promoter could be used to overexpress wildtype or mutant proteins specifically in *Xenopus* ADE.

mcer-1 regulatory region.

In vivo experiments, where a *mcer-1* promoter deletion was microinjected into *Xenopus laevis* embryos showed that the elements necessary for driving expression in the ADE are present within the 1.4 kb fragment upstream of the ATG. Our results also showed that, although expression was predominantly found in the ADE, in a small percentage of embryos, deletions up to the 1.4 kb fragment resulted in additional reporter marker expression in the involuting mesendoderm. A small 763 bp fragment was able to drive expression predominantly in the involuting mesendoderm but had a reduced ability to drive expression to the ADE during gastrula stages. Fragments smaller than 647 bp, were no longer able to induce LacZ expression. In addition, while deleting the fragment between -1421 and -763 only led to a decrease of LacZ expression in the ADE and increase of LacZ activity exclusively in the involuting mesendoderm, deletion of the -763 to -647 portion completely abolished LacZ expression. The elements required for *mcer-1* expression during gastrula stages in the frog embryo, are therefore likely to be present in the 0.76 kb to 1.4 kb region upstream of the translation start site. Within this region, we were able to identify two distinct enhancers, one required for specific expression (bases -1421 to -763) and one required for general promoter activity (bases -763 to -647).

Although our analysis of the 4.0 kb *mcer-1* promoter fragment did not contain a consensus TATA box sequence, initiator or downstream core promoter element, a TGTGG sequence was present, which can also position the RNA polymerase II at the transcription start site (Saltzman and Weinmann, 1989; Holtzman *et al.,* 1991).

Several binding sites for known transcription factors were identified in the two regulatory regions mentioned above. Among them there are genes that have been described to play a role in anterior-posterior axis formation/patterning and are expressed in the mouse AVE and in its topological equivalent in the frog: *otx2*, *lim-1*, *gsc*, *Sox17* and *HNF3β* (Thomas and Beddington, 1996; Belo *et al.,* 1997; Perea-Gomez *et al.,* 2001).

Deletion of the region located between base -1421 and -763 in the *mcer-1* promoter resulted in the removal of binding elements for a homeodomain transcription factor, Nkx2.5, GATA, AP-1, Gsh-2, SIP-1, Msx-1, FoxH1, TCF/LEF, Sox and Lim-1. As a result of this deletion, reporter gene expression in the ADE was reduced. In this portion of the *mcer-1* promoter we could find several TAAT sites which are known to be homeodomain-binding sites. In particular, the presence of putative sites for bicoid-type homeodomains could be of interest. Evidence has suggested that *otx2*, a member of the bicoid homeobox gene family, is required for *cerberus* expression and is coexpressed with *Xcer* and *mcer-1* in the involuting mesendoderm and in the AVE, respectively (Simeone *et al.,* 1992; Simeone *et al.,* 1993; Pannese *et al.,* 1995). Moreover, Otx2 binding sites have been found in upstream regions of *Xcer*, *mcer-1*, h*cer* and r*cer genes*. Indeed, these sites were shown to be required for the expression of *Xcer* (Yamamoto *et al.,* 2003). Although *mcer-1* is expressed in either *otx2*$^{-/-}$ or *cripto*$^{-/-}$ single mutants, its expression was abolished in *otx2*$^{-/-}$;*cripto*$^{-/-}$ double homozygous mutant embryos (Kimura *et al.,* 2001). Thus, Otx2 could be a potential regulator of the *mcer-1* expression in the AVE. The homeobox protein Goosecoid (Gsc) has also been reported to recognize the same target sequences as Otx2, which could lead to binding competition between Otx2 and Gsc (Wilson *et al.,* 1993). Resembling *otx2*, *gsc* is expressed in the dorsal mesendoderm of the frog embryo at the beginning of gastrulation, as well as in the mouse AVE (Steinbeisser and De Robertis, 1993; Belo *et al.,* 1997). However, the fact the homozygous *gsc* mutants presented no gastrulation defects (Rivera-Perez *et al.,* 1995; Yamada *et al.,* 1995) argues against its possible role in regulating *mcer-1* expression during gastrulation.

One of the possible candidates that might be involved in regulation of *mcer-1* is Lim-1. *Lim-1* is coexpressed with *mcer-1* in the mouse AVE, during gastrula stages. Similarly, its *Xenopus* counterpart, *Xlim-1*, is coexpressed with *Xcer* at the early gastrula stage in the ADE of the *Xenopus* embryo. Previous work has demonstrated that *Xcer* is a direct target of Xlim-1 (Yamamoto *et al.,* 2003) and that *mcer-1* expression is abolished in *lim-1* null mutant mouse embryos (Shawlot *et al.,* 1998).

Consensus sequences for SOX-type DNA binding proteins were also found in the *mcer-1* regulatory regions and were shown to be necessary for its expression. Among the *Sox* genes known to be expressed during gastrulation (Hudson *et al.,* 1997; Penzel *et al.,* 1997; Mizuseki *et al.,* 1998; Sasai, 2001), *Sox17* plays an important role in endoderm

formation by regulating the transcription of several endodermal markers, such as *HNF3β* (Ruiz i Altaba *et al.,* 1993) and *endodermin* (Clements *et al.,* 2003).

The importance of the Nodal/activin and Wnt signaling pathways in regulating *cerberus* expression has already been described (Bouwmeester *et al.,* 1996; Osada and Wright, 1999; Zorn *et al.,* 1999; Agius *et al.,* 2000). Both *Xcer* and *mcer-1* were shown to be induced by Nodal (Waldrip *et al.,* 1998; Osada *et al.,* 2000; Brennan *et al.,* 2001). The Nodal response elements that bind FoxH1 and Smad2/4 transcription factors have been well characterized (Chen *et al.,* 1997). Unlike what was described for *Xcer* promoter, in the *mcer-1* promoter we were able to detect three Smad and four FoxH1 elements. The presence of three Smad binding sites in the *mcer-1* promoter has already been described (Katoh and Katoh, 2006). Our analysis of *mcer-1* promoter deletion constructs showed that the promoter fragment containing the Smad binding sites is no longer able to drive the reporter expression, suggesting that these regulatory elements are not sufficient to activate transcription. Yamamoto *et al.* (2003) have shown that Nodal regulation of *Xcer* gene transcription was achieved through the direct binding of the Nodal effectors, Xlim-1 and Xotx2 to the *Xcer* promoter. In addition, the same authors have demonstrated that, although *Xcer* promoter had no Tcf/Lef binding sites, Wnt signaling was able to regulate *Xcer* expression in an indirect way, via Siamois. Two Tcf/Lef binding sites (Brannon *et al.,* 1997; Laurent *et al.,* 1997; McKendry *et al.,* 1997) are present in the *mcer-1* 4.0 kb promoter fragment. Altogether, these findings suggested that the Nodal/activin and Wnt signaling pathways may regulate *mcer-1* expression in a direct way.

Mouse *cer-1* gene regulation might also be achieved via binding of transcriptional repressors, as seen for the regulation of other genes during frog gastrulation, such as *gsc* (Trindade *et al.,* 1999; Mochizuki *et al.,* 2000), *Xbra* (Lerchner *et al.,* 2000) and *Xlim-1* (Rebbert and Dawid, 1997). The 1.4 kb *mcer-1* regulatory fragment contains core motifs for the binding of two possible repressors, SIP-1 and Msx-1. SIP-1 is a member of the δEF1 family of zinc finger/homeodomain-like transcriptional repressors (Sekido *et al.,* 1997; Verschueren *et al.,* 1999), and shown to interact with the activated form of Smad proteins and interfere with transcription of several genes, including *Xbra* and *endodermin* (Verschueren *et al.,* 1999; Ahmed *et al.,* 2004). Furthermore, the *Xenopus* homologue of *SIP-1*, *XSIP-1*, is expressed during early gastrula stages in the dorsal ectoderm although, weakly in the midline (van Grunsven *et al.,* 2000). On the other hand, *Xmsx-1*, member of the Xvent family, has been reported as BMP-4 downstream target gene and is expressed,

during gastrulation, in marginal zone and animal pole area, both laterally and ventrally, but excluded from the dorsal side (Maeda *et al.,* 1997). Previous studies have demonstrated the requirement of *Xmsx-1* not only for neural induction but also during head induction and formation (Ishimura *et al.,* 2000; Yamamoto *et al.,* 2001). Additionally, it was shown to function as a negative regulator of *Xcer*, *Xhex* and *Xdkk-1* expression via Nodal signaling (Yamamoto *et al.,* 2001). One could hypothesize that XSIP-1 and Xmsx-1 transcription factors might play a role in restricting *mcer-1* expression to the involuting and non-involuting anterior dorsal endoderm. While, Xmsx-1 would repress *mcer-1* expression both in the ventral and lateral marginal zone as well as in the animal pole region, restricting its expression to the dorsal side of the embryo, XSIP-1 would repress *mcer-1* in the dorsal ectoderm.

Within the -763/-647 region of *mcer-1* promoter, shown to be essential to activate *mcer-1* expression in *Xenopus* embryos, we also found motifs for Sox5, HNF3β, Gsh2, Otx2 and Gsc transcription factors. Previous studies have shown that *HNF3β* is expressed in the organizer of vertebrate embryos, including those of mouse and frog (Ruiz i Altaba *et al.,* 1993). Indeed, genetic studies have shown that *HNF3β* expression in the AVE is necessary for proper development (Dufort *et al.,* 1998) and that *HNF3β-/-·lim-1-/-* and *FoxA2-/-* mutant mouse embryos display a severe reduction or absence of expression of m*cer-1* in the AVE (Perea-Gomez *et al.,* 1999; Yang and Klingensmith, 2006).

Evolutionary conservation of Cerberus regulation

M*cer-1* and *Xcer* genes have similar expression patterns during gastrulation (Bouwmeester *et al.,* 1996; Belo *et al.,* 1997). Moreover, the Cerberus-related proteins encoded by these genes seem to have a similar activity, which is to restrict the trunk signaling molecules to the posterior region of the embryo. While both XCer and mCer-1 are able to bind and antagonize Nodal and BMP-4 signals, only XCer is able to bind to Xwnt8 and inhibit its signaling pathway (Piccolo *et al.,* 1999; Belo *et al.,* 2000; Silva *et al.,* 2003). The comparison between the 4.0 kb cis-regulatory fragment of *mcer-1* and the 5′ regulatory sequences of human, rat and *Xenopus cerberus*-related genes using VISTA programs found a high degree of similarity between the mammalian sequences but was unable to detect any evolutionary conserved regions in the *Xcer* promoter when compared to the mammalian promoters. Nevertheless, the *mcer-1* promoter was only activated in the dorsal anterior structures when injected into *Xenopus* animal dorsal blastomeres,

demonstrating regional specificity. In our study, the cross-species analysis of the *mcer-1* upstream promoter region revealed that the upstream regulators of *mcer-1* AVE enhancer are present in the frog ADE and IDME, and suggested that their regulation at the mechanistic level is conserved.

Comparison of the mouse, human and rat *cerberus* promoters reveals a region of high similarity corresponding to nucleotides -797 to -590 of the *mcer-1* promoter (Table I). Within this region are located a Sox5 and an Otx2/Gsc binding sites. A similar juxtaposition of Sox5 and Otx2/Gsc sites is also present in both human and rat promoters. In addition, the observations that *mcer-1* expression is abolished in mice lacking functional Otx2 and Cripto proteins (Kimura *et al.*, 2001), and Otx2 binds directly to *Xcer* promoter, which is important for its regulation (Yamamoto *et al.*, 2003), suggest that *mcer-1* might also be directly regulated by Otx2.

Taken together, the results obtained in this study are supported by previous work that suggested that the regulation of *mcer-1* expression in the AVE resulted from a molecular cascade involving HNF3b, Lim-1, Otx2, ActRIB and Smad2 (Shawlot *et al.*, 1998; Waldrip *et al.*, 1998; Perea-Gomez *et al.*, 1999; Brennan *et al.*, 2001; Yamamoto *et al.*, 2003; Yang and Klingensmith, 2006). Finally, it is necessary to mention that further experiments need to be performed to understand which of the above mentioned *cis*-regulatory elements are essential and/or sufficient for promoter activity in the *Xenopus* ADE. Furthermore, we will investigate the effects of overexpressing different transcription factors in the regulation of *mcer-1*, investigate their direct binding and activation and identify the sequence motifs involved. Future experiments will also include generation of transient transgenic mice to validate the results obtained in the frog and show whether the elements necessary for activating *mcer-1* promoter in the ADE of *Xenopus* embryos and in the mouse AVE are the same.

Experimental Procedures

Xenopus **embryo manipulations**

Xenopus eggs were obtained from females injected with 300 IU of human chorionic gonadotrophin (Sigma), and *in vitro* fertilization was done with macerated testis. Eggs were dejellied with a 2% cysteine hydrochloride pH 8 solution and the embryos were microinjected in 1X MBS-H (88 mM NaCl, 1 mM KCl, 2.4 mM NaHCO$_3$, 0.82 mM MgSO$_4$, 0.41 mM CaCl$_2$, 0.33 mM Ca(NO$_3$)$_2$, 10 mM HEPES pH 7.4, 10 µg/ml streptomycin sulfate

and 10 µg/ml penicillin). Embryos were grown in 0.1XMBS-H until gastrulation and staged according to Nieuwkoop and Faber (1967).

Constructs

The mcer-1 4.0 reporter construct used in this study was generated as described in a previous work (McerP-LacZ; Silva *et al.,* 2003). The deletion constructs of the *mcer-1* 5′ flanking region were generated by restriction enzyme digestion.

The *XCer* 6.0 kb 5′ genomic region subcloned in pBluescriptIIKS+ (Stratagene) was a gift from A.T. Tavares. This 6.0 kb upstream region was then subcloned into pBluescriptIIKS+ containing a ß-galactosidase CDS with a nuclear localization signal and the SV40 polyA signal.

RT-PCR

Total RNA was prepared from embryos with Trizol reagent (Invitrogen) and treated with RNase-free DNase I (Promega). First strand cDNA primed by random hexamers was synthesized with AMV reverse transcriptase (Roche) and PCR was performed using standard conditions and the following sets of primers: LacZ-F (5′-CACCAGCAGCAGTTTTTCCAGTTCC-3′) and LacZ-R (5′-CGTAATCAGCACCGCATCAGCAAGT-3′), 27 cycles, 55 $^{\circ}$C; Xcer-F (5′-GCTGAACTATTTGATTTCACC-3′), Xcer-R (5′-ATGGCTTGTATTCTGTGGGGCG-3′), 35 cycles, 55°C.

β-galactosidade staining of *Xenopus laevis* embryos

Embryos injected with promoter driven NLS-LacZ constructs were selected at the desired stage, transferred to glass vials and fixed for 15 min, at RT, in freshly prepared MEMFA. The embryos were washed in 1xPBS at RT followed by a short rinse with LacZ-staining solution [2mM MgCl$_2$, 5mM K$_3$Fe(CN)$_6$, 5mM K$_4$Fe(CN)$_6$.3H$_2$O, PBS (pH 7.4)]. The staining solution was exchanged to LacZ-staining solution containing 1mg/mL X-Gal and incubated at 37°C. The staining reaction was stopped by several washes with 1xPBS. Finally, the embryos were refixed in MEMFA for 2h at RT and hemi-sectioned along the dorsal-ventral axis to check for internal staining.

Acknowledgments

References

Agius E, Oelgeschlager M, Wessely O, Kemp C, De Robertis EM. 2000. Endodermal Nodal-related signals and mesoderm induction in Xenopus. Development 127:1173-1183.

Ahmed N, Howard L, Woodland HR. 2004. Early endodermal expression of the Xenopus Endodermin gene is driven by regulatory sequences containing essential Sox protein-binding elements. Differentiation 72:171-184.

Barnes JD, Crosby JL, Jones CM, Wright CV, Hogan BL. 1994. Embryonic expression of Lim-1, the mouse homolog of Xenopus Xlim-1, suggests a role in lateral mesoderm differentiation and neurogenesis. Dev Biol 161:168-178.

Bauer DV, Huang S, Moody SA. 1994. The cleavage stage origin of Spemann's Organizer: analysis of the movements of blastomere clones before and during gastrulation in Xenopus. Development 120:1179-1189.

Bell E, Munoz-Sanjuan I, Altmann CR, Vonica A, Brivanlou AH. 2003. Cell fate specification and competence by Coco, a maternal BMP, TGFbeta and Wnt inhibitor. Development 130:1381-1389.

Belo JA, Bachiller D, Agius E, Kemp C, Borges AC, Marques S, Piccolo S, De Robertis EM. 2000. Cerberus-like is a secreted BMP and nodal antagonist not essential for mouse development. Genesis 26:265-270.

Belo JA, Bouwmeester T, Leyns L, Kertesz N, Gallo M, Follettie M, De Robertis EM. 1997. Cerberus-like is a secreted factor with neutralizing activity expressed in the anterior primitive endoderm of the mouse gastrula. Mech Dev 68:45-57.

Biben C, Stanley E, Fabri L, Kotecha S, Rhinn M, Drinkwater C, Lah M, Wang CC, Nash A, Hilton D, Ang SL, Mohun T, Harvey RP. 1998. Murine cerberus homologue mCer-1: a candidate anterior patterning molecule. Dev Biol 194:135-151.

Blum M, Gaunt SJ, Cho KW, Steinbeisser H, Blumberg B, Bittner D, De Robertis EM. 1992. Gastrulation in the mouse: the role of the homeobox gene goosecoid. Cell 69:1097-1106.

Bouwmeester T, Kim S, Sasai Y, Lu B, De Robertis EM. 1996. Cerberus is a head-inducing secreted factor expressed in the anterior endoderm of Spemann's organizer. Nature 382:595-601.

Brannon M, Gomperts M, Sumoy L, Moon RT, Kimelman D. 1997. A beta-catenin/XTcf-3 complex binds to the siamois promoter to regulate dorsal axis specification in Xenopus. Genes Dev 11:2359-2370.

Brennan J, Lu CC, Norris DP, Rodriguez TA, Beddington RS, Robertson EJ. 2001. Nodal signalling in the epiblast patterns the early mouse embryo. Nature 411:965-969.

Brickman JM, Jones CM, Clements M, Smith JC, Beddington RS. 2000. Hex is a transcriptional repressor that contributes to anterior identity and suppresses Spemann organiser function. Development 127:2303-2315.

Chen X, Weisberg E, Fridmacher V, Watanabe M, Naco G, Whitman M. 1997. Smad4 and FAST-1 in the assembly of activin-responsive factor. Nature 389:85-89.

Cho KW, Blumberg B, Steinbeisser H, De Robertis EM. 1991. Molecular nature of Spemann's organizer: the role of the Xenopus homeobox gene goosecoid. Cell 67:1111-1120.

Clements D, Cameleyre I, Woodland HR. 2003. Redundant early and overlapping larval roles of Xsox17 subgroup genes in Xenopus endoderm development. Mech Dev 120:337-348.

De Roberts EM, Blum M, Niehrs C, Steinbeisser H. 1992. Goosecoid and the organizer. Dev Suppl:167-171.

Dufort D, Schwartz L, Harpal K, Rossant J. 1998. The transcription factor HNF3beta is required in visceral endoderm for normal primitive streak morphogenesis. Development 125:3015-3025.

Glinka A, Wu W, Delius H, Monaghan AP, Blumenstock C, Niehrs C. 1998. Dickkopf-1 is a member of a new family of secreted proteins and functions in head induction. Nature 391:357-362.

Hanes SD, Brent R. 1989. DNA specificity of the bicoid activator protein is determined by homeodomain recognition helix residue 9. Cell 57:1275-1283.

Hashimoto H, Rebagliati M, Ahmad N, Muraoka O, Kurokawa T, Hibi M, Suzuki T. 2004. The Cerberus/Dan-family protein Charon is a negative regulator of Nodal signaling during left-right patterning in zebrafish. Development 131:1741-1753.

Hen R, Borrelli E, Sassone-Corsi P, Chambon P. 1983. An enhancer element is located 340 base pairs upstream from the adenovirus-2 E1A capsite. Nucleic Acids Res 11:8747-8760.

Holtzman EJ, Soper BW, Stow JL, Ausiello DA, Ercolani L. 1991. Regulation of the G-protein alpha i-2 subunit gene in LLC-PK1 renal cells and isolation of porcine genomic clones encoding the gene promoter. J Biol Chem 266:1763-1771.

Hudson C, Clements D, Friday RV, Stott D, Woodland HR. 1997. Xsox17alpha and -beta mediate endoderm formation in Xenopus. Cell 91:397-405.

Ishimura A, Maeda R, Takeda M, Kikkawa M, Daar IO, Maeno M. 2000. Involvement of BMP-4/msx-1 and FGF pathways in neural induction in the Xenopus embryo. Dev Growth Differ 42:307-316.

Jones CM, Broadbent J, Thomas PQ, Smith JC, Beddington RS. 1999. An anterior signalling centre in Xenopus revealed by the homeobox gene XHex. Curr Biol 9:946-954.

Katoh M, Katoh M. 2006. CER1 is a common target of WNT and NODAL signaling pathways in human embryonic stem cells. Int J Mol Med 17:795-799.

Kimura C, Shen MM, Takeda N, Aizawa S, Matsuo I. 2001. Complementary functions of Otx2 and Cripto in initial patterning of mouse epiblast. Dev Biol 235:12-32.

Laurent MN, Blitz IL, Hashimoto C, Rothbacher U, Cho KW. 1997. The Xenopus homeobox gene twin mediates Wnt induction of goosecoid in establishment of Spemann's organizer. Development 124:4905-4916.

Lerchner W, Latinkic BV, Remacle JE, Huylebroeck D, Smith JC. 2000. Region-specific activation of the Xenopus brachyury promoter involves active repression in ectoderm and endoderm: a study using transgenic frog embryos. Development 127:2729-2739.

Maeda R, Kobayashi A, Sekine R, Lin JJ, Kung H, Maeno M. 1997. Xmsx-1 modifies mesodermal tissue pattern along dorsoventral axis in Xenopus laevis embryo. Development 124:2553-2560.

Marques S, Borges AC, Silva AC, Freitas S, Cordenonsi M, Belo JA. 2004. The activity of the Nodal antagonist Cerl-2 in the mouse node is required for correct L/R body axis. Genes Dev 18:2342-2347.

McKendry R, Hsu SC, Harland RM, Grosschedl R. 1997. LEF-1/TCF proteins mediate wnt-inducible transcription from the Xenopus nodal-related 3 promoter. Dev Biol 192:420-431.

Mesnard D, Filipe M, Belo JA, Zernicka-Goetz M. 2004. The anterior-posterior axis emerges respecting the morphology of the mouse embryo that changes and aligns with the uterus before gastrulation. Curr Biol 14:184-196.

Mizuseki K, Kishi M, Matsui M, Nakanishi S, Sasai Y. 1998. Xenopus Zic-related-1 and Sox-2, two factors induced by chordin, have distinct activities in the initiation of neural induction. Development 125:579-587.

Mochizuki T, Karavanov AA, Curtiss PE, Ault KT, Sugimoto N, Watabe T, Shiokawa K, Jamrich M, Cho KW, Dawid IB, Taira M. 2000. Xlim-1 and LIM domain binding protein 1 cooperate with various transcription factors in the regulation of the goosecoid promoter. Dev Biol 224:470-485.

Moody SA. 1987a. Fates of the blastomeres of the 16-cell stage Xenopus embryo. Dev Biol 119:560-578.

Moody SA. 1987b. Fates of the blastomeres of the 32-cell-stage Xenopus embryo. Dev Biol 122:300-319.

Newman CS, Chia F, Krieg PA. 1997. The XHex homeobox gene is expressed during development of the vascular endothelium: overexpression leads to an increase in vascular endothelial cell number. Mech Dev 66:83-93.

Nieuwkoop PD, Faber J. 1967. Normal table of Xenopus laevis (Daudin). Amsterdam: North Holland.

Osada SI, Saijoh Y, Frisch A, Yeo CY, Adachi H, Watanabe M, Whitman M, Hamada H, Wright CV. 2000. Activin/nodal responsiveness and asymmetric expression of a Xenopus nodal-related gene converge on a FAST-regulated module in intron 1. Development 127:2503-2514.

Osada SI, Wright CV. 1999. Xenopus nodal-related signaling is essential for mesendodermal patterning during early embryogenesis. Development 126:3229-3240.

Pannese M, Polo C, Andreazzoli M, Vignali R, Kablar B, Barsacchi G, Boncinelli E. 1995. The Xenopus homologue of Otx2 is a maternal homeobox gene that demarcates and specifies anterior body regions. Development 121:707-720.

Penzel R, Oschwald R, Chen Y, Tacke L, Grunz H. 1997. Characterization and early embryonic expression of a neural specific transcription factor xSOX3 in Xenopus laevis. Int J Dev Biol 41:667-677.

Perea-Gomez A, Rhinn M, Ang SL. 2001. Role of the anterior visceral endoderm in restricting posterior signals in the mouse embryo. Int J Dev Biol 45:311-320.

Perea-Gomez A, Shawlot W, Sasaki H, Behringer RR, Ang S. 1999. HNF3beta and Lim1 interact in the visceral endoderm to regulate primitive streak formation and anterior-posterior polarity in the mouse embryo. Development 126:4499-4511.

Piccolo S, Agius E, Leyns L, Bhattacharyya S, Grunz H, Bouwmeester T, De Robertis EM. 1999. The head inducer Cerberus is a multifunctional antagonist of Nodal, BMP and Wnt signals. Nature 397:707-710.

Rebbert ML, Dawid IB. 1997. Transcriptional regulation of the Xlim-1 gene by activin is mediated by an element in intron I. Proc Natl Acad Sci U S A 94:9717-9722.

Rivera-Perez JA, Mallo M, Gendron-Maguire M, Gridley T, Behringer RR. 1995. Goosecoid is not an essential component of the mouse gastrula organizer but is required for craniofacial and rib development. Development 121:3005-3012.

Rodriguez Esteban C, Capdevila J, Economides AN, Pascual J, Ortiz A, Izpisua Belmonte JC. 1999. The novel Cer-like protein Caronte mediates the establishment of embryonic left-right asymmetry. Nature 401:243-251.

Ruiz i Altaba A, Prezioso VR, Darnell JE, Jessell TM. 1993. Sequential expression of HNF-3 beta and HNF-3 alpha by embryonic organizing centers: the dorsal lip/node, notochord and floor plate. Mech Dev 44:91-108.

Saltzman AG, Weinmann R. 1989. Promoter specificity and modulation of RNA polymerase II transcription. Faseb J 3:1723-1733.

Sasai Y. 2001. Roles of Sox factors in neural determination: conserved signaling in evolution? Int J Dev Biol 45:321-326.

Sekido R, Murai K, Kamachi Y, Kondoh H. 1997. Two mechanisms in the action of repressor deltaEF1: binding site competition with an activator and active repression. Genes Cells 2:771-783.

Shawlot W, Deng JM, Behringer RR. 1998. Expression of the mouse cerberus-related gene, Cerr1, suggests a role in anterior neural induction and somitogenesis. Proc Natl Acad Sci U S A 95:6198-6203.

Silva AC, Filipe M, Kuerner KM, Steinbeisser H, Belo JA. 2003. Endogenous Cerberus activity is required for anterior head specification in Xenopus. Development 130:4943-4953.

Simeone A, Acampora D, Gulisano M, Stornaiuolo A, Boncinelli E. 1992. Nested expression domains of four homeobox genes in developing rostral brain. Nature 358:687-690.

Simeone A, Acampora D, Mallamaci A, Stornaiuolo A, D'Apice MR, Nigro V, Boncinelli E. 1993. A vertebrate gene related to orthodenticle contains a homeodomain of the bicoid class and demarcates anterior neuroectoderm in the gastrulating mouse embryo. Embo J 12:2735-2747.

Steinbeisser H, De Robertis EM. 1993. Xenopus goosecoid: a gene expressed in the prechordal plate that has dorsalizing activity. C R Acad Sci III 316:959-971.

Taira M, Jamrich M, Good PJ, Dawid IB. 1992. The LIM domain-containing homeo box gene Xlim-1 is expressed specifically in the organizer region of Xenopus gastrula embryos. Genes Dev 6:356-366.

Thomas P, Beddington R. 1996. Anterior primitive endoderm may be responsible for patterning the anterior neural plate in the mouse embryo. Curr Biol 6:1487-1496.

Thomas PQ, Brown A, Beddington RS. 1998. Hex: a homeobox gene revealing peri-implantation asymmetry in the mouse embryo and an early transient marker of endothelial cell precursors. Development 125:85-94.

Trindade M, Tada M, Smith JC. 1999. DNA-binding specificity and embryological function of Xom (Xvent-2). Dev Biol 216:442-456.

van Grunsven LA, Papin C, Avalosse B, Opdecamp K, Huylebroeck D, Smith JC, Bellefroid EJ. 2000. XSIP1, a Xenopus zinc finger/homeodomain encoding gene highly expressed during early neural development. Mech Dev 94:189-193.

Verschueren K, Remacle JE, Collart C, Kraft H, Baker BS, Tylzanowski P, Nelles L, Wuytens G, Su MT, Bodmer R, Smith JC, Huylebroeck D. 1999. SIP1, a novel zinc finger/homeodomain repressor, interacts with Smad proteins and binds to 5'-CACCT sequences in candidate target genes. J Biol Chem 274:20489-20498.

Waldrip WR, Bikoff EK, Hoodless PA, Wrana JL, Robertson EJ. 1998. Smad2 signaling in extraembryonic tissues determines anterior-posterior polarity of the early mouse embryo. Cell 92:797-808.

Wilson D, Sheng G, Lecuit T, Dostatni N, Desplan C. 1993. Cooperative dimerization of paired class homeo domains on DNA. Genes Dev 7:2120-2134.

Yamada G, Mansouri A, Torres M, Stuart ET, Blum M, Schultz M, De Robertis EM, Gruss P. 1995. Targeted mutation of the murine goosecoid gene results in craniofacial defects and neonatal death. Development 121:2917-2922.

Yamamoto S, Hikasa H, Ono H, Taira M. 2003. Molecular link in the sequential induction of the Spemann organizer: direct activation of the cerberus gene by Xlim-1, Xotx2, Mix.1, and Siamois, immediately downstream from Nodal and Wnt signaling. Dev Biol 257:190-204.

Yamamoto TS, Takagi C, Hyodo AC, Ueno N. 2001. Suppression of head formation by Xmsx-1 through the inhibition of intracellular nodal signaling. Development 128:2769-2779.

Yang YP, Klingensmith J. 2006. Roles of organizer factors and BMP antagonism in mammalian forebrain establishment. Dev Biol 296:458-475.

Yokouchi Y, Vogan KJ, Pearse RV, 2nd, Tabin CJ. 1999. Antagonistic signaling by Caronte, a novel Cerberus-related gene, establishes left-right asymmetric gene expression. Cell 98:573-583.

Zhu L, Marvin MJ, Gardiner A, Lassar AB, Mercola M, Stern CD, Levin M. 1999. Cerberus regulates left-right asymmetry of the embryonic head and heart. Curr Biol 9:931-938.

Zorn AM, Butler K, Gurdon JB. 1999. Anterior endomesoderm specification in Xenopus by Wnt/beta-catenin and TGF-beta signalling pathways. Dev Biol 209:282-297.

II.3 Screening for *Xenopus* orthologs of novel genes expressed in the mouse AVE

II.3.1 Developmental Expression of *XAd4* in *Xenopus laevis*

Developmental Expression of *XAd4* in *Xenopus laevis*

Ana Cristina Silva[1,2], Mário Filipe[1], Herbert Steinbeisser[3], and José António Belo[1,2,4]

In preparation

[1]Instituto Gulbenkian de Ciência, Rua da Quinta Grande, 6, Apartado 14, 2781-901 Oeiras, Portugal; [2]Centro de Biomedicina Molecular e Estrutural, Universidade do Algarve, Campus de Gambelas, 8000-010 Faro, Portugal; [3]Institute of Human Genetics, University of Heidelberg, Im Neuenheimer Feld 366, 69120 Heidelberg, Germany; [4]Author for correspondence: José A. Belo, Tel: +351214407942, Fax: +351214407970, e-mail: jbelo@igc.gulbenkian.pt.

Developmental Expression of *XAd4* in *Xenopus laevis*

Ana Cristina Silva[1,2], Mário Filipe[1], Herbert Steinbeisser[3], and José António Belo[1,2,4]

[1]Instituto Gulbenkian de Ciência, Rua da Quinta Grande, 6, Apartado 14, 2781-901 Oeiras, Portugal; [2]Centro de Biomedicina Molecular e Estrutural, Universidade do Algarve, Campus de Gambelas, 8000-010 Faro, Portugal; [3]Institute of Human Genetics, University of Heidelberg, Im Neuenheimer Feld 366, 69120 Heidelberg, Germany; [4]Author for correspondence: José A. Belo, Tel: +351214407942, Fax: +351214407970, e-mail: jbelo@igc.gulbenkian.pt.

Abstract

Since Spemann and Mangold organizer's properties were described, many genes that are expressed in this region have been isolated. In a recent screening performed in our lab in search for novel genes expressed in the mouse Anterior Visceral Endoderm (AVE), a novel gene named m*Ad4* (mouse *Anterodistally expressed* gene #4) was identified to be specifically expressed in the mouse AVE. *XAd4* is the *Xenopus* homologue of the mouse *Ad4* gene and encodes for a 103 aminoacid protein (11.2kDa). Here, we report the embryonic expression of *Xenopus Ad4*. *XAd4* is expressed throughout early embryonic development. *XAd4* is already expressed in the unfertilized egg. During gastrulation *XAd4* transcripts are present in the dorsal mesoderm. Later in development, *XAd4* is strongly transcribed in the cement gland and weakly expressed in the head mesenchyme, otic vesicle and eye.

1. Results and Discussion

Early work by Spemann and Mangold showed that the dorsal blastopore lip of the amphibian gastrula (later dubbed the Spemann organizer) could induce a complete secondary axis when transplanted to the ventral side of a host embryo (reprinted in Spemann and Mangold, 2001). Similar gastrula organizing centers have been identified in other vertebrates, like the embryonic shield in teleostean fishes (Shih and Fraser, 1996) and the Hensen's node in chick (Waddington, 1933) and mouse (Beddington, 1994). Subsequent work by Spemann and colleagues has shown that the young dorsal blastopore lip and its derived prechordal mesendoderm exhibit head inducing activity, while the

older dorsal blastopore lip and the chordamesoderm that originates from it are only able to induce trunk structures (Spemann, 1931; Mangold, 1933). Based on the above observations, where change in the inductive properties of the dorsal blastopore lip occur in the course of development, led them to suggest the existence of two distinct organizing centers that segregate from the amphibian organizer, the head and trunk organizers, each with a unique ability to induce a specific part of the central nervous system.

Various embryological, genetic and molecular studies indicate that the Anterior Visceral Endoderm (AVE) is required for induction of the anterior nervous system (Thomas and Beddington, 1996; Bouwmeester and Leyns, 1997; Beddington and Robertson, 1998, 1999). The findings that the anterior endoderm of the *Xenopus laevis* organizer, and the mouse AVE express homologous genes (Beddington and Robertson, 1998) has implicated both regions in head induction. Thereby, it has been proposed that the anterior endoderm in *Xenopus* is the topological equivalent of the mouse AVE and the *Xenopus* head organizer (Bouwmeester and Leyns, 1997; Beddington and Robertson, 1998). However, in recent years several studies argue against an essential role for *Xenopus* anterior endoderm in head induction (de Souza and Niehrs, 2000).

In order to gain further insight into the molecular mechanisms involved in the early specification of the anterior neuroectoderm a microarray based on differential screening was performed to identify novel genes expressed in the AVE of E5.5 mouse embryos (Mário Filipe, unpublished). One of the novel genes identified in the screen was designated as mouse *Anterodistally expressed* gene #4 (*Ad4*; Genbank Acc. no. NM_133697) gene. This gene encodes for a 99 aminoacid protein, with unknown function and predicted to be integral to membrane. Using the mouse *Ad4* clone sequence to search NCBI databases (http://www.ncbi.nlm.nih.gov/BLAST/), we identified a potential *Xenopus* ortholog with closest homology to the mouse clone. *XAd4* (GenBank BU906457) was the only ortholog found for m*Ad4* and encodes a 11.2kDa protein (103 a.a.) that shares 73.1% identity with the mouse counterpart (Fig. 1A,C). Bioinformatic analysis of *XAd4* proteic sequence showed that in *XAd4* no putative domains were detected and, in similarity to *mAd4*, the protein is predicted to go to the membrane (http://smart.embl-heidelberg.de). Homologues could also be found in other vertebrates including human, rat, chicken and zebrafish (Fig. 1). This novel family of proteins shows a high level of conservation among different species, particularly in the amino terminal region (Fig. 1A).
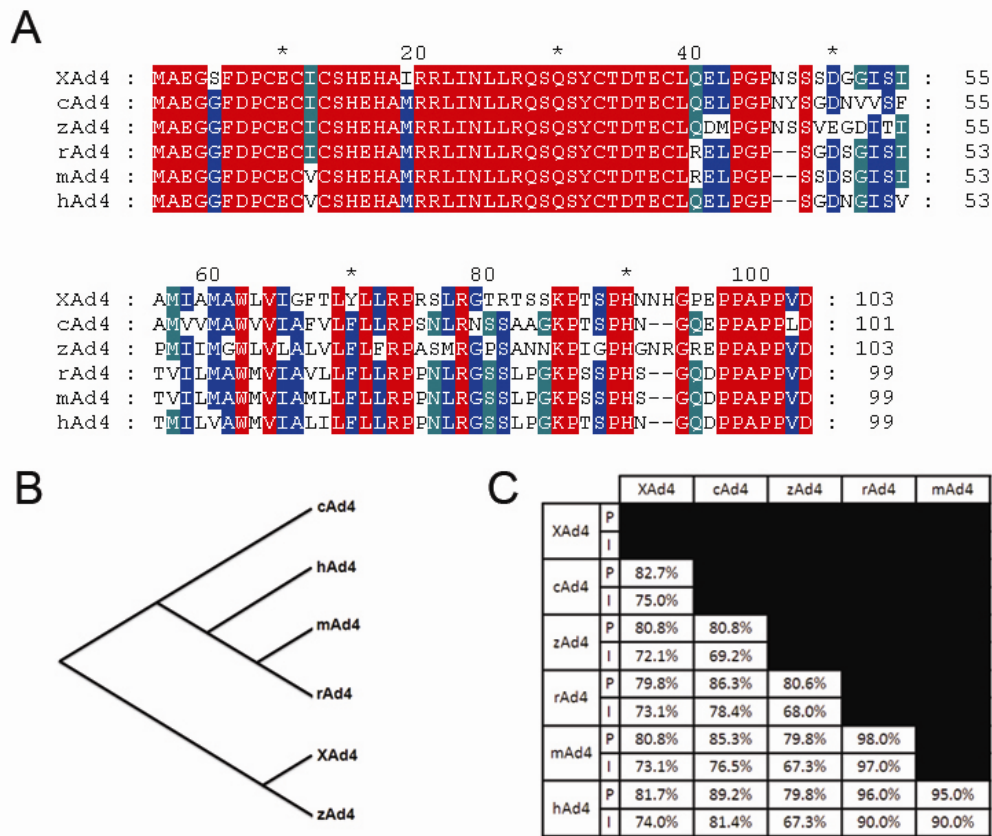
Figure 1 – Comparison of the predicted amino acid sequences of *Xenopus* Ad4 and those from other species. (A) Sequence alignment between vertebrate Ad4 proteins. Dashes represent gaps introduced into the amino acid sequence for optimal sequence homology. Letters with red background indicate identity between all clones while letters with blue and green background indicate identity between only five or four of them, respectively. (B) Homology tree showing relationship between *Xenopus laevis* (XAd4), chicken (cAd4), zebrafish (zAd4), rat (rAd4), mouse (mAd4) and human (hAd4) Ad4 proteins. (C) Percentage of amino acid homology (Positives, P, and Identity,I) between vertebrate Ad4 protein sequences.

The EST for *Xenopus XAd4* was ordered to RZPD (GenBank Acc. CA982906; http://www.rzpd.de). The clone was then sequenced and spatio-temporal expression pattern of this novel gene was analyzed by *in situ* hybridization and developmental RT-PCR.

As shown by RT-PCR, *XAd4* transcripts were present in all stages analyzed (Figure 2I). From the unfertilized egg until late gastrula stages (St12/13; Fig. 2I, lanes 1 to 13) the levels of *XAd4* transcripts are unchanged. From neurula stages onwards, expression of *XAd4* slightly decays (Fig. 2I, lanes 14 to 16). By performing whole-mount *in situ* hybridization we were able to see that in the unfertilized egg and in the early stages of cleavage (St2 and St4), *XAd4* mRNA was localized in the animal hemisphere (Figure 2A,B and not shown, respectively). Although the *in situ* hybridization staining only developed in the animal hemisphere one can not exclude the possibility of *XAd4* also being

111

expressed in the vegetal hemisphere due to the quenching of the RNA *in situ* signals in the yolk-rich vegetal cells. At late blastula stages, *XAd4* expression was observed in both dorsal and ventral marginal zone as well as in the entire ectoderm (Fig. 2C). At the on set of gastrulation *XAd4* transcripts can still be detected in the entire marginal zone, although very weak in the ventral side (not shown). As gastrulation proceeds, the ventral domain is completely abolished (Fig. 2D). This ventral expression domain of *XAd4* observed in the transition from blastula to gastrula stages might be the maternal component that has not been degraded yet. By mid- to late- gastrula stages *XAd4* transcripts were detected in the deep zone of internal involution and axial mesoderm (Fig. 2E). From neurula stages onwards, *XAd4* transcripts were shown to be strongly expressed in the cement gland (Fig. 2F-H). In addition, weak expression of *XAd4* was also detected in the head mesenchyme, the eye, branchial arches and otic vesicle (Fig. 2F-H). The expression pattern of this gene during neurula and tail bud stages makes it a very good cement gland marker.
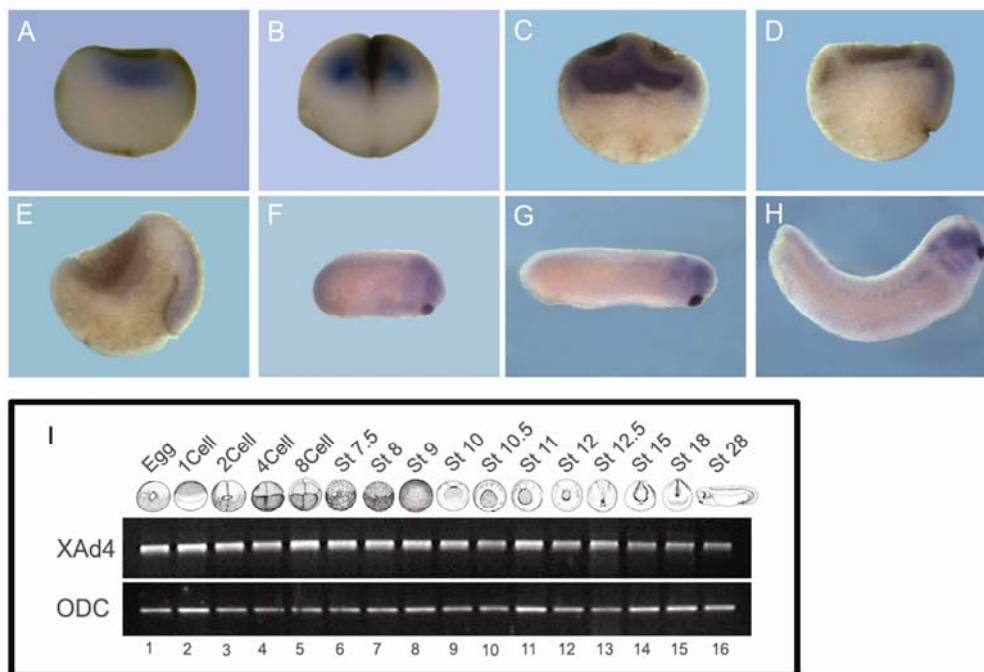
Figure 2 – Expression of *XAd4* through early *Xenopus laevis* development. (A-H) Whole-mount *in situ* hybridization for *XAd4*. *XAd4* is expressed in the animal pole of (A) Stage VI oocytes and at the (B) 2-cell stage. (C) Stage 8 *XAd4* transcripts are found in both dorsal and ventral marginal zone. (D) During early gastrula stages *XAd4* transcripts are restricted to the dorsal side of the embryo. (E) By mid gastrula stages *XAd4* can be detected in the deep zone of internal involution and involuting mesoderm. (F-H) During tailbud stages, *XAd4* is found to be strongly expressed in the cement gland and also in other head structures (lateral view, anterior to the right and dorsal up). (I) RT-PCR analysis of *XAd4* transcripts in *Xenopus laevis* embryos at different stages. *XAd4* is expressed in all stages tested. ODC was used as a loading control for the RT-PCR.

2. Experimental Procedures

2.1. Manipulation of *Xenopus* Embryos

Unfertilized eggs were squeezed out manually from pigmented female *Xenopus laevis* which had been injected with 300-400 units of human chorionic gonadotropin (Sigma). Eggs were fertilized *in vitro* with macerated testis, dejellied in 2% L-cysteine-HCl (pH 8.0), and grown in 0.1xMBS-H (8.8 mM NaCl, 0.1 mM KCl, 0.24 mM NaHCO$_3$, 82 μM MgSO$_4$, 41 μM CaCl$_2$, 33 μM Ca(NO$_3$)$_2$, 1 mM HEPES pH 7.4)at 14–21°C until the desired stages. Embryos were staged according to Nieuwkoop and Faber (1967).

2.2. Cloning of *Xenopus Ad4*

Xenopus Ad4 was identified by using the translated nucleotide sequence of the mouse Ad4 as queries to perform TBLASTX comparisons against NCBI's translated nucleotide (nt) and EST databases (dbest). Protein sequence alignments and homology scores were derived from the NCBI's BL2SEQ alignment program. SMART (Simple Modular Architecture Research Tool, http://smart.embl-heidelberg.de/) and PHI-BLAST (Pattern Hit Initiated BLAST) bioinformatic tools were used to analyze the domain architecture of the proteins. Xenopus laevis Ad4 EST was obtained from the RZPD (Berlin). The clone were sequenced from both the 5' and 3' ends using a DNA ABI Prism 377 (Applied biosystem) to confirm identity between the database entries and the cDNA inserts.

2.3. Analysis of gene expression by RT-PCR

Total RNA was isolated from 3-4 whole-mount embryos using Trizol™ reagent (Invitrogen), according to the manufacturer's protocol. First strand cDNA primed with random hexamers was synthesized with H minus M-MuLV reverse transcriptase (Fermentas) and PCR was performed using standard conditions and the following sets of primers: XAd4_Fw (5'-GTTTTGATCCCTGTGAGTGCATC-3') and XAd4_Rev (5'-GGTTCCGGACCATGATTATTG-3'), 25 cycles, 55 °C.

2.4. Whole-Mount *in Situ* Hybridization

Embryos to be used for *in situ* hybridization were incubated until the proper stages, fixed in MEMFA (0.1 M Mops [pH 7.4], 2 mM EGTA, 1 mM MgSO$_4$, 3.7% formaldehyde) solution, for 2h at RT or ON at 4°C, and stored in methanol at −20°C until

use. Gastrula embryos were hemi-sectioned before carrying out the procedure in order to improve probe penetration. Whole-mount and hemi-section *in situ* hybridization and antisense probe preparation were carried out as described (Epstein *et al.*, 1997). Probes were purified with a Quick Spin Mini RNA column (Roche). Hybridized RNAs were detected with alkaline-phosphatase-conjugated anti-DIG-antibody (Roche) and developed using BM purple or NBT/BCIP (both from Roche). Stained embryos were bleached by illumination in 1% H_2O_2, 4% formamide and 0.5x SSC pH 7.0. Embryos were refixed in MEMFA and photographed under bright light with a Leica DC 200 camera couple to a Leica MZIII stereoscope.

3. Acknowledgements

References

Spemann, H. (1931). Über den Anteil von Implantat und Wirtskeim an der Orientierung und Beschaffenheit der induzierten Embryonalanlage.

Mangold, H. (1933). Über die Induktionsfähighkeit der verschiedenen Bezirke der Neurula von Urodelen. Naturwissenshaften 21, 761-766.

Waddington, C.H. (1933). Induction by the primitive streak and its derivatives in the chick. J. Exp. Biol. 10, 38-46.

Nieuwkoop, P.D., Faber, J. (1967). Normal table of Xenopus laevis (Daudin). North Holland, Amsterdam.

Beddington, R.S. (1994). Induction of a second neural axis by the mouse node. Development 120, 613-20.

Shih, J., Fraser, S.E. (1996). Characterizing the zebrafish organizer: microsurgical analysis at the early-shield stage. Development 122, 1313-22.

Thomas, P., Beddington, R. (1996). Anterior primitive endoderm may be responsible for patterning the anterior neural plate in the mouse embryo. Curr Biol 6, 1487-96.

Bouwmeester, T., Leyns, L. (1997). Vertebrate head induction by anterior primitive endoderm. Bioessays 19, 855-63.

Epstein, M., Pillemer, G., Yelin, R., Yisraeli, J.K., Fainsod, A. (1997). Patterning of the embryo along the anterior-posterior axis: the role of the caudal genes. Development 124, 3805-14.

Beddington, R.S., Robertson, E.J. (1998). Anterior patterning in mouse. Trends Genet 14, 277-84.

Beddington, R.S., Robertson, E.J. (1999). Axis development and early asymmetry in mammals. Cell 96, 195-209.

De Souza, F.S., Niehrs, C. (2000). Anterior endoderm and head induction in early vertebrate embryos. Cell Tissue Res 300, 207-17.

Spemann, H., Mangold, H. (2001). Induction of embryonic primordia by implantation of organizers from a different species. 1923. Int J Dev Biol 45, 13-38.

II.3.2 Comparative expression of Shisa family members during early vertebrate development

II.3.2.1 Comparative expression of mouse and chicken Shisa homologues during early development

Comparative expression of mouse and chicken Shisa homologues during early development

Mário Filipe[1,3], Lisa Gonçalves[1,2,3], Margaret Bento[1,2,3], Ana Cristina Silva[1,2], and José António Belo[1,2,4]

[1]Instituto Gulbenkian de Ciência, Rua da Quinta Grande, 6, Apartado 14, 2781-901 Oeiras, Portugal; [2]Centro de Biomedicina Molecular e Estrutural, Universidade do Algarve, Campus de Gambelas, 8000-010 Faro, Portugal; [3]These authors contributed equally to this work; [4]Author for correspondence: José A. Belo, Tel: +351214407942, Fax: +351214407970, e-mail: jbelo@igc.gulbenkian.pt.

Comparative expression of mouse and chicken Shisa homologues during early development

Mário Filipe[1,3], Lisa Gonçalves[1,2,3], Margaret Bento[1,2,3] Ana Cristina Silva[1,2], and José António Belo[1,2,4]

[1]Instituto Gulbenkian de Ciência, Rua da Quinta Grande, 6, Apartado 14, 2781-901 Oeiras, Portugal; [2]Centro de Biomedicina Molecular e Estrutural, Universidade do Algarve, Campus de Gambelas, 8000-010 Faro, Portugal; [3]These authors contributed equally to this work; [4]Author for correspondence: José A. Belo, Tel: +351214407942, Fax: +351214407970, e-mail: jbelo@igc.gulbenkian.pt

Abstract

During vertebrate embryogenesis, fibroblast growth factor (FGF) and Wnt signaling have been implicated in diverse cellular processes, including cell growth, differentiation, and tissue patterning. The recently identified *Xenopus* Shisa protein promotes head formation by inhibiting Wnt and FGF signaling through its interaction with the immature forms of Frizzled and FGF receptors in the endoplasmic reticulum (ER), which prevents their post-translational maturation. Here we describe the mouse and chicken homologues of *Xenopus* Shisa. The mouse and chicken Shisa proteins share, respectively, 33.6% and 33.8% identity with the *Xenopus* homolog. *In situ* hybridization analysis shows that mouse *Shisa* is expressed throughout embryonic development, predominantly in the anterior visceral endoderm (AVE), headfolds, somites, forebrain, optic vesicle and limb buds. Cross-species comparison shows that the expression pattern of *cShisa* closely mirrors that of *mShisa*. Our observations indicate that the Shisa family genes are typically expressed in tissues known to require the modulation of Wnt and FGF signaling.

Introduction

The establishment of the anteroposterior (AP) axis in vertebrates has been postulated to be under the control of two distinct head and trunk organizing centers (Mangold, 1933; Spemann, 1931). In mammals, the head inducing activitiy is thought to reside in the anterior visceral endoderm (AVE) and later in the axial mesendoderm while trunk inducing and patterning activities reside in the more posterior primitive streak/node (Belo *et al.,* 1997; Bouwmeester and Leyns, 1997; Beddington and Robertson, 1999).

The AVE is an extra-embryonic tissue required for early anterior neural specification in the mouse embryo (Thomas and Beddington, 1996). The AVE is induced at the distal tip of the 5.5 dpc (days *post coitum*) embryo and then migrates to the prospective anterior side, where it imparts anterior identity upon the underlying epiblast. (Rodriguez *et al.,* 2005; Yamamoto *et al.,* 2004; Srinivas *et al.,* 2004; Rivera-Perez *et al.,* 2003).

Signaling molecules play crucial roles in developmental events and their actions are highly regulated by endogenous modulators and antagonists in order to obtain precisely balanced outputs. The process of neural AP patterning involves the integration of various signals such as retinoic acid (RA), fibroblast growth factors (FGF) and members of the Wnt family. The combined inhibition of BMP-4, Nodal and Wnt8 signaling has been demonstrated to be necessary for the specification of anterior neural tissues (Silva *et al.,* 2003; Glinka *et al.,* 1997; Piccolo *et al.,* 1999). Several secreted antagonists of the BMP, Nodal and Wnt pathways, such as Cer1, Lefty1 and Dkk-1, are expressed in the mouse AVE underlying the prospective anterior neuroectoderm (Belo *et al.,* 1997; Glinka *et al.,* 1998; Oulad-Abdelghani *et al.,* 1998). Likewise, the acknowledged topological and functional equivalent of the AVE in chick, the hypoblast, also expresses Nodal, BMP and Wnt antagonists, such as Caronte, Dkk-1 and Crescent (Pfeffer *et al.,* 1997; Rodríguez Esteban *et al.,* 1999; Foley *et al.,* 2000).

Development of the vertebrate limb bud involves a series of cell and axis specification and patterning processes directed by specialized structures such as the zone of polarizing activity (ZPA), the apical ectodermal ridge (AER), and the non-ridge ectoderm. The organizing and patterning activities of these regions are mediated by specific genes which have been shown to be regulated by a complex network of TGF-β, BMP, FGF and Wnt signaling pathways (reviewed in Capdevila and Izpisua Belmonte,

2001). FGFs expressed in the AER, like FGF2, 4 and 8, promote the proliferation of the mesenchymal limb bud cells in the progress zone and are absolutely required for limb outgrowth. Wnt3A, initially expressed in the limb surface ectoderm and subsequently restricted to the AER cells, plays an essential role in controlling the induction of the AER. Another Wnt factor, Wnt7A is expressed in the dorsal ectoderm and is involved in the specification of dorsal identities in the limb. FGFs have also been shown to oppose TGFβ2-induced chondrogenesis, and this inhibition is necessary to keep the proliferating mesenchimal cells of the progress zone in an undifferentiated state and maintain limb outgrowth. A strong argument can be made, therefore, for the important role that modulation mechanisms for such signaling pathways must play in the positioning and outgrowth of the limbs.

Metameric organization of the vertebrate body plan is established by somitogenesis, a process by which the paraxial mesoderm becomes segmented into somites, which later will give rise to the vertebrae, skeletal muscles and part of the dermis (reviewed in Pourquié, 2001). Wnt and FGF signaling pathways are key elements in almost all steps of this process. Correct specification of paraxial mesoderm, a pre-requisite event for somitogenesis, is dependent on Wnt and FGF patterning signals (Yoshikawa *et al.,* 1997; Deng *et al.,* 1994; Sun *et al.,* 1999). The precise spatial and temporal formation of somites relies on the concerted action of two major mechanistic components: the segmentation clock, a molecular oscillator that drives the cyclic expression of a set of genes, setting the periodicity of somite formation; and the determination front, a dynamic morphogen gradient that confers positional responsiveness of the presomitic mesoderm (PSM) cells to the clock signals, thereby defining the segmentation boundaries (reviewed in Pourquié, 2004; Dubrulle and Pourquié, 2004a; Aulehla and Hermann, 2004). Progression of the determination front involves the establishment of a caudorostral gradient of FGF8/Wnt3A activities along the PSM (Dubrulle *et al.,* 2001; Dubrulle and Pourquie, 2004b; Aulehla *et al.,* 2003). Furthermore, evidences suggest that the oscillations in notch signaling, which controls the expression of cyclic genes linked to the segmentation clock, are dependent on Wnt3A in the posterior PSM (Aulehla *et al.,* 2003). The formed somites undergo a maturation process in response to signals emerging from surrounding structures, which leads to the differentiation of three compartments, the sclerotome, the myotome and the dermatome. The sclerotome gives rise to the vertebrae and ribs and forms from a ventromedial epithelium that has acquired mesenchymal

character. The dorsolateral epithelium that remains forms a cap, the dermomyotome, gives rise to the dermatome, from which the dorsal skin dermis originates, and to the myotome, which will form skeletal muscle. Instructive Wnt and FGF signals, among others, are responsible for the specification of the different cell fates in the somite. Particullarly, Wnt signaling from the dorsal neural tube and adjacent ectoderm (Stern *et al.,* 1995; Wagner *et al.,* 2000) and FGFs from the somite itself (Crossley and Martin, 1995; Grass *et al.,* 1996; Pirskanen *et al.,* 2000) have an important role in the specification and maintenance of myogenic fates.

A recently described *Xenopus* protein termed Shisa, was shown to promote head formation through the inhibition of both Wnt and FGF signaling pathways by a novel ER retention mechanism (Yamamoto et. al, 2005). Secreted antagonists that competitively bind to caudalizing/ventralizing factors (Piccolo *et al.,* 1999; Piccolo *et al.,* 1996; Zimmerman *et al.,* 1996) or to their receptors preventing ligand binding (Mao *et al.,* 2001), play a major role in the head-inducing activity of the organizer. However, Shisa, which is expressed in the organizer and anterior endomesoderm as well as in the anterior neuroectoderm, is able to inhibit Wnt and FGF signals in a cell-autonomous fashion. It does so by physically interacting with the immature forms of the Wnt and FGF receptors within the ER and preventing their post-translational modification and trafficking to the cell surface (Yamamoto *et al.,* 2005).

Here we report the identification of the mouse and chicken homologues of *Xenopus* Shisa. We present a detailed description of the expression patterns of *mShisa* and *cShisa* during mouse and chick development and compare them with *XShisa* expression in *Xenopus*.

Results and discussion

Cloning and sequence analysis of mouse and chicken *Shisa*

In order to gain further insight into the molecular mechanisms involved in the early steps of forebrain specification, we have carried out a screening for differentially expressed genes in the mouse AVE (Filipe *et al.,* unpublished results). Briefly, a transgenic mouse line was generated in which EGFP is expressed in the AVE, under the control of the promoter region of the Cer-l gene (TgN(Cerl-GFP)328Belo; Mesnard *et al.,* 2004). In this transgenic line the AP axis reorientation could be followed, by the fluorescently

labelled AVE cells, even before gastrulation. Gene expression profiling using GeneChips ® (Affymetrix ®) identified several new transcripts expressed in the AVE at the very early stages of AP axis establishment.

One of the novel genes identified in this screening and provisory named MAd2 (Mouse Anterodistally expressed gene 2, probe set ID 1423852_at), was found to display a particularly interesting dynamic expression pattern that warranted a more detailed analysis. A BLAST search (Altschul *et al.*, 1990) of the *Xenopus laevis* EST database using the MAd2 sequence as query, returned a potential homolog, which was recently reported by Yamamoto *et al.* (2005) as *Shisa*. In view of this, the MAd2 gene was henceforth designated as mouse *Shisa* (GenBank accession no. DQ342342). The EST clone BC057640, obtained from RZPD (IMAGp998G149268Q3), was sequenced and found to contain the entire putative coding sequence (CDS) of *mShisa* as well as 5' and 3' untranslated regions (UTRs). This putative CDS consists of an 888-bp open reading frame (ORF) that encodes a predicted 295-amino acid protein with a calculated molecular weight of 31.6 kDa, whose sequence is identical to that reported by Yamamoto *et al.* (2005) for the mouse Shisa homolog.

The cDNA sequence of *mShisa* was then used to Blast the *Gallus gallus* sequence databases for potential homologs. This search led to the identification of two mRNAs (GenBank accession no. NM_204501, AF257354) and three EST clones (GenBank accession no. DR424805, BU205915, BM488505). An 855-bp ORF from the AF257354 RNA was identified as the putative *cShisa* CDS, which encodes for a 284-aa protein with a predicted molecular weight of 29.9 kDa, The *cShisa* cDNA sequence was then assembled *in silico* from the retrieved sequences and submitted to GenBank with the accession no. DQ342343. Sequence comparison of the Shisa homologs reveals two highly conserved cysteine-rich domains (CRD) (Fig. 1). The three proteins are also relatively well conserved over their entire sequence, with the murine and chicken Shisa showing, respectively, 33.6% and 33.8% overall identity and 49.5% and 49.2% overall similarity to the *Xenopus* protein. The Shisa proteins of the two amniote vertebrates are even more closely related to each other, sharing 81% identity and 85.8% similarity.

The gene structure of the mouse and chicken *Shisa* was deduced from cDNA-genomic alignments and by using the Genscan gene prediction program (http://genes.mit.edu/GENSCAN.html; Burge and Karlin, 1997). The mouse *Shisa* gene is composed of two exons, each containing one of the CRDs and separated by a 3234-bp

phase 1 intron, inserted between the first and second base of the codon for the first Valine in the conserved sequence VPIYVPFLIV. An identical two-exon gene structure was reported for two other mammalian homologs, the rat and human *Shisa* (Katoh and Katoh, 2005). Despite the still preliminary nature of the first draft of the chicken genome assembly, which did not allow the unequivocal determination of the exon structure of the *cShisa* gene, it was nevertheless possible to identify a 1140-bp intron placed at the exactly same position as the mouse *Shisa* intron. Another evidence supporting the homology of the murine and chicken *Shisa* comes from the chromosomal location of these two genes, which map to syntenic regions in the mouse chromosome 14C3 and chicken chromosome 1, as annotated in the Ensembl genome databases (v.37 - Feb2006; http://www.ensembl.org/; Birney *et al.*, 2006).
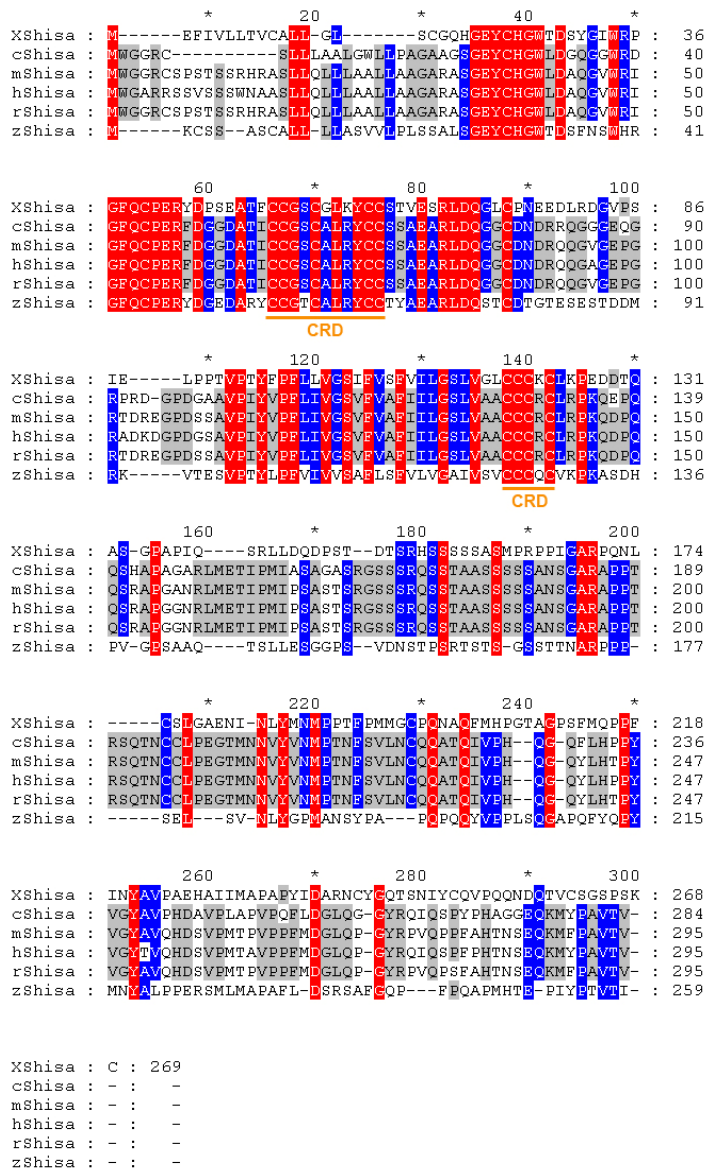
Fig. 1. Sequence alignment of XShisa, cShisa, mShisa, rShisa, hShisa and zShisa. Predicted amino acid sequence of cysteine-rich domains underlined in orange. Identical amino acids among all are shaded red while identical amino acids in only two sequences are shaded blue.

Expression of *mShisa* during mouse development

In situ hybridization analysis was used to examine the expression of *mShisa* transcripts during mouse embryogenesis.

The expression of *mShisa* can be seen as early as 5.5 dpc and continues throughout embryonic development (Fig. 2). At pre- to early streak stages *mShisa* is specifically expressed in the AVE as it migrates to the anterior side (Fig. 2A,B, C). By late streak stage, expression is found in a patch of anterior definitive endoderm cells that has replaced the AVE (Fig. 2D).

In early allantoic bud embryos (Fig. 2E), around E7.25-7.5, *mShisa* transcripts can only be detected in the anterior definitive endoderm and subjacent cranial mesoderm (Fig. 2E′-E‴) while by early headfold stage, *mShisa* is also induced in the anterior neural plate (Fig. 2F′). Up to this point, *mShisa* expression seems to be excluded from the midline axial mesendoderm (Fig. 2F). As the embryo reaches stage E8.0, *mShisa* is expressed in the cephalic mesenchyme and presumptive forebrain neuroectoderm (Fig. 2G-G″). Expression is also present in the endoderm lining the foregut pocket and in the rostral end of the notochordal plate (Fig. 2G″).

By E8.5, *mShisa* expression marks the prospective eye and forebrain regions (Fig. 2H-H″). Expression of *mShisa* is maintained in the optic vesicles of E9.0-9.5 embryos (Fig. 2I-I′, 2J), and the same is true for the expression in the forebrain, which can be more precisely located to the surface ectoderm and neuroepithelium of the prosencephalic vesicle (Fig. 2J′). Other expression domains found at this stage include the pharyngeal pouches (Fig. 2J), the lateral region of the invaginating otic pit (Fig. 2H″,I′) and the ventral endoderm of the foregut and immediately adjacent mesenchyme (2J′). Later in development, *mShisa* expression in the forebrain appears to become progressively confined to the dorsal telencephalon (Fig. 2K).

With the onset of somitogenesis, *mShisa* starts to be expressed in the forming somites, but is apparently absent from the presomitic mesoderm (Fig. 2H,I,J,K). Somitic expression of *mShisa* is restricted to the dorsolateral part that constitutes the dermomyotome (Fig. 2I″,K′). This expression pattern persists through later stages, albeit gradually decreasing to lower levels in older somites (Fig. 2H,I,J,K).
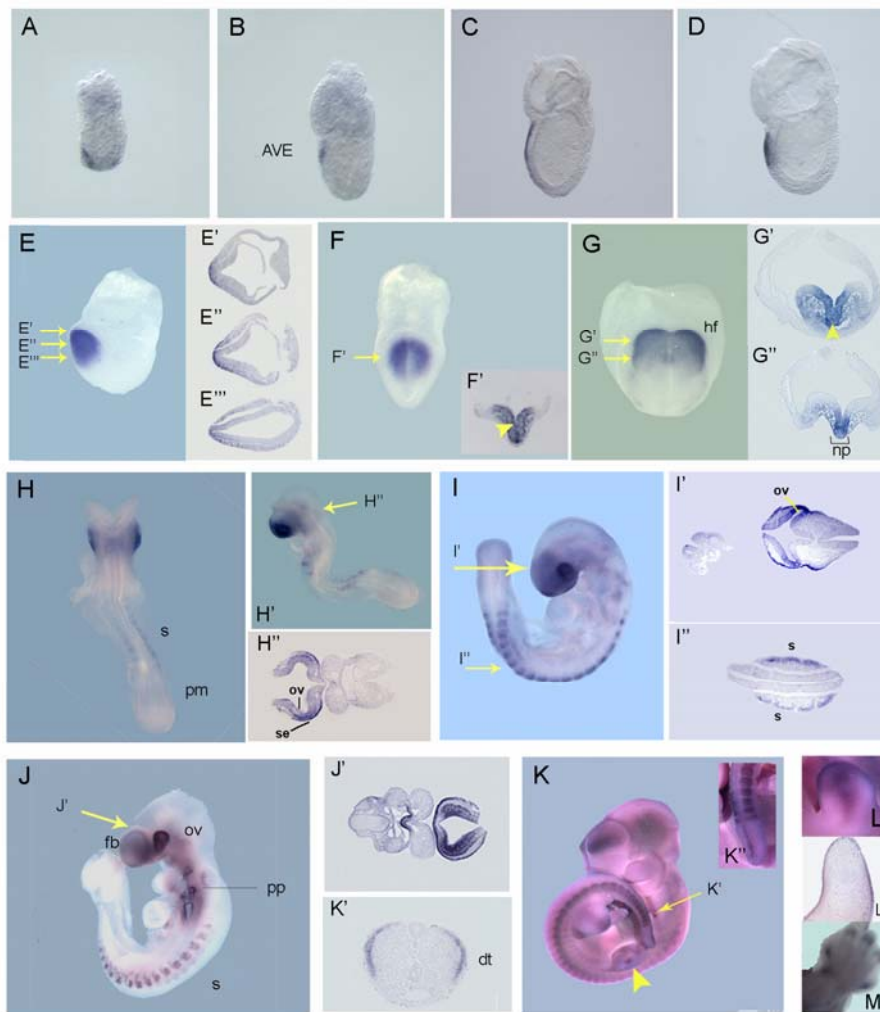
Fig. 2. Expression pattern of *mShisa* during mouse development. Analysis performed by *in situ* hybridization. All sections are 8-µm. The level at which each section was taken is indicated on panels with yellow arrows and the sections are shown next to the relevant panels. **A, B, C, D:** *mShisa* is expressed in the AVE in E5.5, E6.5, E6.75 and E7.0 mouse embryo. **E:** At E7.25 *mShisa* is detected in the prospective head fold. **E′, E″, E‴:** Transverse sections of an E7.25 embryo show that *mShisa* is only expressed in the anterior definitive endoderm and subjacent cranial mesoderm. **F:** In an E7.5 embryo, *mShisa* is expressed in the head folds. **F′:** Transverse section of E7.5 embryo shows that *mShisa* is also induced in the anterior neural plate. **G:** In an E8.0 embryo *mShisa* is expressed in the head folds. Transverse sections show mShisa is present in the cephalic mesenchyme, in the presumptive forebrain neuroectoderm, in the endoderm lining the foregut pocket (**G′**) and in the rostral end of the notochordal plate (**G″**). **H, H′:** At E8.5 *mShisa* transcripts are expressed in the prospective eye, forebrain and somites. **H″:** Transverse section of E8.0 embryo shows that *mShisa* is expressed in the optic pit and surface ectoderm. **I:** At E9.0 *mShisa* is expressed in the eye, somites and forebrain. **I′, I″:** Transverse sections of E9.0 embryo show expression of *mShisa* in the optic vesicle, optic eminence and somites. **J:** At E9.5, *mShisa* is expressed in the eye, forebrain, somites and pharyngeal pouches. **J′:** Transverse section shows that *mShisa* is present in the surface ectoderm and in the ventral endoderm of the foregut and immediately adjacent mesenchyme. **K:** At E11.5 transcripts of *mShisa* are expressed in the dorsal telencephalon, in the eye, in the somites and limb buds. **K′:** Transverse section of the tail at E11.5 shows *mShisa* in the somite is restricted to the dermomyotome. **K″:** Amplification of the tail shows that *mShisa* is absent from the presomitic mesoderm. **L:** Amplification of the limb bud at E11.5 shows *mShisa* expression. **L′:** Sagital section of the limb bud at E11.5 shows that *mShisa* expression is restricted to the surface ectoderm. **K**: Amplification of the limb at 13.5 shows *mShisa* is detected in the tip of the forming digits. AVE, anterior visceral endoderm; dt, dermatome; fb, forebrain; fg, foregut; hf, head fold; np, notochordal plate; ov, optic vesicle; pm, presomitic mesoderm; pp, pharyngeal pouches; s, somite; se, surface ectoderm.

130

Expression of *mShisa* in the developing limb buds can first be seen in a proximal domain (arrowhead, Fig. 2K) that subsequently shifts towards the distal tip as the bud grows (Fig. 2L). The expression in the limb bud is restricted to the ectoderm, as shown in Figure 2L'. At E13.5, *mShisa* expression can still be detected in the tip of the forming digits (Fig. 2M), in the region undergoing chondrogenesis.

Expression of *cShisa* during chick development

Embryos from pre-streak to mid-limb stages of development (Hamburger and Hamilton, 1951) were examined by *in situ* hybridization (Fig. 3). Our observations reveal the expression pattern of *cShisa* is very similar to that of its murine counterpart.

At pre-streak stages (Hamburger and Hamilton stage 1, HH1), *cShisa* transcripts were strongly detected in the hypoblast (Fig. 3A,A'). As gastrulation begins and the primitive streak is formed, *cShisa* expression becomes restricted to the anterior part of the embryo, more specifically to the endodermal layer (Stage HH 3+, Fig. 3B,B',B''). By stage HH5 (Fig. 3C), *cShisa* is expressed in the prospective neural plate tissue. Transverse sections showed that *cShisa* transcripts are still present in the endodermal layer and start also to be expressed in mesodermal cells (Fig. 3C',C'',C'''). This expression pattern is consistent with the observation that *XShisa* is essential for vertebrate head formation (Yamamoto *et al.,* 2005). At stage HH6, *cShisa* mRNA is present in high levels in the head folds and neural plate region (Fig. 3D). Transverse sections show that *cShisa* transcripts are localized to the ectodermal cells (Fig. 3D',D'').

With the beginning of somitogenesis, *cShisa* starts also to be expressed in the somitic territories. At stage HH7, *cShisa* can be detected in the first forming somite (not shown). By stage HH9⁻ *cShisa* is strongly expressed in the head folds and in the developing somites (Fig. 3E). A dynamic expression pattern is observed throughout somitogenesis (Fig. 3E-H). *cShisa* transcripts are absent from the posterior region of the presomitic mesoderm but can be detected at low levels at its rostral end. The expression is strongest in the newly formed somites and gradually decreases as the somites mature. A transverse section at somite level of a stage HH7 embryo shows that *cShisa* is expressed in the entire somite as well as in the lateral plate mesoderm and notochord (Fig. 3E'). Later in development, *cShisa* transcripts are also present in the prospective eye, forebrain, branchial arches and otic vesicle (Fig. 3F-H). As the optic vesicles evaginate, expression is seen in the lens vesicle and anterior surface ectoderm of the fronto-nasal mass (Fig 3H-

H''). At stage HH25, *cShisa* expression in the somite is restricted to the dermomyotome (Fig. 3H',H''), resembling that of *mShisa* (fig 2K').
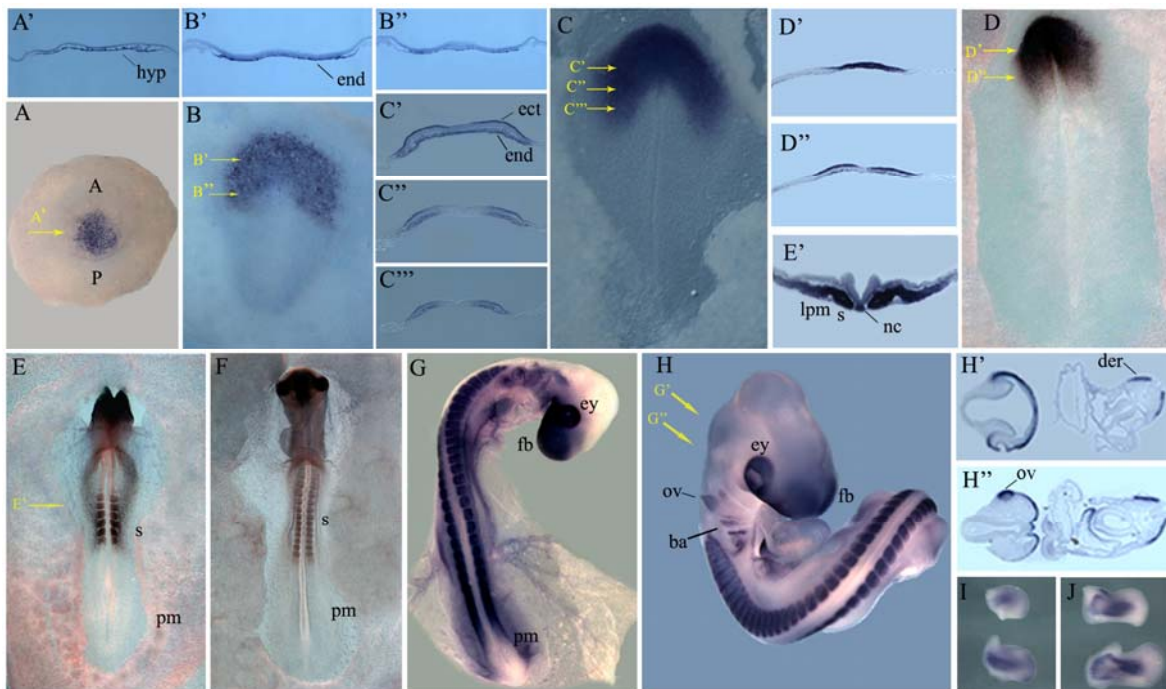
Fig. 3. Localization of cShisa transcripts in developing chicken embryos detected by in situ hybridization. A, C, E and F are ventral views while B and D are dorsal views of whole-mount embryos. All sections are transverse 16 μm cryo-sections. The level at which each section was taken is indicated on panels with yellow arrows and the sections are shown next to the relevant panels. **A:** *cShisa* is expressed in the hypoblast in stage HH1 chicken embryo. Anterior is to the top. **A':** Transverse section of a HH1 chicken embryo showing cShisa expression exclusively in the hypoblast. **B, B':** Stage HH3+ embryo showing expression of *cShisa* restricted to the endodermal layer. **C:** At HH5 *cShisa* transcripts are expressed in the prospective neural plate. **C', C'', C''':** Transverse sections of the embryo in C showing cShisa staining in endoderm and ectoderm. **D:** At HH6, *cShisa* expression appears restricted to the neural plate and primitive folds. **D', D'':** Transverse sections a HH6 embryo show that cShisa transcripts are located in the ectodermal cells. **E:** In stage HH9, *cShisa* is expressed in the head folds and the somites. There is an absence of *cShisa* transcripts within the presomitic mesoderm of the embryo. **E':** Section taken at the level of the somites shows *cShisa* expression within the somite and in the lateral plate mesoderm. The notochord is also positive for *cShisa* expression. **F:** At HH11, *cShisa* transcripts are observed in the forming brain, prospective eye and at the somite level. In the somites *cShisa* expression is strongest in the recently formed somites. **G:** By stage HH18, *cShisa* can be detected in the forebrain, eye, otic vesicle, pharyngeal pouches, branchial arches, somites and the developing limb buds. **H:** *cShisa* expression in HH25 remains in the otic vesicle, forebrain, branchial arches, eye, somites and limb buds. **H',H'':** Transverse sections show that cShisa transcripts in the somite are restricted to the dermatome. **I,J:** cShisa expression in the early limb buds (H, stage HH22; I, stage HH25) has a very dynamic pattern. cShisa starts to be expressed more posteriorly and then migrates towards more distal region. Forelimbs are shown in the top and hindlimbs in the bottom. ba, branchial arches; dt, dermatome; ey, eye; fb, forebrain; hf, head fold; hyp, hypoblast; lpm, lateral plate mesoderm; ov, otic vesicle; nc, notochord; np, neural plate; pm, presomitic mesoderm; s, somite.

During early limb bud stages, *cShisa* starts to be detected in the more proximal region of the limb buds (not shown) and later, as limbs develop, the expression shifts towards the distal region (Fig. 3I,J). This expression pattern in the limb buds resembles the one observed for *MyoD*, a marker of differentiating myogenic cells (Gamer *et al.*, 2001; Fig. 3I,J).

As demonstrated above, the murine and chicken *Shisa* are very closely related to each other both in terms of their sequence similarity and the evolutionarily conserved expression pattern. The early expression of *mShisa* and *cShisa* in the AVE / hypoblast and anterior neuroectoderm also recapitulates the deep endomesoderm and prospective head ectoderm expression previously described for the *Xenopus Shisa*, the founding member of this gene family (Yamamoto *et al.,* 2005). Mouse and chicken *Shisa* are, however, additionally expressed in structures like the somites, pharyngeal region and the eye.

Being members of the *XShisa* family, an antagonist of Wnt and FGF signalling (Yamamoto *et al.,* 2005), the conserved expression patterns of both *mShisa* and *cShisa* reflect the importance they may have during embryonic development of the mouse and chick embryos, patterning topological equivalent regions in these vertebrate embryos.

Assuming, based on their homology with the *Xenopus* protein, that the mouse and chicken Shisa also function as antagonists of Wnt and FGF signalling, then their expression in the AVE and hypoblast may seem, at a first glance, hard to conciliate with the role attributed to these tissues in early neural induction. In fact, recent findings strongly suggest that, at least in chicken, FGF and Wnt signalling are required for neural induction at a very early stage, even before gastrulation. However it should be taken into consideration that Shisa acts cell-autonomously and therefore its expression in the AVE/hypoblast is unlikely to inhibit FGF signalling in the overlying epiblast. Shisa might instead play an indirect role in promoting neural induction by participating in the specification and/or maintenance of the AVE/hypoblast identities, for example through repression of the autocrine action of FGF-8, which is expressed in the AVE (Crossley and Martin, 1995). Later on Shisa is expressed in the neural plate and it's plausible, then, that, like in *Xenopus*, it inhibits the caudalizing Wnt and FGF signals in this tissue. A similar reasoning can be applied to the function of Shisa in the developing limb buds, where Wnt and FGF signaling is known to direct outgrowth and patterning. *Shisa* is expressed in the ectoderm layer of the limbs, where most of the Wnt and FGF signalling centers are also located. Again it is conceivable that Shisa is not antagonizing these signalling pathways in the target mesenchymal cells but is instead acting on some of the signalling centers, perhaps protecting them from their own signals. During somitogenesis Shisa might be involved in the process of somite differentiation and condensation through the inhibition the FGF signalling coming from the posterior presomitic mesoderm. Subsequently expression in the dorsolateral compartment of the somite suggests that Shisa could be

repressing the FGF- and Wnt-mediated myogenic signals in these cells, which as a result will be specified as dermatome.

These considerations are however purely hypothetical and a more conclusive characterization of the biological function of the mouse and chicken Shisa in embryonic development will require further biochemical and genetic analyses.

Experimental Procedures

Chicken and mouse embryo collection.

Fertilized chicken eggs were purchased from local suppliers. Eggs were incubated at 37˚C in a humidified incubator until the desired developmental stage. Embryos were staged according to Hamburger and Hamilton (1951).

Mouse embryos were obtained crossing B6SJL/F1 hybrids maintained on a 19h to 5h dark cycle and mated overnight. Noon of the day of vaginal plug detection was designated 0.5 dpc. Embryos were dissected from the uterus in PBS and further staged by morphological landmarks (Downs and Davies, 1993).

Cloning of *mShisa* and *cShisa* cDNAs

The EST clone BC057640, containing the entire predicted coding sequence of *mShisa* as well as the 5' and 3'-UTR was obtained from RZPD (IMAGp998G149268Q3)

To isolate a fragment of the *cShisa* coding sequence (323-829), total RNA from stage 22 chick embryos (Hamburger and Hamilton, 1951) was isolated using Trizol® reagent (Invitrogen) according to the manufacturer's protocol. Random-primed cDNA synthesized from these samples with H minus M-MuLV reverse transcriptase (Fermentas) was subjected to 25 cycles of amplification by PCR, at an annealing temperature of 55˚C. The following primers were used: forward, 5'- CATTGTCGGCTCCGTCTTCGTC -3'; reverse, 5'- TTCTGCTCTCCGCCTGCATG -3'. The PCR product was cloned into the pGEM-T Easy vector (Promega). The sequence of PCR-amplified *cShisa* cDNA was determined on an ABI sequencer. The sequence of chicken *Shisa* cDNA was deposited in the GeneBank database under the accession number DQ342343.

Whole-mount in situ hybridization and histology

Single whole mount *in situ* hybridization and antisense-probe preparation were performed as previously described (Belo *et al.*, 1997). Digoxigenin labeled *mShisa* antisense RNA probe was synthesized by linearizing the BC05764 clone with *Bgl*II and transcribing with T7 RNA polymerase. To generate the digoxigenin labeled *cShisa* antisense RNA probe, the plasmid containing *cShisa* coding sequence fragment (pGEM-Teasy.*cShisa*) was linearized using *Sal*I and transcribed using T7 RNA polymerase.

After staining, embryos were re-fixed in 4% paraformaldehyde and photographed using a Leica DFCM20 digital camera. Some embryos were embedded in 15% sucrose, 7.5% gelatin, frozen, and sectioned (16 µm) using a Leica CMM0S0 S cryostat; others were embedded in paraffin and sectioned (8 µm) using a microtome Leica RM2135. The sections were examined and photographed using a Leica DM LB2 microscope and a Leica DFCM20 digital camera.

References

Altschul SF, Gish W, Miller W, Myers EW, Lipman DJ. 1990. Basic local alignment search tool. J Mol Biol 215:403-410.

Aulehla A, Herrmann BG. 2004. Segmentation in vertebrates: clock and gradient finally joined. Genes Dev 18:2060–2067.

Aulehla A, Wehrle C, Brand-Saberi B, Kemler R, Gossler A, Kanzler B, Herrmann BG. 2003. Wnt3a plays a major role in the segmentation clock controlling somitogenesis. Dev Cell 4:395–406.

Belo JA, Bouwmeester T, Leyns L, Kertesz N, Gallo M, Follettie M, De Robertis EM. 1997. Cereberus-like is a secreted factor with neutralizing activity expressed in the anterior-primitive endoderm of the mouse gastrula. Mech Dev 68:45–57.

Bainter JJ, Boos A, Kroll KL. 2001. Neural induction takes a transcriptional twist. Dev Dyn 222:315.

Birney E, Andrews D, Caccamo M, Chen Y, Clarke L, Coates G, Cox T, Cunningham F, Curwen V, Cutts T, Down T, Durbin R, Fernandez-Suarez XM, Flicek P, Gräf S, Hammond M, Herrero J, Howe K, Iyer V, Jekosch K, Kähäri A, Kasprzyk A, Keefe D, Kokocinski F, Kulesha E, London D, Longden I, Melsopp C, Meidl P, Overduin B, Parker A, Proctor G, Prlic A, Rae M, Rios D, Redmond S, Schuster M, Sealy I, Searle S, Severin J, Slater G, Smedley D, Smith J, Stabenau A, Stalker J, Trevanion S, Ureta-Vidal A, Vogel J, White S, Woodwark C, Hubbard TJP. 2006. Ensembl 2006. Nucleic Acids Res 34: D556-D561.

Burge C, Karlin S. 1997. Prediction of complete gene structures in human genomic DNA. J Mol Biol 268:78.

Capdevila J, Izpisua Belmonte JC. 2001. Patterning Mechanisms Controlling Vertebrate Limb Development. Annu Rev Cell Dev Biol 17:87–132.

Crossley PH, Martin GR. 1995. The mouse Fgf8 gene encodes a family of polypeptides and is expressed in regions that direct outgrowth and patterning in the developing embryo. Development 121:439.

Deng CX, Wynshaw-Boris A, Shen MM, Daugherty C, Ornitz DM, Leder P. 1994. Murine FGFR-1 is required for early postimplantation growth and axial organization. Genes Dev 8:3045–3057.

Downs KM, Davies T. 1993. Staging of gastrulating mouse embryos by morphological landmarks in the dissecting microscope. Development 118:1255–1266.

Dubrulle J, McGrew MJ, Pourquie O. 2001. FGF signaling controls somite boundary position and regulates segmentation clock control of spatiotemporal Hox gene activation. Cell 106:219–232.

Dubrulle J, Pourquie O. 2004a. Coupling segmentation to axis formation. Development 131:5783–5793.

Dubrulle J, Pourquie O. 2004b. fgf8 mRNA decay establishes a gradient that couples axial elongation to patterning in the vertebrate embryo. Nature 427:419–422.

Foley AC, Skromne I, Stern CD. 2000. Reconciling different models of forebrain induction and patterning: a dual role for the hypoblast. Development 127:3839–3854.

Gamer LW, Cox KA, Small C, Rosen V. 2001. Gdf11 is a negative regulator of chondrogenesis and myogenesis in the developing chick limb. Dev Biol 229:407–420.

Glinka A, Wu W, Delius H, Monaghan AP, Blumenstock C, Niehrs C. 1998. Dickkopf-1 is a member of a new family of secreted proteins and functions in head induction. Nature 391:357–362.

Glinka A, Wu W, Onichtchouk D, Blumenstock C, Niehrs C. 1997. Head induction by simultaneous repression of Bmp and Wnt signalling in Xenopus. Nature 389:517–519.

Grass S, Arnold HH. Braun T. 1996. Alterations in somite patterning of Myf-5-deficient mice: a possible role for FGF-4 and FGF-6. Development 122:141.

Hamburger V, Hamilton HL. 1951. A series of normal stages in the development of the chick embryo. J Morphol 88:49–92.

Katoh Y, Katoh M. 2005. Comparative genomics on Shisa orthologs. Int J Mol Med 16:181

Klebes A, Biehs B, Cifuentes F, Kornberg TB. 2002. Expression profiling of Drosophila imaginal discs. Genome Biol 3:0038.

Mangold O. 1933. Über die Induktionsfähigkeit der verschiedenen Bezirke der Neurula von Urodelen. Naturwissenschaften 21: 761–766 .

Mao B, Wu W, Li Y, Hoppe D, Stannek P, Glinka A, Niehrs C. 2001. LDL-receptor-related protein 6 is a receptor for Dickkopf proteins. Nature 411:321–325.

Mesnard D, Filipe M, Belo JA, Zernicka-Goetz M. 2004. The anterior-posterior axis emerges respecting the morphology of the mouse embryo that changes and aligns with the uterus before gastrulation. Curr Biol 14:184-196.

Oulad-Abdelghani M, Chazaud C, Bouillet P, Mattei MG, Dolle P, Chambon P. 1998. Stra3/lefty, a retinoic acid-inducible novel member of the transforming growth factor-beta superfamily. Int J Dev Biol 42:23–32.

Pfeffer PL, De Robertis EM, Izpisua-Belmonte JC. 1997. Crescent, a novel chick gene encoding a Frizzled-like cysteine-rich domain, is expressed in anterior regions during early embryogenesis. Int J Dev Biol 41:449–458.

Piccolo S, Sasai Y, Lu B, De Robertis EM. 1996. Dorsoventral patterning in Xenopus: inhibition of ventral signals by direct binding of chordin to BMP-4. Cell 86:589–598.

Piccolo S, Agius E, Leyns L, Bhattacharyya S, Grunz H, Bouwmeester T, De Robertis EM. 1999. The head inducer Cereberus is a multifunctional antagonist of Nodal, BMP and Wnt signals. Nature 397:707–710.

Pirskanen A, Kiefer JC, Hauschka SD. 2000. IGFs, insulin, Shh, bFGF, and TGF-beta1 interact synergistically to promote somite myogenesis in vitro. Dev Biol 224:189.

Pourquie O. 2001 Vertebrate somitogenesis. Annu Rev Cell Dev Biol 17:311–350.

Pourquié O. 2004. The chick embryo: a leading model in somitogenesis studies. Mech Dev 121:1069–1079.

Rivera-Perez JA, Mager J, Magnuson T. 2003. Dynamic morphogenetic events characterize the mouse visceral endoderm. Dev Biol 261:470–487.

Rodriguez Esteban C, Capdevila J, Economides AN, Pascual J, Ortiz A, Izpisua Belmonte JC. 1999. The novel Cer-like protein Caronte mediates the establishment of embryonic left-right asymmetry. Nature 401:243–251.

Rodriguez TA, Srinivas S, Clements MP, Smith JC, Beddington RS. 2005. Induction and migration of the anterior visceral endoderm is regulated by the extra-embryonic ectoderm. Development 132:2513–2520.

Silva AC, Filipe M, Kuerner KM, Steinbeisser H, Belo JA. 2003. Endogenous Cereberus activity is required for anterior head specification in Xenopus. Development 130, 4943–4953.

Spemann H. 1931. Über den Anteil von Implantat und Wirtskeim an der Orientierung und Beschaffenheit der induzierten Embryonalanlage. W Roux Arch Entwicklungsmech 123: 390–516.

Srinivas S, Rodriguez T, Clements M, Smith JC, Beddington RS. 2004. Active cell migration drives the unilateral movements of the anterior visceral endoderm. Development 131:1157–1164.

Stern HM, Hauschka SD. 1995. Neural tube and notochord promote in vitro myogenesis in single somite explants. Dev Biol 167:87.

Sun X, Meyers EN, Lewandoski M, Martin GR. 1999. Targeted disruption of Fgf8 causes failure of cell migration in the gastrulating mouse embryo. Genes Dev 13:1834–1846.

Thomas P, Beddington R. 1996. Anterior primitive endoderm may be responsible for patterning the anterior neural plate in the mouse embryo. Curr Biol 6: 1487–1496.

Wagner J, Schmidt C, Nikowits W Jr, Christ B. 2000.Compartmentalization of the somite and myogenesis in chick embryos are influenced by wnt expression. Dev Biol 228:86.

Yamamoto A, Nagano T, Takehara S, Hibi M, Aizawa S. 2005. Shisa promotes head formation through the inhibition of receptor protein maturation for the caudalizing factors, Wnt and FGF. Cell 120:223–235.

Yamamoto M, Saijoh Y, Perea-Gomez A, Shawlot W, Behringer RR, Ang SL, Hamada H, Meno C. 2004. Nodal antagonists regulate formation of the anteroposterior axis of the mouse embryo. Nature 428:387–392.

Yoshikawa Y, Fujimori T, McMahon AP, Takada S. 1997. Evidence that absence of Wnt-3a signaling promotes neuralization instead of paraxial mesoderm development in the mouse. Dev Biol 183:234–242.

Zimmerman LB, De Jesus-Escobar JM, Harland RM. 1996. The Spemann organizer signal noggin binds and inactivates bone morphogenetic protein 4. Cell 86:599-606.

II.3.2.2 Developmental Expression of Shisa-2 in *Xenopus laevis*

Developmental Expression of *Shisa-2* in *Xenopus laevis*

Ana Cristina Silva[1,2], Mário Filipe[1], Marta Vitorino[2], Herbert Steinbeisser[3] and José António Belo[1,2,4]

[1]Instituto Gulbenkian de Ciência, Rua da Quinta Grande, 6, Apartado 14, 2781-901 Oeiras, Portugal; [2]Centro de Biomedicina Molecular e Estrutural, Universidade do Algarve, Campus de Gambelas, 8000-010 Faro, Portugal; [3]Institute of Human Genetics, University of Heidelberg, Im Neuenheimer Feld 366, 69120 Heidelberg, Germany; [4]Author for correspondence: José A. Belo, Tel: +351214407942, Fax: +351214407970, e-mail: jbelo@igc.gulbenkian.pt.

Developmental Expression of *Shisa-2* in *Xenopus laevis*

Ana Cristina Silva[1,2], Mário Filipe[1], Marta Vitorino[2], Herbert Steinbeisser[3] and José António Belo[1,2,4]

[1]Instituto Gulbenkian de Ciência, Rua da Quinta Grande, 6, Apartado 14, 2781-901 Oeiras, Portugal; [2]Centro de Biomedicina Molecular e Estrutural, Universidade do Algarve, Campus de Gambelas, 8000-010 Faro, Portugal; [3]Institute of Human Genetics, University of Heidelberg, Im Neuenheimer Feld 366, 69120 Heidelberg, Germany; [4]Author for correspondence: José A. Belo, Tel: +351214407942, Fax: +351214407970, e-mail: jbelo@igc.gulbenkian.pt.

ABSTRACT

Shisa is an antagonist of Wnt and FGF signaling, that functions cell autonomously in the endoplasmic reticulum (ER) to inhibit the post-translational maturation of Wnt and FGF receptors. In this paper we report the isolation of a second *Xenopus* Shisa gene (*XShisa*-2). *Xenopus* Shisa-2 shows 30.7% identity to XShisa. RT-PCR analysis indicates that *XShisa-2* mRNA is present throughout early development, and shows an increased expression during neurula and tailbud stages. At neurula stages *Xenopus Shisa-2* is initially expressed in the presomitic paraxial mesoderm and later in the developing somites. The expression profiles and pattern of *XShisa* and *XShisa-2* differ significantly. During gastrulation only *XShisa* mRNA is present in the Spemann-Mangold organizer and later on becomes restricted to the neuroectoderm and the prechordal plate.

TEXT

Secreted growth factors of the Wnt and Fibroblast growth factor (FGF) families have an essential role in vertebrate development (Logan and Nusse, 2004; Böttcher and Niehrs, 2005). However, Wnt activities need to be inhibited for the correct development of the head and heart (Glinka *et al.,* 1997; Marvin *et al.,* 2001; Schneider and Mercola, 2001).

The head formation promoting factors Dickkopf (Dkk) and Cerberus are secreted Wnt antagonists that regulate this signaling pathway in the extracellular space (Glinka *et al.*, 1998; Piccolo *et al.*, 1999; Mukhopadhyay *et al.*, 2001; Silva *et al.*, 2003). Shisa, a recently identified protein, has been shown to inhibit Wnt as well as FGF signaling in a cell autonomous manner. It binds to the immature form of Frizzled and the FGF receptors in the ER and prevents the post-translational modifications necessary for their function (Yamamoto et. al., 2005).

FGF signaling is critical for specification of the paraxial mesoderm identity (Pourquié, 2001). In mutant mice for FGF8 and FGFR1, no paraxial mesoderm (PM) is formed (Deng *et al.*, 1994; Yamaguchi *et al.*, 1994; Sun *et al.*, 1999). Additionally, studies in *Xenopus* have shown that eFGF is able to induce XmyoD expression in the mesoderm and specifies the myogenic cells (Fisher *et al.*, 2002). Interestingly, *fgf8* expressed in the caudal presomitic mesoderm (PSM) was recently shown to inhibit myogenesis (Dubrulle *et al.*, 2001). Wnts were also shown to be involved in the initial steps of myogenesis in mammals (Cossu and Borello, 1999). In *Xenopus* embryos, injection of *Xwnt8* RNA leads to an enlargement of the PM territory (Christian & Moon 1993), whereas injection of dominant-negative *Xwnt8* impairs the formation of the somitic territory (Hoppler *et al.* 1996). In higher vertebrates, Wnt3a plays a critical role in maintaining the PM fate in the posterior somites (Takada *et al.* 1994) and like Fgf8, Wnt3a gradients are also important in controlling segmentation in the PSM (Aulehla *et al.*, 2003). In this paper we report the isolation of *XShisa*-2, an ortholog of the mouse *Shisa*, and describe its expression during *Xenopus laevis* embryogenesis. The expression pattern of this gene suggests that it may regulate the activities of Wnts and FGFs during *Xenopus* somitogenesis.

We have carried out a screening for differentially expressed genes in the mouse Anterior Visceral Endoderm (AVE; Filipe *et al.*, unpublished results). One of the genes identified in the screen was previously named as *mouse anterodistally expressed gene-2* (GenBank Acc. NM_145463). Through a BLAST search using this gene as query, we have identified two potential *Xenopus* homologs. One of these homologs was recently reported by Yamamoto et. al., (2005) as *Shisa*. The other homolog, here designated as *Xenopus Shisa-2* (*XShisa*-2), has been reported as three EST sequences (GenBank accession no. BC077953, CF286494 and BJ042155). The EST BJ042155 was obtained from NIBB (clone XL050n07; http://xenopus.nibb.ac.jp/) and the insert was completely sequenced. When compared with mouse Shisa, the sequence obtained from BC077953 shows homology to

the 5′ of the mRNA where as BJ042155 shows homology to the 3′ of the mRNA sequence. These two ESTs show partial overlapping, indicating that the ORF of Shisa-2 could be obtained from these two ESTs. When the combined sequences from these two ESTs were subjected to bioinformatic analysis, a putative open reading frame was obtained. After cloning of the full-length cDNA, we observed that this gene, *Xenopus Shisa-2* (GenBank accession no. DQ342341) contains an open reading frame of 867 nucleotides encoding a 288 amino acid protein with a predicted molecular mass of 31.1 kDa. Similarly to *Xenopus* Shisa, Shisa-2 contains a signal peptide, two conserved cysteine-rich domains (CRD) in the amino-terminal half and a putative transmembrane domain N-terminally to the second CRD. The predicted amino acid sequence of *X*Shisa-2 has close similarity to *X*Shisa (Identity = 30.7%, Positives = 46.3%; Fig. 1A). Comparison of *Xenopus* Shisa and Shisa-2 sequences with that of mouse Shisa reveals higher conservation between *X*Shisa-2 and mouse Shisa (I = 76.9%, P = 84.4%) than between *X*Shisa and mouse Shisa (I = 31.9%, P = 45.2%; Fig. 1A), suggesting that *X*Shisa-2 is the true ortholog of the previously described mouse protein.

The temporal expression of *XShisa-2* was analyzed by RT-PCR using total RNAs isolated from different developmental stages (Fig. 1B). Transcripts encoding *XShisa-2* are present in all stages analyzed (from mature oocyte until stage 48) and its expression is upregulated in neurula and early tailbud stages.

The spatial expression of *XShisa-2* during early *Xenopus* development was characterized by whole-mount *in situ* hybridization. *XShisa-2* transcripts were not detectable by *in situ* hybridization until gastrulation. At late gastrula/early neurula stages *XShisa-2* is restricted to two stripes in the dorsal side but excluded from the dorsal midline (Figure 2A). A sagittal section shows that the cells expressing *XShisa-2* are in the posterior portion of the paraxial mesoderm, but not in the neuroectoderm (Figure 2B,C).

147
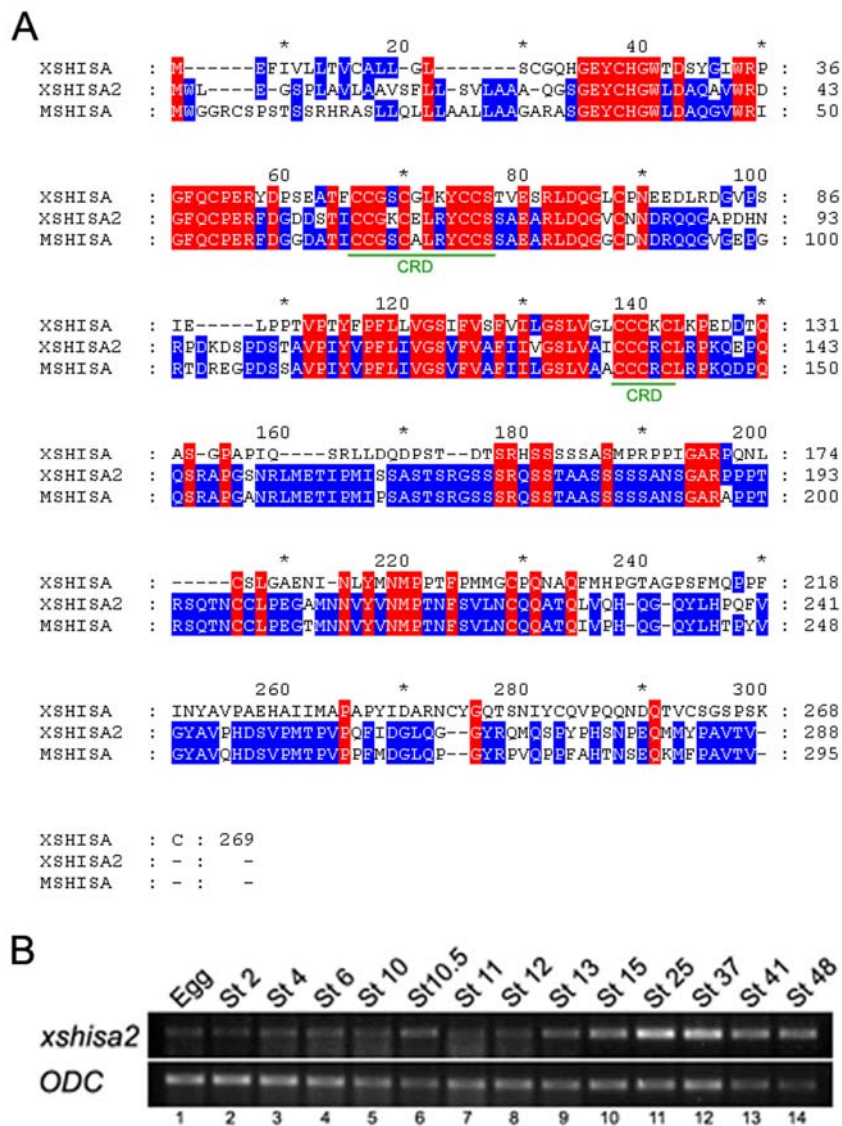
Figure 1. Sequence alignment of Shisa family members and temporal expression of *XShisa-2* during *Xenopus* development. (A) Comparison of the predicted amino acid sequence of *X. laevis* Shisa-2 with *X. laevis* Shisa and mouse Shisa. XShisa-2 shares 76.9% of identity (positives - 84.4%) with mShisa-2 and 30.7% identity (positives - 46.3%) with XShisa. Identical amino acids among all are shaded red while identical amino acids in only two sequences are shaded blue. The absence of residues at the corresponding region is indicated by dashes. The two conserved cysteine-rich domains (CRD) are shown in green. GenBank accession numbers for *X. laevis Shisa-2*: DQ342341. (B) Temporal expression pattern of *Xenopus Shisa-2* by RT-PCR analysis. RT-PCR was performed with total RNA from different developmental stages. *XShisa-2* transcripts are present maternally at very low levels, increase in the beginning of neurulation and continue to be expressed during early development. Stages are indicated on top. ODC was used as a loading control.

As somitogenesis commences, *XShisa*-2 transcripts localize to a paraxial region, lateral to the involuting neural tube (Figure 3B). As development proceeds, a dynamic expression pattern is observed in forming somites (Figure 3). Its expression is stronger in the presomitic mesoderm and decreases as somites are formed. *XmyoD* is expressed in all myogenic cells throughout somitogenesis (Hopwood *et al.*, 1989). *Paraxial protocadherin*

(*PAPC*) expression in the PSM is restricted to the anterior halves of somitomeres 2, 3 and 4 and is expressed uniformly from somitomere 1 to the unsegmented portion of the PSM, the tailbud domain (TBD; Kim *et al.*, 2000). Comparing *XShisa*-2, *XmyoD* and *PAPC* expression pattern one can observe that *XmyoD* and *PAPC* domains extend more posteriorly than the XShisa-2 expression domain (Figure 3D,H,H') which ends after the more posterior *PAPC* segmented stripe (S2) and is not expressed in the unsegmented portion of the presomitic mesoderm. A transverse section of the trunk region of a stage 27 embryo shows *XShisa*-2 expression in the entire somite (Figure 3G''). From early tailbud stages onwards *XShisa*-2 is also expressed in the developing eye region. A complex expression pattern is also observed in the head at late tailbud stages, including the lens, the branchial arches (Figure 3K'). Unlike *XShisa-2*, *XShisa* is expressed during tailbud stages exclusively in the head region (Figure 3I).
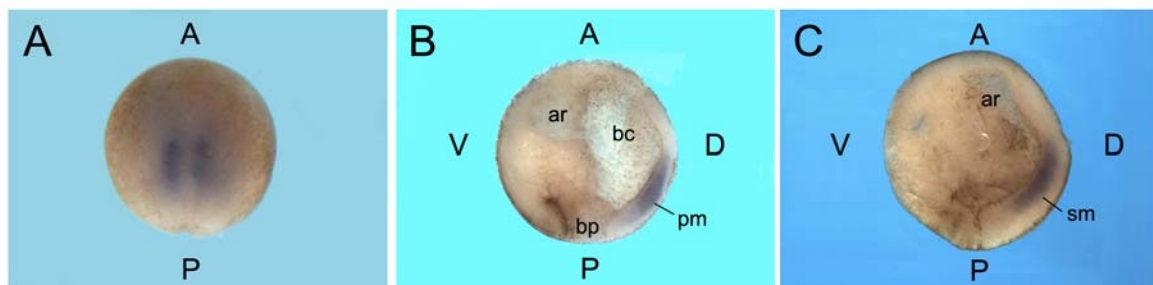
Figure 2. *XShisa-2* expression in the end of gastrulation and beginning of neurulation. Whole mount *in situ* hybridization with a *Shisa-2* DIG-labeled antisense RNA probe was performed on embryos in the end of gastrulation and beginning of neurulation. A) *XShisa-2* expression by the end of gastrulation (st 13) is restricted to two narrow stripes on the dorsal side of the embryo but not in the notochord. Posterior dorsal view. (B-C) Hemisection of st 12 and st 14 embryos show that *XShisa2* mRNA is restricted to the posterior portion of the paraxial mesoderm. Hemisections with dorsal to the right. A, anterior; P, posterior; D, dorsal; V, ventral; ar, archenteron; bc, blastocoel; pm, paraxial mesoderm; sm, somitic mesoderm.

In this work, we report the isolation and developmental expression pattern of a second *Xenopus Shisa* gene, *XShisa-2*. The founding member of this increasing family, *XShisa*, was reported to exert its activity through a novel mechanism by which both the Wnt and the FGF signaling pathways are inhibited. This activity was used by *XShisa* to pattern the anterior region of the *Xenopus* embryo. As reported here, *XShisa-2*, a closely related member of this family has an expression pattern opposite to that of *XShisa*, at the level of the posterior mesoderm where it might be involved in formation/segmentation of the somites. The similarity to *Xenopus* Shisa raises the question of whether XShisa-2 also functions as antagonists of Wnt and FGF signaling. Further biochemical and genetic analyses should help to clarify the biological function of *XShisa-2* during embryonic

development. Taken together, this fam.ily of genes might be employing the same strategy, inhibition of the maturation of Wnt and FGF receptors, to pattern both the anterior and the posterior regions of the *Xenopus* embryo.
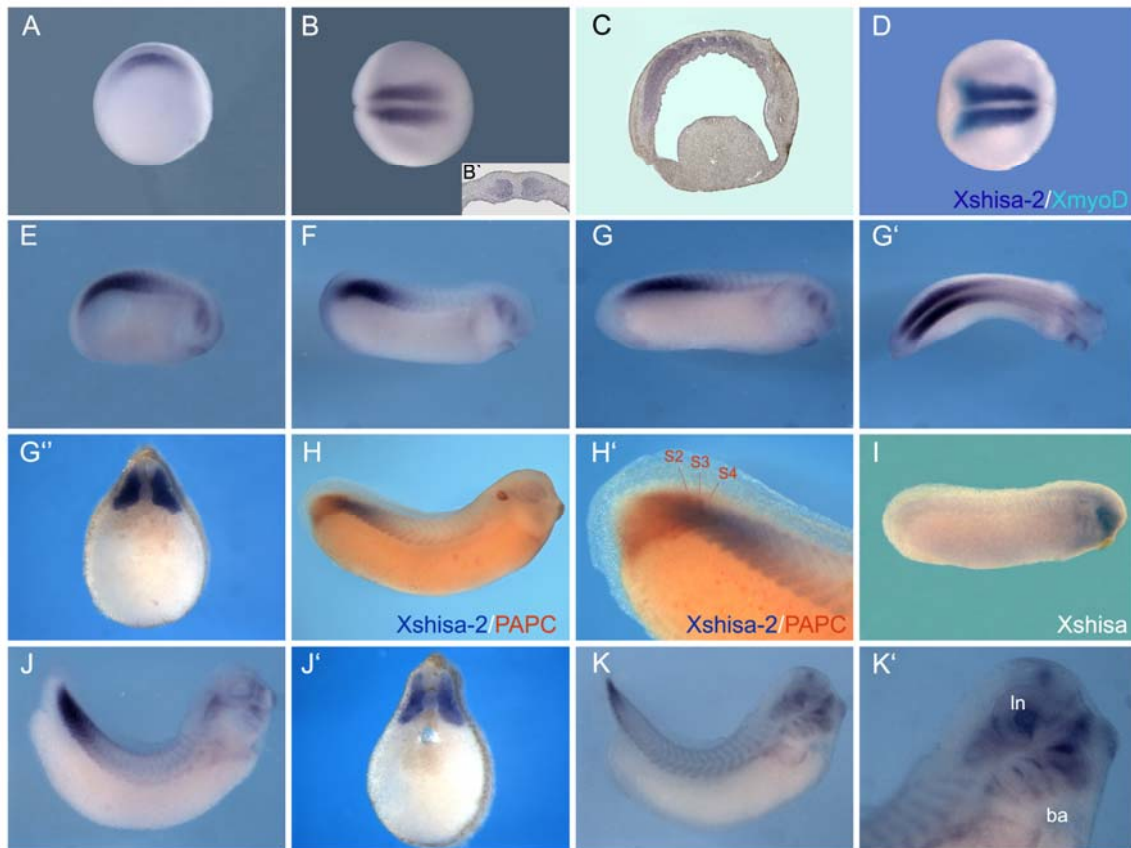
Figure 3. Expression pattern of *XShisa-2* during tailbud stages. From early tailbud stage onward, a dynamic pattern is observed in the forming somites. (A-B) At stage 18, *XShisa-2* becomes progressively reduced in the anterior paraxial mesoderm. (B') Transversal section showing *XShisa-2* expression in the entire somite region. (C) Parasagittal section of a stage 18 embryos. (D) Double whole mount *in situ* hybridization with *XShisa-2* DIG-labeled antisense RNA probe and *XmyoD* Fluo-labelled antisense RNA probe. The expression domain of *XmyoD* extends more posteriorly than *XShisa-2* expression domain. (E-H,J-K) Expression of *XShisa-2* is stronger in the presomitic mesoderm and decreases as somites form. Transverse sections through the trunk region of stage 27 (G'') and 30 (J') embryos show *XShisa*-2 expression in the entire somite. (H,H') Double whole mount *in situ* hybridization with *Shisa-2* and PAPC shows that *XShisa-2* is not expressed in the unsegmented region of the presomitic mesoderm. (I) Whole mount *in situ* hybridization with *XShisa* shows expression restricted to the head region, a distinct expression pattern than the one observed for *XShisa-2*. (K') A complex expression pattern is also observed in the head, including the lens, ln, and branchial arches, ba. (A,C,E-G,H-J,K,K') Lateral view. (B,D,G'). Dorsal view. All embryos are oriented with anterior to the right.

150

Experimental Procedures

Xenopus **embryo manipulations**

Xenopus eggs were obtained from females injected with 300 IU of human chorionic gonadotrophin (Sigma), and were fertilized *in vitro*. Eggs were dejellied with 2% cysteine hydrochloride pH 8. Embryos were grown in 0.1XMBS-H (1X MBS-H = 88 mM NaCl, 1 mM KCl, 2.4 mM NaHCO$_3$, 0.82 mM MgSO$_4$, 0.41 mM CaCl$_2$, 0.33 mM Ca(NO$_3$)$_2$, 10 mM HEPES pH 7.4, 10 µg/ml streptomycin sulfate and 10 µg/ml penicillin) and staged according to Nieuwkoop and Faber (1967).

Cloning of *Xenopus Shisa-2*

The EST containing the *Xenopus laevis Shisa-2* partial coding sequence, GenBank Acc. BJ042155, was obtained from NIBB (clone XL050n07; http://xenopus.nibb.ac.jp/).

To isolate the full length *XShisa*-2 coding sequence, total RNA from late neurula (stage 18) *Xenopus laevis* embryos (Nieuwkoop and Faber, 1967) was isolated using Trizol® reagent (Invitrogen) according to the manufacturer's protocol. First strand cDNA was synthesized with H minus M-MuLV reverse transcriptase (Fermentas) using random hexamers as primers. The following primers were used to amplify the *XShisa*-2 gene product by PCR: forward, 5'-TTTATCGATATGTGGTTGGAGGGCTCCCCCCTG -3'; reverse, 5'- TTTCTCGAGCTACACAGTCACGGCTGGGTACATC -3', 65 °C, 25 cycles). The PCR product was cloned into pCRII-TOPO® (Invitrogen). The sequence of *XShisa*-2 cDNA described here has been deposited in GenBank under accession number DQ342341.

Whole mount *in situ* **hybridization and Histology**

Single and double whole mount *in situ* hybridization and anti-sense probe preparation was carried out as previously described (Belo *et al.*, 1997; Epstein *et al.*, 1997). Digoxigenin-labeled *XShisa-2* antisense RNA probe was synthesized by linearizing the XL050n07 clone (pBS(SK)*XShisa-2*) using *XbaI* and transcribing using T7 RNA polymerase. The probe was then partially fragmented for 6 min at 60 °C in hydrolysis buffer [40mM NaHCO$_3$, 60mM Na$_2$CO$_3$, pH 10.2] followed by sodium acetate/ethanol precipitation. To generate the fluorescein labeled XmyoD and PAPC antisense RNA probes, plasmids containing XmyoD and PAPC fragments were linearized using *HindIII* and *XbaI* respectively, and transcribed using T7 RNA polymerase. Stained embryos (stage 18 and above) were bleached by illumination in 1% H$_2$O$_2$, 4% formamide and 0.5xSSC pH 7.0.

For histology, Xenopus embryos previously *in situ* hybridized were fixed ON at 4°C in 4% PFA, embedded in gelatin and sectioned to 16mm with a cryostat.

RT-PCR

Total RNA was prepared from pools of 5 embryos with Trizol® reagent (Invitrogen) according to the manufacturer's protocol. First strand cDNA primed by random hexamers was synthesized with H minus M-MuLV reverse transcriptase (Fermentas) and PCR was performed using standard conditions and the following sets of primers: *Shisa-2*-F (5'-TCCTTCTCTCAGTGCTGGCG-3') and *Shisa-2*-R (5'-ATCGGGACTGTCCTTGTCCG-3'), 55°C, 25 cycles; *ODC*-F (5'-CAGCTAGCTGTGGTGTGG-3') and *ODC*-R (5'-CAACATGGAAACTCACACC-3'), 57°C, 21 cycles.

ACKNOWLEDGMENTS

REFERENCES

AULEHLA, A., WEHRLE, C., BRAND-SABERI, B., KEMLER, R., GOSSLER, A., KANZLER, B., and HERRMANN, B.G. (2003). Wnt3a plays a major role in the segmentation clock controlling somitogenesis. Dev. Cell 4: 395–406.

BELO, J. A., BOUWMEESTER, T., LEYNS, L., KERTESZ, N., GALLO, M., FOLLETTIE, M., AND DE ROBERTIS, E. M. (1997). Cerberus-like is a secreted factor with neutralizing activity expressed in the anterior primitive endoderm of the mouse gastrula. *Mech. Dev.* 68, 45–57.

BÖTTCHER, R., AND NIEHRS, C. (2005). Fibroblast Growth Factor Signaling during Early Vertebrate Development. *Endocrine Reviews* 26: 63–77.

CHRISTIAN, J.L., and MOON, R.T. (1993). Interactions between Xwnt-8 and Spemann organizer signaling pathways generate dorsoventral pattern in the embryonic mesoderm of *Xenopus*. Genes Dev. 7: 13–28.

COSSU, G., and BORELLO, U. (1999). Wnt signaling and the activation of myogenesis in mammals. EMBO J. 18: 6867–6872.

DENG, C.X., WYNSHAW-BORIS, A., SHEN, M.M., DAUGHERTY, C., ORNITZ, D.M., AND LEDER, P. (1994). Murine FGFR-1 is required for early postimplantation growth and axial organization. *Genes Dev.* 8: 3045–3057.

DUBRULLE, J., MCGREW, M.J., and POURQUIÉ, O. (2001). FGF signaling controls somite boundary position and regulates segmentation clock control of spatiotemporal Hox gene activation. Cell 106: 219–232.

EPSTEIN, M., PILLEMER, G., YELIN, R., YISRAELI, J.K., AND FAINSOD, A., (1997). Patterning of the embryo along the anterior-posterior axis: the role of the caudal genes. *Development* 124: 3805–3814.

FISHER, M.E., ISAACS, H.V., and POWNALL, M.E. (2002). eFGF is required for activation of XmyoD expression in the myogenic cell lineage of *Xenopus laevis*. *Development* 129: 1307–1315.

GLINKA, A., WU, W., ONICHTCHOUK, D., BLUMENSTOCK, C., AND NIEHRS, C. (1997). Head induction by simultaneous repression of Bmp and Wnt signalling in *Xenopus*. *Nature* 389: 517–519.

GLINKA, A., WU, W., DELIUS, H., MONAGHAN, A.P., BLUMENSTOCK, C., AND NIEHRS, C. (1998). Dickkopf-1 is a member of a new family of secreted proteins and functions in head induction. *Nature* 391: 357–362.

HOPPLER, S., BROWN, J.D. and MOON, R.T. (1996). Expression of a dominant negative Wnt blocks induction of MyoD in *Xenopus* embryos. *Genes Dev.* 10: 2805–2817.

HOPWOOD, N.D., PLUCK, A., AND GURDON, J.B. (1989). MyoD expression in the forming somites is an early response to mesoderm induction in *Xenopus* embryos. *EMBO J.* 8: 3409–3417.

KIM, S.H., JEN, W.C., DE ROBERTIS, E.M., AND KINTNER, C. (2000). The protocadherin PAPC establishes segmental boundaries during somitogenesis in xenopus embryos. *Curr. Biol.* 10:821–830.

LOGAN, C.Y., AND NUSSE, R. (2004). The Wnt Signaling Pathway in Development and Disease. Annu. *Rev. Cell Dev. Biol.* 20: 781–810.

MARVIN, M. J., DI ROCCO, G., GARDINER, A., BUSH, S.M., AND LASSAR, A.B. (2001). Inhibition of Wnt activity induces heart formation from posterior mesoderm. *Genes Dev.* 15: 316–327.

MUKHOPADHYAY, M., SHTROM, S., RODRIGUEZ-ESTEBAN, C., CHEN, L., TSUKUI, T., GOMER, L., DORWARD, D.W., GLINKA, A., GRINBERG, A., HUANG, S.P., NIEHRS, C., BELMONTE, J.C., AND WESTPHAL, H. (2001). Dickkopf1 is required for embryonic head induction and limb morphogenesis in the mouse. *Dev. Cell* 1, 423–434.

NIEUWKOOP, P.D. and FABER, J. (1967). Normal Table of *Xenopus laevis* (Daudin). Amsterdam, North Holland Publishing Company.

POURQUIÉ, O. (2001).Vertebrate Somitogenesis. Annu. Rev. Cell Dev. Biol. 17: 311–350.

PICCOLO, S., AGIUS, E., LEYNS, L., BHATTACHARYYA, S., GRUNZ, H., BOUWMEESTER, T., AND DE ROBERTIS, E.M. (1999). The head inducer Cerberus is a multifunctional antagonist of Nodal, BMP and Wnt signals. *Nature* 397: 707–710.

SCHNEIDER, V.A., AND MERCOLA M.(2001). Wnt antagonism initiates cardiogenesis in *Xenopus* laevis. *Genes Dev*. 15:304–315.

SILVA, A.C., FILIPE, M., KUERNER, K.-M., STEINBEISSER, H., AND BELO, J.A. (2003) Endogenous Cerberus activity is required for anterior head specification in *Xenopus*. *Development*, 130: 4943–4953.

SUN, X., MEYERS, E.N., LEWANDOSKI, M., AND MARTIN, G.R. (1999). Targeted disruption of Fgf8 causes failure of cell migration in the gastrulating mouse embryo. *Genes Dev.* 13:1834–1846.

TAKADA, S., STARK, K.L., SHEA, M.J., VASSILEVA, G., MCMAHON, J.A., and MCMAHON, A.P. (1994). Wnt-3a regulates somite and tailbud formation in the mouse embryo. *Genes Dev*. 8: 174–189.

YAMAGUCHI, T.P., HARPAL, K., HENKEMEYER, M., AND ROSSANT, J. (1994). fgfr-1 is required for embryonic growth and mesodermal patterning during mouse gastrulation. *Genes Dev.* 8:3032–3044.

YAMAMOTO, A., NAGANO, T., TAKEHARA, S., HIBI, M., AND AIZAWA, S. (2005). Shisa promotes head formation through the inhibition of receptor protein maturation for the caudalizing factors, Wnt and FGF. *Cell* 120: 223–235.

II.4 The role of *Xenopus laevis Shisa-2* during early development

The role of *Xenopus laevis Shisa-2* during early development

Ana Cristina Silva[1,2], Herbert Steinbeisser[3], and José António Belo[1,2,4]

[1]Instituto Gulbenkian de Ciência, Rua da Quinta Grande, 6, Apartado 14, 2781-901 Oeiras, Portugal; [2]Centro de Biomedicina Molecular e Estrutural, Universidade do Algarve, Campus de Gambelas, 8000-010 Faro, Portugal; [3]Institute of Human Genetics, University of Heidelberg, Im Neuenheimer Feld 366, 69120 Heidelberg, Germany; [4]Author for correspondence: José A. Belo, Tel: +351214407942, Fax: +351214407970, e-mail: jbelo@igc.gulbenkian.pt.

The role of *Xenopus laevis Shisa-2* during early development

Ana Cristina Silva[1,2], Herbert Steinbeisser[3], and José António Belo[1,2,4]

[1]Instituto Gulbenkian de Ciência, Rua da Quinta Grande, 6, Apartado 14, 2781-901 Oeiras, Portugal; [2]Centro de Biomedicina Molecular e Estrutural, Universidade do Algarve, Campus de Gambelas, 8000-010 Faro, Portugal; [3]Institute of Human Genetics, University of Heidelberg, Im Neuenheimer Feld 366, 69120 Heidelberg, Germany; [4]Author for correspondence: José A. Belo, Tel: +351214407942, Fax: +351214407970, e-mail: jbelo@igc.gulbenkian.pt.

Abstract

Secreted growth factors like Wnts and FGFs play crucial roles during early development and must be tightly regulated for proper development of the embryo. Recently isolated gene *Shisa* regulates both Wnt and FGF signaling by promoting the maturation of their receptors in the endoplasmic reticulum (ER). Here, we present a loss-of-function study using an antisense morpholino against *Shisa-2*, a recently isolated *Shisa* family member. Knockdown of Shisa-2 resulted in embryos exhibiting narrower somites. In addition, *Xenopus* embryos depleted of Shisa-2 showed smaller eyes and smaller otic vesicles. Analysis at the molecular level showed that in the absence of Shisa-2, the position where segmentation occurs is shifted anteriorly. During late gastrula stages, Shisa-2Mo injected embryos also displayed mild convergent-extension defects. These results suggest that Shisa-2 plays an important role in otic placode, eye and somite formation during *Xenopus* development.

Introduction

The patterning of the vertebrate embryo is largely dependent on morphogen signaling. Morphogens are secreted proteins that are produced by a restricted group of cells. They diffuse away from the source cells and induce distinct cellular responses in a concentration dependent manner. These signaling molecules function by activating specific intracellular cascades that regulate gene expression and ultimately control cell behavior. Among morphogens are the members of the wingless (Wnt) and fibroblast growth factor (FGF) families.

FGFs belong to a large family of secreted growth factors that act through binding and activating the cell surface FGF receptors (FGFR), which are tyrosine kinase receptors containing three immunoglobulin-like domains and a heparin-binding sequence (for review see, Bottcher and Niehrs, 2005). The FGFRs then transmit the extracellular signals to various signal transduction pathways through tyrosine phosphorylation. The main signaling pathway activated by the stimulation of the FGFRs is the Ras/MAP kinase pathway (Bottcher and Niehrs, 2005).

FGF signaling regulates different cellular processes that include cell growth, chemotaxis, cell migration, differentiation, cell survival and apoptosis. During embryonic development FGF signaling has been shown to be involved in different processes, from early to late events, including patterning, morphogenesis, differentiation, regulation of cell proliferation or migration (for review see Goldfarb, 1996; Bottcher and Niehrs, 2005; Thisse and Thisse, 2005).

Like FGF signaling, Wnt signaling has also been implicated in the regulation of a great variety of developmental processes that include tissue patterning, cell proliferation, cell differentiation, cell polarity and cell migration. In addition, Wnt signaling pathway has been shown to be crucial in organogenesis and in the maintenance of adult tissues. Abnormal Wnt signaling activities may lead to severe developmental defects and various diseases (Nusse, 2005).

Wnt ligands are secreted glycoproteins that bind and signal through Frizzled (Fz) receptors. Fzs are seven-transmembrane molecules and activation of the Wnt signaling cascade requires not only the Fz receptors, but also the presence of a long single pass transmembrane molecule of the low-density lipoprotein receptor-related protein family (LRP), LRP5/6 (Pinson *et al.,* 2000; Tamai *et al.,* 2000; Mao *et al.,* 2001). Wnt ligands are able to activate different signaling pathways. The most well studied branch is the Wnt canonical/β-catenin pathway and is involved in both cell adhesion and signaling. This branch involves the activation of Dishevelled (Dsh), that binds to Axin and GBP leading to the inhibition of GSK3β, and ultimately to the stabilization of β-catenin (Li *et al.,* 1999; Umbhauer *et al.,* 2000; Wong *et al.,* 2003). β-catenin is then translocated to the nucleus where it interacts with LEF1/TCF transcription factors and activates gene expression (van Noort and Clevers, 2002; Nusse, 2005). The Wnt signaling that does not involve β-catenin is designated as the non-canonical Wnt signaling and includes the Wnt /PCP and the Wnt/Ca^{2+} pathways. The Wnt/PCP pathway regulates cell adhesion and cell migration

(Moon *et al.,* 1993; Du *et al.,* 1995; Heisenberg *et al.,* 2000; Veeman *et al.,* 2003). In the vertebrate embryo, the convergent extension movements occurring during gastrulation and responsible for the anterior-posterior axis elongation are regulated by the Wnt/PCP pathway (Keller *et al.,* 2000; Mlodzik, 2002; Wallingford *et al.,* 2002). The Wnt/Ca^{2+} pathway involves modulation of intracellular calcium levels and has been shown to play a role in tissue separation (Slusarski *et al.,* 1997; Winklbauer *et al.,* 2001).

Due to the great importance of these two signaling pathways during embryonic development, their activities have to be tightly regulated and an increasing number of positive and negative regulators are being identified. Recently, Yamamoto *et al.,* (2005) reported the isolation and characterization of the founding member of a new family of genes, S*hisa-1*. They were able to show that *Shisa-1* functioned as an inhibitor of Wnt and FGF signaling pathways, by binding directly to the immature forms of Frizzled and FGF receptors in the endoplasmic reticulum (ER) and preventing their pos-translational maturation and translocation to the cellular membrane. Overexpression studies showed that *Shisa-1* mRNA was able to promote enlarged cement glands and anterior head structures. On the contrary, loss-of-function analyses, using antisense morpholino oligonucleotides, showed a requirement of *Shisa-1* in head formation. *Shisa-1* morphants exhibited small heads with small eyes and cement glands (Yamamoto *et al.,* 2005).

We have reported the isolation of a second member of the Shisa gene family, *Shisa-2* (Silva *et al.,* 2006). *Shisa-2* is expressed in the somites, eye, otic vesicle, head mesenchyme and brachial arches. In the present study, we have generated an antisense morpholino oligonucleotide that was able to deplete *Shisa-2* in the *Xenopus laevis*. Depletion of *Shisa-2* resulted in a delay in the maturation of the presomitic mesoderm which ultimately led to a decrease in somite number and size. It was also found that *Shisa-2* is required for proper eye and otic vesicle development. These findings suggest that Shisa-2, like was described for Shisa-1, may function as an inhibitor of both FGF and Wnt signaling and plays an important role in processes where FGF and Wnt signaling have to be tightly regulated for proper development of the embryo.

Results

Antisense morpholino oligonucleotide inhibits Shisa-2 activity

In *Xenopus laevis* embryos *Shisa-2* expression could be found in the presomitic mesoderm and recently formed somites and, later on, in each somite as well as in the otic vesicle, eye, branchial arches and head mesenchyme (Fig.1A-C; Silva *et al.,* 2006). To study the role of *Xenopus Shisa-2* we took a loss-of-function approach using antisense morpholino oligonucleotides (MOs) against *Shisa-2*. MOs are antisense oligodeoxynucleotides in which the riboside moieties are substituted with nitrogen-containing morpholine moieties and are phosphorodiamidate linked. They have the ability to block translation of the target mRNAs with high specificity and stability when introduced into cells (Summerton and Weller, 1997). This approach has been used successfully to study the function of genes during embryonic development in several model systems, including *Xenopus*, chicken and zebrafish (Heasman, 2002). Due to the pseudo-tetraploid nature of the *Xenopus laevis* genome, it is likely that many genes are represented by extra copies. To address this, we have designed a morpholino oligonucleotide against the translation starting site, which shows great degree of conservation between the duplicated copies of *Xenopus* genes (Shisa-2Mo; Fig.1D).

We first tested the efficiency and specificity of the Shisa-2 morpholino to downregulate Shisa-2 protein expression in a cell free transcription/translation system. Translation of Shisa-2-myc RNA containing the sequences complementary to Shisa-2Mo was blocked, as shown by western blot analysis using the anti-myc antibody (Fig 1E). In contrast, translation of a Shisa-2-myc construct (Shisa-2 (mut)-myc), where the morpholino target sequences were mutated, or even of an unrelated control Fz7-myc RNA, was not affected (Fig.1E). An unrelated standard control morpholino oligonucleotide (CoMo) showed no inhibitory effects (Fig 1E).

Yamamoto *et al.,* (2005) have shown that when *Xenopus* Shisa-1 was expressed in HEK 293T cells, it could be detected both in the endoplasmic reticulum (ER) as well as in the extracellular medium (Yamamoto *et al.,* 2005). We have also tested if Shisa-2 could be secreted by injecting *XShisa-2* DNA into the nuclei of *Xenopus laevis* oocytes and culturing them for 24h. Unlike XShisa-1, XShisa-2 was only detected in the cell lysate and not in the medium (Fig 1F). This indicates that Shisa-2 is not secreted and may only function in the

ER. This difference can also be due to the different system used, which needs further investigation.
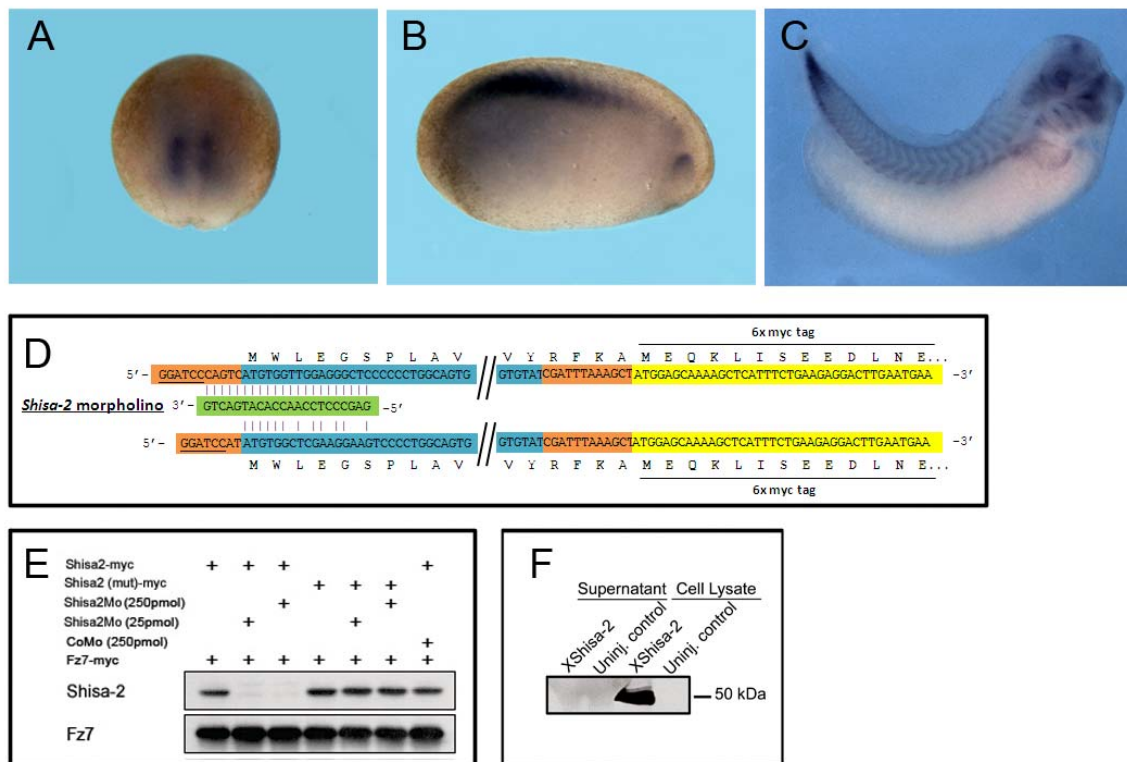
Figure 1 – Expression of *Xenopus Shisa-2* and morpholino oligonucleotide design and testing. (A-C) *XShisa-2* mRNA can be detected by *in situ* hybridization by late gastrulation in the paraxial mesoderm and later in development is highly expressed in the anterior portion of the presomitic mesoderm and in the newly formed somites. It can also be detected at lower levels in the remaining somites, in the eye, otic placodes and head mesenchyme. (D) Schematic structure and alignment of the *Xenopus Shisa-2* morpholino oligonucleotide (Shisa-2Mo) with the Shisa-2-myc (top) and Shisa-2(mut)-myc (bottom) expression constructs. The Shisa-2(mut)-myc expression is a mutated version of the Shisa-2-myc where the morpholino target sequence was mutated but maintains the same aminoacid sequence. (E) *In vitro* transcription/translation of XShisa-2-myc protein was blocked in the presence of Shisa-2Mo but not in the presence of the standard control morpholino, CoMo. Transcription/translation of the Shisa-2(mut)-myc rescue construct could not be blocked by Shisa-2Mo. Western blot analysis using anti-Myc antibody. (E) Secretion experiment for XShisa-2. Culture medium (Supernatant) and whole cell lysate from *Xenopus laevis* oocytes microinjected with the XShisa-2-myc expression construct were analyzed by Western blot using an anti-myc antibody. The predicted molecular weight of Shisa-2-myc protein is of 43 kDa.

Morpholino knockdown of Shisa-2 impairs somite formation

To assess the endogenous role of Shisa-2 during embryonic development, Shisa-2Mo or CoMo were injected unilaterally at the 4 cell stage, so that the uninjected side could serve as an internal control (throughout the present study, embryos were injected in a similar way unless otherwise stated). Shisa-2 morphants seamed normal until neurulation but morphological defects became visible from tailbud stages onwards. By tailbud stages, in the Shisa-2Mo injected side it was clearly seen that the somitic tissue was much narrower than in the control side, causing the dorsal fin to bend towards the

morpholino injected side (Fig. 2B-B''). In addition, in the Shisa-2 depleted side, the eye field was significantly reduced in size (Fig. 2E,E'). CoMo injected embryos developed normally and none of the above mentioned defects were observed (Fig. 2A-A'',D,D'). The phenotypes observed in Shisa-2 morphant embryos are detected in tissues which formation/patterning is FGF and/or Wnt signaling dependent. These observations suggest that Shisa-2 may function, like Shisa-1, as an inhibitor of Wnt and FGF signaling.
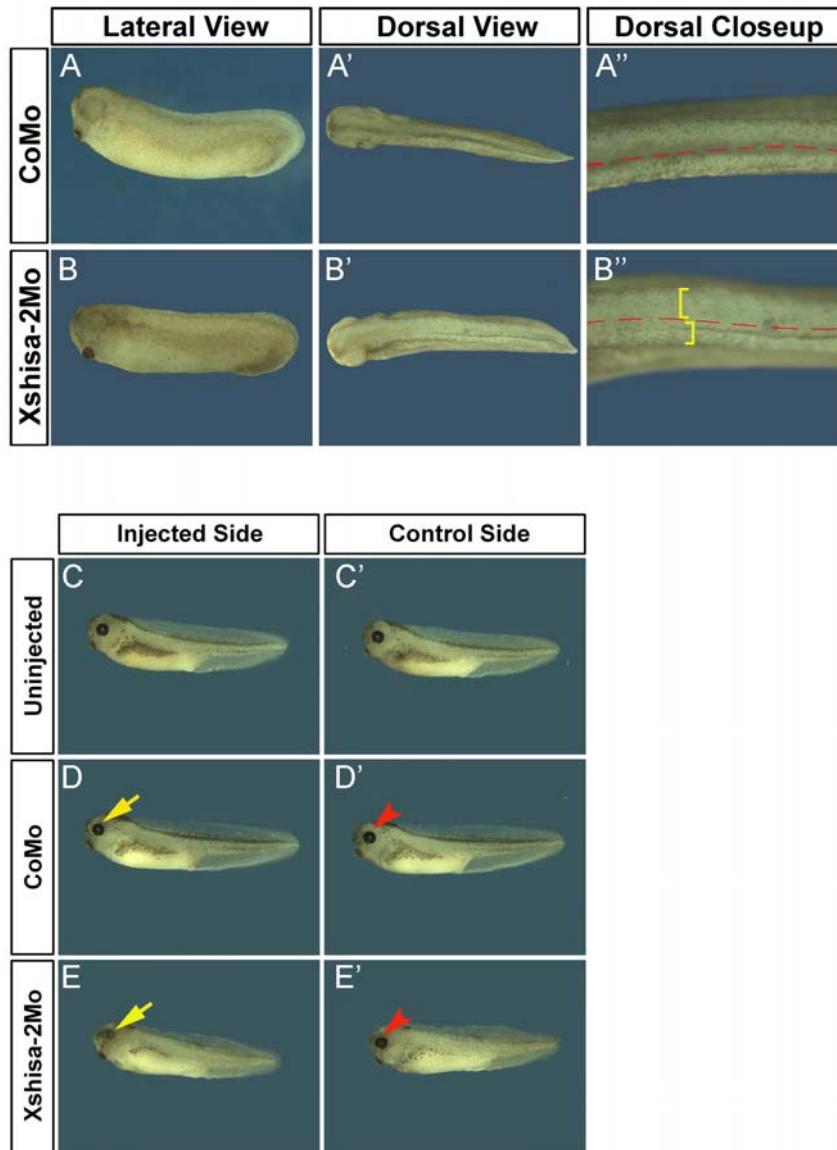
Figure 2 – *In vivo* requirement of *XShisa-2* during early development. *Xenopus laevis* embryos were unilaterally microinjected in the marginal zone of a 4 cell stage embryo with either (B-B'',E,E') Shisa-2 morpholino oligo (Shisa-2Mo, 5pmol) or (A-A'',D,D') a standard control morpholino oligo (CoMo, 5pmol) and grown until tailbud stages. (B-B'') Tailbud embryos injected with Shisa-2Mo developed mild defects that include a decrease in somitic tissue and bent dorsal fins (92%, n=75) when compared to the uninjected side or with embryos injected with (A-A'') CoMo. (E,E') Microinjection of Shisa-2Mo also resulted in embryos displaying smaller eyes (85%, n=62) in the injected side. (C-D')This phenotype was not observed in wild type or CoMo injected embryos.

166

Shisa-2 does not affect presomitic mesoderm formation but reduces somite size

To investigate the molecular and cellular defects observed in Shisa-2 morphant embryos, we analyzed the expression of known marker genes by whole mount in situ hybridization. It is well known that FGF signaling is necessary for mesoderm induction and for the specification of myogenic cell fate (Isaacs *et al.*, 1994; Fisher *et al.*, 2002; Bottcher and Niehrs, 2005). Because *Shisa-1* was shown to interfere with FGF signaling (Yamamoto *et al.*, 2005) we decided to analyze the expression pattern of two FGF downstream target genes, *Xbra*, a pan-mesodermal marker and *XmyoD*, a myogenic marker (Hopwood *et al.*, 1989) in Shisa-2 morphants (Fig. 3). For this purpose, four cell stage embryos were injected with 5pmol of either Shisa-2Mo or CoMo and grown until late gastrula/early neurula stages. Morphant embryos injected dorsally show no change in the *Xbra* ring around the blastopore (Fig. 3B). On the other hand, the axial domain of *Xbra* was wider and did not elongate properly in Shisa-2Mo injected embryos compared to CoMo injected or wildtype embryos (Fig. 3A and data not shown). In addition, unilateral depletion of Shisa-2 produced no effect on the expression of *XmyoD* when compared with the non injected side (Fig. 3D). These data suggest that the removal of Shisa-2 results in impaired convergent-extension without affecting mesoderm formation or the patterning of the embryo (anteroposterior or dorsoventral patterning). The defects in convergent extension may result from an excess of non-canonical Wnt/PCP pathway.
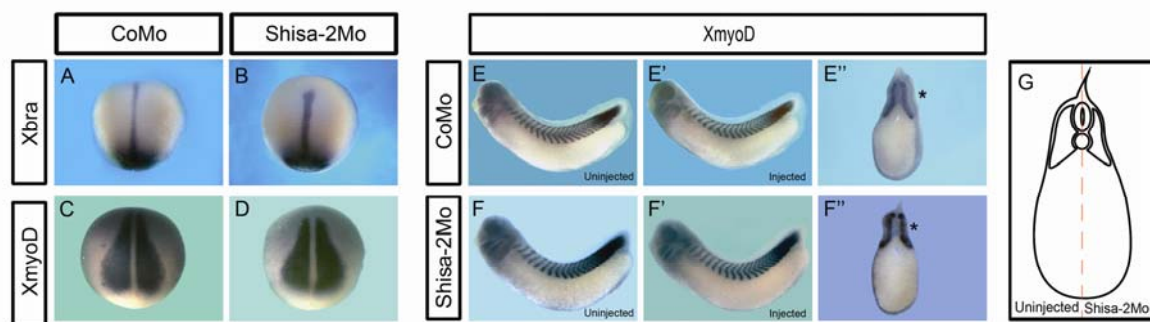
Figure 3 – Mesoderm induction and somite formation in Shisa-2 morphants. (A,B) Four cell stage embryos were injected dorsally (2.5pmol/blastomere) with (A) CoMo or (B) Shisa-2Mo and grown until stage 13, followed by *in situ* hybridization against *Xbra*. In the Shisa-2Mo injected embryos the axial domain of *Xbra* was shorter and wider (76%, n=25) than in the CoMo injected embryos (9%, n=23) while the ring around the blastopore was not affected. (C,E,E') CoMo or (D,F,F') Shisa-2Mo injection into the right blatomeres at the four-cell stage did not change *XmyoD* expression pattern. (E'',F'') Section at the level of the somites in a tailbud stage embryo. Injected side images were flipped horizontally in order to obtain a better comparison (F'') Injection of XShisa-2MO in the right side of the embryos resulted in embryos exhibiting narrow somites when compared with the non injected side (83%, n=42; injected side is marked with a black asterisk). (E'') CoMo injected embryos do not show significant difference between the injected side and the non injected side (6%, n=37). (G) Schematic drawing of the phenotype observed in the Shisa-2 morphants at the level of the somites.

The expression pattern of *XmyoD* was also analyzed in tailbud stage embryos injected unilaterally with either Shisa-2Mo or CoMo (Fig. 3E,E',F,F') and, similarly to what was observed for the earlier stages, in Shisa-2 morphants, *XmyoD* expression pattern was unaffected (Fig. 3F,F'). Nevertheless, when morpholino injected embryos, stained for *XmyoD*, were transversely sectioned at the somite level, the difference in somite size between the injected and the control side was apparent (Fig. 3F'',G), which could not be observed in CoMo injected embryos (Fig. 3E'') or uninjected embryos (not shown). These results suggest that *Shisa-2* plays no role during mesoderm formation and does not affect determination and position of the myogenic cells within the embryo. Nevertheless, *Shisa-2* is necessary for the formation of somites with proper size.

Shisa-2 is required for correct segmentation of the presomitic mesoderm

Somites are formed by a segmentation process that occurs in the presomitic mesoderm (PSM) in a cyclic way. This segmentation process has been proposed to be a result of a segmentation clock acting within cells of the PSM and of a wavefront which controls where the somite boundaries will be formed. This wavefront has been defined as a morphogenetic gradient of the signaling molecules: fibroblast growth factor (FGF), Wnts and retinoic acid (RA) (Dubrulle and Pourquie, 2004b). To analyze a possible role of *Shisa-2* in the PSM segmentation process we injected Shisa-2Mo unilaterally in the marginal zone of four cell stage embryos and let the embryos grow until early-tailbud or tailbud stages and performed WISH for different PSM gene markers. *Paraxial protocadherin* (*PAPC*) and *Thylacine2* (*thy2*, member of the *mesp* gene family) expression in the PSM has been precisely mapped and are suitable anterior PSM markers (Fig. 4A; Sparrow *et al.*, 1998; Kim *et al.*, 2000b). Knockdown experiments of Shisa-2 have shifted both *thy2* (Fig. 4B,C) and *PAPC* (Fig. 4D,E) expression anteriorly. Next, we tested whether in Shisa-2 morphants the expression pattern of known genes expressed in the unsegmented portion of the PSM, the tailbud domain (TBD), was also affected. We found that in the Shisa-2Mo injected side, the expression domains of *Xbra* (Fig. 4F,G; Smith *et al.*, 1991), and *Cyp26* (downstream target of RA; de Roos *et al.*, 1999; Fig. 4H,I) in the PSM were expanded anteriorly, similarity to what we had observed before for the anterior PSM markers *PAPC* and *thy2*. These results suggest that Shisa-2 depletion results in a delay in the segmentation process of the PSM cells, probably due to an increase in FGF and Wnt signaling.
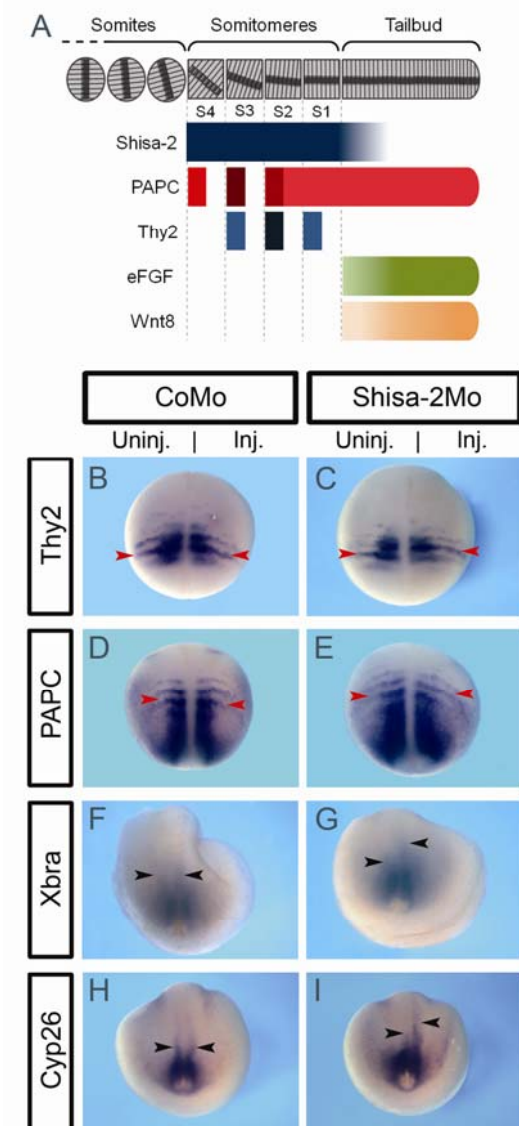
Figure 4 – *Shisa-2* **controls the position of the segmentation plane.** (A) Schematic diagram showing the expression pattern of several genes expressed in the PSM of *Xenopus* embryos in relation to both *Shisa-2* expression and somite formation. Color intensity was used to reflect the intensity of staining. (B-I) *In situ* hybridization analysis of morpholino injected embryos for different molecular markers, (B,C) *thy2*, (D,E) *PAPC*, (F,G) *Xbra* and (H,I) *Cyp26*. Four-cell stage embryos were injected with either CoMo (B,D,F,H) or Shisa-2Mo (C,E,G,I) and grown until early tailbud stages. Note that knock-down of Shisa-2 results in an anterior shift of the expression domain of (C) *thy2*, (E) *PAPC*, (G) *Xbra* and (I) *Cyp26* when compared with the non injected side. By contrast, these shifts were not seen in the CoMo injected embryos (B,D,F,H). Posterior view of the embryos. Red arrowheads indicate the location of the S-II/*Thy2* or S-III/*PAPC* stripes while the black arrowheads mark the anterior border of *Xbra* and *Cyp26* expression in the PSM.

Shisa-2 is necessary for eye and otic vesicle formation

To confirm the small eye phenotype observed in Shisa-2Mo injected embryos we analyzed the expression of different eye markers (Fig. 5) such as, *Pax6* (Hirsch and Harris, 1997), *Xrx1* (marks only retina; Casarosa *et al.*, 1997), *Sox2* (Mizuseki *et al.*, 1998) and *Cyp26* (lens marker; de Roos *et al.*, 1999). For that, we have injected embryos unilaterally with either CoMo or with Shisa-2Mo and grown them until tailbud stages. *In situ* hybridization for *Pax6* showed that in the Shisa-2 depleted embryos the prospective eye field in the injected side was reduced when compared with the uninjected control side (Fig. 5B). Nevertheless, none of the remaining *Pax6* expression domains was affected by the knock-down of Shisa-2. In addition, Shisa-2 depletion leads to the reduction in *Xrx1* expression (Fig. 5D), indicating that eye formation is affected by the loss of Shisa-2. Microinjection of CoMo did not affect any of the expression domains of *Pax6* nor the expression of *Xrx1*

(Fig. 5A,C). Analysis of the expression pattern of the pan-neuroectodermal marker S*ox2* confirmed the small eye phenotype observed for the Shisa-2Mo injected embryos. However, Shisa-2 depletion did not interfere with the formation of neural tissue (Fig. 5F). Later in development, at the late tailbud stage, analysis of the expression pattern of the RA downstream target *Cyp26* showed that the expression of *Cyp26,* in Shisa-2 morphants, is downregulated specifically in the lens (Fig. 5I-J').
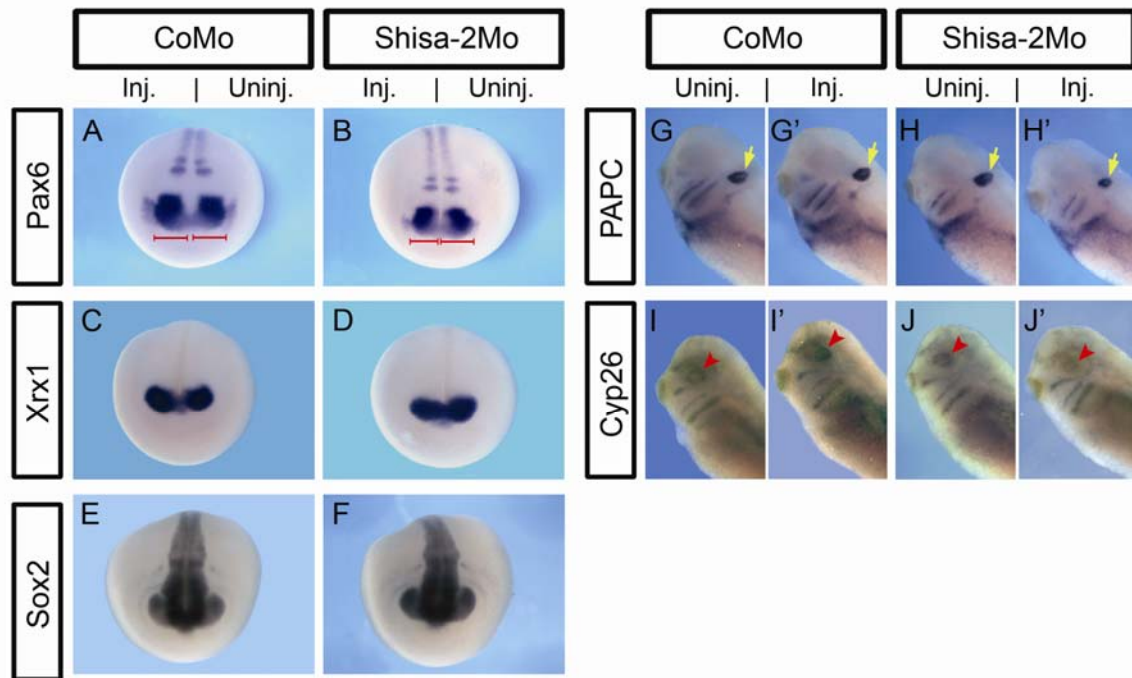
Figure 5 – Loss of Shisa-2 function interferes with eye and otic vesicle development. *Xenopus* embryos were injected unilaterally with 5 pmol of either (B,D,F,H,H',J,J') Shisa-2Mo or (A,C,E,G,G',I,I') CoMo in the marginal zone at the 4-cell stage and fixed at (A-F) early and (G-J') late tailbud stages. CoMO injected embryos show normal expression of (A) *Pax6*, (C) *Xrx1*, (E) *sox2*, (G,G') *PAPC* and (I,I') *Cyp26*. *In situ* hybridization for (B) *Pax6*, (D) *Xrx1* and (E) *Sox2* in Shisa-2Mo injected embryos shows that the eye field is reduced in the injected side compared with the uninjected side that serves as an internal control. (H,H') *In situ* hybridization against *PAPC* shows a reduction in the otic vesicle in the injected side of the Shisa-2Mo morphant embryos when compared with the control. (J,J') *Cyp26* lens domain in the Shisa-2 depleted embryos is downregulated. Morpholino injected side images of late tailbud embryos were flipped horizontally for a better comparison with the non injected side.

To further investigate the function of *Shisa-2* during *Xenopus* development, we decided next to focus on the otic vesicle, which also expresses *Shisa-2* (Fig.1 B,C). To do so, whole-mount *in situ* hybridization for PAPC was performed in early tailbud and tailbud stages embryos, unilaterally injected with either Shisa-2Mo or CoMo (Fig. 5G-H'). One could observe that in the Shisa-2Mo injected embryos, the otic vesicle was clearly smaller in the injected side when compared to the uninjected control side of the same embryo (Fig. 5H,H'). In contrast, the otic vesicle was not affected by the CoMo injection (Fig. 5G,G').

170

Discussion

In this study we have characterized the function of a second member of the *Shisa* gene family. *Shisa-2* was previously reported as being strongly expressed in the anterior part of the presomitic mesoderm and in the recently formed somites. As the embryo develops, *Shisa-2* expression pattern moves posteriorly and keeps being expressed at low levels in more mature somites. In addition, *Shisa-2* was also reported as being expressed in the head region, namely in the eye, otic vesicles and branchial arches. Due to this very interesting expression pattern, its possible role in inhibiting FGF and Wnt signaling and the fact that the formation/induction of the above mentioned structures is directly related to both FGF and Wnt signaling pathway, we decided to study the role of *Shisa-2* during *Xenopus* by performing loss-of-function studies using antisense morpholino oligonucleotides.

Role of Shisa-2 in Somitogenesis

Depletion of Shisa-2 in the frog embryo results in anteriorization of the PSM as a result of a delay in the maturation of the presomitic mesoderm (PSM) cells. This phenotype can be related to a possible role of Shisa-2 in inhibiting FGF and Wnt signaling.

Somitogenesis is the process by which the presomitic mesodermal cells become segmented into epithelial block designated as somites. This segmentation process is generated in a rhythmic fashion from the caudal portion of the mesenchymal PSM. Several proposed models have attempted to explain how somites are formed from the PSM. In the clock and wavefront model view, the position where the segmental boundaries in the PSM will be formed depends on the "determination front" and the time at which each segment will be formed will be determined by a molecular oscillator, the segmentation clock. The determination front is determined by a morphogenetic gradient of Wnt, FGF and RA signaling originated in the anterior and posterior ends of the PSM (Dubrulle *et al.*, 2001; Sawada *et al.*, 2001; Aulehla *et al.*, 2003; Diez del Corral *et al.*, 2003; Moreno and Kintner, 2004). *Fgf8* mRNA is expressed in the PSM in a graded way (anterior-to-posterior), highly expressed in the posterior unsegmented region of the PSM and at low levels in the anterior end of the PSM (Dubrulle and Pourquie, 2004a). Studies have shown that increasing the levels of FGF signaling in the PSM, by either overexpressing *fgf8* mRNA or by grafting FGF8 beads, resulted in somites with smaller

sizes while, blocking FGF signaling has led to the formation of larger somites (Dubrulle *et al.*, 2001). This gradient has, thereby, been shown to be necessary and responsible for maintaining the immature state of the cells in the posterior portion of the PSM (the tail bud domain, TBD, in the frog). In the opposite direction (from anterior-to-posterior), the RA gradient is set and has been determined to be necessary for the activation of segmentation genes (Diez del Corral *et al.*, 2003; Moreno and Kintner, 2004; Vermot and Pourquie, 2005). RA gradient seems necessary for restricting FGF gradient to the anterior region of the PSM, and vice versa (Diez del Corral *et al.*, 2003; Moreno and Kintner, 2004). This mutual inhibition apparently determines the position where segmentation will occur, which corresponds to the domain of expression of the *mesp* genes (Moreno and Kintner, 2004; Delfini *et al.*, 2005; Morimoto *et al.*, 2005). The Wnt signaling pathway has also been reported to be necessary for placing the determination wavefront (Aulehla *et al.*, 2003). In chick embryos, *Wnt3a* has a gradient expression in the PSM and misexpression of *Axin2*, an inhibitor of Wnt signaling pathway, in the PSM results in larger somites while increasing the levels of *Wnt3a* in the PSM leads to the formation of smaller somites (Aulehla *et al.*, 2003).

In summary, the gradient of both Wnt and FGF signaling needs to be tightly regulated in order for a proper segmentation program to occur. Shisa-2 might function cell autonomously to insure an appropriate wavefront position. Our data suggests that Shisa-2 functions as an antagonist of FGF and Wnt signaling. This assumption results from the fact that Shisa-2Mo injected embryos display a mild convergent extension phenotype, which typically has been associated with perturbations in the non-canonical Wnt signaling pathway (Sokol, 1996; Medina *et al.*, 2000; Habas *et al.*, 2001; Cheyette *et al.*, 2002). On the other hand, the expression pattern of *Xbra*, a known FGF downstream target gene was shown to be shifted anteriorly in the PSM of Shisa-2Mo injected embryos. These results, along with high homology at the aminoacid level between Shisa-1 and Shisa-2, support the idea of a mode of action for Shisa-2 similar to the one described for Shisa-1, functioning therefore as a Wnt and FGF inhibitor, within the ER, by interacting directly with the immature forms of Frizzled and FGF receptor, preventing their maturation and transport to the cell surface.

Frizzled-2 and -7 as well as FGFR1 have been reported to be expressed at the somite level and in the PSM (Deardorff and Klein, 1999; Golub *et al.*, 2000; Sumanas *et al.*, 2000) and might be the endogenous targets of Shisa-2. Shisa-2 might thereby be able to

control the morphogenetic gradient of FGF and Wnts by regulating the levels by which their receptors appear at the cell surface. Our data shows that in Shisa-2 depleted embryos, the regulation of the gradient of FGF and Wnt ligands in the PSM by RA and Axin2, among other molecules is not sufficient to place the determination front in the correct place. Shisa-2 might therefore act to generate a gradient of Frizzled and FGFR at the cell surface that can, in turn, be transduced in a stronger FGF and Wnt signaling in the posterior region portion of the PSM which decreases towards the anterior portion of the PSM, reaching a minimum at the level where segmentation will take place.

The narrow somite phenotype observed in the Shisa-2 morphants could also be explained by an increase of both FGF and Wnt signaling. As mentioned above, an increase of either FGF or Wnt signaling results in the formation of smaller somites due to a reduction in the number of cells that incorporate the somites (Dubrulle *et al.*, 2001; Aulehla *et al.*, 2003). In the *Xenopus* embryo, the somites form when a group of PSM cells segregate and perform a rotation of 90º, acquiring a final orientation parallel to the AP axis (Jen *et al.*, 1997). In the absence of Shisa-2 there will be and increase of FGF and Wnt signaling which leads to a reduction of the number of cells that will segregate from the remaining PSM. Once this cell population rearranges itself it will result in a somite with the same length although narrower (Fig 6).
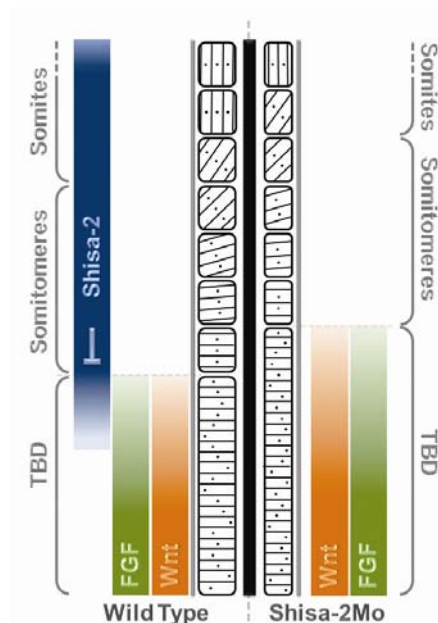
Figure 6 –Proposed model of the function of *Shisa-2* in somitogenesis. In the wild type embryo, the segmentation process occurring in the PSM is regulated by different signaling pathways including FGF and Wnt signaling. *Fgf* and *Wnt* signals that are expressed in a caudal to rostral decreasing gradient control the maturation of the PSM and determine the position where segmentation will take place. *Shisa-2* is also expressed in a gradient with high levels in the rostral portion of the PSM and in the recently formed somites and gradually decreases towards the anterior of the embryo and towards the caudal unsegmented portion of the PSM. By possibly inhibiting FGF and Wnt signaling, *Shisa-2* is responsible for the correct positioning of the segmentation plane. In the Shisa-2 morphant embryos, depletion of Shisa-2 protein creates and excess of Wnt and FGF signaling that extends more anteriorly than in the wild type embryo preventing higher number of cells from entering the segmentation program. In addition, the excess of FGF and Wnt signaling leads to a reduced number of cells segregating from the PSM which results, after cell rearrangement, in narrower somites.

Shisa-2 and placode formation

In the present study we have shown that *Xenopus Shisa-2* is not only required during somitogenesis but our experiments also showed that loss of Shisa-2 function led to an impairment in eye and otic vesicle formation.

Several studies performed in different vertebrate model organisms have shown that canonical Wnt signaling inhibits eye formation (de Iongh *et al.,* 2006). In the zebrafish *headless* mutant, a mutation of the *Tcf3* gene, which is a transcriptional repressor of the Wnt signaling cascade, causes loss of eyes, forebrain and part of the midbrain (Kim *et al.,* 2000a). A mutation in *Axin*, as seen in the zebrafish mutant *masterblind*, results in a fate transformation where eye and telencephalon structures become posterior diencephalon (Heisenberg *et al.,* 2001). Likewise, overexpression of Wnt pathway, like a *GSK-3β* dominant negative, results in eye reduction that can be rescued by coinjection of Wnt antagonists (Nambiar and Henion, 2004). On the other hand, microinjection of Wnt antagonists, like *dkk-1* or *cerberus*, into wild-type embryos leads to enlarged eyes and anterior structures (Bouwmeester *et al.,* 1996; Glinka *et al.,* 1998; Shinya *et al.,* 2000). Consistent with these results, mutant mice where β-catenin was inactivated specifically in the periocular ectoderm formed ectopic lenses while a constitutively active form of β-catenin suppresses lens development (Smith *et al.,* 2005). In the vertebrate embryo, several components of the Wnt signaling pathway are expressed in the eye field (de Iongh *et al.,* 2006).

Similarly to Wnt canonical signaling, the activation of FGF signaling before gastrulation has been shown to lead to the formation of small eyes whereas inhibition of FGF signaling causes eye field enlargement (Moore *et al.,* 2004). Overexpressing the mouse or *Xenopus Hip*, a Wnt, FGF and Hedgehog (HH) antagonist, in the frog embryo results in increased eye sizes (Cornesse *et al.,* 2005). On the other hand, loss-of-function experiments have shown that XHip depletion results in the suppression of the lens placode formation (Cornesse *et al.,* 2005). In the same study, the authors have shown that microinjection of a dominant-negative FGFR induces larger lens placodes and that lens placode suppression could be achieved by microinjecting *fgf8* mRNA (Cornesse *et al.,* 2005). The eye and otic vesicle phenotype observed in Shisa-2 morphant embryos are therefore in favor of the idea of an increase in Wnt and FGF signaling in these structures. Nevertheless, additional functional data, including rescue experiments, need to be

performed to support this view and to determine whether Shisa-2 is inhibiting *in vivo* both signaling pathways in the eye and otic vesicle or only one of them.

In summary, our studies show that Shisa-2 is not only required for the segmentation process but it is also necessary during other morphological processes like eye and otic vesicle formation.

Experimental Procedures

Manipulation of *Xenopus* Embryos

Unfertilized eggs were squeezed out manually from pigmented female *Xenopus laevis* which had been injected with 300-400 units of human chorionic gonadotropin (Sigma). Eggs were *in vitro* fertilized with macerated testis, dejellied in 2% L-cysteine-HCl (pH 8.0), injected in 1xMBS-H (88 mM NaCl, 1 mM KCl, 2.4 mM $NaHCO_3$, 0.82 mM $MgSO_4$, 0.41 mM $CaCl_2$, 0.33 mM $Ca(NO_3)_2$, 1 mM HEPES pH 7.4) and grown in 0.1xMBS-H at 14–21°C until the desired stages. Embryos were staged according to Nieuwkoop and Faber (1967).

Microinjection of *Xenopus laevis* Oocytes

A portion of ovarian tissue was surgically removed from an adult sacrificed female *Xenopus laevis*. The excised ovary tissue was teared into small pieces and incubated in 0.2% (w/v) collagenase in 1x MBS-H solution without Ca^{2+} and Mg^{2+} for 2h at RT, with gentle rocking, until complete defolliculization was achieved. Oocytes were then extensively washed in 1xMBS-H to completely remove the collagenase and transferred to a glass Petri dish containing oocyte culture medium and set aside overnight at RT. On the following morning, healthy stage 4 and 5 oocytes were picked and transferred to fresh oocyte culture medium. Oocytes were then turned with the animal pole upwards and DNA nuclear injection was performed by injecting in the center of the animal pole. After injection, oocytes were cultured in oocyte culture medium supplemented with 0.5mg/mL bovine serum albumin (BSA), at 20°C for 1 day.

Plasmid constructs and morpholino Oligonucleotide

The *Xenopus* Shisa-2 morpholino oligonucleotide (Shisa-2Mo) was synthesized and obtained from Gene Tools LLC. Shisa-2Mo was designed to complement the region between base -5 upstream of the AUG and base +17 downstream of the AUG

(5′-GAGCCCTCCAACCACATGACTG-3′). The standard control morpholino oligonucleotide was also obtained from Gene Tools LLC (5'-CCTCTTACCTCAGTTACAATTTATA-3').

To test the efficiency and specificity of Shisa-2Mo two C-terminal myc-tagged constructs were generated: Shisa-2-myc, that contains *Xenopus Shisa-2* complete CDS plus the 5 bp upstream of the ATG in order to contain the antisense morpholino oligonucleotide consensus sequence; and Shisa-2(mut)-myc, a full-length *Shisa-2* construct where the first 17 nucleotides after the ATG were mutated in order to maintain the same aminoacid sequence but no longer be targeted by the morpholino. The Shisa-2-myc construct was generated by PCR amplification of pCRII-TOPO.Shisa-2 (Silva *et al.,* 2006) to include the 5′UTR sequence and mutate the stop codon. For that, the following primers were used: Shisa2myc_Fw (5′-TTAGGATCCCAGTCATGTGGTTGGAGGGCTCC-3′); Shisa2myc_Rev (5′-AAAATCGATACACAGTCACGGCTGGG-3′). The PCR product was cloned into pGEM-T easy (Promega) and then the BamHI/ClaI fragment was subcloned into pCS2+-6xmyc (pCS2+MT). To introduce the mutation to generate the Shisa-2(mut)-myc rescue construct a two-step partial amplification of pCRII-TOPO.Shisa-2 was performed using the following primers: Shisa-2(mut)-myc_Fw1 (5′-TCGAAGGAAGTCCCCTGGCAGTGTTGG-3′); Shisa-2(mut)-myc_Fw2 (5′-TTAGGATCCATATGTGGCTCGAAGGAAGTCCC-3′); Shisa-2(mut)-myc_Rev (5′-AGGGATGGTCTCCATCAGCCGGTTACTTCC-3′). The PCR product (485 bp) was cloned into pGEM-T easy and the 448 bp BamHI-SacI fragment was used to replace the BamHI-SacI fragment from pCS2.Shisa-2-6xmyc.

In vitro translation and Western Blot analysis

For *in vitro* transcription/translation the TNT®* Coupled Reticulocyte Lysate System (Promega) was used according to the manufacturer's instructions. For protein secretion assay, *Xenopus* oocytes were extracted in 20mM HEPES pH 7.4, 130mM NaCl, 2mM EDTA, 1mM EGTA and 1% NP-40 supplemented with a cocktail of protease inhibitors (Calbiochem). To test for the presence of secreted proteins upon oocyte injection the oocyte culture medium was collected and proteins in the medium were precipitated using 4 volumes of cold acetone and resuspended in 1x SDS-PAGE loading buffer. Proteins were heated in loading buffer and separated by denaturing SDS-PAGE using a 12% polyacrylamide gel (Laemmli, 1970). Subsequently, proteins were transferred to a

nitrocellulose membrane (Towbin *et al.,* 1979), detected with a monoclonal mouse anti-c-myc (Oncogene) and developed using a chemiluminescent substrate (Pierce).

Whole-Mount in Situ Hybridization

Embryos to be used for in situ hybridization were incubated until the proper stages, fixed in MEMFA (0.1 M Mops [pH 7.4], 2 mM EGTA, 1 mM MgSO$_4$, 3.7% formaldehyde) solution, for 2h at RT or ON at 4°C, and stored in methanol at −20°C until use. Whole-mount in situ hybridization and antisense probe preparation were carried out as described (Epstein *et al.,* 1997). Probes were purified with a Quick Spin Mini RNA column (Roche). To generate the digoxigenin labeled antisense RNA probes, plasmids containing Cyp26, PAPC, Pax6, Thy2, XmyoD and Xrx1 fragments were linearized using *EcoRI*, *XbaI*, *NotI*, *PvuII*, *HindIII* and *BamHI* respectively, and transcribed using T7 RNA polymerase. Plasmids containing Shisa-2 and Xbra were cut with *XbaI* and *SalI* respectively, and transcribed using SP6 RNA polymerase. Hybridized RNAs were detected with alkaline-phosphatase-conjugated anti-DIG-antibody (Roche) and developed using BM purple or NBT/BCIP (both from Roche). Stained embryos were bleached, by illumination, in 1% H$_2$O$_2$, 4% formamide and 0.5x SSC pH 7.0. Embryos were refixed in MEMFA and photographed under bright light with a Leica DFCM20 camera, mounted on a Leica MZIII stereoscope.

Acknowledgements

References

Aulehla A, Wehrle C, Brand-Saberi B, Kemler R, Gossler A, Kanzler B, Herrmann BG. 2003. Wnt3a plays a major role in the segmentation clock controlling somitogenesis. Dev Cell 4:395-406.

Bottcher RT, Niehrs C. 2005. Fibroblast growth factor signaling during early vertebrate development. Endocr Rev 26:63-77.

Bouwmeester T, Kim S, Sasai Y, Lu B, De Robertis EM. 1996. Cerberus is a head-inducing secreted factor expressed in the anterior endoderm of Spemann's organizer. Nature 382:595-601.

Casarosa S, Andreazzoli M, Simeone A, Barsacchi G. 1997. Xrx1, a novel Xenopus homeobox gene expressed during eye and pineal gland development. Mech Dev 61:187-198.

Cheyette BN, Waxman JS, Miller JR, Takemaru K, Sheldahl LC, Khlebtsova N, Fox EP, Earnest T, Moon RT. 2002. Dapper, a Dishevelled-associated antagonist of beta-catenin and JNK signaling, is required for notochord formation. Dev Cell 2:449-461.

Cornesse Y, Pieler T, Hollemann T. 2005. Olfactory and lens placode formation is controlled by the hedgehog-interacting protein (Xhip) in Xenopus. Dev Biol 277:296-315.

de Iongh RU, Abud HE, Hime GR. 2006. WNT/Frizzled signaling in eye development and disease. Front Biosci 11:2442-2464.

de Roos K, Sonneveld E, Compaan B, ten Berge D, Durston AJ, van der Saag PT. 1999. Expression of retinoic acid 4-hydroxylase (CYP26) during mouse and Xenopus laevis embryogenesis. Mech Dev 82:205-211.

Deardorff MA, Klein PS. 1999. Xenopus frizzled-2 is expressed highly in the developing eye, otic vesicle and somites. Mech Dev 87:229-233.

Delfini MC, Dubrulle J, Malapert P, Chal J, Pourquie O. 2005. Control of the segmentation process by graded MAPK/ERK activation in the chick embryo. Proc Natl Acad Sci U S A 102:11343-11348.

Diez del Corral R, Olivera-Martinez I, Goriely A, Gale E, Maden M, Storey K. 2003. Opposing FGF and retinoid pathways control ventral neural pattern, neuronal differentiation, and segmentation during body axis extension. Neuron 40:65-79.

Du SJ, Purcell SM, Christian JL, McGrew LL, Moon RT. 1995. Identification of distinct classes and functional domains of Wnts through expression of wild-type and chimeric proteins in Xenopus embryos. Mol Cell Biol 15:2625-2634.

Dubrulle J, McGrew MJ, Pourquie O. 2001. FGF signaling controls somite boundary position and regulates segmentation clock control of spatiotemporal Hox gene activation. Cell 106:219-232.

Dubrulle J, Pourquie O. 2004a. Coupling segmentation to axis formation. Development 131:5783-5793.

Dubrulle J, Pourquie O. 2004b. fgf8 mRNA decay establishes a gradient that couples axial elongation to patterning in the vertebrate embryo. Nature 427:419-422.

Epstein M, Pillemer G, Yelin R, Yisraeli JK, Fainsod A. 1997. Patterning of the embryo along the anterior-posterior axis: the role of the caudal genes. Development 124:3805-3814.

Fisher ME, Isaacs HV, Pownall ME. 2002. eFGF is required for activation of XmyoD expression in the myogenic cell lineage of Xenopus laevis. Development 129:1307-1315.

Glinka A, Wu W, Delius H, Monaghan AP, Blumenstock C, Niehrs C. 1998. Dickkopf-1 is a member of a new family of secreted proteins and functions in head induction. Nature 391:357-362.

Goldfarb M. 1996. Functions of fibroblast growth factors in vertebrate development. Cytokine Growth Factor Rev 7:311-325.

Golub R, Adelman Z, Clementi J, Weiss R, Bonasera J, Servetnick M. 2000. Evolutionarily conserved and divergent expression of members of the FGF receptor family among vertebrate embryos, as revealed by FGFR expression patterns in Xenopus. Dev Genes Evol 210:345-357.

Habas R, Kato Y, He X. 2001. Wnt/Frizzled activation of Rho regulates vertebrate gastrulation and requires a novel Formin homology protein Daam1. Cell 107:843-854.

Heasman J. 2002. Morpholino oligos: making sense of antisense? Dev Biol 243:209-214.

Heisenberg CP, Houart C, Take-Uchi M, Rauch GJ, Young N, Coutinho P, Masai I, Caneparo L, Concha ML, Geisler R, Dale TC, Wilson SW, Stemple DL. 2001. A mutation in the Gsk3-binding domain of zebrafish Masterblind/Axin1 leads to a fate transformation of telencephalon and eyes to diencephalon. Genes Dev 15:1427-1434.

Heisenberg CP, Tada M, Rauch GJ, Saude L, Concha ML, Geisler R, Stemple DL, Smith JC, Wilson SW. 2000. Silberblick/Wnt11 mediates convergent extension movements during zebrafish gastrulation. Nature 405:76-81.

Hirsch N, Harris WA. 1997. Xenopus Pax-6 and retinal development. J Neurobiol 32:45-61.

Hopwood ND, Pluck A, Gurdon JB. 1989. MyoD expression in the forming somites is an early response to mesoderm induction in Xenopus embryos. Embo J 8:3409-3417.

Isaacs HV, Pownall ME, Slack JM. 1994. eFGF regulates Xbra expression during Xenopus gastrulation. Embo J 13:4469-4481.

Jen WC, Wettstein D, Turner D, Chitnis A, Kintner C. 1997. The Notch ligand, X-Delta-2, mediates segmentation of the paraxial mesoderm in Xenopus embryos. Development 124:1169-1178.

Keller R, Davidson L, Edlund A, Elul T, Ezin M, Shook D, Skoglund P. 2000. Mechanisms of convergence and extension by cell intercalation. Philos Trans R Soc Lond B Biol Sci 355:897-922.

Kim CH, Oda T, Itoh M, Jiang D, Artinger KB, Chandrasekharappa SC, Driever W, Chitnis AB. 2000a. Repressor activity of Headless/Tcf3 is essential for vertebrate head formation. Nature 407:913-916.

Kim SH, Jen WC, De Robertis EM, Kintner C. 2000b. The protocadherin PAPC establishes segmental boundaries during somitogenesis in xenopus embryos. Curr Biol 10:821-830.

Laemmli UK. 1970. Cleavage of structural proteins during the assembly of the head of bacteriophage T4. Nature 227:680-685.

Li L, Yuan H, Weaver CD, Mao J, Farr GH, 3rd, Sussman DJ, Jonkers J, Kimelman D, Wu D. 1999. Axin and Frat1 interact with dvl and GSK, bridging Dvl to GSK in Wnt-mediated regulation of LEF-1. Embo J 18:4233-4240.

Mao B, Wu W, Li Y, Hoppe D, Stannek P, Glinka A, Niehrs C. 2001. LDL-receptor-related protein 6 is a receptor for Dickkopf proteins. Nature 411:321-325.

Medina A, Reintsch W, Steinbeisser H. 2000. Xenopus frizzled 7 can act in canonical and non-canonical Wnt signaling pathways: implications on early patterning and morphogenesis. Mech Dev 92:227-237.

Mizuseki K, Kishi M, Matsui M, Nakanishi S, Sasai Y. 1998. Xenopus Zic-related-1 and Sox-2, two factors induced by chordin, have distinct activities in the initiation of neural induction. Development 125:579-587.

Mlodzik M. 2002. Planar cell polarization: do the same mechanisms regulate Drosophila tissue polarity and vertebrate gastrulation? Trends Genet 18:564-571.

Moon RT, Campbell RM, Christian JL, McGrew LL, Shih J, Fraser S. 1993. Xwnt-5A: a maternal Wnt that affects morphogenetic movements after overexpression in embryos of Xenopus laevis. Development 119:97-111.

Moore KB, Mood K, Daar IO, Moody SA. 2004. Morphogenetic movements underlying eye field formation require interactions between the FGF and ephrinB1 signaling pathways. Dev Cell 6:55-67.

Moreno TA, Kintner C. 2004. Regulation of segmental patterning by retinoic acid signaling during Xenopus somitogenesis. Dev Cell 6:205-218.

Morimoto M, Takahashi Y, Endo M, Saga Y. 2005. The Mesp2 transcription factor establishes segmental borders by suppressing Notch activity. Nature 435:354-359.

Nambiar RM, Henion PD. 2004. Sequential antagonism of early and late Wnt-signaling by zebrafish colgate promotes dorsal and anterior fates. Dev Biol 267:165-180.

Nieuwkoop PD, Faber J. 1967. Normal table of Xenopus laevis (Daudin). Amsterdam: North Holland.

Nusse R. 2005. Wnt signaling in disease and in development. Cell Res 15:28-32.

Pinson KI, Brennan J, Monkley S, Avery BJ, Skarnes WC. 2000. An LDL-receptor-related protein mediates Wnt signalling in mice. Nature 407:535-538.

Sawada A, Shinya M, Jiang YJ, Kawakami A, Kuroiwa A, Takeda H. 2001. Fgf/MAPK signalling is a crucial positional cue in somite boundary formation. Development 128:4873-4880.

Shinya M, Eschbach C, Clark M, Lehrach H, Furutani-Seiki M. 2000. Zebrafish Dkk1, induced by the pre-MBT Wnt signaling, is secreted from the prechordal plate and patterns the anterior neural plate. Mech Dev 98:3-17.

Silva AC, Filipe M, Vitorino M, Steinbeisser H, Belo JA. 2006. Developmental expression of Shisa-2 in Xenopus laevis. Int J Dev Biol 50:575-579.

Slusarski DC, Yang-Snyder J, Busa WB, Moon RT. 1997. Modulation of embryonic intracellular Ca2+ signaling by Wnt-5A. Dev Biol 182:114-120.

Smith AN, Miller LA, Song N, Taketo MM, Lang RA. 2005. The duality of beta-catenin function: a requirement in lens morphogenesis and signaling suppression of lens fate in periocular ectoderm. Dev Biol 285:477-489.

Smith JC, Price BM, Green JB, Weigel D, Herrmann BG. 1991. Expression of a Xenopus homolog of Brachyury (T) is an immediate-early response to mesoderm induction. Cell 67:79-87.

Sokol SY. 1996. Analysis of Dishevelled signalling pathways during Xenopus development. Curr Biol 6:1456-1467.

Sparrow DB, Jen WC, Kotecha S, Towers N, Kintner C, Mohun TJ. 1998. Thylacine 1 is expressed segmentally within the paraxial mesoderm of the Xenopus embryo and interacts with the Notch pathway. Development 125:2041-2051.

Sumanas S, Strege P, Heasman J, Ekker SC. 2000. The putative wnt receptor Xenopus frizzled-7 functions upstream of beta-catenin in vertebrate dorsoventral mesoderm patterning. Development 127:1981-1990.

Summerton J, Weller D. 1997. Morpholino antisense oligomers: design, preparation, and properties. Antisense Nucleic Acid Drug Dev 7:187-195.

Tamai K, Semenov M, Kato Y, Spokony R, Liu C, Katsuyama Y, Hess F, Saint-Jeannet JP, He X. 2000. LDL-receptor-related proteins in Wnt signal transduction. Nature 407:530-535.

Thisse B, Thisse C. 2005. Functions and regulations of fibroblast growth factor signaling during embryonic development. Dev Biol 287:390-402.

Towbin H, Staehelin T, Gordon J. 1979. Electrophoretic transfer of proteins from polyacrylamide gels to nitrocellulose sheets: procedure and some applications. Proc Natl Acad Sci U S A 76:4350-4354.

Umbhauer M, Djiane A, Goisset C, Penzo-Mendez A, Riou JF, Boucaut JC, Shi DL. 2000. The C-terminal cytoplasmic Lys-thr-X-X-X-Trp motif in frizzled receptors mediates Wnt/beta-catenin signalling. Embo J 19:4944-4954.

van Noort M, Clevers H. 2002. TCF transcription factors, mediators of Wnt-signaling in development and cancer. Dev Biol 244:1-8.

Veeman MT, Axelrod JD, Moon RT. 2003. A second canon. Functions and mechanisms of beta-catenin-independent Wnt signaling. Dev Cell 5:367-377.

Vermot J, Pourquie O. 2005. Retinoic acid coordinates somitogenesis and left-right patterning in vertebrate embryos. Nature 435:215-220.

Wallingford JB, Fraser SE, Harland RM. 2002. Convergent extension: the molecular control of polarized cell movement during embryonic development. Dev Cell 2:695-706.

Winklbauer R, Medina A, Swain RK, Steinbeisser H. 2001. Frizzled-7 signalling controls tissue separation during Xenopus gastrulation. Nature 413:856-860.

Wong HC, Bourdelas A, Krauss A, Lee HJ, Shao Y, Wu D, Mlodzik M, Shi DL, Zheng J. 2003. Direct binding of the PDZ domain of Dishevelled to a conserved internal sequence in the C-terminal region of Frizzled. Mol Cell 12:1251-1260.

Yamamoto A, Nagano T, Takehara S, Hibi M, Aizawa S. 2005. Shisa promotes head formation through the inhibition of receptor protein maturation for the caudalizing factors, Wnt and FGF. Cell 120:223-235.

II.5 Characterization of XADTK1, a member of a novel family of tyrosine (serine/threonine or tyrosine) kinases, expressed in the Xenopus organizer

Characterization of XADTK1, a member of a novel family of tyrosine (serine/threonine or tyrosine) kinases, expressed in the Xenopus organizer

Ana Cristina Silva[1,2], Marta Vitorino[2], Mário Filipe[1], Herbert Steinbeisser[3], and José António Belo[1,2,4]

In preparation

[1]Instituto Gulbenkian de Ciência, Rua da Quinta Grande, 6, Apartado 14, 2781-901 Oeiras, Portugal; [2]Centro de Biomedicina Molecular e Estrutural, Universidade do Algarve, Campus de Gambelas, 8000-010 Faro, Portugal; [3]Institute of Human Genetics, University of Heidelberg, Im Neuenheimer Feld 366, 69120 Heidelberg, Germany; [4]Author for correspondence: José A. Belo, Tel: +351214407942, Fax: +351214407970, e-mail: jbelo@igc.gulbenkian.pt.

Characterization of XADTK1, a member of a novel family of tyrosine (serine/threonine or tyrosine) kinases, expressed in the *Xenopus* organizer

Ana Cristina Silva[1,2], Marta Vitorino[2], Mário Filipe[1], Herbert Steinbeisser[3], and José António Belo[1,2,4]

[1]Instituto Gulbenkian de Ciência, Rua da Quinta Grande, 6, Apartado 14, 2781-901 Oeiras, Portugal; [2]Centro de Biomedicina Molecular e Estrutural, Universidade do Algarve, Campus de Gambelas, 8000-010 Faro, Portugal; [3]Institute of Human Genetics, University of Heidelberg, Im Neuenheimer Feld 366, 69120 Heidelberg, Germany; [4]Author for correspondence: José A. Belo, Tel: +351214407942, Fax: +351214407970, e-mail: jbelo@igc.gulbenkian.pt.

Summary

The mouse anterior visceral endoderm (AVE) has been proposed to play a role in the establishment of the AP axis and in anterior neural induction. In order to gain further insight into the molecular mechanisms involved in head formation, a differential screening for mouse AVE specific genes was performed. One of the novel genes expressed in the mouse AVE, *Anterior Distal Tyrosine Kinase 1* (*mADTK1*), encodes for a protein that contains a predicted Serine/Threonine protein kinase catalytic domain. Based on a bioinformatics analysis we have isolated two *Xenopus* orthologs, *XADTK1* and *XADTK2*. XADTK1 protein shows 61.7% identity to mADTK1 whereas XADTK2 shows 42% identity. Both *Xenopus* ADTK proteins are 40.9% identical to each other. Both *Xenopus* orthologs of *mADTK1* were shown to be maternally expressed at low levels in the animal pole and in the organizer during gastrulation. By neurula stages XADTK1 was expressed in the prospective eye field, in the neural folds as well as in the otic placode and later on it could also be detected in the notochord. *XADTK2* was expressed in the anterior ventral mesoderm region and later on became restricted to the foregut, head region and notochord. We have performed morpholino antisense mediated knock-down of XADTK1 and have observed that depletion of XADTK1 resulted in neural tube closure defects. In addition, XADTK1 morphants show impairment in neural crest and eye formation.

Introduction

During the vertebrate embryonic development, the fertilized egg in order to become a multi-cellular organism has to undergo several stages of development, gastrulation, neurulation and organogenesis in which different morphogenetic processes take place such as proliferation, adhesion, differentiation, migration and apoptosis.

One of the most crucial stages in development is gastrulation. During this stage, the three germ layers are established as well as the primary body axes, cells rearrange themselves as a result of gastrulation movements and are brought to their final position in the embryo. The inductive interactions occurring during gastrulation are crucial for neurulation and organogenesis and understanding the molecular bases of these inductive interactions has interested many researchers. Innumerous work has been performed in order to identify and characterize novel molecules expressed during gastrulation that may play a crucial role in the correct establishment of the embryonic axes and patterning of the embryo.

Two important developmental processes that that place in the vertebrate embryo and can be traced back to gastrulation events are the neural tube closure and the migration of neural crest (NC) cells.

As the embryo goes trough neurulation, the dorsal ectoderm thickens and becomes a flat sheet of cells designated the neural plate. At the same time the border of the neural plate rises and forms the neural folds which rolls up and fuse at the midline, forming the neural tube that subsequently differentiates into the central nervous system. Neural tube closure in *Xenopus laevis* involves several cell movements such as medial migration, direct protrusive activity, cell intercalation and convergent extension (Davidson and Keller, 1999). Failure in this process causes neural tube defects that are among the most common birth defects and can be divided into rostral neural tube defects (anencephaly/exencephaly) and caudal neural tube closure defects (craniorachischisis) (Wallingford, 2006). Studies performed in vertebrate embryos have shown that impairment in neural tube closure can arise from defects either in cell fate, cell shape or cell movement (Cabrera *et al.,* 2004; Copp *et al.,* 2003; Wallingford, 2006). The molecular network underlying neural tube closure is still largely unknown but regulators of actin dynamics have been implicated in neural tube closure in mice and frog (Haigo *et al.,* 2003; Wallingford, 2006). In addition, signaling cascades such as the hedgehog and the Wnt non-canonical pathways have been shown to play a crucial role in neural tube closure

(Franco *et al.,* 1999; Park *et al.,* 2006; Ueno and Greene, 2003; Wallingford, 2006; Ybot-Gonzalez *et al.,* 2002).

It has been shown that non-canonical Wnt signaling not only regulates neural tube closure but is also involved in neural crest formation and migration (De Calisto *et al.,* 2005). The neural crest is a transient embryonic structure composed of a migratory population of multipotent cells. Neural crest induction occurs at the end of gastrulation and is thought to involve signals coming from the neural plate, non-neural ectoderm and paraxial mesoderm, which include Wnt, FGF and BMP signaling (Bonstein *et al.,* 1998; Huang and Saint-Jeannet, 2004; Mancilla and Mayor, 1996; Marchant *et al.,* 1998; Mayor *et al.,* 1997; Mayor *et al.,* 1999; Monsoro-Burq *et al.,* 2003; Selleck and Bronner-Fraser, 1995; Villanueva *et al.,* 2002). Neural crest cells are induced at the border between the non-neural ectoderm and the neural plate that correspond to the neural folds. Upon neural tube closure, the neural crest cells, which are located at the dorsal most region of the neural tube, undergo an epithelial-to-mesenchymal transition that allows them to delaminate from the neuroepithelium in a rostrocaudal wave and migrate throughout the embryo along specific routes (for a review, see LaBonne and Bronner-Fraser, 1999; Le Douarin and Kalcheim, 1999 ; Thiery, 2003). Upon migration, neural crest cells differentiate into a variety of cell type that include neurons and glia of the peripheral nervous system, craniofacial cartilage and bone, endocrine cells, smooth muscle cells and melanocytes (Aybar and Mayor, 2002; Baker and Bronner-Fraser, 1997; Knecht and Bronner-Fraser, 2002; LaBonne and Bronner-Fraser, 1999; Mayor and Aybar, 2001). Due to the fact that neural crest cells contribute to multiple cell lineages, abnormal development of the neural crest may lead to dramatic defects in many different organs.

In this report we have isolated two members of a novel gene family, *XADTK1* and *XADTK2* (*Xenopus Anterior Distal Tyrosine Kinase*), where the mouse homologue was identified in a screening for genes differentially expressed in the mouse anterior visceral endoderm (AVE). *XADTK1* and *2* encode for defective tyrosine kinase proteins. We show that during normal development *XADTK1* and *2* are present in the organizer during gastrulation. We have inhibited endogenous XADTK1 activity using a morpholino oligonucleotide targeted to the translational initiation site of *XADTK1*. Depletion of XADTK1 resulted in gastrulation defects and an open anterior neural tube defect as a result from an improper hingepoint formation and bending of the neural folds. In addition, loss of XADTK1 activity causes downregulation of cranial crest markers. These

data presented here suggest that XADTK1 plays a role during neural tube closure and cranial crest formation.

Materials and Methods

Manipulation of *Xenopus* Embryos

Unfertilized eggs were squeezed out manually from pigmented female *Xenopus laevis* which had been injected with 300-400 units of human chorionic gonadotropin (Sigma). Eggs were *in vitro* fertilized with macerated testis, dejellied in 2% L-cysteine-HCl (pH 8.0), injected in 1xMBS-H (88 mM NaCl, 1 mM KCl, 2.4 mM NaHCO$_3$, 0.82 mM MgSO$_4$, 0.41 mM CaCl$_2$, 0.33 mM Ca(NO$_3$)$_2$, 1 mM HEPES pH 7.4) and grown in 0.1xMBS-H at 14–21°C until the desired stages. Embryos were staged according to Nieuwkoop and Faber (1967).

Axis perturbation Assays

To perform UV treatment, fertilized embryos were dejellied 15min after fertilization was done and healthy embryos were transferred to quartz dishes containing 0.1xMBS-H. Embryos were irradiated for 60sec with short-wave (254nm) UV light in an inverted UVGL-25 lamp. After treatment, the embryos were left in place until after the first cleavage was completed after which they were transferred to 0.1xMBS-H agarose-coated dishes and allowed to grow below 20°C, along with untreated embryos. At stage 10.5 embryos were fixed and stored.

LiCl treatment was performed at the 32-cell stage by incubating embryos in 0.3 M LiCl in 0.1xMBS-H, for 10min at RT, with gently swirling. Embryos were then washed in 0.1xMBS-H and allowed to grow at RT, along with untreated control embryos. Embryos were collected and fixed at gastrula stages.

Cloning of *Xenopus ADTK1* and *ADTK2*

Xenopus ADTK1 and *ADTK2* was identified by using the translated nucleotide sequence of the mouse *ADTK1* as queries to perform TBLASTX comparisons against NCBI's translated nucleotide (nt) and EST databases (dbest). Protein sequence alignments and homology scores were derived from the NCBI's BL2SEQ alignment program. SMART (Simple Modular Architecture Research Tool, http://smart.embl-heidelberg.de/) and PHI-BLAST (Pattern Hit Initiated BLAST) bioinformatics' tools were used to analyze the

domain architecture of the proteins. *Xenopus laevis ADTK1* EST containing the full open reading frame of XADTK1 (Genbank accession number: BJ630561, pBlueScript SK vector) was obtained from the NIBB (http://*Xenopus*.nibb.ac.jp/).

No *XADTK2* full open reading frame EST clone was found in any of the searched databases. In addition, no partial coding sequence *XADTK2* clone was retrievable from the stock centers and was kindly gifted by M. Taira (Genbank accession number: BP673009, pCS105 vector). To isolate the full length *XADTK2* coding sequence, total RNA from gastrula stages (stages 10-12) *Xenopus laevis* embryos (Nieuwkoop and Faber, 1967) was isolated using Trizol® reagent (Invitrogen) according to the manufacturer's protocol. First strand cDNA was synthesized with H minus M-MuLV reverse transcriptase (Fermentas) using random hexamers as primers. The following primers were used to amplify the *ADTK2* gene product by PCR: forward, 5'-TTTGGATCCAGTGATGAAGAACACC-3'; reverse, 5'-GCAGATGGGAAGATGATCGATTTT-3', 55 °C, 25 cycles). The PCR product was cloned into pCS2+.

All clones were sequenced from both the 5' and 3' ends using a DNA ABI Prism 377 (Applied biosystem) to confirm identity between the database entries and the cDNA inserts.

RT-PCR

Total RNA was prepared from pools of 5 embryos with Trizol® reagent (Invitrogen) according to the manufacturer's protocol. First strand cDNA primed by random hexamers was synthesized with H minus M-MuLV reverse transcriptase (Fermentas) and PCR was performed using standard conditions and the following sets of primers: XADTK1-F (5'-ACTGCAAAGGCTTCAGCACC-3') and XADTK1-R (5'-TCGGTGTGGCTGATACAAGG-3'), 55°C, 25 cycles; XADTK2-F (5'-GGGAGATGCACTGGCGTCAATG-3') and XADTK2-R (5'-TGCAGAACTCGGCAGCCTCTTC-3'), 55°C, 25 cycles; ODC-F (5'-CAGCTAGCTGTGGTGTGG-3') and ODC-R (5'-CAACATGGAAACTCACACC-3'), 57°C, 21 cycles.

Plasmid constructs and morpholino Oligonucleotide

The *Xenopus ADTK1* morpholino oligonucleotide (XADTK1Mo) was synthesized and obtained from Gene Tools LLC. XADTK1Mo was designed to complement the region between base -1 upstream of the AUG and base +24 downstream of the AUG (5′-CACTGCGATCTTCCTGCGTCTCATG- 3′). The standard control morpholino oligonucleotide was also obtained from Gene Tools LLC (5'-CCTCTTACCTCAGTTACAATTTATA-3').

To test the efficiency and specificity of XADTK1Mo two C-terminal myc-tagged constructs were generated: XADTK1-myc, that contains *Xenopus* XADTK1 complete CDS plus the 1 bp upstream of the ATG in order to contain the antisense morpholino oligonucleotide consensus sequence; and XADTK1(mut)-myc, a full-length XADTK1 construct where the first 24 nucleotides after the ATG were mutated in order to maintain the same aminoacid sequence but no longer be targeted by the morpholino. The XADTK1-myc construct was generated by PCR amplification of pBSII(SK).XADTK1 to mutate the stop codon. For that, the following primers were used: XADTK1myc_Fw (5′-TTTGGATCCCATCATGAGACGCAGG-3′); XADTK1myc_Rev (5′-AAAATCGATAGCCTGTCAGTTTCAGGTACG-3′). The PCR product was cloned into pGEM-T easy (Promega) and then the BamHI/ClaI fragment as subcloned into pCS2+-6xmyc (pCS2+MT). To introduce the mutations to generate the XADTK1(mut)-myc rescue construct, a two-step partial amplification of pCS2.XADTK1-6xmyc was performed using the following primers: XADTK1(mut)-myc_Fw1 (5′-AGGCGAAAAATTGCTGTCGCTGCTGCTTTTTGTCTCTCC-3′); XADTK1(mut)-myc_Fw2 (5′-TTTGGATCCTATGCGTAGGCGAAAAATTGCTGTCG-3′); XADTK1(mut)-myc_Rev (5′-TGCCATTGAGGAGCGATTTATAGACGGCTTTGG-3′). The PCR product (473 bp) was cloned into pGEM-T easy and the 167 bp BamHI-SacI fragment was used to replace the BamHI-SacI fragment from pCS2.XADTK1-6xmyc.

In *vitro* translation and Western Blot analysis

For *in vitro* transcription/translation the TNT® Coupled Reticulocyte Lysate System (Promega) was used according to the manufacturer's instructions. In brief, 225 ng of XADTK1-myc or XADTK1(mut)-myc plasmid was transcribed/translated in presence or absence of 25 pmol/250 pmol of respective morpholino or 250pmol of CoMo. The

reaction was carried out in 10µl total volume and 5 µl of this was loaded on each lane in a 12% SDS-PAGE. 25 ng of EGFP-myc was added to each reaction tube, which serves as a loading control. For protein expression, *Xenopus* embryos were extracted in 20mM HEPES pH 7.4, 130mM NaCl, 2mM EDTA, 1mM EGTA, 1% NP-40 supplemented with a cocktail of protease inhibitors (Calbiochem). Proteins were heated in sample buffer and separated by denaturing SDS-PAGE using a 12% polyacrylamide gel (Laemmli, 1970). Subsequently, proteins were transferred to a nitrocellulose membrane (Towbin *et al.,* 1979), detected with a monoclonal mouse anti-c-myc (Oncogene) and developed using a chemiluminescent substrate (Pierce).

Whole-Mount *in situ* Hybridization

Embryos to be used for *in situ* hybridization were incubated until the proper stages, fixed in MEMFA (0.1 M Mops [pH 7.4], 2 mM EGTA, 1 mM MgSO4, 3.7% formaldehyde) solution, for 2h at RT or ON at 4ºC, and stored in methanol at −20°C until use. Whole-mount *in situ* hybridization and antisense probe preparation were carried out as described (Epstein *et al.,* 1997). Probes were purified with a Quick Spin Mini RNA column (Roche). To generate the digoxigenin labeled antisense RNA probes, plasmids containing XADTK1, Sox2, Twist and Pax6 fragments were linearized using *EcoRI*, *EcoRI*, *EcoRI* and *NotI* respectively, and transcribed using T7 RNA polymerase. Plasmid containing Slug was cut with *BglII* and transcribed using SP6 RNA polymerase while plasmid containing XADTK2 fragment was cut with *SalI* and transcribed with T3 RNA polymerase. To generate the fluorescein-labeled antisense RNA probes, plasmid containing Otx2 fragment was cut with *EcoRI* and transcribed using T3 RNA polymerase and plasmid containing Troponin fragment was cut with *NotI* and transcribed with T7 RNA polymerase. Hybridized RNAs were detected with alkaline-phosphatase-conjugated anti-DIG-antibody (Roche) or anti-Fluo-antibody (Roche) and developed using BM purple (Roche) or NBT/BCIP (both from Roche). Stained embryos were bleached by illumination in 1% H_2O_2, 4% formamide and 0.5x SSC, pH 7.0. Embryos were refixed in MEMFA and photographed under bright light with a Leica DFCM20 camera, mounted on a Leica MZIII stereoscope.

Results

Identification and isolation of *XADTK1* and *XADTK2*

A microarray based differential screening was carried out with the aim to identify genes that are differentially expressed in the Anterior Visceral Endoderm (AVE) of E5.5 mouse embryos (Mario Filipe, unpublished). In this screening 288 genes were shown to be upregulated in the anterior distal (Ad) samples by the GeneChip arrays. Of those clones, 17 - 50%, depending on the criteria of selection used, were considered as genes that are either specifically expressed or enriched in the AVE of the mouse embryo. Some of the genes from this list were selected for validation of correct spatial expression by whole mount *in situ* hybridization analysis. One of these clones, referred as *ADTK1* (Antero Distal Tyrosine Kinase 1), was chosen to search for the *Xenopus laevis* ortholog. *mADTK1* encodes for a novel protein with a putative tyrosine kinase and shown by *in situ* hybridization to be, at E5.5, AVE specific. Using mouse ADTK1 protein sequences as a query to search NCBI databases (http://www.ncbi.nlm.nih.gov/BLAST/), we identified two potential *Xenopus* orthologs with closest homology to the mouse clone, which were therefore referred to as *Xenopus ADTK1* and *Xenopus ADTK2* (Table 1). In this search we empirically assumed that a gene was the ortholog of the analyzed mouse gene when their E-values were ≤ e–100.

XADTK1 (GenBank BJ630561) encodes a 489 a.a. protein with a predicted molecular weight of 55.9kDa (Fig. 1A). Bioinformatic analysis (http://smart.embl-heidelberg.de) of *XADTK1* proteic sequence showed that XADTK1 contains a predicted Serine/Threonine/Tyrosine protein kinase catalytic domain (between a.a. 134 and 381; Fig. 1B). The predicted product of the *XADTK1* gene has 61.9% identity to mADTK1 while the Serine/Threonine/Tyrosine protein kinase catalytic domain of both proteins shares 75% identity. The second *Xenopus* ortholog of mADTK1, XADTK2 (GenBank BP673009) shares 42% of identity with mADTK1. The region of higher identity corresponds to the region predicted to be a Serine/Threonine/Tyrosine protein kinases catalytic domain (between a.a. 83 and 336; Fig. 1B), sharing 57.4% identity. *XADTK2* encodes for a 449 a.a. protein with a predicted molecular weight of 51.0kDa (Fig. 1A). Both *Xenopus* proteins share 40.9% identity through the overall protein and 57.8% identity in the region predicted to be protein kinases catalytic domain. Bioinformatic analysis has detected the absence of some consensus residues typical of protein kinases (Hanks and Hunter, 1995).

Fig. 1 (previous page) – *XADTK1* **and** *XADTK2* **expression pattern and protein alignment with the mouse sequence.** (A) Comparison of the predicted amino acid sequence of mouse ADTK1 (AnteroDistal Tyrosine Kinase1) with the two *Xenopus* orthologs, XADTK1 and XADTK2. XADTK1 shares 61.9% of identity (P- 70.1%) with mADTK1 and 40.9% identity (P- 52.6%) with XADTK2. XADTK2 shares 42% identity (P- 53.6%) with mADTK1. Identical amino acids among all are shown in red while identical amino acids in only two sequences are shown in blue. The absence of residues at the corresponding region is indicated by dashes. (B) Schematic drawing of XADTK1 and comparison with mADTK1 and XADTK2. Serine/Threonine/Tyrosine protein kinase catalytic domain (STYKc domain) shown in Orange. (C) Temporal expression pattern of *Xenopus ADTK1* and ADTK2 by RT-PCR analysis. Both genes are expressed maternally at low levels. *XADTK1* transcripts peaks at gastrulation and are down-regulated after the onset of neurulation while *XADTK2* expression increases until neurula stages. ODC was used as a loading control for the RT-PCR. (D-Q') Expression pattern of *XADTK1* and *XADTK2* during *Xenopus* developemt. (D,K) *XADTK1* and *XADTK2* are expressed in the animal pole of mature oocytes. (E) Zygotic *XADTK1* is detectable at early gastrula stages in the anterior dorsal endoderm. (F) At late-gastrula stages *XADTK1* mRNA is expressed in the involuting mesoderm. (G) During early neurula stages, *XADTK1* transcripts can be detected in the neural folds, dorsal view, anterior down. (H) Stage 17, neurula, anterior view. *XADTK1* expression is seen in the prospective eye field, neural folds and otic placode. (I-J') In tailbud stages (27, and 31; lateral view, anterior to the right and dorsal up), *XADTK1* is expressed in the neural tube roof, otic vesicle, notochord, eye, lateral plate mesoderm, and head mesenchyme. (L,M) By early gastrula stages *XADTK2* transcripts can be detected in the (L) dorsal blastopore lip and the (M) ADE. (N) At stage 12, *XADTK2* is present in the involuting mesoderm. (O-Q') *XADTK2* expression at tailbud stages is restricted to the lateral plate mesoderm, foregut and eye and isthmus. (R) Double whole mount *in situ* hybridization for *XADTK2* (blue) and *otx2* (Cabrera *et al.*) shows that *XADTK2* expression in the brain is restricted to the mid-hindbrain boundary (S) Double whole mount *in situ* hybridization for *XADTK2* (blue) and *Troponin* (Cabrera *et al.*) showing that *XADTK2* expression is absente from the heart. (T) Summary of expression of *XADTK1* and *XADTK2* during early gastrula stages, in comparison with *Xcer*.

In particular, the GXGXXG motif in subdomain I, the HRDL motif in subdomain VIb and the DFG domain in subdomain VII are changed to GXGXXK, LLDF and DLD (DDA for XADTK2),respectively. These data suggests that XADTK1 and XADTK2 do not have protein kinase activity.

Table 1 Results of sequence based BLAST search to identify the *Xenopus* orthologs of novel mouse AVE genes.

Mouse Clone	Mouse Acc. no.	Domains/homology	*Xenopus* Clone	*Xenopus* Acc. no.
mADTK1	BC022157 *	Protein kinase, tyrosine kinase and serine/threonine kinase catalytic domain	*XADTK1*	BJ630561
			XADTK2	BP673009 *

*these Accession numbers contain only partial coding sequences.

An EST for *XADTK1* was obtained from NIBB (http://*Xenopus*.nibb.ac.jp/). The *XADTK2* clone (gift from M. Taira) was unretrievable from the stock centers and for that the complete coding sequence was amplified by RT-PCR from total gastrula embryo RNA using gene specific primers. The clones were then sequenced and spatio-temporal expression pattern of these genes were analyzed by *in situ* hybridization and developmental RT-PCR.

Expression pattern of *XADTK1* and *XADTK2* during early embryogenesis

To analyze the expression of *XADTK1*, whole-mount *in situ* hybridization was performed on embryos at different stages. As shown by *in situ* hybridization and RT-PCR, *XADTK1* was expressed maternally at low levels, in the animal hemisphere of the embryo (Fig. 1C,D). Due to the fact that RNA *in situ* signals are known to be quenched in the yolk-rich vegetal cells, one can not exclude that *XADTK1* maternal transcripts might be distributed ubiquitously. *XADTK1* expression was found to increase after mid-blastula transition (MBT), peak during late gastrula stages, after which its expression seams to decline (Fig. 1C). At the beginning of gastrulation, *XADTK1* is expressed exclusively in the anterior dorsal endoderm (ADE; Fig. 1E), overlapping with the expression domain of previously known organizer genes, *dkk-1* and *cerberus* (Bouwmeester *et al.,* 1996; Glinka *et al.,* 1998). Unlike *dkk-1* and *cerberus*, *XADTK1* transcripts were not detected in blastocoel floor (Fig. 1E). As gastrulation proceeds, *XADTK1* mRNA was expressed not only in the ADE but also in the involuting dorsal mesoderm, including the prospective prechordal plate (Fig. 1F). During neurula stages *XADTK1* transcripts were present in the prospective eye field, in the neural folds as well as in the otic placode (Fig. 1G,H). At tailbud stages (stage 25 and 31; Fig. 1I-J'), *XADTK1* expression was restricted to the eye, otic vesicle, neural tube roof, notochord, lateral plate mesoderm, and head mesenchyme.

RT-PCR analysis demonstrated that *XADTK2* is expressed maternally at very low levels while zygotic *XADTK2* transcription starts immediately after MBT, gradually increasing until late gastrula (Fig. 1C,K). The levels of XADTK2 are maintained during neurula stages and decreases after early tailbud stages (Fig. 1C). Whole-mount *in situ* hybridization of early gastrula stage *Xenopus* embryos shows that the expression is restricted to the dorsal blastopore lip and to the ADE (Fig. 1L,M). Sagittally hemisectioned embryos at stage 11 showed expression throughout the anterior neural ectoderm (ANE) and in the dorsal involuting mesoderm (Fig. 1N). During early tailbud and tailbud stages *XADTK2* transcripts could be detected in the lateral plate mesoderm as well as in the pronephros, notochord and the eye (Fig. 1O,P). *XADTK2* expression by late tailbud stages is restricted to the foregut, notochord and head region, including the eye field and the isthmus (Fig. 1Q,Q'). We performed a double *in situ* hybridization for *XADTK2* and *otx2*, which stains the fore-midbrain. *XADTK2* expression in the brain is located posterior to *otx2* expression domain, confirming that *XADTK2* is expressed in the isthmus (Fig. 1R). By comparing *XADTK2* and *troponin* expression pattern during late tailbud stages, we could

confirm that they are not co-localized and thus, *XADTK2* is not expressed in the heart field (Fig. 1S).

In summary, although during later stages both genes are expressed in different tissues, they are expressed in organizer region, more precisely in the ADE, during gastrulation (Fig. 1T). This data, together with the fact that *mADTK1* is expressed in the mouse AVE, which is the topological equivalent of the frog ADE, suggests that this novel gene family has conserved its expression through evolution.

XADTK1 and *XADTK2* expression is regulated by Wnt canonical signaling

Xenopus embryos can be submitted to several physical and chemical treatments in order to perturb the dorsal-ventral axis formation (Sive *et al.*, 2000). The expression pattern of genes involved in the early patterning of the frog embryos, like organizer genes, can be expanded or reduced when *Xenopus* embryos are submitted to LiCl and UV, respectively. Treatment of recently fertilized embryos with UV leads to cortical rotation inhibition and results in ventralized embryos (Heasman, 1997). On the other hand, treatment of early blastula embryos with LiCl generates dorsalized embryos. Lithium acts through inhibition of GSK-3β, allowing activation of the Wnt signaling pathway required for dorsal axis formation (Heasman, 1997).

In order to test if these novel genes are regulated by signals involved in specification of dorso-ventral axis, the expression pattern of these genes were monitored by whole-mount *in situ* hybridization of UV or LiCl treated embryos and untreated control embryos. *In situ* hybridization of gastrula stage embryos submitted to UV treatment (ventralized embryos) showed that mRNA levels of *XADTK1* and *XADTK2* were greatly reduced when compared to the untreated controls (Fig. 2, compare A,E with B,F respectively). In contrast, dorsalized embryos, obtained by treating with LiCl, caused an expansion of *XADTK1* and *XADTK2* expression (Fig. 2 C,D,G,H). We can conclude from these results that the expression of both *XADTK1* and *XADTK2* during gastrula stages is positively regulated by maternal β-Catenin and thereby by the Wnt canonical-signaling.
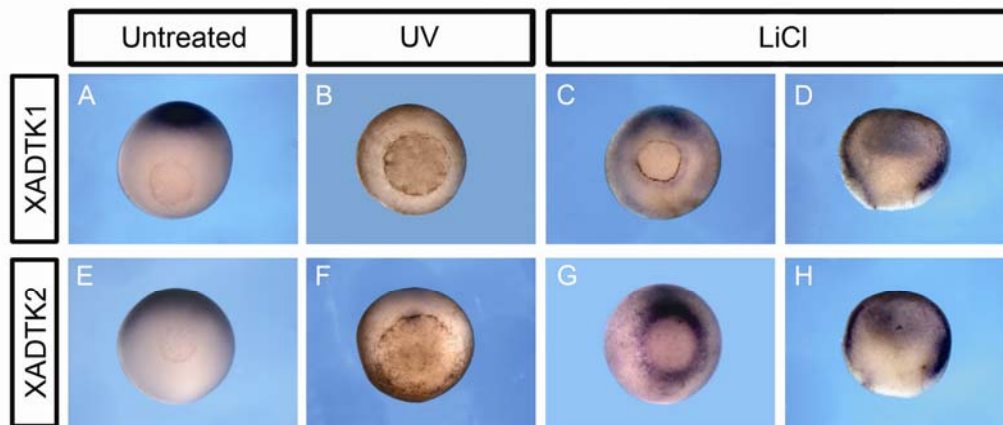
Fig. 2 – Axis perturbation assays. Whole-mount *in situ* hybridization of gastrula stages for untreated embryos (A,E) or treated with UV (B,F) or LiCl (C,D,G,H) and hybridized with (A-D) *XADTK1* or (E-H) *XADTK2* probe. Whole-mount embryos are shown in a vegetal view with dorsal side to the top and ventral side to the bottom. Hemisections are shown with the dorsal to the right. At gastrula stages, *XADTK1* and *XADTK2* transcripts were shown to be greatly reduced by treatment with UV and up-regulated upon treatment with LiCl (red arrowhead - endogenous expression, black arrow – ectopic expression). These results indicate that the expression of *XADTK1* and *XADTK2* may be regulated by signaling events specifying dorsal axis.

XADTK1 depletion disrupts anterior neural tube closure

To investigate the function of this novel gene family we decided to focus our study on the role of *XADTK1* during early *Xenopus* development. To understand the endogenous function of *XADTK1*, we designed a morpholino antisense oligonucleotide to knock-down its protein expression in the embryo (Heasman, 2002; Summerton and Weller, 1997). *XADTK1* morpholino (XADTK1MO) was designed according to the manufacture's instructions, towards the translation initiation site of *XADTK1* (Fig. 3B). In addition, we have generated a XADTK1 tagged expression construct by fusing, in frame, *XADTK1* complete coding sequence to 6xmyc (XADTK1-myc). This construct was injected into fertilized eggs and protein extract from late blastula stage embryos was analyzed by western blot. XADTK1-myc was shown to be expressed as a single band that runs between 70 and 85 kDa in a 12% Acrylamide gel (expected molecular weight of 67.6 kDa; Fig. 3A). The difference to the predicted molecular weight might be due to some post-translational modification like phosphorylation or glycosylation.

In order to test the efficiency and specificity of the *XADTK1* morpholino to down-regulate XADTK1 protein we have performed an *in vitro* transcription/translation assay using a cell free transcription/translation system (Promega). Translation of XADTK1-myc mRNA, which contained the sequence complementary to XADTK1Mo, was blocked by this morpholino in a concentration-dependent manner (Fig. 3C). On the other hand, translation of a XADTK1-myc expression construct (XADTK1(mut)-myc) where the

morpholino target sequence was mutated, or even of an unrelated EGFP-myc mRNA was not affected (Fig. 3C). An unrelated standard control morpholino oligonucleotide (CoMo) showed no inhibitory effects (Fig. 3C).
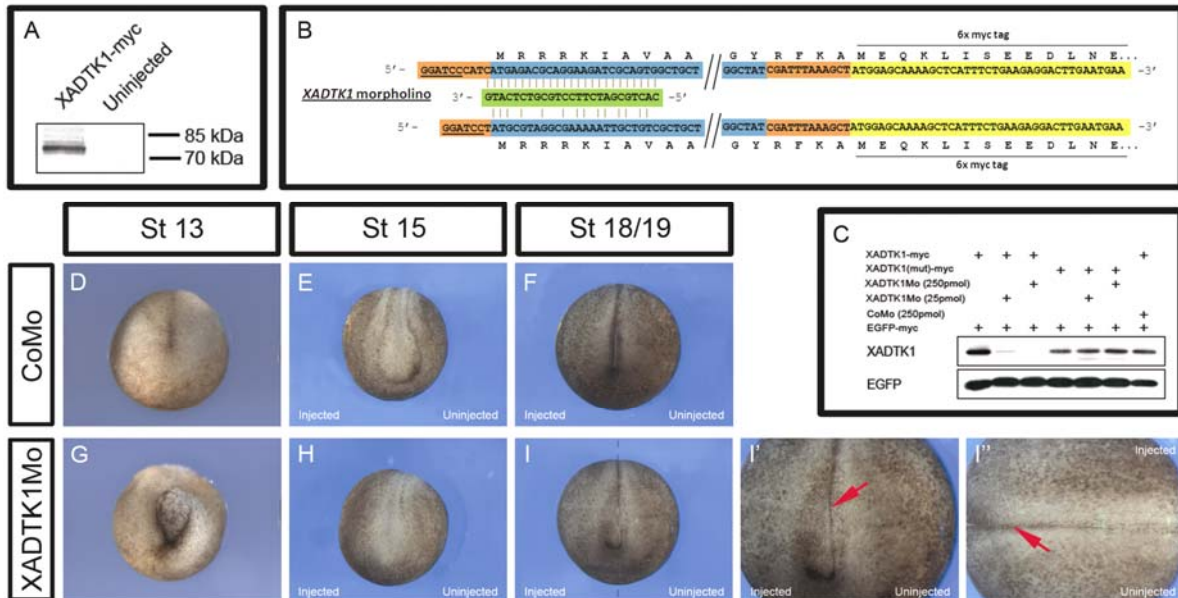
Fig. 3 – *In Vivo* Requirement of *XADTK1* during early development. (A) Western blotting of protein extract from gastrula embryos injected with XADTK1-myc RNA or of uninjected control embryos of the same stage. In a 12% Acrylamide Western Blot, XADTK1-myc (588 a.a., predicted to have 67.6 kDa) runs between 70 and 85 kDa. (B) Schematic structure and alignment of the *Xenopus* ADTK1 morpholino oligonucleotide (XADTK1Mo) with the XADTK1-myc (Gonzalez *et al.*) and XADTK1(mut)-myc (bottom) expression constructs. The XADTK1(mut)-myc expression is a mutated version of the XADTK1-myc where the morpholino taget sequence was mutated but maintains the same aminoacid sequence. (C) *In vitro* transcription/translation of XADTK1-myc protein was blocked in the presence of XADTK1Mo but not in the presence of the standard control morpholino, CoMo. Transcription/translation of the XADTK1(mut)-myc rescue construct could not be blocked by XADTK1Mo. Each reaction was carried out in presence of EGFP-myc, which serves as a loading control. (D-I') Four-cell stage embryos were injected either (D,G) dorsally or (E,F,H-I'') unilaterally with a total of 5pmol of either (G-I'') XADTK1Mo or (D-F) CoMo and analyzed at stage 13 (D,G), 15 (E,H) or 18/19 (F,I-I''). Injection of XADTK1Mo caused (G) gastrulation and (H,I) neural tube closure defects that was not observed in (D-F) CoMo injected embryos. (I',I'') Close up of the stage 18/19 XADTK1Mo unilaterally injected embryos. In embryos injected unilaterally with XADTK1MO, no hingepoint is formed on the injected side. In contrary, hingepoints can be clearly visible in the anterior neural plate in the uninjected control side (arrow).

Xenopus embryos at the 4 cell stage were injected in both dorsal blastomeres with 5pmol of XADTK1Mo or with CoMo. At the late gastrula stages (stage 12/13) XADTK1Mo injected embryos displayed some gastrulation defects that were not seen in the CoMo injected embryos (Fig. 3D,G). However, if the embryos were left to grow until later stages they would recover from this gastrulation phenotype and appeared to develop normally although with some delay (not shown).

In order to better evaluate the effects of XADTK1 depletion, 4 cell stage embryos were unilaterally injected with 5pmol of either XADTK1Mo or CoMo, serving the

uninjected side as an internal control. At the neurula stages, while CoMo injected embryos developed with no apparent phenotype (Fig. 3E,F), XADTK1Mo injected embryos displayed a delay and defect in anterior neural tube closure (Fig. 3H-I''). The neural tube defects in the XADTK1 depleted embryos could already be detected by stage 15 (Fig. 3H). At this stage, in the XADTK1Mo injected side the embryo fail to form a well-defined neural fold. In addition, the neural folds seamed to be broader and more widely apart when compared with the non injected side and with the CoMo injected embryos (Fig. 3E,H). The phenotype observed for the XADTK1 morphants was more pronounced at stage 18/19 embryos where, in the CoMo injected embryos, the neural tube was almost closed (Fig. 3F,I). In the XADTK1Mo injected embryos, while the control uninjected side developed normally and the neural folds were placed already at or very closely to the dorsal midline, in the XADTK1Mo injected side, the neural folds were still far from the midline (Fig. 3I).

During neurulation, the neural folds have to elevate, bend and converge in order for the neural tube to close (Jacobson and Gordon, 1976; Schoenwolf and Smith, 1990). The bending of the neural plate is achieved by apical constriction in two discrete regions, designated as hingepoints, which form a distinct line of bending in each side of the neural plate. Hingepoints can be easily visualized by an increase in pigment concentration due to shortened surface in the apically constricting cells. In XADTK1 morphants, no hingepoint is formed on the injected side (Fig. 3I,I'). However, an obvious darker line of bending was observed in the control side (Fig. 3I,I', arrow). In CoMo injected embryos, both the injected and control sides displayed normal hingepoints (not shown).

Although in the more severe cases the anterior neural tube remained slightly open (data not shown), most of the XADTK1Mo injected embryos eventually closed their neural tubes despite the delay.

Embryos lacking XADTK1 activity develop with defects in cranial neural crest formation

To gain further insight into the role of *XADTK1* in the developing embryo, we decided to examine the expression pattern of some known markers for neural crest, eye and neural plate, based on the tissues were *XADTK1* is expressed.

As *slug* (Mayor *et al.*, 1995) is one of the earliest genes to be activated in response to neural crest inducting signals we have analyzed its expression pattern in XADTK1Mo

injected embryos. Unilateral microinjection of 5pmol of XADTK1Mo into four-cell stage embryos, cause a mild (not shown) or severe reduction (Fig. 4B) of *slug* expression on the injected side, at stage 15. To further characterize XADTK1 morphants the expression pattern of an additional neural crest marker, *Xtwist* (Hopwood *et al.*, 1989) was analyzed at early tailbud stage. *Xtwist* expression pattern was severely (Fig. 4D) reduced in XADTK1Mo injected embryos. Analysis of the pan-neural marker *Sox2* (Mizuseki *et al.*, 1998) in XADTK1 depleted embryos showed that in the XADTK1Mo injected side *Sox2* was slightly expanded when comparing with the control side (Fig. 4J,J'). In addition, the expression of *Pax6* in the developing eye reduced in embryos lacking XADTK1 function (Fig. 4H). Injection of the CoMo at the same concentration produced no effect in the expression of any of the analyzed markers (Fig. 4A,C,G,I,I'). In summary, the results suggest that *XADTK1* is necessary not only for neural tube closure but also for neural crest and eye formation.
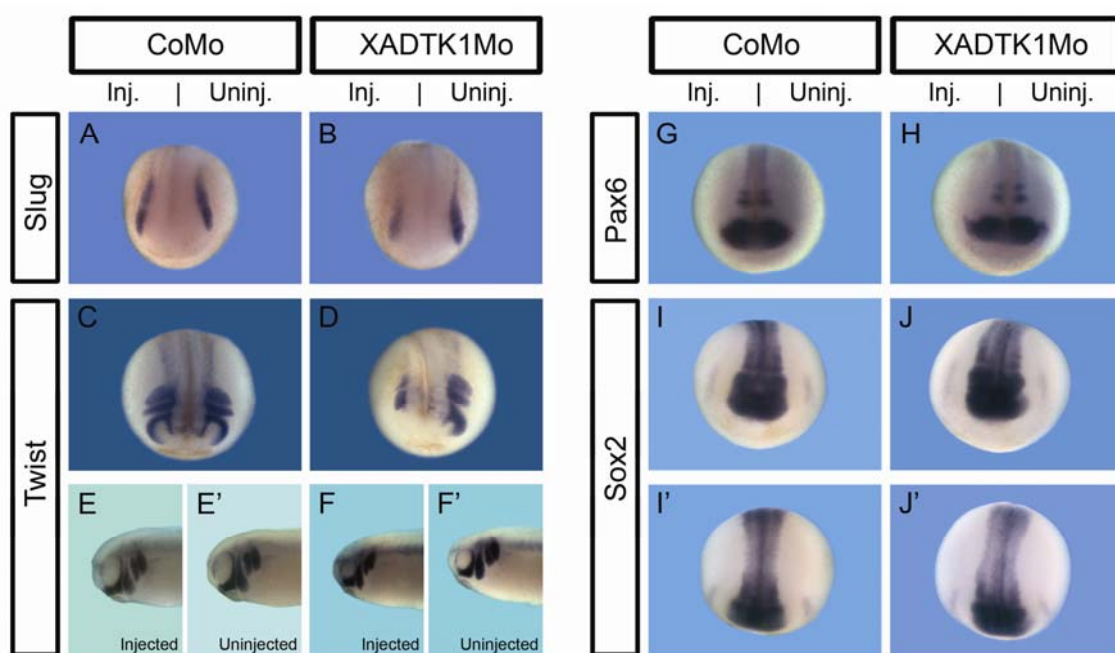
Fig. 4 – *XADTK1* disruption impairs neural crest and eye formation and leads an expansion of neural tissues. (B,D) Unilateral injection of XADTK1Mo leads to the down-regulation of neural crest markers (A,B) *slug* and (C,D) *twist*, when compared with (A,C) CoMo injected embryos. (F,F') Expression of *twist* in stage 28 XADTK1Mo injected embryos showed no neural crest migration defects although *twist* expression was reduced and the branchial stream was the most affected. (E,E') Injection of the CoMo had no effect. Morpholino injected side images of late tailbud embryos were flipped horizontally for a better comparison with the non injected side. CoMo injected embryos show normal expression of (G) *Pax6* and (I,I') *sox2*. *In situ* hybridization for (H) *Pax6* in XADTK1 depleted embryos showed a down-regulation in *Pax6* prospective eye domain while staining for the (J,J') pan-neural marker *sox2* showed a slightly expanded neural tissue in the injected side compared to the uninjected control side.

During late neurula stages, the neural crest cells undergo an epithelial-to-mesenchymal transition allowing them to migrate to specific places and differentiate. To evaluate the role of *XADTK1* in neural crest migration we have unilaterally injected the CoMo or the XADTK1Mo into four-cell stage embryos and analyzed *Xtwist*'s expression pattern in tailbud stage embryos. In CoMo injected embryos there was no difference in the extent of cranial neural crest migration between the injected and uninjected sides (Fig. 4E,E'). On the other hand, in the XADTK1Mo injected embryos, although no migration phenotype was observed, the shape of the streams seemed to be affected in the injected side compared to the control side (Fig. 4F,F'). In XADTK1Mo injected side all streams appeared to be narrower, in particular, the branchial stream (Fig. 4F). In summary, these data suggests that *XADTK1* is required for the specification of neural crest cells but not for the migration of the neural crest cells.

In order to better evaluate the XADTK1 morphants, embryos unilaterally injected with either CoMo or XADTK1Mo and hybridized with a *slug* antisense probe were cross-sectioned. In embryos injected with CoMo the bending of the hingepoints resulted in the formation of a concave neural plate (Fig. 5A'). On the uninjected side of the XADTK1Mo injected embryos the concave neural plate could be readily observed (Fig. 5B'). However, in the XADTK1 depleted neural plates although the neural fold was elevated, no hingepoint could be detected, and thereby it fails to bend properly (Fig. 5B'). In addition, the notochord did not display the usual rod-like shape (Fig. 5B') that could be observed in the CoMo injected embryos (Fig. 5A'). These observations suggest that *XADTK1* plays a role not only in neural crest formation and neural tube closure but also in notochord formation.

Discussion

In a screening to search for novel genes differentially expressed in the mouse anterior visceral endoderm, a novel gene, *mADTK1* was identified and through *in situ* hybridization was confirmed to be specifically expressed in the AVE at pre-gastrula stages. In this study we report the cloning of two members of a novel gene family, *Xenopus ADTK1* and *ADTK2* and the functional characterization of *XADTK1* during early *Xenopus laevis* development. By performing bioinformatic analysis we have detected that this novel gene family encodes for proteins containing a putative Serine/Threonine/Tyrosine protein kinase catalytic domain. In all these ADTK family

members the kinase catalytic domain contains alterations in the consensus motifs. Both the phenylalanine and glycine residues of the DFG motif which coordinates the Mg^{2+}-ATP are changed in both XADTK1 and XADTK2. In addition, the ATP-binding motif, GXGXXG, and the HRDL are altered to GXGXXK and LLDF in both *Xenopus* proteins. Since the kinase domain in all these proteins is defective in several of the motifs crucial for the kinase activity (Hanks and Hunter, 1995), it is assumed that it lacks catalytic activity. In some preliminary experiments (data not shown) we tried to perform kinase assays using common substrates like casein, MBP and histones. As expected, in *in vitro* kinase assays XADTK1 over-expressed in *Xenopus* embryos, and was not able to phosphorylate any of the used substrates. Unfortunately, we can not rule out the possibility that in our *in vitro* kinase assays the conditions provided, such as buffer, temperature and substrate, were not optimal for this protein.
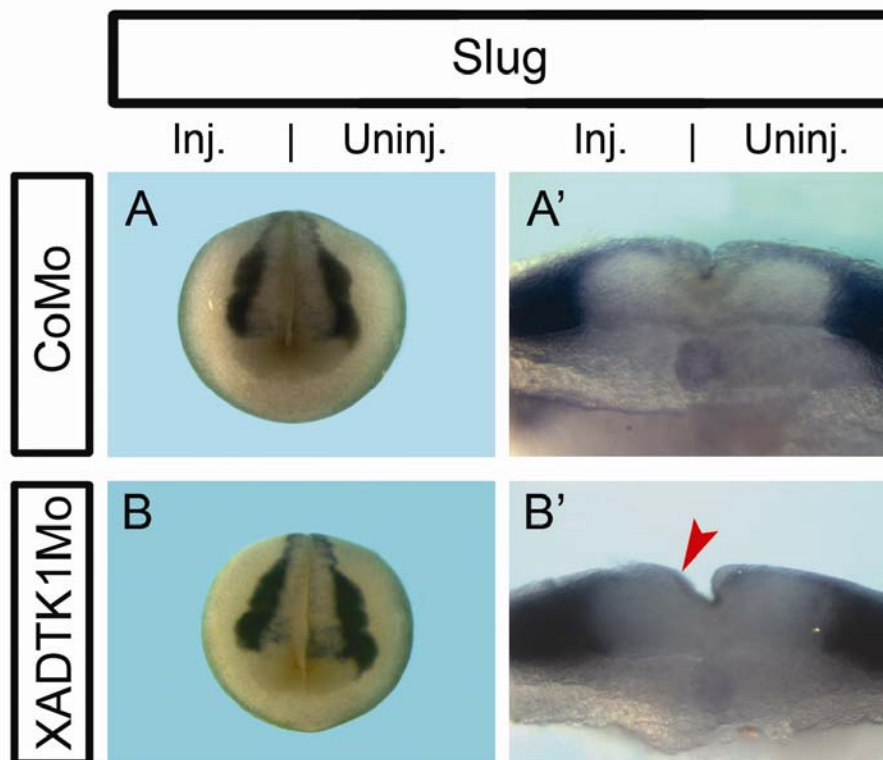
Fig. 5 – XADTK1 depletion impairs neural tube bending. (A,A') CoMo or (B,B') XADTK1Mo unilaterally injected embryos were hybridized with a *slug* probe at stage 18. (A) In CoMo injected embryos the expression pattern of *slug* was unchanged while (B) XADTK1Mo injected embryos *slug*'s expression was slightly down-regulated and posteriorly shifted. (A',B') Coss-section of the embryos presented in (A) and (B), respectively. (A') In both the injected and uninjected side of CoMo injected embryos the neural folds are elevated and due to neural plate bending at the hingepoints, the neural plate is concave. (B') In the XADTK1Mo injected embryos, in the control side it is possible to detect a elevated concave neural plate while in the XADTK1 depleted side, although the neural plate has elevated, it has not bended, remaining convex (arrow).

In recent years an increased number of studies have reported the isolation and characterization of defective kinases that are still able to function in signal transduction pathways (Kroiher *et al.,* 2001). One of these defective kinases is the *Xenopus* PTK7 (Jung *et al.,* 2004) that was found to be a regulator of the PCP pathway and is required for neural convergent extension and neural tube closure (Lu *et al.,* 2004). Although XPTK7 lacks kinase activity, it is thought that it might recruit other kinases and its presence is necessary for their phosphorylation (Lu *et al.,* 2004). It is then feasible to speculate, from the data presented in this paper that, like XAPTK7, XADTK1 and the other ADTK family members might also have an important role in development by recruiting other molecules although their catalytic activity might be impaired. In future, we intend to restore the defective domains in XADTK1 and test if this mutated version is able to phosphorylate substrates such as caseine, MBP or histone. This will provide a direct comparison between the kinase activity of the wild type and the mutant molecule.

In this study we have presented the spatio-temporal expression of both *XADTK1* and *XADTK2*. Both whole mount *in situ* hybridization and RT-PCR analysis have shown that both *XADTK1* and *2* are maternally expressed and present a very dynamic zygotic expression, detectable from gastrula stages onwards. Although throughout early frog development both genes are generally expressed in similar places some differences can be observed. While *Xenopus ADTK1* is expressed during gastrula stages in the anterior dorsal endoderm (ADE) and later on in the involuting mesendoderm, *XADTK2* is also expressed in the dorsal blastopore lip and in the dorsal neural ectoderm. The finding that the *Xenopus* orthologs of *mADTK1* are expressed in the topological equivalent of the mouse AVE, the frog ADE suggests that the expression of this gene family is evolutionary conserved. During latter stages, *XADTK1* is expressed in tissues including the neural folds, eyes, otic vesicle and notochord. On the other hand, tissues expressing *XADTK2* include eye, isthmus, foregut and notochord. The very dynamic expression patterns observed for both *Xenopus ADTK* genes suggest that they might play multiple roles during embryonic development.

In order to characterize this gene family we have performed axis perturbation assays (UV and LiCl treatment) in *Xenopus* embryos. Our results have shown that both *XADTK1* and *XADTK2* expression during gastrulation is regulated by Wnt canonical signaling which suggests that these genes might play a role in the patterning of the embryo. In addition, preliminary results (data not shown) using the animal cap assay

indicate that *XADTK1* might also be regulated by early Wnt non-canonical and TGF-β signaling. Further experiments have still do be performed in order to determine the signaling pathways involved in the regulation of these novel genes.

The role of *XADTK1* was investigated by using antisense morpholino oligonucleotides (Heasman, 2002). While XADTK1 depleted embryos developed with several defects, microinjection of a standard control morpholino oligonucleotide caused no effect in development, suggesting that the observed phenotypes are specific to XADTK1Mo.

Disruption of *XADTK1* function during early *Xenopus* development led to gastrulation and anterior neural tube closure defects. The gastrulation defects suggest that gastrulation movements are impaired, namely convergent extension. In the vertebrate embryo, convergent extension movements occurring during gastrulation are responsible for elongation of the anterior-posterior axis. Several studies have shown that the non-canonical Wnt signaling is involved in regulation of convergent extension movements (Keller *et al.*, 2000; Mlodzik, 2002; Wallingford *et al.*, 2002). Preliminary data indicate that *XADTK1* is downstream of Wnt non-canonical signaling together with the gastrulation defects suggest that *XADTK1* might be involved in Wnt non-canonical signaling.

The process of neurulation involves different events, like neural fold elevation, bending and convergion, for the neural tube to close. Our loss-of-function experiments have shown that XADTK1 depletion causes neural tube closure defects which seam to result from impairment in neural plate bending. Defects in neural tube closure can be associated to the disruption of different signaling pathways, such as Hedgehog and PCP pathway, as well as with defects in actin cytoskeleton (Wallingford, 2005). Disruption of components of the PCP pathway like *dishevelled* results in posterior neural tube closure defects while disruption of the hedgehog signaling or the actin cytoskeleton results in anterior neural tube defects (Wallingford, 2005; Wallingford and Harland, 2002). Recently, two genes, *fuzzy* and *inturned*, found to be important for anterior neural tube closure and ciliogenesis, were found to be regulators of both PCP and hedgehog signaling (Park *et al.*, 2006; Wallingford, 2006). Hedgehog signaling has also been reported to control the positioning of hingepoints in the mouse neural plate (Ybot-Gonzalez *et al.*, 2002). Currently, experiments are being performed to test if *XADTK1* is functioning in any of the above signaling cascades and to uncover possible interacting partners.

The fact that our morpholino injected embryos are able to recover from the gastrulation and neural tube closure defects might be due to the fact that *XADTK2* expression superimposes *XADTK1* expression. Thus, *XADTK1* and *XADTK2* might have redundant roles during early embryonic development. Loss-of-function studies of XADTK2 either alone or in combination with XADTK1 should answer this question.

Beside the defects in neural tube closure embryos injected with XADTK1Mo also displayed neural crest defects. Expression of three neural crest markers, *slug* and *Xtwist* during late neurula stages is down-regulated in XADTK1 morphants, indicating that depletion of XADTK1 affects neural crest specification. During tailbud stages, *Xtwist* expression in XADTK1Mo injected embryos although down regulated did not show defects in neural crest migration. Consistent with this, our results suggest that depletion of XADTK1 disrupts the proper neural crest formation rather than disrupting neural crest migration. Finally, we have shown that the eye field in XADTK1 morphants is smaller than in the CoMo injected embryo, as could be seen by *Pax6 in situ* hybridization. These results indicate that XADTK1 might not only play a role in neural crest formation but also during eye formation.

Acknowledgements

References

Aybar, M. J. and Mayor, R. (2002). Early induction of neural crest cells: lessons learned from frog, fish and chick. *Curr Opin Genet Dev* **12**, 452-8.

Baker, C. V. and Bronner-Fraser, M. (1997). The origins of the neural crest. Part I: embryonic induction. *Mech Dev* **69**, 3-11.

Bonstein, L., Elias, S. and Frank, D. (1998). Paraxial-fated mesoderm is required for neural crest induction in Xenopus embryos. *Dev Biol* **193**, 156-68.

Bouwmeester, T., Kim, S., Sasai, Y., Lu, B. and De Robertis, E. M. (1996). Cerberus is a head-inducing secreted factor expressed in the anterior endoderm of Spemann's organizer. *Nature* **382**, 595-601.

Cabrera, R. M., Hill, D. S., Etheredge, A. J. and Finnell, R. H. (2004). Investigations into the etiology of neural tube defects. *Birth Defects Res C Embryo Today* **72**, 330-44.

Copp, A. J., Greene, N. D. and Murdoch, J. N. (2003). The genetic basis of mammalian neurulation. *Nat Rev Genet* **4**, 784-93.

Davidson, L. A. and Keller, R. E. (1999). Neural tube closure in Xenopus laevis involves medial migration, directed protrusive activity, cell intercalation and convergent extension. *Development* **126**, 4547-56.

De Calisto, J., Araya, C., Marchant, L., Riaz, C. F. and Mayor, R. (2005). Essential role of non-canonical Wnt signalling in neural crest migration. *Development* **132**, 2587-97.

Epstein, M., Pillemer, G., Yelin, R., Yisraeli, J. K. and Fainsod, A. (1997). Patterning of the embryo along the anterior-posterior axis: the role of the caudal genes. *Development* **124**, 3805-14.

Franco, P. G., Paganelli, A. R., Lopez, S. L. and Carrasco, A. E. (1999). Functional association of retinoic acid and hedgehog signaling in Xenopus primary neurogenesis. *Development* **126**, 4257-65.

Glinka, A., Wu, W., Delius, H., Monaghan, A. P., Blumenstock, C. and Niehrs, C. (1998). Dickkopf-1 is a member of a new family of secreted proteins and functions in head induction. *Nature* **391**, 357-62.

Gonzalez, E. M., Fekany-Lee, K., Carmany-Rampey, A., Erter, C., Topczewski, J., Wright, C. V. and Solnica-Krezel, L. (2000). Head and trunk in zebrafish arise via coinhibition of BMP signaling by bozozok and chordino. *Genes Dev* **14**, 3087-92.

Haigo, S. L., Hildebrand, J. D., Harland, R. M. and Wallingford, J. B. (2003). Shroom induces apical constriction and is required for hingepoint formation during neural tube closure. *Curr Biol* **13**, 2125-37.

Hanks, S. K. and Hunter, T. (1995). Protein kinases 6. The eukaryotic protein kinase superfamily: kinase (catalytic) domain structure and classification. *Faseb J* **9**, 576-96.

Heasman, J. (1997). Patterning the Xenopus blastula. *Development* **124**, 4179-91.

Heasman, J. (2002). Morpholino oligos: making sense of antisense? *Dev Biol* **243**, 209-14.

Hopwood, N. D., Pluck, A. and Gurdon, J. B. (1989). A Xenopus mRNA related to Drosophila twist is expressed in response to induction in the mesoderm and the neural crest. *Cell* **59**, 893-903.

Huang, X. and Saint-Jeannet, J. P. (2004). Induction of the neural crest and the opportunities of life on the edge. *Dev Biol* **275**, 1-11.

Jacobson, A. G. and Gordon, R. (1976). Changes in the shape of the developing vertebrate nervous system analyzed experimentally, mathematically and by computer simulation. *J Exp Zool* **197**, 191-246.

Jung, J. W., Shin, W. S., Song, J. and Lee, S. T. (2004). Cloning and characterization of the full-length mouse Ptk7 cDNA encoding a defective receptor protein tyrosine kinase. *Gene* **328**, 75-84.

Keller, R., Davidson, L., Edlund, A., Elul, T., Ezin, M., Shook, D. and Skoglund, P. (2000). Mechanisms of convergence and extension by cell intercalation. *Philos Trans R Soc Lond B Biol Sci* **355**, 897-922.

Knecht, A. K. and Bronner-Fraser, M. (2002). Induction of the neural crest: a multigene process. *Nat Rev Genet* **3**, 453-61.

Kroiher, M., Miller, M. A. and Steele, R. E. (2001). Deceiving appearances: signaling by "dead" and "fractured" receptor protein-tyrosine kinases. *Bioessays* **23**, 69-76.

LaBonne, C. and Bronner-Fraser, M. (1999). Molecular mechanisms of neural crest formation. *Annu Rev Cell Dev Biol* **15**, 81-112.

Laemmli, U. K. (1970). Cleavage of structural proteins during the assembly of the head of bacteriophage T4. *Nature* **227**, 680-5.

Le Douarin, N. M. and Kalcheim, C. (1999). The Neural Crest. New York: Cambridge University Press.

Lu, X., Borchers, A. G., Jolicoeur, C., Rayburn, H., Baker, J. C. and Tessier-Lavigne, M. (2004). PTK7/CCK-4 is a novel regulator of planar cell polarity in vertebrates. *Nature* **430**, 93-8.

Mancilla, A. and Mayor, R. (1996). Neural crest formation in Xenopus laevis: mechanisms of Xslug induction. *Dev Biol* **177**, 580-9.

Marchant, L., Linker, C., Ruiz, P., Guerrero, N. and Mayor, R. (1998). The inductive properties of mesoderm suggest that the neural crest cells are specified by a BMP gradient. *Dev Biol* **198**, 319-29.

Mayor, R. and Aybar, M. J. (2001). Induction and development of neural crest in Xenopus laevis. *Cell Tissue Res* **305**, 203-9.

Mayor, R., Guerrero, N. and Martinez, C. (1997). Role of FGF and noggin in neural crest induction. *Dev Biol* **189**, 1-12.

Mayor, R., Morgan, R. and Sargent, M. G. (1995). Induction of the prospective neural crest of Xenopus. *Development* **121**, 767-77.

Mayor, R., Young, R. and Vargas, A. (1999). Development of neural crest in Xenopus. *Curr Top Dev Biol* **43**, 85-113.

Mizuseki, K., Kishi, M., Matsui, M., Nakanishi, S. and Sasai, Y. (1998). Xenopus Zic-related-1 and Sox-2, two factors induced by chordin, have distinct activities in the initiation of neural induction. *Development* **125**, 579-87.

Mlodzik, M. (2002). Planar cell polarization: do the same mechanisms regulate Drosophila tissue polarity and vertebrate gastrulation? *Trends Genet* **18**, 564-71.

Monsoro-Burq, A. H., Fletcher, R. B. and Harland, R. M. (2003). Neural crest induction by paraxial mesoderm in Xenopus embryos requires FGF signals. *Development* **130**, 3111-24.

Nieuwkoop, P. D. and Faber, J. (1967). Normal table of Xenopus laevis (Daudin). Amsterdam: North Holland.

Park, T. J., Haigo, S. L. and Wallingford, J. B. (2006). Ciliogenesis defects in embryos lacking inturned or fuzzy function are associated with failure of planar cell polarity and Hedgehog signaling. *Nat Genet* **38**, 303-11.

Schoenwolf, G. C. and Smith, J. L. (1990). Mechanisms of neurulation: traditional viewpoint and recent advances. *Development* **109**, 243-70.

Selleck, M. A. and Bronner-Fraser, M. (1995). Origins of the avian neural crest: the role of neural plate-epidermal interactions. *Development* **121**, 525-38.

Sive, H. L., Grainger, R. M. and Harland, R. M. (2000). Early development of Xenopus laevis : a laboratory manual. Cold Spring Harbor, N.Y.: Cold Spring Harbor Laboratory Press.

Summerton, J. and Weller, D. (1997). Morpholino antisense oligomers: design, preparation, and properties. *Antisense Nucleic Acid Drug Dev* **7**, 187-95.

Thiery, J. P. (2003). Epithelial-mesenchymal transitions in development and pathologies. *Curr Opin Cell Biol* **15**, 740-6.

Towbin, H., Staehelin, T. and Gordon, J. (1979). Electrophoretic transfer of proteins from polyacrylamide gels to nitrocellulose sheets: procedure and some applications. *Proc Natl Acad Sci U S A* **76**, 4350-4.

Ueno, N. and Greene, N. D. (2003). Planar cell polarity genes and neural tube closure. *Birth Defects Res C Embryo Today* **69**, 318-24.

Villanueva, S., Glavic, A., Ruiz, P. and Mayor, R. (2002). Posteriorization by FGF, Wnt, and retinoic acid is required for neural crest induction. *Dev Biol* **241**, 289-301.

Wallingford, J. B. (2005). Neural tube closure and neural tube defects: studies in animal models reveal known knowns and known unknowns. *Am J Med Genet C Semin Med Genet* **135**, 59-68.

Wallingford, J. B. (2006). Planar cell polarity, ciliogenesis and neural tube defects. *Hum Mol Genet* **15 Spec No 2**, R227-34.

Wallingford, J. B., Fraser, S. E. and Harland, R. M. (2002). Convergent extension: the molecular control of polarized cell movement during embryonic development. *Dev Cell* **2**, 695-706.

Wallingford, J. B. and Harland, R. M. (2002). Neural tube closure requires Dishevelled-dependent convergent extension of the midline. *Development* **129**, 5815-25.

Ybot-Gonzalez, P., Cogram, P., Gerrelli, D. and Copp, A. J. (2002). Sonic hedgehog and the molecular regulation of mouse neural tube closure. *Development* **129**, 2507-17.

Chapter III

Discussion

One of the most interesting and most studied subjects in developmental biology is the formation of the antero-posterior axis and more specifically head induction during vertebrate embryogenesis. Transplantation experiments, performed in the early twentieth century in newt embryos, have shown that head induction takes place during gastrulation as a result of the inductive properties of the Spemann's organizer, which has been defined as a source of neuralizing signaling whose function is to inhibit the ventral posteriorizing signaling that results in the patterning of the central nervous system along the antero-posterior axis (reprinted in Spemann and Mangold, 2001). Although in the last decades the molecular mechanisms underlying these events have been gradually revealed it is not yet fully understood.

Additional experiments in the amphibian embryo have shown that in the frog the organizer region can be divided into three parts. One of these parts, the anterior dorsal endoderm (ADE) has been proposed to be the head organizing center. However, in recent years several studies have argued against the role of the ADE in head induction (de Souza and Niehrs, 2000).

In this thesis we have addressed the role of ADE in head induction by analyzing the function and regulation of molecules expressed in the frog ADE or in its topological equivalent in other vertebrate embryos.

III.1 The role of Cerberus in head formation

The early work performed in amphibian embryos by Spemann and Mangold has indicated the existence of separate head- and trunk-inducing regions within the Spemann's organizer (Mangold, 1933; Spemann, 1931; Spemann, 1938). They have realized that different parts of the organizer had the ability to induce head or trunk and/or tail structures. While early gastrulae organizers had the ability to induce secondary axis containing heads when transplanted to the ventral side amphibian embryo, old gastrula organizers are only able to induce secondary trunks and/or tails. However, in other vertebrate embryos such as mammals the group of cells containing the head inducing activity is not located within the node but studies have demonstrated that they might be located in the anterior visceral endoderm (AVE; reviewed by Beddington and Robertson, 1999).

The *Xenopus laevis* organizer region can be divided, according to their fate map, into three different regions, the anterior endoderm, the prechordal endomesoderm and

the chordamesoderm (de Souza and Niehrs, 2000). During gastrula stages these tissues migrate towards the future side of the embryo and, due to their different organizer-inducing activities, pattern the overlying ectoderm along the anteroposterior axis and thereby are responsible for the induction and patterning of the future central nervous system. Traditionally, the prechordal endomesoderm had been considered to be the head organizing center (Niehrs, 1999). Likewise, the posterior chordamesoderm was considered to be the trunk organizing center (Niehrs, 1999). However, the isolation of *cerberus* (*Xcer*), a multiple inhibitor of Wnt, BMP and Nodal signaling, shown to be a potent head inducing molecule expressed in the ADE, has also implicated the anterior endoderm in head induction (Bouwmeester *et al.*, 1996). Later on, the discovery of the mouse homologue of *Xcer*, mouse *cerberus-like* (m*cer-1*) that was expressed in the AVE, the region considered to be the topological and functional equivalent to the frog ADE, gave emphasis to the role of the ADE as an head organizing center (Belo *et al.*, 1997; Biben *et al.*, 1998; Shawlot *et al.*, 1998). Unfortunately, the fact that the knockout mouse for m*cer-1* develops without any visible phenotype has argued against the role of Cerberus in head formation (Belo *et al.*, 2000; Shawlot *et al.*, 2000).

We have addressed this question of the role of Cerberus in head formation by performing loss-of-function studies using an antisense morpholino oligonucleotide against *Xcer* and by taking advantage of sensitized/compound system approaches. Using these approaches we were able to show that *Xcer* is involved in head induction and patterning. This result has been supported by the work of other groups (Hino *et al.*, 2003; Kuroda *et al.*, 2004). In our study, the XcerMo alone did not produced any visible head phenotypes but resulted in progressive loss of anterior structures when injected in embryos where the levels of BMP-4, Xnr-1 or/and Xwnt-8 had been raised specifically in the ADE. However, the morpholino designed by Kuroda and colleagues was able to partially inhibit head formation (Kuroda *et al.*, 2004). These differences can be due to the existence of pseudoalleles in the *Xenopus laevis* genome (Kobel and Du Pasquier, 1986). At the time that we designed the *Xcer* morpholino sequence we compared it with the available *Xcerberus* EST sequences, present in the general publicly accessible databases, and all 5'UTR sequences were complementary to the designed morpholino. However, later on a new EST sequence became available that showed a second allele for *Xcer* in which the 5'UTR was no longer complementary to our XCerMo. The morpholino oligo designed by Kuroda and colleagues (2004) already contemplated this second allele and for

this reason was already able to knockdown both copies of *Xcer*. In brief, the morpholino oligo used in our study inhibits only one allele of *Xcer* whereas the one used by Kuroda and colleagues inhibits both alles, thus producing a stronger phenotype. Neverthless they both lead to similar conclusions on the role of Cerberus in head formation (Kuroda *et al.,* 2004; Silva *et al.,* 2003).

Early work in amphibian embryos had shown that the organizer is a source of secreted factors with BMP, Wnt or Nodal inhibitory activities (Niehrs, 2004). Among these are Frzb-1, Crescent, sFRP-2, and Dkk-1 as Wnt inhibitors, Chordin and Noggin as BMP inhibitors and Lefty as Nodal inhibitor (De Robertis and Kuroda, 2004). The presence of these secreted molecules in the same group of cells as Cerberus or in its close vicinity may partially compensate for the loss of Cerberus. Indeed, when depletion of XCer is followed by the depletion of XBMP-3b, a Nodal and BMP inhibitor, the embryos develop without anterior structures, whereas alone no phenotype could be observed (Hino *et al.,* 2003). Due to possible redundancy with other secreted factors within the organizer, we have used a sensitized system where we have saturated the organizer and thereby the secreted factors produced there with BMP-4, Wnt-8 and/or Xnr-1. In these way, we were able to show that when, in addition, we remove Cerberus, head formation was severely affected. With this we were able not only to show that endogenous Cerberus is indeed involved in head formation but also to show *in vivo* that it is required to inhibit these three signaling cascades (Piccolo *et al.,* 1999; Silva *et al.,* 2003).

Other studies however, contradict the role of Cerberus/ADE in head formation. Schneider and Mercola (1999) suggest that Cerberus is not involved in head induction but might be important for heart formation. In those experiments they removed the Cerberus-expressing cells and have shown that head formation was not affected but that instead heart defects developed. Recently, it has been shown the requirement of *Xenopus* Cerberus in the induction of cardiogenic mesoderm in the frog (Foley *et al.,* 2007). Nevertheless, it is possible that Cerberus role in head induction might occur before gastrulation begins since Cerberus is already expressed at stage 9 (Bouwmeester *et al.,* 1996). In this way, by stage 10 when the authors removed the Cerberus-expressing cells, Cerberus protein that was already present in the embryo might already have diffused to the adjacent ectoderm which would then account for the lack of head phenotype in these embryos. In addition, in conjugate assays it has been shown that the ADE where Cerberus is expressed is able to induce the expression of anterior neural markers in dorsal

ectoderm/neuralized explants (Lupo *et al.*, 2002 and this thesis). Furthermore, in this thesis we have shown that if we remove XCer from these conjugates, anterior neural marker induction no longer occurs. Taken together, it is possible that Cerberus expression can be divided in two distinct phases: one, before gastrulation, that might be involved in head formation and requires at least its Wnt and BMP inhibitory activity; and a second phase, during gastrulation, that would be required in heart formation. It would be interesting to test this hypothesis by repeating the experiment performed by Schneider and Mercola, (1999) in XcerMo injected embryos. If these embryos would develop with additional head defects it would support the above mentioned hypothesis.

III.2 The use of promoters to express molecules in a time and space restricted way

Throughout this thesis we have demonstrated that the 4kb mouse *cerberus-like* promoter fragment has the ability to mimic endogenous *Xcer* temporal and spatial expression and direct the expression of different molecules to the ADE of the frog embryo. Normally, when BMP-4, Wnt-8 and Xnr-1 are expressed in embryos using vectors with constitutively active or ubiquitous promoters, the embryos develop with very dramatic phenotypes. Thus, the crucial role that this signaling molecules play during the early embryonic development (Heasman, 2006), together with the strong phenotypes induced when expressed at early stages, compromises their use when trying to study later events. In our work we were able to overcome this problem and restrict in space and time the expression of these molecules, which allowed us to demonstrate *in vivo* the requirement for XCer to inhibit these molecules for a proper head induction and patterning. Taken together, this promoter fragment proved to be a very useful tool for the targeted expression of other molecules in the ADE during gastrula stages. Previous reports have demonstrated the usefulness of using specific promoters, such as the heat shock promoters as tools to control the expression of certain molecules (Hess *et al.*, 2007; Michiue and Asashima, 2005). However, in many studies such as ours, the proteins expressed as a result of the specific promoter's activity can be detected much later than the endogenous protein would, which might result from a higher stability of either the RNA or the protein or even both (Aulehla *et al.*, 2007; Tavares *et al.*, 2007). This higher stability might be good when the goal of using these promoters is to mark a specific tissue or to determine its derivative tissues, however, when the goal is to express molecules within a specific time-window it might become a problem. In this case, the solution would be to shorten both

the protein and the RNA turnover. RNA instability might be achieved, for example, by fusing the 3'UTR of segmental genes, such as *hairy2a* or *esr5*, downstream of the coding sequence (Aulehla *et al.*, 2007; Davis *et al.*, 2001) while adding in the C-terminal end a PEST domain would regulate protein stability (Artavanis-Tsakonas *et al.*, 1999).

In summary, the study of *cis*-regulatory regions of promoter fragments of known genes can be a very valuable tool to drive expression of specific molecules in a temporally and spatially controlled manner. That is not only useful in developmental biology to help understanding different events and mechanisms that occur during embryonic development, but it could also be very useful in other fields such as cancer and disease.

III.3 Cerberus regulation throughout evolution: the use of cross-species studies

Although *Xcer* orthologous genes (c*cer* and m*cer-1*) are expressed in the topological equivalent structures of the frog ADE, during later stages their expression patterns differ significantly ((Belo *et al.*, 1997; Bouwmeester *et al.*, 1996; Rodriguez Esteban *et al.*, 1999) These variations may result from differences in the *cis*-regulatory elements in their genomic sequences or from differences in the expression pattern of their upstream regulators, or both. In our work we have analyzed, using cross-species studies, a fragment of the *cis*-regulatory region of the m*cer-1* gene shown to direct the expression of a reporter gene specifically to the mouse AVE. Our results suggested that although the upstream *cis*-regulatory region between mouse and *Xenopus cerberus* show very little similarity, the regulatory elements seam to be conserved. It would also be interesting to see how the *cis*-regulatory region of *Xcer* would behave in the mouse embryo. These types of studies are quite important to determine how gene regulation has evolved with time. To analyze the promoter region of m*cer-1* we performed transient expression of reporter constructs in *Xenopus* embryos instead of using transgenic frogs. This type of approach results in a salt and pepper expression due to the fact that not all cells receive the DNA. In addition, it has been reported that it may also happen that the reporter gene expression pattern might differ from the endogenous expression pattern (Yang *et al.*, 2002), which could be due to the presence of a repressor that cannot inhibit the high amount of reporter construct present in the cell. In agreement with this, we intend to generate transient transgenic frogs to validate our results.

III.4 In search of novel genes expressed in the anterior endoderm

Since the isolation of the first organizer-specific gene, *goosecoid*, many screens have been performed in order to isolate novel organizer genes (De Robertis *et al.,* 2001; Lemaire and Kodjabachian, 1996). During the work reported in this thesis we took advantage of a differential screening performed in the lab to identify novel mouse AVE specific genes and searched for the orthologs in the frog. Our purpose with this search was to establish the evolutionary conservation between the expression pattern of these novel genes in the mouse and *Xenopus* embryos, with the aim of determine a conserved function of these genes in head formation in mouse and frog.

We started by identifying and analyzing the expression pattern of the *Xenopus* orthologs of three novel mouse genes (*mADTK1, mAd4, mShisa*). We were able to identify two *Xenopus* orthologs for two of these genes (*ADTK* and *Shisa*), which we named *XADTK1, -2* and *Shisa-1, -2*, respectively. By *in situ* hybridization we were able to show that from the five novel *Xenopus* genes (*XADTK1, XADTK2, XShisa-1, XShisa-2* and *XAd4*), three were expressed in the topological equivalent structure of the mouse AVE, the ADE (*XADTK1, XADTK2* and *XShisa-1*). We have analyzed the expression pattern of m*ADTK1* and m*Shisa* chick orthologs and shown that they were expressed in the hypoblast. These results reinforce the idea that these structures are equivalent in terms of gene expression. Three of the identified genes (*XADTK1, XADTK2* and *XAd4*) belong to novel families of genes with no known function while the two other belong to the recently identified Shisa gene family. One interesting observation that resulted from this study is that if we would superimpose the expression pattern of *XADTK1* and *XADTK2* and compare it with the expression pattern of the mouse counterpart, one would see that they are expressed in topological equivalent regions throughout development. A similar result was obtained in the case of *Shisa* genes. The similar expression pattern between frog and mouse genes suggests that these genes might be playing the same role in these two organisms and that their function might remain the same throughout evolution. Functional studies using morpholino antisense based knock-downs in *Xenopus* and mouse knockout models should address this question.

Although the work presented here on these novel molecules is still very preliminary and many more experiments have to be performed to determine their role in development and the molecular mechanisms behind their function. Nevertheless it is clear that there are still many molecules to be identified in the organizer region.

III.5 The role of Shisa-2 during *Xenopus* embryonic development

The search for the *Xenopus* orthologs of novel mouse AVE specific genes resulted in the isolation of two Shisa-related genes, *Shisa-1* and *Shisa-2*, at the time named *XAd2L2* and *XAd2L1*, respectively. *XAd2L2* was soon after reported as being a novel organizer gene, named *Shisa-1* (Yamamoto *et al., 2005)*. Shisa-1 was shown to inhibit Wnt and FGF signaling by binding to the immature forms of Fz and FGFR, in the ER, prevent their maturation and posterior translocation to the cellular membrane (Yamamoto *et al.,* 2005). In our studies we have shown that *Shisa-2*, unlike *Shisa-1*, is not an organizer gene and its expression is restricted to the paraxial mesoderm in late gastrula stage embryos. Later on, *Shisa-2* transcripts were strongly detected in the anterior portion of the presomitic mesoderm and recently formed somites, and at low levels in the more mature somites (Silva *et al.,* 2006). Although *Shisa-2* was not expressed in the ADE, its very dynamic expression pattern prompted us to analyze the role of *Shisa-2* during *Xenopus* development. Through our *Shisa-2* morpholino antisense based knock-down we were able to show that Shisa-2 is required for determining the segmentation plane. Previous work has shown that both FGF and Wnt signaling is necessary in the PSM to maintain its immature state and for the segmentation process to occur these signaling pathways need to be inhibited (Dubrulle *et al.,* 2001). The expression of both FGF and Wnt ligands in the PSM is tightly regulated by retinoic acid signaling (Diez del Corral *et al.,* 2003; Moreno and Kintner, 2004; Vermot and Pourquie, 2005). This mutual regulation generates a gradient which has been shown to determine where the somite will form (Delfini *et al.,* 2005; Moreno and Kintner, 2004; Morimoto *et al.,* 2005). In this light, and because both FGF and Wnts are morphogenic proteins, Shisa-2 may function in the anterior portion of the PSM to ensure that even if there is an excess of ligands in the extracellular space, there will be a limited number of receptors available in the cell surface to transduce the signal to the inside of the cell. The results obtained in this study have been supported by a recent study performed by Nagano and colleagues (2006) that reported the isolation of Xenopus Shisa-2 and Shisa-3 and analyzed the role of XShisa-2 in somitogenesis.

In addition, Shisa-2 depleted embryos displayed mild convergent extension phenotypes. It is likely that this phenotype is due to inhibition of non-canonical Wnt signaling. When analyzing the expression pattern of *Xbra*, a FGF downstream target gene,

we were able to see that mesoderm formation had not been affected. These results suggest that during this stages FGF signaling is not being regulated by Shisa-2.

Our results have also shown that Shisa-2 is required not only for the segmentation process, but is also involved in other processes like eye and otic vesicle formation. Indeed, Shisa-2 depleted embryos develop with smaller eyes and smaller otic vesicles. These results are supported by studies from frog, fish and mouse that have shown the importance of Wnt or FGF signaling in the formation and patterning of these structures (Cornesse *et al.,* 2005; de Iongh *et al.,* 2006; Heisenberg *et al.,* 2001; Kim *et al.,* 2000; Moore *et al.,* 2004; Nambiar and Henion, 2004; Smith *et al.,* 2005).

III.6 The role of XADTK1 during *Xenopus* development

As mentioned before we have isolated three novel genes expressed in the frog ADE. Two of these genes, *XADTK1* and *XADTK2*, belong to a novel gene family. Bioinformatics analysis has shown that these genes encode for proteins containing a protein kinase catalytic domain. However, they have no similarity to any of the known kinase families and should constitute a novel family of kinases. Conversely, we have identified *ADTK1* orthologs in mouse, human, fish, rat and chicken but not in drosophila, suggesting that *ADTK* genes are unique to the vertebrate.

Both *XADTK1* and *XADTK2* genes exhibit very interesting expression patterns throughout early development and are coexpressed in different tissues such as the ADE and IDME, during gastrula stages and, in the notochord and eye in later stages of development. In this thesis we have decided to focus on *XADTK1* and determine its function in the embryo. Our loss of function experiments, using a morpholino against *XADTK1* has shown that embryos lacking XADTK1 develop neural tube closure defects. This type of defects might be related to defects in non-canonical Wnt signaling or Hedgehog signaling (Wallingford, 2005). While non-canonical Wnt signaling defects in neural tube closure arise from defects in convergent extension movements, Hedgehog related defects are usually associated with cilia (Wallingford, 2006). Ongoing experiments are trying to determine in which of these signaling cascades *XADTK1* is involved in.

Morphological data has shown that the neural tube closure defects observed in the morpholino injected embryos might be caused by the lack of hingepoint formation in the neural plate. A similar phenotype is observed in Shroom depleted embryos (Haigo *et al.,* 2003). Like XADTK1, also Shroom is expressed in the neural folds. Functional

characterization of shroom has shown that it is involved in apical constriction and neural tube closure, however, the mechanism by which Shroom acts remains unknown (Haigo *et al.*, 2003). The similarity between the phenotypes observed in Shroom and XADTK1 morphants suggests that XADTK1 might be involved in actin regulation and consequently in apical constriction.

On the other hand, preliminary data has shown that non canonical Wnt signaling is able to induce XADTK1 expression in animal cap assays (not shown). This result supports the idea that XADTK1 might be a non canonical Wnt target gene. However, non canonical Wnt signaling is associated with posterior neural tube closure defects and XADTK1 morphants display anterior neural tube closure defects which have been associated with apical constriction and Hedgehog signaling (Wallingford, 2005). Interestingly, two recently characterized genes, *fuzzy* and *inturned*, were shown to be involved in both non canonical Wnt and Hedgehog signaling pathways (Park *et al.*, 2006). Loss-of-function experiments resulted in neural tube closure defects (Park *et al.*, 2006), similarly to what we have shown in this thesis for XADTK1.

In addition, to the neural tube defects observed in XADTK1 morphants, these embryos also shown neural crest formation defects. Although XADTK1 morphants display neural crest formation defects, molecular analysis has shown that neural crest migration is not affected. It is feasible to hypothesize that these defects could be traced back to gastrulation, where neural crest cells are first induced (Bonstein *et al.*, 1998; Mancilla and Mayor, 1996).

In conclusion, the work reported in this thesis contributed for the better understanding of the mechanisms involved in the genetic control of early development in the frog, namely the role of the ADE and XCerberus in head induction and Anterior-Posterior patterning.

III.7 Current and Future perspectives

By the end of this PHD thesis several questions still remain without answer, others have been raised, laying the ground and the leads for the experiments to follow. A more thorough analysis of the m*cer-1* promoter, using shorter fragments and mutated binding sites for the putative regulators, will tell us which are the factors most likely to regulate its activity to the *Xenopus* ADE. In addition, these results should be validated in the mouse by performing transient transgenic experiments. Those results would not only help in

225

understanding the regulation of m*cer-1* but also in clarifying the initial steps in early embryonic development, namely how the anterior-posterior axis is formed in the mouse.

Through this work we have shown that the 4kb m*cer-1* promoter fragment is a very useful tool to accurately drive the expression of specific molecules in the ADE. Currently, we are taking advantage of this promoter fragment together with a recently described technique to generate a *Xenopus laevis* transgenic line that will express EGFP specifically in the ADE. This transgenic line will be very valuable in studies where experiments such as transplantation experiments or screenings where this tissue may need to be selectively removed.

As referred in this study, a screening to search for novel genes expressed in the mouse AVE was performed in the laboratory and proved to be a good source of novel genes expressed in the AVE. We have analyzed the expression pattern of five novel *Xenopus* genes and isolated three others not mentioned in this thesis. The data presented here regarding the characterization of some of these novel genes is still at an early stage. Concerning the *XAd4* gene, we have cloned both an unlabelled and tagged full-length open reading-frame constructs and we intend to characterize this gene by performing gain- and loss-of-function experiments using a *XAd4* morpholino oligo.

Regarding the study of the function of *Shisa-2* during early development we intend to further analyze the requirement for *Shisa-2* in both eye and ear formation. It would also be interesting to evaluate if Hedgehog signaling is inhibited by Shisa-2.

In order to continue the characterization of the *ADTK* genes in the frog, we intend to determine the proteins interacting with XADTK1 by performing a GST-pull down. In addition, we are currently trying to determine the subcellular localization of XADTK1 in both HEK 293 cell lines and in *Xenopus* embryos. The outcome of these experiments will allow a better understanding of the mechanism of action of XADTK1. In order to further analyze the phenotypes described here for the XADTK1 loss-of-function experiments we plan to perform time-lapse movies of the neural tube closure and to perform staining of the cartilage to determine the defects caused by disruption of the XADTK1 protein in the cranial neural crest derivatives. We would also like to take advantage of the animal cap assay to determine if *XADTK1* is involved in different signaling cascades, such as non-canonical Wnt signaling and Hedgehog signaling. In addition, we intend to analyze the phenotypes generated in XADTK1 gain-of-function experiments in depth. Finally, we have already generated a morpholino oligonucleotide against *XADTK2* and are currently

performing both gain- and loss-of-function experiments to determine the role of *XADTK2* in *Xenopus laevis* development. Together with this, the combined depletion of XADTK1 and XADTK2 will enable us to determine if they are able to compensate for each other and if their function is redundant.

In conclusion, I think that the experiments described above highlight some of the experimental lines that should be the natural follow-up from the point where this thesis ended. During the course of this thesis, I was able to better clarify some pertinent developmental issues and many others have been raised. I do believe that the future work may help in elucidating the function of the anterior dorsal endoderm during embryonic development and in understanding the molecular mechanisms underlying these events.

References

Acampora, D., Avantaggiato, V., Tuorto, F., Briata, P., Corte, G., and Simeone, A. (1998). Visceral endoderm-restricted translation of Otx1 mediates recovery of Otx2 requirements for specification of anterior neural plate and normal gastrulation. *Development* **125,** 5091-104.

Acampora, D., Mazan, S., Lallemand, Y., Avantaggiato, V., Maury, M., Simeone, A., and Brulet, P. (1995). Forebrain and midbrain regions are deleted in Otx2-/- mutants due to a defective anterior neuroectoderm specification during gastrulation. *Development* **121,** 3279-90.

Agathon, A., Thisse, C., and Thisse, B. (2003). The molecular nature of the zebrafish tail organizer. *Nature* **424,** 448-52.

Agius, E., Oelgeschlager, M., Wessely, O., Kemp, C., and De Robertis, E. M. (2000). Endodermal Nodal-related signals and mesoderm induction in Xenopus. *Development* **127,** 1173-83.

Amaya, E., Musci, T. J., and Kirschner, M. W. (1991). Expression of a dominant negative mutant of the FGF receptor disrupts mesoderm formation in Xenopus embryos. *Cell* **66,** 257-70.

Ang, S. L., Conlon, R. A., Jin, O., and Rossant, J. (1994). Positive and negative signals from mesoderm regulate the expression of mouse Otx2 in ectoderm explants. *Development* **120,** 2979-89.

Artavanis-Tsakonas, S., Rand, M. D., and Lake, R. J. (1999). Notch signaling: cell fate control and signal integration in development. *Science* **284,** 770-6.

Aulehla, A., and Herrmann, B. G. (2004). Segmentation in vertebrates: clock and gradient finally joined. *Genes Dev* **18,** 2060-7.

Aulehla, A., Wehrle, C., Brand-Saberi, B., Kemler, R., Gossler, A., Kanzler, B., and Herrmann, B. G. (2003). Wnt3a plays a major role in the segmentation clock controlling somitogenesis. *Dev Cell* **4,** 395-406.

Aulehla, A., Wiegraebe, W., Baubet, V., Wahl, M. B., Deng, C., Taketo, M., Lewandoski, M., and Pourquie, O. (2007). A beta-catenin gradient links the clock and wavefront systems in mouse embryo segmentation. *Nat Cell Biol*.

Bachiller, D., Klingensmith, J., Kemp, C., Belo, J. A., Anderson, R. M., May, S. R., McMahon, J. A., McMahon, A. P., Harland, R. M., Rossant, J., and De Robertis, E. M. (2000). The organizer factors Chordin and Noggin are required for mouse forebrain development. *Nature* **403,** 658-61.

Bachvarova, R. F., Skromne, I., and Stern, C. D. (1998). Induction of primitive streak and Hensen's node by the posterior marginal zone in the early chick embryo. *Development* **125,** 3521-34.

Beddington, R. S. (1994). Induction of a second neural axis by the mouse node. *Development* **120,** 613-20.

Beddington, R. S., and Robertson, E. J. (1999). Axis development and early asymmetry in mammals. *Cell* **96,** 195-209.

Bell, E., Munoz-Sanjuan, I., Altmann, C. R., Vonica, A., and Brivanlou, A. H. (2003). Cell fate specification and competence by Coco, a maternal BMP, TGFbeta and Wnt inhibitor. *Development* **130,** 1381-9.

Belo, J. A., Bachiller, D., Agius, E., Kemp, C., Borges, A. C., Marques, S., Piccolo, S., and De Robertis, E. M. (2000). Cerberus-like is a secreted BMP and nodal antagonist not essential for mouse development. *Genesis* **26,** 265-70.

Belo, J. A., Bouwmeester, T., Leyns, L., Kertesz, N., Gallo, M., Follettie, M., and De Robertis, E. M. (1997). Cerberus-like is a secreted factor with neutralizing activity expressed in the anterior primitive endoderm of the mouse gastrula. *Mech Dev* **68,** 45-57.

Belo, J. A., Leyns, L., Yamada, G., and De Robertis, E. M. (1998). The prechordal midline of the chondrocranium is defective in Goosecoid-1 mouse mutants. *Mech Dev* **72,** 15-25.

Biben, C., Stanley, E., Fabri, L., Kotecha, S., Rhinn, M., Drinkwater, C., Lah, M., Wang, C. C., Nash, A., Hilton, D., Ang, S. L., Mohun, T., and Harvey, R. P. (1998). Murine cerberus homologue mCer-1: a candidate anterior patterning molecule. *Dev Biol* **194,** 135-51.

Binnerts, M. E., Wen, X., Cante-Barrett, K., Bright, J., Chen, H. T., Asundi, V., Sattari, P., Tang, T., Boyle, B., Funk, W., and Rupp, F. (2004). Human Crossveinless-2 is a novel inhibitor of bone morphogenetic proteins. *Biochem Biophys Res Commun* **315,** 272-80.

Birsoy, B., Kofron, M., Schaible, K., Wylie, C., and Heasman, J. (2006). Vg 1 is an essential signaling molecule in Xenopus development. *Development* **133,** 15-20.

Bonstein, L., Elias, S., and Frank, D. (1998). Paraxial-fated mesoderm is required for neural crest induction in Xenopus embryos. *Dev Biol* **193,** 156-68.

Boterenbrood, E. C., and Nieuwkoop, P. D. (1973). "The formation of the mesoderm in Urodelan amphibians: V. Its regional induction by the endoderm."

Bouwmeester, T., Kim, S., Sasai, Y., Lu, B., and De Robertis, E. M. (1996). Cerberus is a head-inducing secreted factor expressed in the anterior endoderm of Spemann's organizer. *Nature* **382,** 595-601.

Brent, A. E., and Tabin, C. J. (2002). Developmental regulation of somite derivatives: muscle, cartilage and tendon. *Curr Opin Genet Dev* **12,** 548-57.

Chen, S., and Kimelman, D. (2000). The role of the yolk syncytial layer in germ layer patterning in zebrafish. *Development* **127,** 4681-9.

Cheng, A. M., Thisse, B., Thisse, C., and Wright, C. V. (2000). The lefty-related factor Xatv acts as a feedback inhibitor of nodal signaling in mesoderm induction and L-R axis development in xenopus. *Development* **127,** 1049-61.

Christian, J. L., and Moon, R. T. (1993). Interactions between Xwnt-8 and Spemann organizer signaling pathways generate dorsoventral pattern in the embryonic mesoderm of Xenopus. *Genes Dev* **7,** 13-28.

Clements, D., Friday, R. V., and Woodland, H. R. (1999). Mode of action of VegT in mesoderm and endoderm formation. *Development* **126,** 4903-11.

Coffinier, C., Ketpura, N., Tran, U., Geissert, D., and De Robertis, E. M. (2002). Mouse Crossveinless-2 is the vertebrate homolog of a Drosophila extracellular regulator of BMP signaling. *Mech Dev* **119 Suppl 1,** S179-84.

Cole, S. E., Levorse, J. M., Tilghman, S. M., and Vogt, T. F. (2002). Clock regulatory elements control cyclic expression of Lunatic fringe during somitogenesis. *Dev Cell* **3,** 75-84.

Collavin, L., and Kirschner, M. W. (2003). The secreted Frizzled-related protein Sizzled functions as a negative feedback regulator of extreme ventral mesoderm. *Development* **130,** 805-16.

Conley, C. A., Silburn, R., Singer, M. A., Ralston, A., Rohwer-Nutter, D., Olson, D. J., Gelbart, W., and Blair, S. S. (2000). Crossveinless 2 contains cysteine-rich domains and is required for high levels of BMP-like activity during the formation of the cross veins in Drosophila. *Development* **127,** 3947-59.

Conlon, F. L., Sedgwick, S. G., Weston, K. M., and Smith, J. C. (1996). Inhibition of Xbra transcription activation causes defects in mesodermal patterning and reveals autoregulation of Xbra in dorsal mesoderm. *Development* **122,** 2427-35.

Cornell, R. A., and Kimelman, D. (1994). Activin-mediated mesoderm induction requires FGF. *Development* **120,** 453-62.

Cornesse, Y., Pieler, T., and Hollemann, T. (2005). Olfactory and lens placode formation is controlled by the hedgehog-interacting protein (Xhip) in Xenopus. *Dev Biol* **277,** 296-315.

Crease, D. J., Dyson, S., and Gurdon, J. B. (1998). Cooperation between the activin and Wnt pathways in the spatial control of organizer gene expression. *Proc Natl Acad Sci U S A* **95,** 4398-403.

Cui, Y., Tian, Q., and Christian, J. L. (1996). Synergistic effects of Vg1 and Wnt signals in the specification of dorsal mesoderm and endoderm. *Dev Biol* **180,** 22-34.

Dale, L., Howes, G., Price, B. M., and Smith, J. C. (1992). Bone morphogenetic protein 4: a ventralizing factor in early Xenopus development. *Development* **115,** 573-85.

Dale, L., Matthews, G., Tabe, L., and Colman, A. (1989). Developmental expression of the protein product of Vg1, a localized maternal mRNA in the frog Xenopus laevis. *Embo J* **8,** 1057-65.

Davis, R. L., Turner, D. L., Evans, L. M., and Kirschner, M. W. (2001). Molecular targets of vertebrate segmentation: two mechanisms control segmental expression of Xenopus hairy2 during somite formation. *Dev Cell* **1,** 553-65.

de Iongh, R. U., Abud, H. E., and Hime, G. R. (2006). WNT/Frizzled signaling in eye development and disease. *Front Biosci* **11,** 2442-64.

De Robertis, E. M., and Kuroda, H. (2004). Dorsal-ventral patterning and neural induction in Xenopus embryos. *Annu Rev Cell Dev Biol* **20,** 285-308.

De Robertis, E. M., Larrain, J., Oelgeschlager, M., and Wessely, O. (2000). The establishment of Spemann's organizer and patterning of the vertebrate embryo. *Nat Rev Genet* **1,** 171-81.

De Robertis, E. M., Wessely, O., Oelgeschlager, M., Brizuela, B., Pera, E., Larrain, J., Abreu, J., and Bachiller, D. (2001). Molecular mechanisms of cell-cell signaling by the Spemann-Mangold organizer. *Int J Dev Biol* **45,** 189-97.

de Souza, F. S., and Niehrs, C. (2000). Anterior endoderm and head induction in early vertebrate embryos. *Cell Tissue Res* **300,** 207-17.

del Barco Barrantes, I., Davidson, G., Grone, H. J., Westphal, H., and Niehrs, C. (2003). Dkk1 and noggin cooperate in mammalian head induction. *Genes Dev* **17,** 2239-44.

Delfini, M. C., Dubrulle, J., Malapert, P., Chal, J., and Pourquie, O. (2005). Control of the segmentation process by graded MAPK/ERK activation in the chick embryo. *Proc Natl Acad Sci U S A* **102,** 11343-8.

Deng, C. X., Wynshaw-Boris, A., Shen, M. M., Daugherty, C., Ornitz, D. M., and Leder, P. (1994). Murine FGFR-1 is required for early postimplantation growth and axial organization. *Genes Dev* **8,** 3045-57.

Diez del Corral, R., Olivera-Martinez, I., Goriely, A., Gale, E., Maden, M., and Storey, K. (2003). Opposing FGF and retinoid pathways control ventral neural pattern, neuronal differentiation, and segmentation during body axis extension. *Neuron* **40,** 65-79.

Ding, J., Yang, L., Yan, Y. T., Chen, A., Desai, N., Wynshaw-Boris, A., and Shen, M. M. (1998). Cripto is required for correct orientation of the anterior-posterior axis in the mouse embryo. *Nature* **395,** 702-7.

Du, S. J., Purcell, S. M., Christian, J. L., McGrew, L. L., and Moon, R. T. (1995). Identification of distinct classes and functional domains of Wnts through expression of wild-type and chimeric proteins in Xenopus embryos. *Mol Cell Biol* **15,** 2625-34.

Dubrulle, J., McGrew, M. J., and Pourquie, O. (2001). FGF signaling controls somite boundary position and regulates segmentation clock control of spatiotemporal Hox gene activation. *Cell* **106,** 219-32.

Dufort, D., Schwartz, L., Harpal, K., and Rossant, J. (1998). The transcription factor HNF3beta is required in visceral endoderm for normal primitive streak morphogenesis. *Development* **125,** 3015-25.

Eyal-Giladi, H., and Khaner, O. (1989). The chick's marginal zone and primitive streak formation. II. Quantification of the marginal zone's potencies--temporal and spatial aspects. *Dev Biol* **134,** 215-21.

Feldman, B., Gates, M. A., Egan, E. S., Dougan, S. T., Rennebeck, G., Sirotkin, H. I., Schier, A. F., and Talbot, W. S. (1998). Zebrafish organizer development and germ-layer formation require nodal-related signals. *Nature* **395,** 181-5.

Finley, K. R., Tennessen, J., and Shawlot, W. (2003). The mouse secreted frizzled-related protein 5 gene is expressed in the anterior visceral endoderm and foregut endoderm during early post-implantation development. *Gene Expr Patterns* **3,** 681-4.

Fisher, M. E., Isaacs, H. V., and Pownall, M. E. (2002). eFGF is required for activation of XmyoD expression in the myogenic cell lineage of Xenopus laevis. *Development* **129,** 1307-15.

Foley, A. C., Korol, O., Timmer, A. M., and Mercola, M. (2007). Multiple functions of Cerberus cooperate to induce heart downstream of Nodal. *Dev Biol* **303,** 57-65.

Foley, A. C., Skromne, I., and Stern, C. D. (2000). Reconciling different models of forebrain induction and patterning: a dual role for the hypoblast. *Development* **127,** 3839-54.

Foley, A. C., and Stern, C. D. (2001). Evolution of vertebrate forebrain development: how many different mechanisms? *J Anat* **199,** 35-52.

Gerhart, J., Danilchik, M., Doniach, T., Roberts, S., Rowning, B., and Stewart, R. (1989). Cortical rotation of the Xenopus egg: consequences for the anteroposterior pattern of embryonic dorsal development. *Development* **107 Suppl,** 37-51.

Gimlich, R. L., and Cooke, J. (1983). Cell lineage and the induction of second nervous systems in amphibian development. *Nature* **306,** 471-3.

Gimlich, R. L., and Gerhart, J. C. (1984). Early cellular interactions promote embryonic axis formation in Xenopus laevis. *Dev Biol* **104,** 117-30.

Glinka, A., Wu, W., Delius, H., Monaghan, A. P., Blumenstock, C., and Niehrs, C. (1998). Dickkopf-1 is a member of a new family of secreted proteins and functions in head induction. *Nature* **391,** 357-62.

Glinka, A., Wu, W., Onichtchouk, D., Blumenstock, C., and Niehrs, C. (1997). Head induction by simultaneous repression of Bmp and Wnt signalling in Xenopus. *Nature* **389,** 517-9.

Gonzalez, E. M., Fekany-Lee, K., Carmany-Rampey, A., Erter, C., Topczewski, J., Wright, C. V., and Solnica-Krezel, L. (2000). Head and trunk in zebrafish arise via coinhibition of BMP signaling by bozozok and chordino. *Genes Dev* **14,** 3087-92.

Goodman, S. A., Albano, R., Wardle, F. C., Matthews, G., Tannahill, D., and Dale, L. (1998). BMP1-related metalloproteinases promote the development of ventral mesoderm in early Xenopus embryos. *Dev Biol* **195,** 144-57.

Griffin, K., Patient, R., and Holder, N. (1995). Analysis of FGF function in normal and no tail zebrafish embryos reveals separate mechanisms for formation of the trunk and the tail. *Development* **121,** 2983-94.

Haegel, H., Larue, L., Ohsugi, M., Fedorov, L., Herrenknecht, K., and Kemler, R. (1995). Lack of beta-catenin affects mouse development at gastrulation. *Development* **121,** 3529-37.

Haigo, S. L., Hildebrand, J. D., Harland, R. M., and Wallingford, J. B. (2003). Shroom induces apical constriction and is required for hingepoint formation during neural tube closure. *Curr Biol* **13,** 2125-37.

Hamilton, L. (1969). The formation of somites in Xenopus. *J Embryol Exp Morphol* **22,** 253-64.

Hansen, C. S., Marion, C. D., Steele, K., George, S., and Smith, W. C. (1997). Direct neural induction and selective inhibition of mesoderm and epidermis inducers by Xnr3. *Development* **124,** 483-92.

Haramoto, Y., Tanegashima, K., Onuma, Y., Takahashi, S., Sekizaki, H., and Asashima, M. (2004). Xenopus tropicalis nodal-related gene 3 regulates BMP signaling: an essential role for the pro-region. *Dev Biol* **265,** 155-68.

Harland, R., and Gerhart, J. (1997). Formation and function of Spemann's organizer. *Annu Rev Cell Dev Biol* **13,** 611-67.

Hashimoto, H., Rebagliati, M., Ahmad, N., Muraoka, O., Kurokawa, T., Hibi, M., and Suzuki, T. (2004). The Cerberus/Dan-family protein Charon is a negative regulator of Nodal signaling during left-right patterning in zebrafish. *Development* **131,** 1741-53.

Heasman, J. (2006). Patterning the early Xenopus embryo. *Development* **133,** 1205-17.

Heasman, J., Crawford, A., Goldstone, K., Garner-Hamrick, P., Gumbiner, B., McCrea, P., Kintner, C., Noro, C. Y., and Wylie, C. (1994). Overexpression of cadherins and underexpression of beta-catenin inhibit dorsal mesoderm induction in early Xenopus embryos. *Cell* **79,** 791-803.

Heasman, J., Kofron, M., and Wylie, C. (2000). Beta-catenin signaling activity dissected in the early Xenopus embryo: a novel antisense approach. *Dev Biol* **222,** 124-34.

Heisenberg, C. P., Houart, C., Take-Uchi, M., Rauch, G. J., Young, N., Coutinho, P., Masai, I., Caneparo, L., Concha, M. L., Geisler, R., Dale, T. C., Wilson, S. W., and Stemple,

D. L. (2001). A mutation in the Gsk3-binding domain of zebrafish Masterblind/Axin1 leads to a fate transformation of telencephalon and eyes to diencephalon. *Genes Dev* **15,** 1427-34.

Hemmati-Brivanlou, A., Kelly, O. G., and Melton, D. A. (1994). Follistatin, an antagonist of activin, is expressed in the Spemann organizer and displays direct neuralizing activity. *Cell* **77,** 283-95.

Hemmati-Brivanlou, A., and Melton, D. A. (1992). A truncated activin receptor inhibits mesoderm induction and formation of axial structures in Xenopus embryos. *Nature* **359,** 609-14.

Hess, K., Steinbeisser, H., Kurth, T., and Epperlein, H. H. (2007). Bone morphogenetic protein-4 and Noggin signaling regulates pigment cell distribution in the axolotl trunk. *Differentiation*.

Hino, J., Nishimatsu, S., Nagai, T., Matsuo, H., Kangawa, K., and Nohno, T. (2003). Coordination of BMP-3b and cerberus is required for head formation of Xenopus embryos. *Dev Biol* **260,** 138-57.

Hoppler, S., Brown, J. D., and Moon, R. T. (1996). Expression of a dominant-negative Wnt blocks induction of MyoD in Xenopus embryos. *Genes Dev* **10,** 2805-17.

Hume, C. R., and Dodd, J. (1993). Cwnt-8C: a novel Wnt gene with a potential role in primitive streak formation and hindbrain organization. *Development* **119,** 1147-60.

Iemura, S., Yamamoto, T. S., Takagi, C., Uchiyama, H., Natsume, T., Shimasaki, S., Sugino, H., and Ueno, N. (1998). Direct binding of follistatin to a complex of bone-morphogenetic protein and its receptor inhibits ventral and epidermal cell fates in early Xenopus embryo. *Proc Natl Acad Sci U S A* **95,** 9337-42.

Jen, W. C., Wettstein, D., Turner, D., Chitnis, A., and Kintner, C. (1997). The Notch ligand, X-Delta-2, mediates segmentation of the paraxial mesoderm in Xenopus embryos. *Development* **124,** 1169-78.

Jones, C. M., Broadbent, J., Thomas, P. Q., Smith, J. C., and Beddington, R. S. (1999). An anterior signalling centre in Xenopus revealed by the homeobox gene XHex. *Curr Biol* **9,** 946-54.

Jones, C. M., Kuehn, M. R., Hogan, B. L., Smith, J. C., and Wright, C. V. (1995). Nodal-related signals induce axial mesoderm and dorsalize mesoderm during gastrulation. *Development* **121,** 3651-62.

Jones, E. A., and Woodland, H. R. (1987). The development of animal cap cells in Xenopus: a measure of the start of animal cap competence to form mesoderm. *Development* **101,** 557-563.

Joubin, K., and Stern, C. D. (2001). Formation and maintenance of the organizer among the vertebrates. *Int J Dev Biol* **45,** 165-75.

Kawano, Y., and Kypta, R. (2003). Secreted antagonists of the Wnt signalling pathway. *J Cell Sci* **116,** 2627-34.

Kazanskaya, O., Glinka, A., and Niehrs, C. (2000). The role of Xenopus dickkopf1 in prechordal plate specification and neural patterning. *Development* **127,** 4981-92.

Keller, R. (2000). The origin and morphogenesis of amphibian somites. *Curr Top Dev Biol* **47,** 183-246.

Keller, R. (2005). Cell migration during gastrulation. *Curr Opin Cell Biol* **17,** 533-41.

Keller, R., Davidson, L. A., and Shook, D. R. (2003). How we are shaped: the biomechanics of gastrulation. *Differentiation* **71,** 171-205.

Keller, R., and Shook, D. (2004). Gastrulation in Amphibians. *In* "Gastrulation : from cells to embryo" (C. D. Stern, Ed.), pp. 171-203. Cold Spring Harbor Laboratory Press, Cold Spring Harbor, N.Y.

Kessler, D. S., and Melton, D. A. (1995). Induction of dorsal mesoderm by soluble, mature Vg1 protein. *Development* **121,** 2155-64.

Khaner, O., and Eyal-Giladi, H. (1989). The chick's marginal zone and primitive streak formation. I. Coordinative effect of induction and inhibition. *Dev Biol* **134,** 206-14.

Khokha, M. K., Yeh, J., Grammer, T. C., and Harland, R. M. (2005). Depletion of three BMP antagonists from Spemann's organizer leads to a catastrophic loss of dorsal structures. *Dev Cell* **8,** 401-11.

Kim, C. H., Oda, T., Itoh, M., Jiang, D., Artinger, K. B., Chandrasekharappa, S. C., Driever, W., and Chitnis, A. B. (2000). Repressor activity of Headless/Tcf3 is essential for vertebrate head formation. *Nature* **407,** 913-6.

Kimelman, D., and Bjornson, C. (2004). Vertebrate mesoderm induction: From frogs to mice *In* "Gastrulation: From Cells to Embryo" (C. D. Stern, Ed.), pp. 363-372. Cold Spring Harbor Press., New York.

Kimura, C., Yoshinaga, K., Tian, E., Suzuki, M., Aizawa, S., and Matsuo, I. (2000). Visceral endoderm mediates forebrain development by suppressing posteriorizing signals. *Dev Biol* **225,** 304-21.

Knoetgen, H., Viebahn, C., and Kessel, M. (1999). Head induction in the chick by primitive endoderm of mammalian, but not avian origin. *Development* **126,** 815-25.

Kobel, H. R., and Du Pasquier, L. (1986). Genetics of polyploid Xenopus. *Trends in Genetics* **2,** 310-315.

Kofron, M., Demel, T., Xanthos, J., Lohr, J., Sun, B., Sive, H., Osada, S., Wright, C., Wylie, C., and Heasman, J. (1999). Mesoderm induction in Xenopus is a zygotic event regulated by maternal VegT via TGFbeta growth factors. *Development* **126,** 5759-70.

Ku, M., and Melton, D. A. (1993). Xwnt-11: a maternally expressed Xenopus wnt gene. *Development* **119,** 1161-73.

Kuroda, H., Wessely, O., and De Robertis, E. M. (2004). Neural induction in Xenopus: requirement for ectodermal and endomesodermal signals via Chordin, Noggin, beta-Catenin, and Cerberus. *PLoS Biol* **2,** E92.

Kurth, T. (2005). A cell cycle arrest is necessary for bottle cell formation in the early Xenopus gastrula: integrating cell shape change, local mitotic control and mesodermal patterning. *Mech Dev* **122,** 1251-65.

LaBonne, C., and Whitman, M. (1994). Mesoderm induction by activin requires FGF-mediated intracellular signals. *Development* **120,** 463-72.

Lawson, A., Colas, J. F., and Schoenwolf, G. C. (2001). Classification scheme for genes expressed during formation and progression of the avian primitive streak. *Anat Rec* **262,** 221-6.

Lee, H. X., Ambrosio, A. L., Reversade, B., and De Robertis, E. M. (2006). Embryonic dorsal-ventral signaling: secreted frizzled-related proteins as inhibitors of tolloid proteinases. *Cell* **124,** 147-59.

Lemaire, P., and Kodjabachian, L. (1996). The vertebrate organizer: structure and molecules. *Trends Genet* **12,** 525-31.

Leyns, L., Bouwmeester, T., Kim, S. H., Piccolo, S., and De Robertis, E. M. (1997). Frzb-1 is a secreted antagonist of Wnt signaling expressed in the Spemann organizer. *Cell* **88,** 747-56.

Liu, P., Wakamiya, M., Shea, M. J., Albrecht, U., Behringer, R. R., and Bradley, A. (1999). Requirement for Wnt3 in vertebrate axis formation. *Nat Genet* **22,** 361-5.

Lupo, G., Harris, W. A., Barsacchi, G., and Vignali, R. (2002). Induction and patterning of the telencephalon in Xenopus laevis. *Development* **129,** 5421-36.

Lustig, K. D., Kroll, K. L., Sun, E. E., and Kirschner, M. W. (1996). Expression cloning of a Xenopus T-related gene (Xombi) involved in mesodermal patterning and blastopore lip formation. *Development* **122,** 4001-12.

Mancilla, A., and Mayor, R. (1996). Neural crest formation in Xenopus laevis: mechanisms of Xslug induction. *Dev Biol* **177,** 580-9.

Mangold, H. (1933). Über die Induktionsfähighkeit der verschiedenen Bezirke der Neurula von Urodelen. *Naturwissenshaften* **21,** 761-766.

Mao, B., Wu, W., Davidson, G., Marhold, J., Li, M., Mechler, B. M., Delius, H., Hoppe, D., Stannek, P., Walter, C., Glinka, A., and Niehrs, C. (2002). Kremen proteins are Dickkopf receptors that regulate Wnt/beta-catenin signalling. *Nature* **417,** 664-7.

Mao, B., Wu, W., Li, Y., Hoppe, D., Stannek, P., Glinka, A., and Niehrs, C. (2001). LDL-receptor-related protein 6 is a receptor for Dickkopf proteins. *Nature* **411,** 321-5.

Marikawa, Y., and Elinson, R. P. (1999). Relationship of vegetal cortical dorsal factors in the Xenopus egg with the Wnt/beta-catenin signaling pathway. *Mech Dev* **89,** 93-102.

Marques, S., Borges, A. C., Silva, A. C., Freitas, S., Cordenonsi, M., and Belo, J. A. (2004). The activity of the Nodal antagonist Cerl-2 in the mouse node is required for correct L/R body axis. *Genes Dev* **18,** 2342-7.

Martinez-Barbera, J. P., and Beddington, R. S. (2001). Getting your head around Hex and Hesx1: forebrain formation in mouse. *Int J Dev Biol* **45,** 327-36.

Martinez-Barbera, J. P., Rodriguez, T. A., and Beddington, R. S. (2000). The homeobox gene Hesx1 is required in the anterior neural ectoderm for normal forebrain formation. *Dev Biol* **223,** 422-30.

Martinez Barbera, J. P., Clements, M., Thomas, P., Rodriguez, T., Meloy, D., Kioussis, D., and Beddington, R. S. (2000). The homeobox gene Hex is required in definitive endodermal tissues for normal forebrain, liver and thyroid formation. *Development* **127,** 2433-45.

McMahon, J. A., Takada, S., Zimmerman, L. B., Fan, C. M., Harland, R. M., and McMahon, A. P. (1998). Noggin-mediated antagonism of BMP signaling is required for growth and patterning of the neural tube and somite. *Genes Dev* **12,** 1438-52.

Meno, C., Gritsman, K., Ohishi, S., Ohfuji, Y., Heckscher, E., Mochida, K., Shimono, A., Kondoh, H., Talbot, W. S., Robertson, E. J., Schier, A. F., and Hamada, H. (1999). Mouse Lefty2 and zebrafish antivin are feedback inhibitors of nodal signaling during vertebrate gastrulation. *Mol Cell* **4,** 287-98.

Meno, C., Shimono, A., Saijoh, Y., Yashiro, K., Mochida, K., Ohishi, S., Noji, S., Kondoh, H., and Hamada, H. (1998). lefty-1 is required for left-right determination as a regulator of lefty-2 and nodal. *Cell* **94,** 287-97.

Michiue, T., and Asashima, M. (2005). Temporal and spatial manipulation of gene expression in Xenopus embryos by injection of heat shock promoter-containing plasmids. *Dev Dyn* **232,** 369-76.

Miller, J. R., Rowning, B. A., Larabell, C. A., Yang-Snyder, J. A., Bates, R. L., and Moon, R. T. (1999). Establishment of the dorsal-ventral axis in Xenopus embryos coincides with the dorsal enrichment of dishevelled that is dependent on cortical rotation. *J Cell Biol* **146,** 427-37.

Mishina, Y., Suzuki, A., Ueno, N., and Behringer, R. R. (1995). Bmpr encodes a type I bone morphogenetic protein receptor that is essential for gastrulation during mouse embryogenesis. *Genes Dev* **9,** 3027-37.

Mizuno, T., Yamaha, E., Wakahara, M., Kuroiwa, A., and Takeda, H. (1996). Mesoderm induction in zebrafish. *Nature* **383,** 131-132.

Moon, R. T., Campbell, R. M., Christian, J. L., McGrew, L. L., Shih, J., and Fraser, S. (1993). Xwnt-5A: a maternal Wnt that affects morphogenetic movements after overexpression in embryos of Xenopus laevis. *Development* **119,** 97-111.

Moon, R. T., and Kimelman, D. (1998). From cortical rotation to organizer gene expression: toward a molecular explanation of axis specification in Xenopus. *Bioessays* **20,** 536-45.

Moore, K. B., Mood, K., Daar, I. O., and Moody, S. A. (2004). Morphogenetic movements underlying eye field formation require interactions between the FGF and ephrinB1 signaling pathways. *Dev Cell* **6,** 55-67.

Morales, A. V., Yasuda, Y., and Ish-Horowicz, D. (2002). Periodic Lunatic fringe expression is controlled during segmentation by a cyclic transcriptional enhancer responsive to notch signaling. *Dev Cell* **3,** 63-74.

Moreno, T. A., and Kintner, C. (2004). Regulation of segmental patterning by retinoic acid signaling during Xenopus somitogenesis. *Dev Cell* **6,** 205-18.

Morimoto, M., Takahashi, Y., Endo, M., and Saga, Y. (2005). The Mesp2 transcription factor establishes segmental borders by suppressing Notch activity. *Nature* **435,** 354-9.

Moser, M., Binder, O., Wu, Y., Aitsebaomo, J., Ren, R., Bode, C., Bautch, V. L., Conlon, F. L., and Patterson, C. (2003). BMPER, a novel endothelial cell precursor-derived protein, antagonizes bone morphogenetic protein signaling and endothelial cell differentiation. *Mol Cell Biol* **23,** 5664-79.

Mukhopadhyay, M., Shtrom, S., Rodriguez-Esteban, C., Chen, L., Tsukui, T., Gomer, L., Dorward, D. W., Glinka, A., Grinberg, A., Huang, S. P., Niehrs, C., Belmonte, J. C., and Westphal, H. (2001). Dickkopf1 is required for embryonic head induction and limb morphogenesis in the mouse. *Dev Cell* **1,** 423-34.

Nagano, T., Takehara, S., Takahashi, M., Aizawa, S., and Yamamoto, A. (2006). Shisa2 promotes the maturation of somitic precursors and transition to the segmental fate in Xenopus embryos. *Development* **133,** 4643-54.

Nambiar, R. M., and Henion, P. D. (2004). Sequential antagonism of early and late Wnt-signaling by zebrafish colgate promotes dorsal and anterior fates. *Dev Biol* **267,** 165-80.

Niehrs, C. (1999). Head in the WNT: the molecular nature of Spemann's head organizer. *Trends Genet* **15,** 314-9.

Niehrs, C. (2004). Regionally specific induction by the Spemann-Mangold organizer. *Nat Rev Genet* **5,** 425-34.

Nieuwkoop, P. D. (1969a). "The formation of the mesoderm in urodelean amphibians. I. Induction by the endoderm."

Nieuwkoop, P. D. (1969b). "The formation of mesoderm in urodelean amphibians. II. The origin of the dorso-ventral polarity of the mesoderm. ."

Nieuwkoop, P. D., and Ubbels, G. A. (1972). "The formation of mesoderm in urodelean amphibians. IV. Quantitative evidence for the purely "ectodermal" origin of the entire mesoderm and of the pharyngeal endoderm."

Nishita, M., Hashimoto, M. K., Ogata, S., Laurent, M. N., Ueno, N., Shibuya, H., and Cho, K. W. (2000). Interaction between Wnt and TGF-beta signalling pathways during formation of Spemann's organizer. *Nature* **403,** 781-5.

Oelgeschlager, M., Kuroda, H., Reversade, B., and De Robertis, E. M. (2003). Chordin is required for the Spemann organizer transplantation phenomenon in Xenopus embryos. *Dev Cell* **4,** 219-30.

Onichtchouk, D., Chen, Y. G., Dosch, R., Gawantka, V., Delius, H., Massague, J., and Niehrs, C. (1999). Silencing of TGF-beta signalling by the pseudoreceptor BAMBI. *Nature* **401,** 480-5.

Oulad-Abdelghani, M., Chazaud, C., Bouillet, P., Mattei, M. G., Dolle, P., and Chambon, P. (1998). Stra3/lefty, a retinoic acid-inducible novel member of the transforming growth factor-beta superfamily. *Int J Dev Biol* **42,** 23-32.

Pandur, P., Maurus, D., and Kuhl, M. (2002). Increasingly complex: new players enter the Wnt signaling network. *Bioessays* **24,** 881-4.

Park, T. J., Haigo, S. L., and Wallingford, J. B. (2006). Ciliogenesis defects in embryos lacking inturned or fuzzy function are associated with failure of planar cell polarity and Hedgehog signaling. *Nat Genet* **38,** 303-11.

Pera, E. M., and De Robertis, E. M. (2000). A direct screen for secreted proteins in Xenopus embryos identifies distinct activities for the Wnt antagonists Crescent and Frzb-1. *Mech Dev* **96,** 183-95.

Perea-Gomez, A., Lawson, K. A., Rhinn, M., Zakin, L., Brulet, P., Mazan, S., and Ang, S. L. (2001a). Otx2 is required for visceral endoderm movement and for the restriction of posterior signals in the epiblast of the mouse embryo. *Development* **128,** 753-65.

Perea-Gomez, A., Rhinn, M., and Ang, S. L. (2001b). Role of the anterior visceral endoderm in restricting posterior signals in the mouse embryo. *Int J Dev Biol* **45,** 311-20.

Perea-Gomez, A., Shawlot, W., Sasaki, H., Behringer, R. R., and Ang, S. (1999). HNF3beta and Lim1 interact in the visceral endoderm to regulate primitive streak formation and anterior-posterior polarity in the mouse embryo. *Development* **126,** 4499-511.

Perea-Gomez, A., Vella, F. D., Shawlot, W., Oulad-Abdelghani, M., Chazaud, C., Meno, C., Pfister, V., Chen, L., Robertson, E., Hamada, H., Behringer, R. R., and Ang, S. L. (2002). Nodal antagonists in the anterior visceral endoderm prevent the formation of multiple primitive streaks. *Dev Cell* **3,** 745-56.

Piccolo, S., Agius, E., Leyns, L., Bhattacharyya, S., Grunz, H., Bouwmeester, T., and De Robertis, E. M. (1999). The head inducer Cerberus is a multifunctional antagonist of Nodal, BMP and Wnt signals. *Nature* **397,** 707-10.

Piccolo, S., Agius, E., Lu, B., Goodman, S., Dale, L., and De Robertis, E. M. (1997). Cleavage of Chordin by Xolloid metalloprotease suggests a role for proteolytic processing in the regulation of Spemann organizer activity. *Cell* **91,** 407-16.

Piccolo, S., Sasai, Y., Lu, B., and De Robertis, E. M. (1996). Dorsoventral patterning in Xenopus: inhibition of ventral signals by direct binding of chordin to BMP-4. *Cell* **86,** 589-98.

Popperl, H., Schmidt, C., Wilson, V., Hume, C. R., Dodd, J., Krumlauf, R., and Beddington, R. S. (1997). Misexpression of Cwnt8C in the mouse induces an ectopic embryonic axis and causes a truncation of the anterior neuroectoderm. *Development* **124,** 2997-3005.

Pourquie, O. (2001). Vertebrate somitogenesis. *Annu Rev Cell Dev Biol* **17,** 311-50.

Pourquie, O. (2003). Vertebrate somitogenesis: a novel paradigm for animal segmentation? *Int J Dev Biol* **47,** 597-603.

Reversade, B., and De Robertis, E. M. (2005). Regulation of ADMP and BMP2/4/7 at opposite embryonic poles generates a self-regulating morphogenetic field. *Cell* **123,** 1147-60.

Rhinn, M., Dierich, A., Shawlot, W., Behringer, R. R., Le Meur, M., and Ang, S. L. (1998). Sequential roles for Otx2 in visceral endoderm and neuroectoderm for forebrain and midbrain induction and specification. *Development* **125,** 845-56.

Rivera-Perez, J. A., Mallo, M., Gendron-Maguire, M., Gridley, T., and Behringer, R. R. (1995). Goosecoid is not an essential component of the mouse gastrula organizer but is required for craniofacial and rib development. *Development* **121,** 3005-12.

Rodaway, A., Takeda, H., Koshida, S., Broadbent, J., Price, B., Smith, J. C., Patient, R., and Holder, N. (1999). Induction of the mesendoderm in the zebrafish germ ring by yolk cell-derived TGF-beta family signals and discrimination of mesoderm and endoderm by FGF. *Development* **126,** 3067-78.

Rodriguez Esteban, C., Capdevila, J., Economides, A. N., Pascual, J., Ortiz, A., and Izpisua Belmonte, J. C. (1999). The novel Cer-like protein Caronte mediates the establishment of embryonic left-right asymmetry. *Nature* **401,** 243-51.

Roeser, T., Stein, S., and Kessel, M. (1999). Nuclear beta-catenin and the development of bilateral symmetry in normal and LiCl-exposed chick embryos. *Development* **126,** 2955-65.

Salic, A. N., Kroll, K. L., Evans, L. M., and Kirschner, M. W. (1997). Sizzled: a secreted Xwnt8 antagonist expressed in the ventral marginal zone of Xenopus embryos. *Development* **124,** 4739-48.

Sasai, Y., Lu, B., Steinbeisser, H., Geissert, D., Gont, L. K., and De Robertis, E. M. (1994). Xenopus chordin: a novel dorsalizing factor activated by organizer-specific homeobox genes. *Cell* **79,** 779-90.

Schneider, V. A., and Mercola, M. (1999). Spatially distinct head and heart inducers within the Xenopus organizer region. *Curr Biol* **9,** 800-9.

Schneider, V. A., and Mercola, M. (2001). Wnt antagonism initiates cardiogenesis in Xenopus laevis. *Genes Dev* **15,** 304-15.

Schroeder, K. E., Condic, M. L., Eisenberg, L. M., and Yost, H. J. (1999). Spatially regulated translation in embryos: asymmetric expression of maternal Wnt-11 along the dorsal-ventral axis in Xenopus. *Dev Biol* **214,** 288-97.

Schulte-Merker, S., Lee, K. J., McMahon, A. P., and Hammerschmidt, M. (1997). The zebrafish organizer requires chordino. *Nature* **387,** 862-3.

Seleiro, E. A., Connolly, D. J., and Cooke, J. (1996). Early developmental expression and experimental axis determination by the chicken Vg1 gene. *Curr Biol* **6,** 1476-86.

Shah, S. B., Skromne, I., Hume, C. R., Kessler, D. S., Lee, K. J., Stern, C. D., and Dodd, J. (1997). Misexpression of chick Vg1 in the marginal zone induces primitive streak formation. *Development* **124,** 5127-38.

Shawlot, W., Deng, J. M., and Behringer, R. R. (1998). Expression of the mouse cerberus-related gene, Cerr1, suggests a role in anterior neural induction and somitogenesis. *Proc Natl Acad Sci U S A* **95,** 6198-203.

Shawlot, W., Min Deng, J., Wakamiya, M., and Behringer, R. R. (2000). The cerberus-related gene, Cerr1, is not essential for mouse head formation. *Genesis* **26,** 253-8.

Shawlot, W., Wakamiya, M., Kwan, K. M., Kania, A., Jessell, T. M., and Behringer, R. R. (1999). Lim1 is required in both primitive streak-derived tissues and visceral endoderm for head formation in the mouse. *Development* **126,** 4925-32.

Silva, A. C., Filipe, M., Kuerner, K. M., Steinbeisser, H., and Belo, J. A. (2003). Endogenous Cerberus activity is required for anterior head specification in Xenopus. *Development* **130,** 4943-53.

Silva, A. C., Filipe, M., Vitorino, M., Steinbeisser, H., and Belo, J. A. (2006). Developmental expression of Shisa-2 in Xenopus laevis. *Int J Dev Biol* **50,** 575-9.

Skromne, I., and Stern, C. D. (2001). Interactions between Wnt and Vg1 signalling pathways initiate primitive streak formation in the chick embryo. *Development* **128,** 2915-27.

Smith, A. N., Miller, L. A., Song, N., Taketo, M. M., and Lang, R. A. (2005). The duality of beta-catenin function: a requirement in lens morphogenesis and signaling suppression of lens fate in periocular ectoderm. *Dev Biol* **285,** 477-89.

Smith, J. C., and Slack, J. M. (1983). Dorsalization and neural induction: properties of the organizer in Xenopus laevis. *J Embryol Exp Morphol* **78,** 299-317.

Smith, W. C., and Harland, R. M. (1992). Expression cloning of noggin, a new dorsalizing factor localized to the Spemann organizer in Xenopus embryos. *Cell* **70,** 829-40.

Spemann, H. (1931). "Über den Anteil von Implantat und Wirtskeim an der Orientierung und Beschaffenheit der induzierten Embryonalanlage. ."

Spemann, H. (1938). "Embryonic Development and Induction." Yale University Press, Yale.

Spemann, H., and Mangold, H. (2001). Induction of embryonic primordia by implantation of organizers from a different species. 1923. *Int J Dev Biol* **45,** 13-38.

Stennard, F., Carnac, G., and Gurdon, J. B. (1996). The Xenopus T-box gene, Antipodean, encodes a vegetally localised maternal mRNA and can trigger mesoderm formation. *Development* **122,** 4179-88.

Stern, C. D. (2000). Conrad H. Waddington's contributions to avian and mammalian development, 1930-1940. *Int J Dev Biol* **44,** 15-22.

Stern, C. D. (2005). Neural induction: old problem, new findings, yet more questions. *Development* **132,** 2007-21.

Stern, C. D. (2006). Neural induction: 10 years on since the 'default model'. *Curr Opin Cell Biol* **18,** 692-7.

Stern, C. D., Yu, R. T., Kakizuka, A., Kintner, C. R., Mathews, L. S., Vale, W. W., Evans, R. M., and Umesono, K. (1995). Activin and its receptors during gastrulation and the later phases of mesoderm development in the chick embryo. *Dev Biol* **172,** 192-205.

Sun, X., Meyers, E. N., Lewandoski, M., and Martin, G. R. (1999). Targeted disruption of Fgf8 causes failure of cell migration in the gastrulating mouse embryo. *Genes Dev* **13,** 1834-46.

Tao, Q., Yokota, C., Puck, H., Kofron, M., Birsoy, B., Yan, D., Asashima, M., Wylie, C. C., Lin, X., and Heasman, J. (2005). Maternal wnt11 activates the canonical wnt signaling pathway required for axis formation in Xenopus embryos. *Cell* **120,** 857-71.

Tavares, A. T., Andrade, S., Silva, A. C., and Belo, J. A. (2007). Cerberus is a feedback inhibitor of Nodal asymmetric signaling in the chick embryo. *Development* **134,** 2051-60.

Thomas, P., and Beddington, R. (1996). Anterior primitive endoderm may be responsible for patterning the anterior neural plate in the mouse embryo. *Curr Biol* **6,** 1487-96.

Thomas, P. Q., Brown, A., and Beddington, R. S. (1998). Hex: a homeobox gene revealing peri-implantation asymmetry in the mouse embryo and an early transient marker of endothelial cell precursors. *Development* **125,** 85-94.

Varlet, I., Collignon, J., and Robertson, E. J. (1997). nodal expression in the primitive endoderm is required for specification of the anterior axis during mouse gastrulation. *Development* **124,** 1033-44.

Vermot, J., and Pourquie, O. (2005). Retinoic acid coordinates somitogenesis and left-right patterning in vertebrate embryos. *Nature* **435,** 215-20.

Vincent, S. D., Dunn, N. R., Hayashi, S., Norris, D. P., and Robertson, E. J. (2003). Cell fate decisions within the mouse organizer are governed by graded Nodal signals. *Genes Dev* **17,** 1646-62.

Wall, N. A., Craig, E. J., Labosky, P. A., and Kessler, D. S. (2000). Mesendoderm induction and reversal of left-right pattern by mouse Gdf1, a Vg1-related gene. *Dev Biol* **227,** 495-509.

Wallingford, J. B. (2005). Neural tube closure and neural tube defects: studies in animal models reveal known knowns and known unknowns. *Am J Med Genet C Semin Med Genet* **135,** 59-68.

Wallingford, J. B. (2006). Planar cell polarity, ciliogenesis and neural tube defects. *Hum Mol Genet* **15 Spec No 2,** R227-34.

Wallingford, J. B., and Harland, R. M. (2002). Neural tube closure requires Dishevelled-dependent convergent extension of the midline. *Development* **129,** 5815-25.

Wang, S., Krinks, M., and Moos, M., Jr. (1997). Frzb-1, an antagonist of Wnt-1 and Wnt-8, does not block signaling by Wnts -3A, -5A, or -11. *Biochem Biophys Res Commun* **236,** 502-4.

Wardle, F. C., Welch, J. V., and Dale, L. (1999). Bone morphogenetic protein 1 regulates dorsal-ventral patterning in early Xenopus embryos by degrading chordin, a BMP4 antagonist. *Mech Dev* **86,** 75-85.

Watabe, T., Kim, S., Candia, A., Rothbacher, U., Hashimoto, C., Inoue, K., and Cho, K. W. (1995). Molecular mechanisms of Spemann's organizer formation: conserved growth factor synergy between Xenopus and mouse. *Genes Dev* **9,** 3038-50.

Weaver, C., Farr, G. H., 3rd, Pan, W., Rowning, B. A., Wang, J., Mao, J., Wu, D., Li, L., Larabell, C. A., and Kimelman, D. (2003). GBP binds kinesin light chain and translocates during cortical rotation in Xenopus eggs. *Development* **130,** 5425-36.

Weaver, C., and Kimelman, D. (2004). Move it or lose it: axis specification in Xenopus. *Development* **131,** 3491-9.

Wessely, O., Agius, E., Oelgeschlager, M., Pera, E. M., and De Robertis, E. M. (2001). Neural induction in the absence of mesoderm: beta-catenin-dependent expression of secreted BMP antagonists at the blastula stage in Xenopus. *Dev Biol* **234,** 161-73.

Winnier, G., Blessing, M., Labosky, P. A., and Hogan, B. L. (1995). Bone morphogenetic protein-4 is required for mesoderm formation and patterning in the mouse. *Genes Dev* **9,** 2105-16.

Xanthos, J. B., Kofron, M., Wylie, C., and Heasman, J. (2001). Maternal VegT is the initiator of a molecular network specifying endoderm in Xenopus laevis. *Development* **128,** 167-80.

Yabe, T., Shimizu, T., Muraoka, O., Bae, Y. K., Hirata, T., Nojima, H., Kawakami, A., Hirano, T., and Hibi, M. (2003). Ogon/Secreted Frizzled functions as a negative feedback regulator of Bmp signaling. *Development* **130,** 2705-16.

Yamaguchi, T. P., Harpal, K., Henkemeyer, M., and Rossant, J. (1994). fgfr-1 is required for embryonic growth and mesodermal patterning during mouse gastrulation. *Genes Dev* **8,** 3032-44.

Yamaguchi, T. P., Takada, S., Yoshikawa, Y., Wu, N., and McMahon, A. P. (1999). T (Brachyury) is a direct target of Wnt3a during paraxial mesoderm specification. *Genes Dev* **13,** 3185-90.

Yamamoto, A., Nagano, T., Takehara, S., Hibi, M., and Aizawa, S. (2005). Shisa promotes head formation through the inhibition of receptor protein maturation for the caudalizing factors, Wnt and FGF. *Cell* **120,** 223-35.

Yamamoto, M., Saijoh, Y., Perea-Gomez, A., Shawlot, W., Behringer, R. R., Ang, S. L., Hamada, H., and Meno, C. (2004). Nodal antagonists regulate formation of the anteroposterior axis of the mouse embryo. *Nature* **428,** 387-92.

Yang, J., Mei, W., Otto, A., Xiao, L., Tao, Q., Geng, X., Rupp, R. A., and Ding, X. (2002). Repression through a distal TCF-3 binding site restricts Xenopus myf-5 expression in gastrula mesoderm. *Mech Dev* **115,** 79-89.

Yokota, C., Kofron, M., Zuck, M., Houston, D. W., Isaacs, H., Asashima, M., Wylie, C. C., and Heasman, J. (2003). A novel role for a nodal-related protein; Xnr3 regulates convergent extension movements via the FGF receptor. *Development* **130,** 2199-212.

Yokouchi, Y., Vogan, K. J., Pearse, R. V., 2nd, and Tabin, C. J. (1999). Antagonistic signaling by Caronte, a novel Cerberus-related gene, establishes left-right asymmetric gene expression. *Cell* **98,** 573-83.

Zeng, L., Fagotto, F., Zhang, T., Hsu, W., Vasicek, T. J., Perry, W. L., 3rd, Lee, J. J., Tilghman, S. M., Gumbiner, B. M., and Costantini, F. (1997). The mouse Fused locus encodes Axin, an inhibitor of the Wnt signaling pathway that regulates embryonic axis formation. *Cell* **90,** 181-92.

Zhang, J., Houston, D. W., King, M. L., Payne, C., Wylie, C., and Heasman, J. (1998). The role of maternal VegT in establishing the primary germ layers in Xenopus embryos. *Cell* **94,** 515-24.

Zhang, J., and King, M. L. (1996). Xenopus VegT RNA is localized to the vegetal cortex during oogenesis and encodes a novel T-box transcription factor involved in mesodermal patterning. *Development* **122,** 4119-29.

Zhu, L., Marvin, M. J., Gardiner, A., Lassar, A. B., Mercola, M., Stern, C. D., and Levin, M. (1999). Cerberus regulates left-right asymmetry of the embryonic head and heart. *Curr Biol* **9,** 931-8.

Zimmerman, L. B., De Jesus-Escobar, J. M., and Harland, R. M. (1996). The Spemann organizer signal noggin binds and inactivates bone morphogenetic protein 4. *Cell* **86,** 599-606.

Zorn, A. M., Butler, K., and Gurdon, J. B. (1999). Anterior endomesoderm specification in Xenopus by Wnt/beta-catenin and TGF-beta signalling pathways. *Dev Biol* **209,** 282-97.

Appendix

In the course of this thesis I have collaborated in other studies that were not included in this thesis due to the fact that those studies were not directly related to the main aim of this thesis and my contribution to those studies although relevant was small. However, I decided to include them in the Appendix of this thesis.

In 2004, I have collaborated in the study intituled "The activity of the Nodal antagonist Cerl-2 in the mouse node is required for correct L/R body axis" (Gene Dev, 18:2342–2347, 2006). For this project I have provided data to show the inhibitory effects of Cerberus-like2 on Nodal and BMP signaling and participated in the writing of the paper.

I have also participated in the study intituled "Identification of alternative promoter usage for the matrix Gla protein gene" (FEBS J. 272(6):1501-10, 2006). For this study I performed RT-PCR and Southern Blot to show the temporal expression of *XlMGP* transcripts during early Xenopus development. I did in situ hybridization for *XlMGP* to determine its localization during embryogenesis and I also performed luciferase assays to show if either or both *XlMGP* transcripts are present during gastrulation. I helped in writing the paper.

Finally I have performed *Xenopus* animal cap luciferase assays to test the activity of several luciferase reporter constructs containing wild-type or mutant fragments of *cCer* regulatory sequences in the presence and absence of Nodal. This work is included in the study intituled "Cerberus is a feedback inhibitor of Nodal asymmetric signaling in the chick embryo" (Development 134, 2051-2060, 2007).

The activity of the Nodal antagonist *Cerl-2* in the mouse node is required for correct L/R body axis

Sara Marques,[1] Ana Cristina Borges,[1,2]
Ana Cristina Silva,[1,2] Sandra Freitas,[1]
Michelangelo Cordenonsi,[3] and
José António Belo[1,2,4]

[1]Instituto Gulbenkian de Ciência, 2781-901 Oeiras, Portugal;
[2]Centro de Biomedicina Molecular e Estrutural, Universidade do Algarve, Campus de Gambelas, 8000-010 Faro, Portugal;
[3]Department of Histology, Microbiology, and Medical Biotechnologies, Section of Histology and Embryology, University of Padua, 35121 Padua, Italy

Correct establishment of the left/right (L/R) body asymmetry in the mouse embryo requires asymmetric activation of the evolutionarily conserved *Nodal* signaling cascade in the left lateral plate mesoderm (L-LPM). Furthermore, the presence of Nodal in the node is essential for its own expression in the L-LPM. Here, we have characterized the function of *cerl-2*, a novel Nodal antagonist, which displays a unique asymmetric expression on the right side of the mouse node. *cerl-2* knockout mice display multiple laterality defects including randomization of the L/R axis. These defects can be partially rescued by removing one *nodal* allele. Our results demonstrate that Cerl-2 plays a key role in restricting the Nodal signaling pathway toward the left side of the mouse embryo by preventing its activity in the right side.

Development of the internal organs proceeds across the left/right (L/R) axis and becomes apparent during organogenesis as a result of asymmetric activation of the conserved *Nodal* signaling cascade in the left lateral plate mesoderm (L-LPM) (for review, see Beddington and Robertson 1999; Capdevila et al. 2000; Hamada et al. 2002). Nodal signaling is a crucial player in the correct establishment of the vertebrate L/R body axis (Capdevila et al. 2000; Wright 2001; Hamada et al. 2002). *Nodal* expression in the perinodal region of the embryonic day 7.0 (E7.0) mouse embryo has been shown to be required for its own activation in L-LPM and thus generate the asymmetric expression of *Nodal*'s downstream genes (Brennan et al. 2002; Saijoh et al. 2003). Leftward flow in the mouse node (nodal flow) generated by specialized cilia

255

(Nonaka et al. 1998) and intracellular calcium signaling (McGrath et al. 2003) has been recently implicated in the initial steps of lateralization. However, the exact mechanism behind the asymmetric Nodal activity in the node remains largely unexplained (for review, see Hamada et al. 2002).

We have identified a novel *Cerberus/Dan* family member, mouse *cerberus-like2* (*cerl-2*), that is asymmetrically expressed on the right side of the node. *cerl-2* encodes a secreted protein with the capability to bind directly to Nodal and to inhibit its signaling pathway in *Xenopus* assays. Inactivation of mouse *cerl-2* resulted in a wide range of laterality defects including randomization of *Nodal* expression domain in the LPM. These findings are consistent with an important role of *cerl-2* in early events of L/R axis specification. In addition, the observed abnormalities can be partially rescued by the removal of one *Nodal* allele. Our results demonstrate that Nodal antagonism in the node, mediated by Cerl-2, is essential for proper specification of the mouse L/R axis.

Results and Discussion

Using a sequence-similarity-based search, we identified an incomplete EST sequence (GenBank accession no. AA289243), later also designated *Dante* (Pearce et al. 1999) and mouse *Coco* (Bell et al. 2003) as the cDNA most related to mouse *cerberus-like* (Belo et al. 1997) in the mammalian database. After cloning of the full-length cDNA, we observed that this gene, here designated *cerberus-like2* (*cerl-2*), is located on mouse Chromosome 8, and is genomically organized into two exons, separated by an intron of 5.92 kb. It encodes a 20-kDa protein with a predicted signal peptide sequence and a cysteine-rich domain (CRD) containing nine cysteines characteristic of the Cerberus/DAN family (Supplementary Fig. S1). The CRD domain is essential for the biological function of these proteins (Belo et al. 1997; Hsu et al. 1998), so it is important to note that only in Cerl-2 is this complete domain present, in contrast to what has been previously described for the incomplete sequence of Dante (Pearce et al. 1999).

Cerl-2 has close similarities to mouse *cerberus-like* ($I = 35\%$, $P = 47\%$), cCaronte ($I = 34\%$, $P = 51\%$), *Xcoco* ($I = 38\%$, $P = 53\%$), and to a hypothetical human protein ($I = 57\%$, $P = 65\%$; Supplementary Fig. S1). The latter is probably the human homolog of mouse Cerl-2, and we named it human Cer2. It also shares some similarities with the recently described zebrafish Charon ($I = 33\%$, $P = 55\%$).

As shown by whole-mount in situ hybridization (WISH), *cerl-2* transcripts can be first detected in a horseshoe-shaped expression pattern in the perinodal region of the early head-fold stage of the mouse embryo (E7.0; Fig. 1A,A'), resembling *Nodal* expression at this stage (Collignon et al. 1996; Lowe et al. 1996). However, by late head-fold stage (E7.5), expression of *cerl-2* begins to decrease in intensity on the left side (Fig. 1B,B'), and by early somitogenesis (E8.0), it can be strongly detected in the right side of the node (Fig. 1C,C'), assuming a complementary expression pattern to that of *Nodal* (Collignon et al. 1996; Lowe et al. 1996). After a thorough in situ hybridization analysis, *cerl-2* transcripts could not
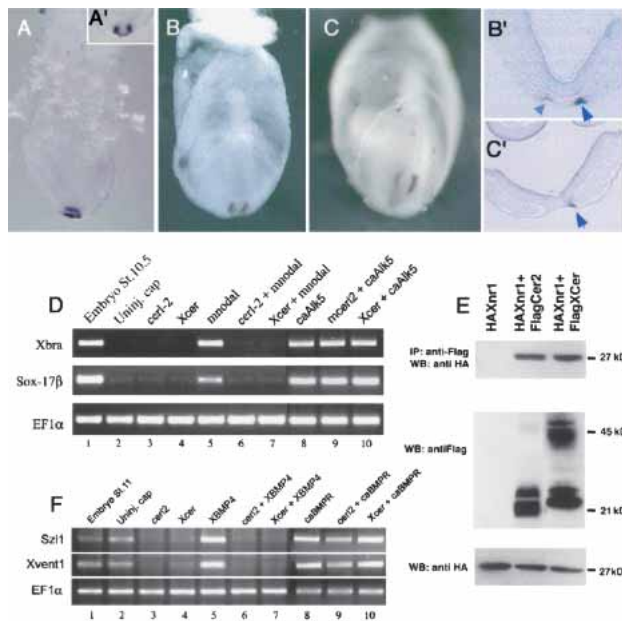
Figure 1. Biological activity of the asymmetrically expressed *cerl-2*. (*A–C*) *cerl-2* expression pattern during early mouse development. (*A,A′*) Lateral and anterior views, respectively, of *cerl-2* expression in the node at E7.0. At E7.5 (*B*), *cerl-2* starts to be asymmetrically up-regulated on the right side of the node, and at E8.0 (*C*) the asymmetry becomes more evident. *B′* and *C′* show frontal sections of the embryos in *B* and *C*, respectively, and provide a detailed view of the perinodal region where *cerl-2* is expressed (arrowheads). (*D–F*) Inhibitory effects of Cerl-2 on Nodal and BMP signaling. (*D*) *cerl-2* inhibits m*Nodal* but not ca*ALK5* mRNA, as assayed by the induction of their target genes *Xbra* and *Sox-17*β. (*E*) Coimmunoprecipitation experiments showing direct binding of Cerl-2 and Xcer to Xnr1. (*F*) *cerl-2* inhibits X*BMP4* but not ca*Br* mRNA, as assayed by the induction of their target genes *Szl1* and *Xvent1*.

be found in later stages of mouse development. Thus, *cerl-2* is expressed at the proper time and place to be involved in an early L/R symmetry-breaking event in the mouse gastrula.

Cerl-2 belongs to a family of secreted antagonists that are inhibitors of TGF-β proteins like Nodal and BMPs, and also of Wnts, whose specificity can be unveiled by heterologous assays in the frog embryo (Piccolo et al. 1999; Belo et al. 2000). To assay Cerl-2 activity against endogenous signals, we injected *cerl-2* mRNA (750 pg) in the marginal zone of *Xenopus* embryos at the four-cell stage and then performed WISH for a mesodermal marker (*Xbra*) at stage 11. We found that embryos injected with *cerl-2* mRNA fail to gastrulate properly and form mesoderm (data not shown), indicating a possible interference with endogenous *nodal* signals. To test this hypothesis, *cerl-2* and *mNodal* mRNAs were coinjected in the animal pole of four-cell-stage embryos, animal caps were explanted at blastula stage, harvested at stage 10.5, and analyzed by RT–PCR for *Xbra* and *Sox17*β (a pan-endodermal marker), two prototypic nodal target genes (Belo et al. 2000). To test whether inhibition of *mNodal* took place upstream or downstream of the Nodal receptor, we performed epistatic experiments with a constitutively active form of the activin receptor (ca*Alk5*). Microinjection of animal caps with either *mNodal* (50 pg) or ca*Alk5* (800 pg) (Fig. 1D, lanes 5,8) induced expression of both *Xbra* and *Sox17*β. Coinjection of *mNodal* with *cerl-2* mRNA (1 ng) completely

blocked mNodal signal (Fig. 1D, lane 6). However, these inductions could not be prevented when *cerl-2* was coinjected along with ca*Alk5*, showing that it acts upstream of this Nodal receptor (Fig. 1D, lane 9). A similar experiment was performed to test if *cerl-2* could also inhibit BMP4 signaling (Fig. 1F). For this experiment, animal caps were harvested at stage 11, and the downstream targets *Szl1* and X*vent1* were analyzed by RT–PCR. Microinjection of X*BMP4* (300 pg) or ca*Br* (a constitutively active BMP4 receptor used for the epistatic experiment) alone induced the expression of both *Szl1* and X*vent1* (Fig. 1F, lanes 5,8). Coinjection of *cerl-2* (1 ng) with caBr (480 pg) did not prevent *Szl1* and X*vent1* expression (Fig. 1F, lane 9), whereas coinjection of Cerl-2 with X*BMP4* inhibited the expression of both markers (Fig. 1F, lane 6). In both experiments Xcer (800 pg) was injected as a control as it is known to inhibit both *Nodal* and *BMP4* signaling. Taken together, these results show that full-length *cerl-2* inhibits *nodal* and *BMP4* but not ca*Alk5* or ca*Br* signaling (Fig. 1D,F), suggesting that Cerl-2 might antagonize Nodal and BMP4 extracellularly.

To determine whether Cerl-2 is able to physically interact with TGFβ proteins, we coinjected synthetic mRNAs encoding a Flag-tagged version of Cerl-2 together with an HA-tagged version of Xnr1 into animal poles. Extracts were immunoprecipitated with anti-Flag antibody and the coprecipitating proteins were analyzed by anti-HA Western blotting. As shown in Figure 1E, HAXnr1 protein was found in a complex with FlagCerl2. All the in vitro experiments—(1) the inhibition of Nodal and its downstream targets by Cerl-2; (2) its activity being upstream of the Nodal receptor; and (3) the biochemical assay showing a physical interaction between the two proteins—suggest that Cerl-2 is a novel Nodal antagonist.

To determine the in vivo role of *cerl-2*, we inactivated this gene in ES cells by replacing the second exon (containing the core CRD) with a LacZ reporter cassette (Fig. 2A). WISH in E7.5 *cerl-2*^{+/−} embryos using a *LacZ* probe revealed that its expression is also asymmetrical in the right side of the node (Fig. 2D,E). The offspring of Cerl-2^{+/−} intercrosses were born according to the correct Mendelian ratio. We observed that 35% of the homozygous mutants (33/94) died within the first 48 h after birth. From those animals that died perinatally (*n* = 33), 18% (6/33) showed left pulmonary isomerism (Fig. 2G), 18% (6/33) thoracic situs inversus (Fig. 2H), and the remaining 64% (21/33) failed to show any apparent laterality defect. However, when these apparently unaffected animals were examined carefully by histological analysis, it was observed that they displayed cardiovascular malformations (Fig. 2J,L), these being their probable cause of death. These defects include incomplete atrial (Fig. 2L) and ventricular septation (data not shown). Of the 65% mutant animals that survived (61/94), 40% become normal adults (37/94), and the remaining 25% (24/94) die between weaning age and 3 mo old, most of them showing heterotaxia of the abdominal organs (Supplementary Fig. S2).

Because of its expression pattern and its Nodal inhibitory activity, together with the observed laterality defects, we decided to investigate the effect of the loss of *cerl-2* in the expression of left–right determinant genes. At early somite stages, *Nodal*, *Lefty1*, *Lefty2*, and *Pitx2* are expressed in the left side of the embryo and are part of an evolutionarily conserved signaling cascade essen-

256
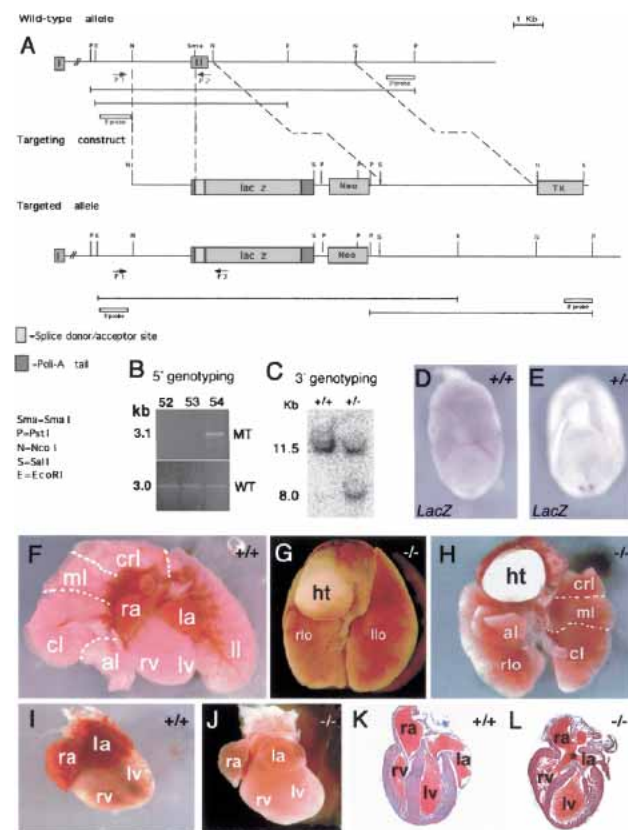
Figure 2. Targeted inactivation of *cerl-2* gene. (*A*) Schematic representation of the wild-type *cerl-2* locus, targeting vector, and targeted allele. The positions of primers, restriction enzyme sites, and the probe used for PCR and Southern blot analysis, respectively, are shown. (*B*) PCR-based 5′-genotyping of wild-type and targeted ES cell DNA. (*C*) Genomic Southern blot of PstI-digested tail DNA, prepared from newborn offspring of a mating of heterozygous mice. (*D,E*) *LacZ* in situ hybridization in wild-type (*D*) and heterozygous (*E*) embryos. (*F–H*) Thoracic organs of newborn wild-type (*F*) and *cerl-2⁻/⁻* littermates displaying left lung isomerism (*G*) or inverted situs (*H*). (*I,J*) Hearts of newborn wild-type and *cerl-2⁻/⁻* littermates, respectively. (*K,L*) Frontal sections of the hearts depicted in *I* and *J*, respectively, showing the atrial septal defects (asterisk) in *cerl-2⁻/⁻*. (al) Accessory lobe; (cl) caudal lobe; (crl) cranial lobe; (ht) heart; (ml) middle lobe; (la) left atrium; (llo) left lobe; (lv) left ventricle; (ra) right atrium; (rlo) right lobe; (rv) right ventricle.

tial for correct L/R morphogenesis (Capdevila et al. 2000; Wright 2001; Hamada et al. 2002). At E8.0, *Nodal* is expressed in the node and in the L-LPM of wild-type embryos (Fig. 3A). WISH in *cerl-2⁻/⁻* embryos (*N* = 60) using a *Nodal* probe revealed that although 40% of the embryos showed normal expression, 50% displayed bilateral expression, and 10% had an inverted pattern of expression in the R-LPM (Fig. 3B–D). Interestingly, *Nodal* expression in the node remains unaffected in these three situations, always being stronger in the left side (red arrows in Fig. 3A–D). This evidence further supports previously described work in which *Nodal* asymmetric expression in the node is reported not to be necessary or linked to its later expression domain in the L-LPM (Brennan et al. 2002; Saijoh et al. 2003). At this same developmental stage, *Lefty1* is expressed along the ventral midline in the prospective floor plate of the wild-type embryo (Fig. 3E), whereas *Lefty2* expression can be detected in the L-LPM (Fig. 3E; Meno et al. 1997). Both

257

genes, *Lefty1* and *Lefty2*, have been described to be downstream targets of *Nodal* and also its inhibitors (for review, see Hamada et al. 2002). By performing WISH using a riboprobe that detects both *Lefty* genes, we found that in *cerl-2⁻/⁻* embryos, *Lefty2* expression in the LPM is very similar to that of *Nodal*, as it would be expected. It can be detected in the left LPM, bilaterally or in the R-LPM (Fig. 3F–H). We could also observe that, in *cerl-2*-null mutants, *Lefty1* expression in the midline is not affected (Fig. 3F–H). Lefty1 was proposed to function as a midline barrier to prevent the diffusion of Nodal-induced signals emanating from the left to the right LPM (Meno et al. 1998). The proper expression of *Lefty1* (Fig. 3F–H) and *Shh* (data not shown) in the prospective floorplate leads us to conclude that the abnormal expression of left
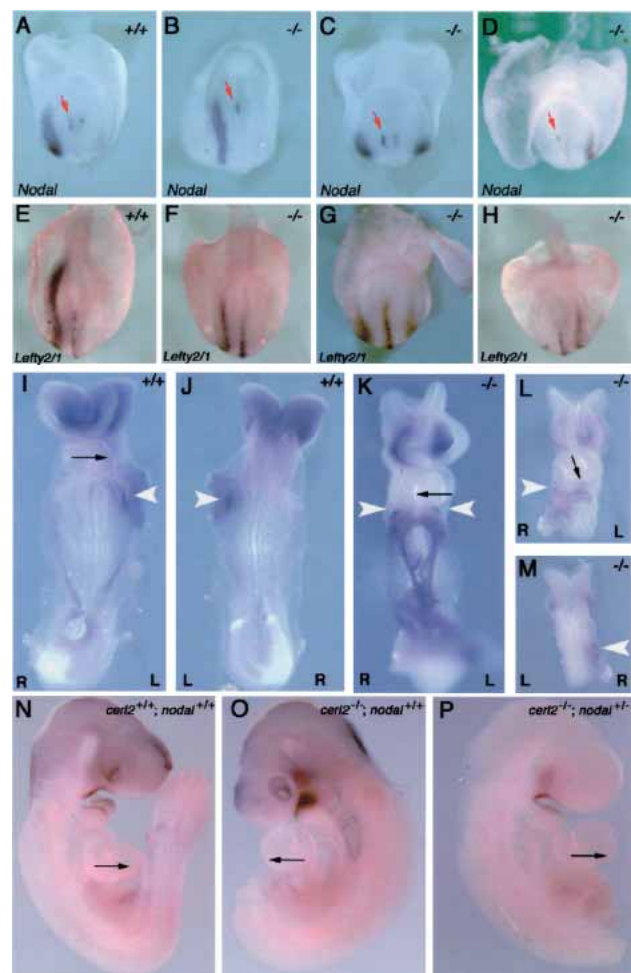
Figure 3. *cerl-2* null mutants display a range of L/R defects. (*A–H*) Posterior views of E8.0 embryos. (*A*) Wild-type *Nodal* expression in the node and left LPM. (*B–D*) *cerl-2⁻/⁻* embryos showing normal (*B*), bilateral (*C*), and right-sided (*D*) expression of *Nodal* in the LPM. (*E*) Wild-type *Lefty2/1* expression in the left LPM and floorplate. (*F–H*) *cerl-2⁻/⁻* embryos displaying normal (*F*), bilateral (*G*), and right-sided (*H*) expression of *Lefty2* in the LPM. (*I,J*) Ventral and dorsal views, respectively, of E8.5 wild-type embryos showing *Pitx2* on the left LPM. (*K–M*) *cerl-2⁻/⁻* embryos presenting bilateral (*K*) and right-sided (*L,M*) expression of *Pitx2* in the LPM. White arrowheads indicate the expression domain of *Pitx2*. (*N–P*) Rescue of *cerl-2* phenotype by reduced Nodal activity. (*N*) E9.5 wild-type embryo showing rightward looping of the heart. (*O*) *cerl-2⁻/⁻* littermate with a reversed heart loop. (*P*) *cerl-2⁻/⁻*; *nodal⁺/⁻* compound mutant with normal looping of the heart.

determinant genes in *cerl-2*^{−/−} embryos is not caused by midline defects. Furthermore, 10% of *cerl-2*^{−/−} embryos show right-sided ectopic expression of *Nodal* (Fig. 3D). In addition, in embryos with bilateral *Nodal* expression in the LPM, this expression starts at the level of the node (Fig. 3C). Taken together, these results strongly indicate that the leaking of left-side determinants takes place at the level of the node, and not later through to a defectively patterned midline.

Pitx2 is a downstream target of Nodal that is responsive to Nodal signaling through an asymmetric enhancer (Shiratori et al. 2001), similar to Lefty2 and Nodal (Adachi et al. 1999; Norris and Robertson 1999; Saijoh et al. 1999). At E8.5, *Pitx2* expression can be detected in the left LPM (Fig. 3I,J; Ryan et al. 1998), and it has been shown to be required for asymmetric development of organ situs (Gage et al. 1999; Kitamura et al. 1999; Lin et al. 1999; Lu et al. 1999). In *cerl-2*^{−/−} embryos, *Pitx2* expression in the LPM ($N = 11$) could be detected bilaterally (38%), in the left (55%), or in the right side (9%) (Fig. 3K–M).

The L/R-determining genetic cascade leads to morphological consequences in the positioning of internal organs, and the first morphological manifestation of L/R axis determination is the orientation of embryonic heart looping (Fujinaga 1997). In wild-type mouse embryos, the linear heart tube loops rightward, whereas 54% (27/50) of *cerl-2*^{−/−} mice exhibited leftward or ventral heart looping (Fig. 3K,L). This comes in agreement with the previous experiments in which we show that Cerl-2 activity is essential for the correct establishment of the left-side determinant genes, and, therefore, it is also necessary for the correct asymmetric development of the organ situs. In fact, besides the mentioned defects in heart looping, later developmentally associated phenotypes like left isomerism, situs inversus, and cardiac malformation were also observed (Fig. 2F–L).

The phenotype of *cerl-2* mutants suggests that Nodal activity is increased in the node, leading to abnormal expression of *Nodal* and its downstream targets in the LPM. Therefore, we hypothesized that by removing one copy of the *Nodal* gene, in the context of the *cerl-2* mutant, Nodal activity in the node would be lowered to a condition more similar to the wild type. To test this, we intercrossed *cerl-2*^{−/−} with *cerl-2*^{+/−}; *Nodal*^{+/−} animals, recovered the embryos at E9.5, and scored them according to the heart loop direction. Indeed, we could observe that in *cerl-2*^{−/−}; *nodal*^{+/−} embryos ($N = 20$), the abnormal heart-looping phenotype was 35% (7/20) (Fig. 3P). Interestingly, from the crosses between *cerl-2*^{−/−} × *cerl-2*^{+/−}; *Nodal*^{+/−} mutants, we also obtained 17 *cerl-2*^{−/−} embryos, and of these nine (52%) showed a heart-looping phenotype, which suggests that although the number of these embryos is less than half those obtained from *cerl-2*^{−/−} crosses, the percentage of defective heart loops remains fairly invariable. This observation (although not statistically significant owing to the relatively small number of embryos analyzed) suggests a qualitative tendency to partially rescue this phenotype. This tendency, as a complement of the other lines of evidence reported here, is in accordance with the proposed mechanisms for Cerl-2 activity. Taken together, our results suggest that the phenotypes in L/R axis determination observed in *cerl-2*^{−/−} embryos may result from an excess of Nodal signaling because of the lack of the Cerl-2 anti-Nodal activity in the mouse node.

In vitro biochemical assays showed that the Cerl-2 molecule also has the ability of inhibiting BMP-4. The lack of this potential inhibition in the mutants is, however, unlikely to be correlated with the in vivo observed phenotypes. Other studies in which BMP-4 antagonism was absent from the node, as in the targeted inactivation of Chordin (Bachiller et al. 2003) and Noggin (McMahon et al. 1998), did not result in L/R asymmetry-related phenotypes.

A gene named *Charon* that might be an ortholog of *cerl-2* has recently been described in zebrafish. In zebrafish, expression of *Southpaw* and *Charon* is not asymmetric. Nevertheless, knockdown of *Charon* using a morpholino oligonucleotide produces a similar phenotype to that of *cerl-2* mutants (Hashimoto et al. 2004). Although in zebrafish the breaking of L/R symmetry is still not very well understood, this unveils a possible conserved evolutionary mechanism of Nodal antagonism in the node, mediated by Cerberus/DAN family members, essential for the correct development of the L/R axis. In the mouse, *Nodal* activity in the node is required for *Nodal* expression in the L-LPM (Brennan et al. 2002; Saijoh et al. 2003) and subsequent activation of *Lefty2* and *Pitx2*. The role we propose for *cerl-2* is to restrict Nodal activity to the left side of the node. The consequent effect of such inhibition is to prevent additional activation of *Nodal*, *Lefty2*, and *Pitx2* in the R-LPM (Fig. 4). In the absence of Cerl-2 antagonistic activity on the node, *Nodal* may be also activated in the R-LPM, leading to bilateral or ectopic expression of this genetic cascade in the R-LPM. In addition, we noticed that *Nodal* expression on the node is still asymmetric on the left side of *cerl-2* mutants, indicating that *cerl-2* doesn't affect the asymmetric expression of *Nodal* in the node. Interestingly, *cerl-2* expression in the node also seems to be independent from *Nodal*. In fact in *Nodal*[neo/neo] mutants that lack (or have low levels of) *Nodal* expression in the node, *cerl-2* (*Dante*) expression domains remain unchanged (Saijoh et al. 2003).

The maintenance of asymmetric expression of *Nodal* in the node of *cerl-2* mutants, and later its randomized expression in the LPM, suggests that it may be uncoupled from asymmetric gene expression within the node, as previously described (Brennan et al. 2002; Saijoh et al. 2003). Although the relevance of *Nodal* asymmetric expression in the node as the cause of its later expression domain in the LPM remains unexplained and con-
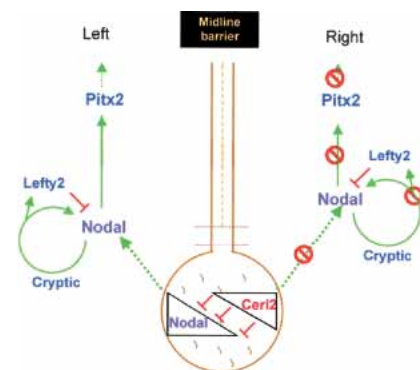
Figure 4. Proposed model for the role of *cerl-2* in generating asymmetric gene expression. *cerl-2* restricts nodal activity to the left side of the node, preventing additional activation of *Nodal*, *Lefty2*, and *Pitx2* in the R-LPM.

258

troversial (Saijoh et al. 2003), our data highlight the importance of tight regulation of Nodal activity in the node by the extracellular antagonism mediated by Cerl-2 as an integral part of the L/R program.

The first known event for inducing asymmetry in *Nodal* expression is the concerted rotational movement of cilia of the node pit cells (the nodal flow); indeed, in *iv/iv* mice that lack such oriented fluid flow, *Nodal* has a randomized asymmetric expression in the node (Supp et al. 1999).

Paradoxically, despite the different expression pattern of *Nodal* in the node, of the *iv/iv* (Supp et al. 1999) and *cerl-2* mutants, they end up displaying a very similar type of randomization, characterized by left, right, or bilateral activation of the "leftness" program in the LPM. This indicates that Cerl-2 plays an important role in the early events of symmetry breaking that take place in the node. Our data suggest a possible explanation in which the L/R asymmetry is controlled by a double-assurance mechanism consisting of two parallel systems, the first relying on the leftward nodal-cilia flow, and the second, on the antagonism between Cerl-2 and Nodal described by the proposed model (Fig. 4).

Materials and methods

Cloning of the full-length CDNA
A cDNA clone (GenBank accession no. AA289245) containing the second exon and the 3′-UTR of *cerl-2* was obtained by database search for proteins similar to mCer-l. A hypothetical human protein (FLJ38607) was found by searching the NCBI database for proteins homologous to *cerl-2* and its corresponding cDNA BLASTed against the mouse genome. A primer designed to align in the predicted 5′-UTR (5′-CGGAATTCCGC CAGAAAACAACTCTCAAGCTGCTCTCC-3′) and a reverse primer complementary to the second exon of *cerl-2* (5′-CCACACCACAGCGT CACCGATGTCCAGC-3′) were used in an RT–PCR with E7.5 mouse total RNA. The resulting 5′-cDNA portion was subcloned into a pGEM-Teasy vector, and the full-length cDNA was assembled into pCS2+ plasmid and sequenced. The GenBank accession number for mouse *cerberus-like2* is AY387409.

Targeted disruption of the cerl-2 gene
A mouse 129/Ola genomic library was screened for *cerl-2* using a partial cDNA clone (GenBank accession no. AA289245), and two positive clones were obtained.

In our targeting vector, a 0.6-kb SmaI/NcoI DNA fragment containing the second exon was replaced with a neomycin and a lacz cassette. The linearized vector was electroporated into 129/Ola embryonic stem cells. One heterozygous embryonic stem cell clone was used to generate chimeric mice by blastocyst injection, and mutant animals were bred in both 129/Ola and 129/Ola × C57BL/6J mixed backgrounds. Genotyping was done by Southern blotting and PCR assays. For Southern blot analysis, genomic DNA was digested with PstI and hybridized with a 3′-probe. The 3′-probe was a 1.0-kb (PstI/XbaI) genomic DNA fragment downstream from the 3′ recombination arm. Primers for PCR analysis were P1 (5′-GGAACCACCTTTGTAGTCAAGACTGG-3′), P2 (5′-GGTGACTT CTTTTTTGCTTTAGCAGG-3′), and P3 (5′-CACACAGCTGTTGCAG AAGAC-3′).

Generation and genotyping of single and compound mutants
cerl-2^{+/−} heterozygous mice were intercrossed with *nodal*^{+/−} heterozygous mice (both of C57/B6 background), originating *cerl-2*^{−/−} or double heterozygous animals. The latter were crossed to *cerl-2*^{+/−} or *cerl-2*^{−/−} mice to obtain *cerl-2*^{−/−}; *nodal*^{+/−} mutants. DNA preparation for genotyping was performed as described previously (Lowe et al. 1996) and analyzed by PCR using the following three oligonucleotides for *cerl-2*: AA289c-P3 (5′-CACACAGCTGTTGCAGAAGAC-3′), GenCer2-fwd (5′-GGAAGATTTTATGCAAGCAAGAGTGTGG-3′), and Lower2 (5′-GGTGACTTCTTTTTTGCTTTAGCAGG-3′), which resulted in bands of 300 bp and 500 bp for the wild-type and mutant alleles, respectively. *nodal* genotyping was performed as described previously (Bachiller et al. 2000).

Whole-mount in situ hybridization and histology
Whole-mount in situ hybridization and antisense probe preparation was carried out as described previously (Belo et al. 1997).

Detailed descriptions of the RNA probes and constructs used are available from the authors on request.

mRNA synthesis, microinjection and RT–PCR analysis
Capped sense mRNAs were synthesized using Ambion mMessage mMachine kit. In vitro fertilization, microinjection of *Xenopus laevis* embryos, and RT–PCR analysis were performed as described previously (Bouwmeester et al. 1996; Belo et al. 2000). The primer sets used are described in http://www.hhmi.ucla.edu/derobertis/protocol_page/oligos. PDF. For all RT–PCR reactions, *ef1* was used as the loading control. Detailed descriptions of the expression constructs used are available from the authors on request.

Coimmunoprecipitation analysis
A Flag-tagged version of *cerl2* was constructed by standard PCR methods and subcloned in pCS2+, using the abovementioned forward primer and the following reverse primer: 5′-CCGCTCGAGTCACTTATCGTCGT CATCCTTGTAATCTCCTCCTCCCAGCTTCGGGCGGCACTGACA CTTCTGG-3′. One nanogram of HA*Xnr1* mRNA and 5 ng of Flag*cerl-2* mRNA were injected into the animal poles of *Xenopus* embryos, and coimmunoprecipitation was performed as previously described (Yeo and Whitman 2001). Anti-Flag mouse monoclonal antibody (Sigma) and anti-HA rabbit polyclonal antibody (Covance) were used for immunoprecipitation and Western blot analysis. Proteins were visualized using ECLWestern blotting detection reagents (Amersham Pharmacia Biotech).

References
Adachi, H., Saijoh, Y., Mochida, K., Ohishi, S., Hashiguchi, H., Hirao, A., and Hamada, H. 1999. Determination of left/right asymmetric expression of nodal by a left side-specific enhancer with sequence similarity to a Lefty-2 enhancer. *Genes & Dev.* **13:** 1589–1600.

Bachiller, D., Klinggensmith, J., Kemp, C., Belo, J.A., Anderson, R.M., May, S.R., MacMahon, J.A., McMahon, A.P., Harland, R.M., Rossant, J., et al. 2000. The organizer factors Chordin and Noggin are required for mouse forebrain development. *Nature* **403:** 658–661.

Bachiller, D., Klingensmith, J., Shaneyder, N., Tran, U., Anderson, R., Rossant, J., and De Robertis, E.M. 2003. The role of chordin/Bmp signals in mammalian pharyngeal development and DiGeorge syndrome. *Development* **130:** 3567–3578.

Beddington, R.S. and Robertson, E.J. 1999. Axis development and early asymmetry in mammals. *Cell* **96:** 195–209.

Bell, E., Munoz-Sanjuan, I., Altmann, C.R., Vonica, A., and Brivanlou, A.H. 2003. Cell fate specification and competence by Coco, maternal BMP, TGFβ and Wnt inhibitor. *Development* **130:** 1381–1389.

Belo, J.A., Bouwmeester, T., Leyns, L., Kertesz, N., Gallo, M., and De Robertis, E.M. 1997. Cerberus-like is a secreted factor with neuralizing activity expressed in the anterior primitive streak endoderm of the mouse gastrula. *Mech. Dev.* **68:** 45–57.

Belo, J.A., Bachiller, D., Agius, E., Kemp, C., Borges, A.C., Marques, S., Piccolo, S., and De Robetis, E.M. 2000. Cerberus-like is a secreted BMP and nodal antagonist not essential for mouse development. *Genesis* **26:** 265–270.

Bouwmeester, T., Kim, S., Sasai, Y., Lu, B., and De Robertis, E.M. 1996. Cerberus is a head-inducing secreted factor expressed in the anterior endoderm of Spemann's organizer. *Nature* **382:** 595–601.

Brennan, J., Norris, D.P., and Robertson, E.J. 2002. Nodal activity in the node governs left–right asymmetry. *Genes & Dev.* **16:** 2339–2344.

259

Capdevila, J., Vogan, K.J., Tabin, C.J., and Izpisua-Belmonte, J.C. 2000. Mechanisms of left–right determination in vertebrates. *Cell* **101:** 9–21.

Collignon, J., Varlet, I., and Robertson, E.J. 1996. Relationship between asymmetric nodal expression and the direction of embryonic turning. *Nature* **381:** 155–158.

Fujinaga, M. 1997. Development of sidedness of asymmetric body structures in vertebrates. *Int. J. Dev. Biol.* **41:** 153–186.

Gage, P.J., Suh, H., and Camper, S.A. 1999. Dosage requirement of Pitx2 for development of multiple organs. *Development* **126:** 4643–4651.

Hamada, H., Meno, C., Watanabe, D., and Saijoh, Y. 2002. Establishment of vertebrate left–right asymmetry. *Nat. Rev. Genet.* **31:** 103–113.

Hashimoto, H., Rebagliati, M., Ahmad, N., Muraoka, O., Kurokawa, T., Hibi, M., and Suzuki, T. 2004. The *Cerberus/Dan*-family protein Charon is a negative regulator of Nodal signaling during left–right patterning in zebrafish. *Development* **131:** 1741–1753.

Hsu, D.R., Economides, A.N., Wang, X., Eimon, P.M., and Harland, R.M. 1998. The *Xenopus* dorsalizing factor Gremlin identifies a novel family of secreted proteins that antagonize BMP activities. *Mol. Cell* **1:** 673–683.

Kitamura, K., Miura, H., Miyagawa-Tomita, S., Yanazawa, M., Katoh-Fukui, Y., Suzuki, R., Ohuchi, H., Suehiro, A., Motegi, Y., Nakahara, Y., et al. 1999. Mouse Pitx2 deficiency leads to anomalies of the ventral body wall, heart, extra- and periocular mesoderm and right pulmonary isomerism. *Development* **126:** 5749–5758.

Lin, C.R., Kioussi, C., O'Connell, S., Briata, P., Szeto, D., Liu, F., Izpisua-Belmonte, J.C., and Rosenfeld, M.G. 1999. Pitx2 regulates lung asymmetry, cardiac positioning and pituitary and tooth morphogenesis. *Nature* **401:** 279–282.

Lowe, L.A., Supp, D.M., Sampath, K., Yokoyama, T., Wright, C.V., Potter, S.S., Overbeek, P., and Kuehn, M.R. 1996. Conserved left–right asymmetry of nodal expression and alterations in murine situs inversus. *Nature* **381:** 158–161.

Lu, M.F., Pressman, C., Dyer, R., Johnson, R.L., and Martin, J.F. 1999. Function of Rieger syndrome gene in left–right asymmetry and craniofacial development. *Nature* **401:** 276–278.

McGrath, J., Somlo, S., Makova, S., Tian, X., and Brueckner, M. 2003. Two populations of node monocilia initiate left–right asymmetry in the mouse. *Cell* **114:** 61–73.

McMahon, J.A., Takada, S., Zimmerman, L.B., Fan, C.M., Harland, R.M., and McMahon, A.P. 1998. Noggin-mediated antagonism of BMP signaling is required for growth and patterning of the neural tube and somite. *Genes* & *Dev.* **12:** 1438–1452.

Meno, C., Ito, Y., Saijoh, Y., Matsuda, Y., Tashiro, K., Kuhara, S., and Hamada, H. 1997. Two closely-related left–right asymmetrically expressed genes, lefty-1 and lefty-2: Their distinct expression domains, chromosomal linkage and direct neuralizing activity in *Xenopus* embryos. *Genes Cells* **2:** 513–524.

Meno, C., Shimono, A., Saijoh, Y., Yashiro, K., Mochida, K., Ohishi, S., Noji, S., Kondoh, H., and Hamada, H. 1998. Lefty-1 is required for left–right determination as a regulator of lefty-2 and nodal. *Cell* **94:** 287–297.

Nonaka, S., Tanaka, Y., Okada, Y., Takeda, S., Harada, A., Kanai, Y., Kido, M., and Hirokawa, N. 1998. Randomization of left–right asymmetry due to loss of nodal cilia generating leftward flow of extraembryonic fluid in mice lacking KIF3B motor protein. *Cell* **95:** 829–837.

Norris, D.P. and Robertson, E.J. 1999. Asymmetric and node-specific nodal expression patterns are controlled by two distinct *cis*-acting regulatory elements. *Genes* & *Dev.* **13:** 1575–1588.

Pearce, J.J., Penny, G., and Rossant, J. 1999. A mouse cerberus/Dan-related gene family. *Dev Biol.* **209:** 98–110.

Piccolo, S., Agius, E., Leyns, L., Bhattacharyya, S., Grunz, H., Bouwmeester, T., and De Robertis, E.M. 1999. The head inducer Cerberus is a multifunctional antagonist of Nodal, BMP and Wnt signals. *Nature* **397:** 707–710.

Ryan, A.K., Blumberg, B., Rodriguez-Esteban, C., Yonei-Tamura, S., Tamura, K., Tsukui, T., de la Pena, J., Sabbagh, W., Greenwald, J., Choe, S., et al. 1998. Pitx2 determines left–right asymmetry of internal organs in vertebrates. *Nature* **394:** 545–551.

Saijoh, Y., Adachi, H., Mochida, K., Ohishi, S., Hirao, A., and Hamada, H. 1999. Distinct transcriptional regulatory mechanisms underlie left–right asymmetric expression of lefty-1 and lefty-2. *Genes* & *Dev.* **13:** 259–269.

Saijoh, Y., Oki, S., Ohishi, S., and Hamada, H. 2003. Left–right patterning of the mouse lateral plate requires nodal produced in the node. *Dev. Biol.* **256:** 160–172.

Shiratori, H., Sakuma, R., Watanabe, M., Hashiguchi, H., Mochida, K., Sakai, Y., Nishino, J., Saijoh, Y., Whitman, M., and Hamada, H. 2001. Two-step regulation of left–right asymmetric expression of pitx2: Initiation by nodal signaling and maintenance by Nkx2. *Mol. Cell* **7:** 137–149.

Supp, D.M., Brueckner, M., Kuehn, M.R., Witte, D.P., Lowe, L.A., MacGrath, J., Corrales, J., and Potter, S.S. 1999. Targeted deletion of the ATP binding domain of left–right dynein confirms its role in specifying development of left–right asymmetries. *Development* **126:** 5495–5504.

Wright, C.V. 2001. Mechanisms of left–right asymmetry: What's right and what's left? *Dev. Cell* **1:** 179–186.

Yeo, C. and Whitman, M. 2001. Nodal signals to Smads through Cripto-dependent and Cripto-independent mechanisms. *Mol. Cell* **7:** 949–957.

260

Identification of alternative promoter usage for the matrix Gla protein gene

Evidence for differential expression during early development in *Xenopus laevis*

Natércia Conceição[1]*, Ana C. Silva[2,3]*, João Fidalgo[1], José A. Belo[2,3] and M. Leonor Cancela[1]

1 University of Algarve CCMAR, Campus de Gambelas, Faro, Portugal
2 CBME, Campus de Gambelas, Faro, Portugal
3 Instituto Gulbenkian de Ciência, Oeiras, Portugal

Correspondence

M. L. Cancela, University of Algarve-CCMAR, Campus de Gambelas, 8005–139 Faro, Portugal
Fax: +351 289818353
Tel: +351 289800971
E-mail: lcancela@ualg.pt

*Note

These two authors contributed equally to this work.

Recent cloning of the *Xenopus laevis* (*Xl*) matrix Gla protein (MGP) gene indicated the presence of a conserved overall structure for this gene between mammals and amphibians but identified an additional 5′-exon, not detected in mammals, flanked by a functional, calcium-sensitive promoter, 3042 bp distant from the ATG initiation codon. DNA sequence analysis identified a second TATA-like DNA motif located at the 3′ end of intron 1 and adjacent to the ATG-containing second exon. This putative proximal promoter was found to direct transcription of the luciferase reporter gene in the *X. laevis* A6 cell line, a result confirmed by subsequent deletion mutant analysis. RT-PCR analysis of *Xl*MGP gene expression during early development identified a different temporal expression of the two transcripts, strongly suggesting differential promoter activation under the control of either maternally inherited or developmentally induced regulatory factors. Our results provide further evidence of the usefulness of nonmammalian model systems to elucidate the complex regulation of MGP gene transcription and raise the possibility that a similar mechanism of regulation may also exist in mammals.

Matrix Gla protein (MGP) is a 10 kDa secreted protein which contains between three and five γ-carboxyglutamic acid residues depending on the species [1,2]. MGP mRNA was originally shown to be present in nearly all tissues analysed [3,4], although it was later shown to be synthesized *in vivo* mainly by chondrocytes and smooth muscle cells (reviewed in [5]). During early mouse development MGP mRNA was detected as early as 9.5 days *post coitus*, before the onset of skeletogenesis [4], indicating a role in early cell differentiation and confirming previous data on the presence of high levels of MGP in rat fetus [6]. Consistent with this hypothesis, MGP mRNA was found to be expressed throughout lung morphogenesis where it may play a role in the epithelium–mesenchymal cell interactions required for normal differentiation and branching of respiratory components of the lung. In addition, MGP mRNA was consistently found in cells from the chondrocytic lineage, becoming more restricted to chondrocytes as development progressed, particularly during limb development [4]. Accordingly, MGP was later unequivocally associated with cartilage formation and mineralization through the use of mouse genetics [7]. Unexpectedly, this study also revealed that MGP played a major role in the inhibition of soft tissue calcification, as MGP null (MGP–/–) mice developed severe vascular calcifications resulting from differentiation of smooth muscle cells in the aortic

medial layer into chondrocyte-like cells capable of producing a typical cartilaginous extracellular matrix progressively undergoing mineralization. A direct correlation between MGP and chondrocyte differentiation and function has also been suggested by Yagami *et al.* [8], who showed that constitutive MGP overexpression in chicken limb resulted in inhibition of cartilage mineralization *in vivo*, with delayed chondrocyte maturation and arrest of endochondral and intramembranous ossification. More recently, MGP mRNA was identified in later embryonic stages of *Xenopus laevis* embryos [1] and of the marine fish *Sparus aurata* [9], further suggesting that its role in cell differentiation must be a common feature in all vertebrates. The available evidence supports the current concept that MGP plays a decisive role during early tissue development and in differentiation of specific cell types, but the mechanisms regulating MGP gene transcription and its mode of action at the molecular level remain largely unknown.

Cloning of the human [10] and mouse [4] MGP genes provided the necessary molecular tools to investigate the functionality of MGP promoter regions in mammals, but, despite this knowledge, little information is available on the mechanisms responsible for regulation of MGP gene transcription. More recently, the cloning of the *X. laevis* MGP cDNA [1] and genomic locus [11] enabled us to investigate the regulation of MGP gene expression in this model organism. In this report, we show that *Xl*MGP mRNA is maternally inherited, and we provide evidence for the presence of alternative promoter usage in this gene during early *X. laevis* development.

Results

Identification of a functional proximal promoter for *X. laevis*

Alignment of the 5′-flanking region of exon IB from the *Xl*MGP gene with the 5′-flanking regions of ATG-containing exons of mouse, rat and human MGP genes identified a conserved DNA region located at the 3′ end of intron 1 of the *Xl*MGP gene and homologous to the known promoter regions of the three mammalian MGP genes considered (Fig. 1). As this region contained a TATA-like sequence (TATAAA) located between +2932 and +2937, the possibility that it may correspond to a proximal promoter for the *Xl*MGP gene was further investigated using LuC fusion genes containing the genomic regions from +2123 to +3013 of the *Xl*MGP gene. Upon transient transfection into A6 cells, the construct spanning this entire region


Fig. 1. Identification of a TATA-like box (bold) in intron 1 of the *Xl*MGP gene. Comparison between intron 1 of the *Xl*MGP gene and promoter regions of human [10], mouse [4] and rat (http://www.ncbi.nlm.nih.gov/genome/guide/rat/) MGP genes. Numbers indicate the position of the last nucleotide shown according to the ATG initiation codon of each gene.

(+2123/+3013LuC) was found to induce luciferase expression to levels comparable to those seen when using the previously described *Xl*MGP gene distal promoter (−949LuC construct [11]) (Fig. 2A). To delineate the functional elements within this region, a series of deletion mutants from the proximal promoter were tested for their effect on *in vitro* LuC activity (Fig. 2A). The +2123/+3013LuC, +2733/+3013LuC and +2852/3013LuC constructs had the strongest promoter activities. In contrast, the +2831/+3013LuC and +2843/+3013Luc constructs had significantly weaker promoter activities in these cells. These findings suggest that a functional basal promoter exists within the +2852 to +3013 region, and that negative regulatory elements exist within the 119 bases upstream from this region. The recovery of promoter activity in the +2123/+3013LuC construct may be accounted for by additional positive regulatory elements in the more 3′ sequences or by release of inhibition from the negative regulation. The +1278/+2083LuC construct showed no luciferase activity, indicating that a sequence randomly picked from intron 1 was not capable of inducing transcription. Taken together, our results demonstrate that the 3′ end of *Xl*MGP intron 1, spanning +2852 to +3013, is sufficient to induce strong reporter gene activity.

Computer analysis of DNA sequences from +2123 to +3013 using the TRANSFAC software (http://www.gene-regulation.com) identified binding sites for various putative nuclear factors. Their approximate locations within the deletion mutant constructs are indicated in Fig. 2A. As expected, most of the identifiable motifs were located between +2733 and the TATA box, the region shown to mediate significant changes in transcription. Interestingly, within this region, consensus sequences homologous to adaptor protein 1 (AP1) and δ-crystallin enhancer factor 1 (δEF1) binding element were identified. Functional promoter analysis in A6 cells including (a) deletion mutations that removed the putative AP1 site, (b) deletion mutations that removed the putative δEF1 elements located more 5′ from the TATA or (c) site-directed mutagenesis on
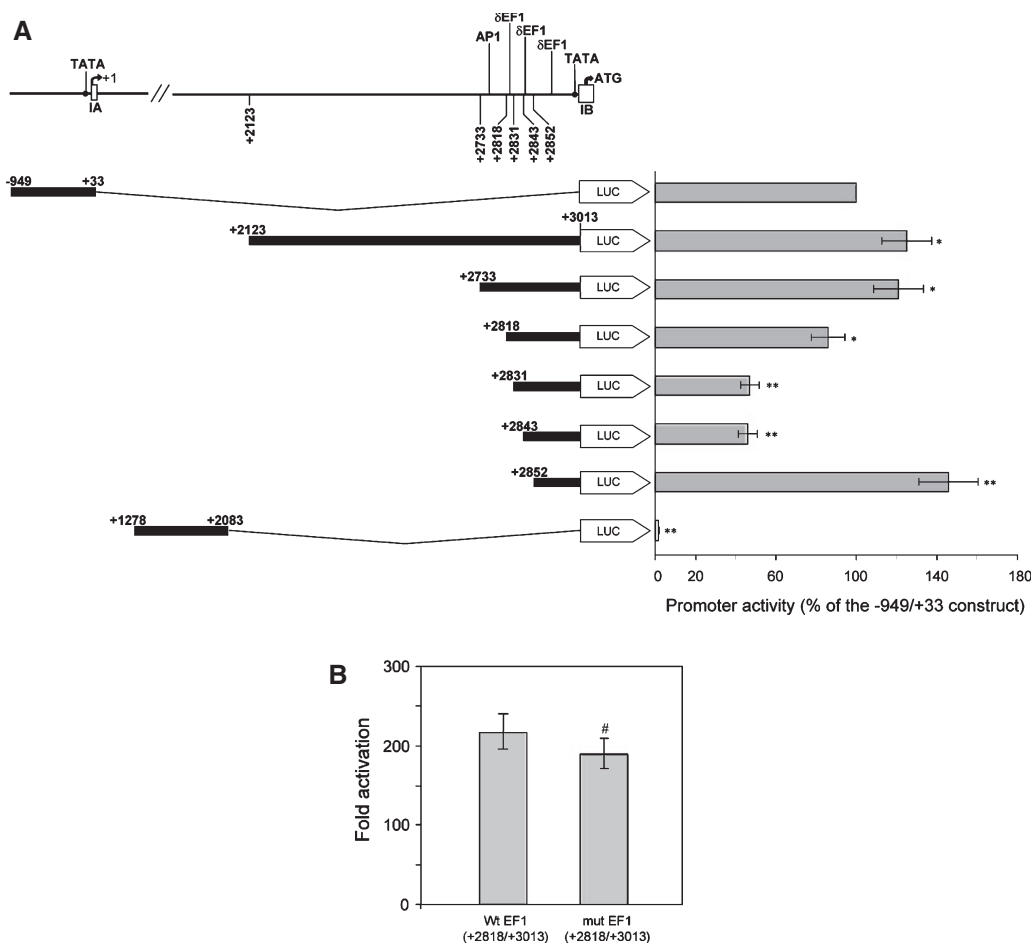
Fig. 2. Relative transcription activity of the *Xl*MGP gene proximal promoter constructs in A6 cells. (A) Schematic representation of the *Xl*MGP gene promoter regions. TATA boxes are indicated by ●. Approximate localization of consensus sequences for putative nuclear factors is indicated. A schematic representation of the *Xl*MGP proximal promoter constructs used for transient transfections is shown to the left (−949/+33LuC and +1278/+2083LuC are not to scale). The nomenclature of the promoter deletions was based on the transcription start site of the *Xl*MGP gene. Constructs used were: −949/+33LuC, +2123/+3013LuC; +2733/+3013LuC; +2818/+3013LuC; +2831/+3013LuC; +2843/+3013LuC; +2852/+3013LuC; and +1278/+2083LuC. A6 cells were harvested 36 h after transfection, and the promoter activity of the different 5′ regions of the *Xl*MGP gene proximal promoter was determined by measuring the relative luciferase activity as described in Experimental Procedures. Each transfection was carried out at least five times, and the standard deviation was always less than 10%. The results are indicated as fold induction over the promoterless pGL2-Basic vector. The activity of different constructs was compared with the activity of −949/+33LuC, considered as 100%. *$P < 0.05$ compared with −949/33LuC; **$P < 0.0001$ compared with −949/33LuC. (B) Mutation of putative δEF1 motifs (mutEF1) inhibits the promoter activation compared with WtEF1(+2818/+3013). #$P < 0.05$ compared with WtEF1(+2818/+3013).

these same putative δEF1 elements (Fig. 2A,B) demonstrated the existence of a basal promoter (from +2852/+3013), but did not confirm the direct involvement of the identified putative AP1 and δEF1 motifs in its transcriptional activation.

Differential MGP gene promoter usage in *X. laevis*

Temporal expression of the two transcripts (*Xl*MGP-IA and *Xl*MGP-IB) was investigated through a PCR strategy by searching for MGP mRNAs starting with either exon IA (longer transcript) or IB (shorter transcript), indicative of transcription directed from either the distal or the proximal promoter (Fig. 3A). Amplification of the longer IA transcript was first detected at stage 10.5 and thereafter remained present, albeit with different intensities up to the last stage analyzed (stage 48) (Fig. 3B). In contrast, the shorter IB transcript was amplified from the unfertilized egg as well as from the initial stages of development, with a peak at stage 8, then decreasing to
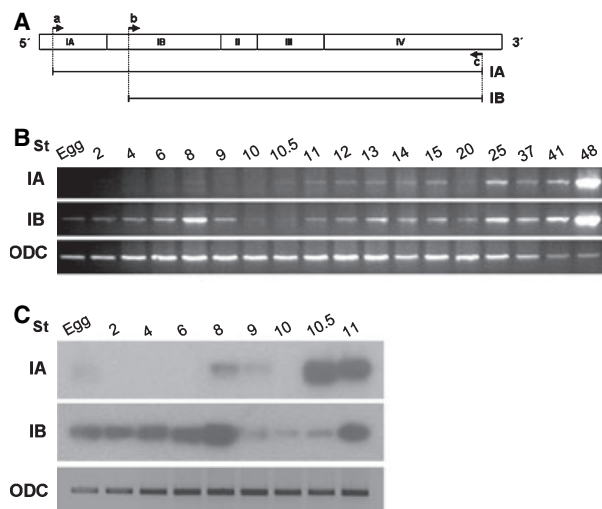
Fig. 3. Temporal expression of *Xl*MGP transcripts. Total RNA isolated from the indicated developmental stage (St) was analyzed by RT-PCR to investigate differential levels of expression of *Xl*MGP transcripts IA and IB. ODC was used as a loading control. RNA extracts used for RT-PCRs were made from pools of five randomly picked embryos. Results obtained for egg and stages 2–11 were further analysed by Southern blot hybridization using MGP 1B and ODC as specific probes labeled with ³²P. (A) Schematic diagram showing localization of the exon-specific oligonucleotide primers used for PCR amplification. a + c for amplification of the larger IA transcript; b + c for amplification of the shorter IB transcript. (B) PCR amplification of the two specific transcripts and of the ODC gene from the same RT reaction. (C) Southern blot hybridization of PCR fragments obtained after amplification of the same RT reactions used for (B) obtained from RNA purified from unfertilized egg and from embryonic stages 2–11. DNA was transferred to a nylon membrane after amplification and hybridized with *Xl*MGP or ODC probes as described in Experimental Procedures.

nearly nondetectable levels by stage 10 (Fig. 3B). These results were confirmed by Southern blot analysis after PCR amplification and using as specific probe transcript IB (Fig. 3C). The fact that this transcript IB was detected from stage 11 onwards may result from the presence, at those stages, of transcript IA, which can be used as a template by the polymerase as, except for the longer 5′ end of IA, the two transcripts are identical (Fig. 3A). This possibility is reinforced by the fact that the pattern of IB amplification obtained follows roughly that observed from this stage on for the larger IA transcript, although stage-specific expression of IB in some stages cannot be excluded.

Using the same approach for adult tissues, transcript IA was always detected in those tissues found to express the MGP gene as well as in the A6 cell line (results not shown).

Localization of MGP in *X. laevis* embryos by *in situ* hybridization

To determine the spatial pattern of *Xl*MGP expression during embryogenesis, we subjected embryos of various developmental stages to whole-mount *in situ* hybridization using digoxigenin-labeled *Xl*MGP antisense or sense RNA as probes [12]. In Fig. 4 we show that during gastrulation (stages 10.5–12) *Xl*MGP transcripts are expressed in the dorsal mesoderm along Brachet's cleft, as well as in the ventral mesoderm (Fig. 4b,d). At the onset of neurulation (stages 13–14), *Xl*MGP mRNA is located in both dorsal and ventral involuting mesoderm (Fig. 4f). The sibling embryos that were hybridized with the sense probe show no staining, and thus serve as control embryos (Fig. 4a,c,e).

From stage 39 to 42 (tadpole stages), *Xl*MGP transcripts are exclusively expressed in the olfactory placodes (Fig. 5, arrows) and in the cement gland (Fig. 5, arrowheads). Detailed comparison of *Xl*MGP-IA expression with that of *Xl*MGP-IB could not be observed because the probe used detects both *Xl*MGP transcripts.

Transcriptional analysis of the promoter constructs after microinjection into *X. laevis* embryos

To investigate whether either or both *Xl*MGP transcripts are present during gastrulation, a series of reporter constructs were injected radially into the marginal zone of four-cell *X. laevis* embryos. A constitutively active luciferase construct, pCMV-Luc and the Xcollagen basal promoter (Xcol-luc [13]) were used as positive controls. Analysis of luciferase activity at stage 11 showed that injection of the −949LuC construct induced a threefold increase in luciferase activity, whereas the +2733/+3013LuC and +2852/+3013LuC constructs showed less activity (Fig. 6 and results not shown). Although small, this difference in increase in luciferase activity is consistent with the other results obtained, namely the intensity of the RT-PCR bands and the weak *in situ* hybridization signal at stage 12. Injection of the −949LuC, +2733/+3013LuC and +2852/+3013LuC constructs in the animal cap resulted in less luciferase activity than in the radially injected ones, confirming the specificity of this activation (results not shown). We therefore conclude that during gastrulation stages, only the distal promoter is activated in the embryo, resulting in generation of the longer *Xl*MGP-IA transcript.
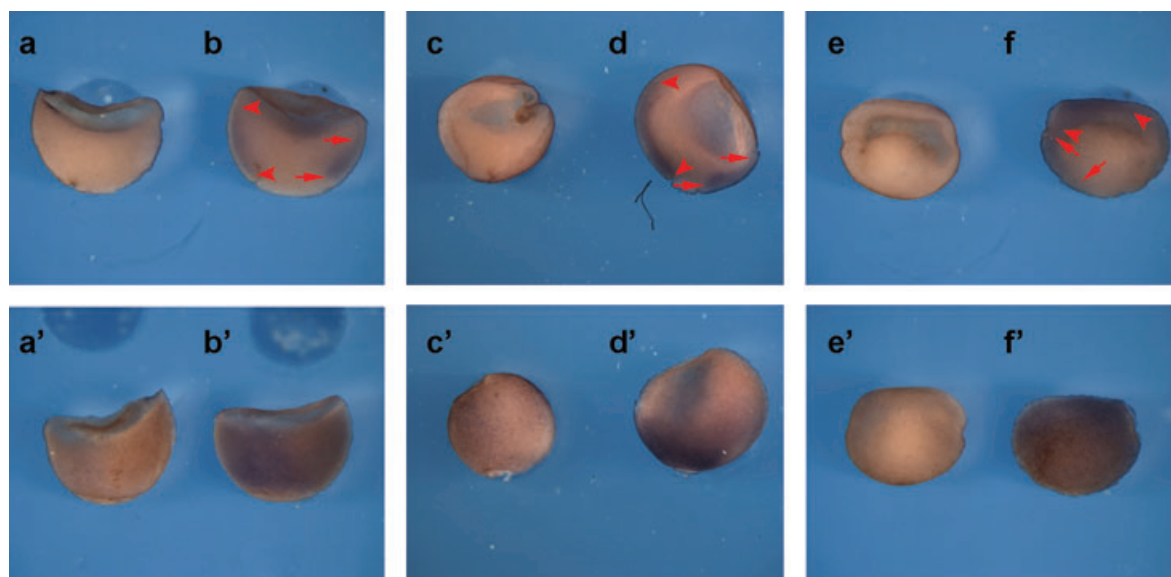
Fig. 4. Expression of *Xl*MGP during gastrulation. Mid-sagittal sections of whole-mount *in situ* hybridizations performed at stages 10.5 (a, a', b, b'), 12 (c, c', d, d') and 13 (e, e', f, f') using either a sense (a, a', c, c', e, e') or an antisense (b, b', d, d', f, f') *Xl*MGP probe. At stage 10.5, *Xl*MGP is expressed in the dorsal mesoderm along Brachet's cleft as well as in the ventral mesoderm (b). At stage 12 (d) and 13 (f), *Xl*MGP keeps on being expressed in both dorsal and ventral involuting mesoderm. The extension of *Xl*MGP's domain of expression is shown by red arrowheads on the dorsal side and by red arrows on the ventral side. The embryos hybridized with the sense probe show no staining (a, a', c, c', e, e').
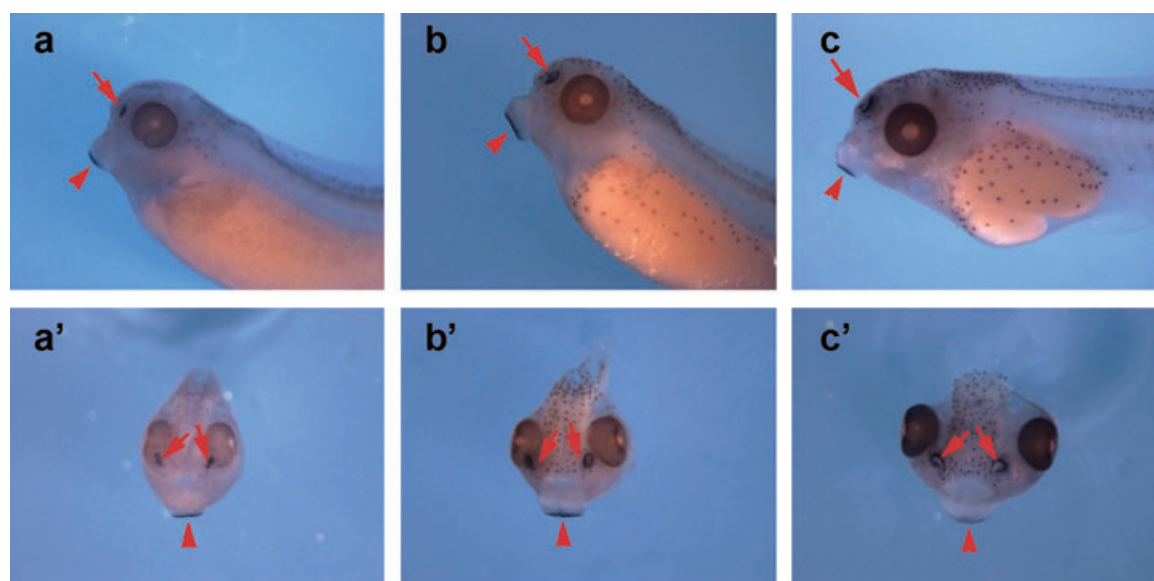
Fig. 5. Expression of *Xl*MGP at tadpole stages. Lateral (a, b, c) and frontal (a', b', c') views of stage 39 (a, a'), 40 (b, b') and 42 (c, c') embryos expressing *Xl*MGP. Throughout these stages *Xl*MGP expression domain is restricted to the olfactory placodes (arrows) and to the cement gland (arrowheads).

Discussion

This report describes the identification of a second functional promoter for the *Xl*MGP gene, a finding not previously reported for any mammalian MGP gene studied. In addition, evidence for maternal inheritance of the shorter MGP transcript and alternative promoter usage during early *X. laevis* development is

267
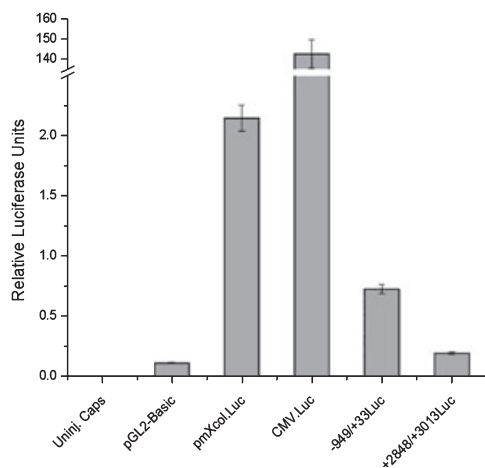
Fig. 6. Transcriptional analysis of the *Xl*MGP promoter constructs after injection in *X. laevis* embryos. Various *Xl*MGP–luciferase reporter constructs were injected radially into the marginal zone of four-cell stage embryos. At stage 11.5, embryos were lysed, and luciferase activities were measured. All values are expressed as relative luciferase units (firefly luciferase activity/ Renilla luciferase activity). Each assay was performed in triplicate and repeated at least twice.

provided. Our findings suggest a novel mechanism of regulation for the MGP gene in *X. laevis* and raise the possibility that MGP gene transcription in mammals may also be more complex than previously described.

Identification of a second, proximal promoter for the *X. laevis* MGP gene

The identification by sequence analysis of a TATA-like motif at the 3′ end of exon IB located 95 nucleotides upstream from the ATG initiation codon and sharing high homology with identical sequences found upstream from the ATG-containing exon in mammalian MGP genes led to the hypothesis of a second functional promoter for the *Xl*MGP gene. Luc reporter constructs and subsequent deletion mutant analysis confirmed this hypothesis and provided clear evidence for the presence of two functional promoters, a result not previously reported for this gene in any mammalian species. Alternative promoter usage has been previously observed in other genes containing 5′ exons comprising only untranslated sequences [14–17], thus providing alternative regulatory mechanisms for gene transcription without changes in the protein sequence.

Computer analysis of the DNA sequences from +2123 to +3013 using the TRANSFAC software identified putative binding sites for various nuclear factors. Their approximate locations within the deletion

mutant constructs are indicated in Fig. 2A (top panel). As expected, most of the identifiable motifs were located between +2733 and the TATA box, the region shown to mediate significant changes in transcription. Among the putative DNA motifs identified were binding sites for AP1, already found in the human MGP gene promoter [10,18], and three consensus sequences homologous to the δEF1 binding element (Fig. 2A). δEF1 is a widely distributed transcription regulator and the vertebrate homologue of the *Drosophila* protein *zfh-1* [19], a factor containing both zinc finger and homeodomain motifs. It is a 124 kDa DNA-binding protein which was initially characterized as a negative regulatory factor involved in the lens-specific regulation of the avian gene encoding δ-crystallin where it binds preferentially to the sequence (C/T)(A/T) C(C/G) in the δ-crystallin enhancer [20]. It is also involved in postgastrulation embryogenesis [21]. However, its broad tissue distribution suggests that it may play a more generalized role in gene transcription, as it has been detected in all murine tissues examined and in limb bud as early as stage 9.5 during mouse development [22,23]. Interestingly, experiments with the δEF1 knockout mouse demonstrated an important role of this nuclear factor in skeletal morphogenesis [23], suggesting possible involvement of this factor in the complex gene transcription regulatory pathway during early development of *Xenopus*. In this context, we cannot exclude MGP as a possible target gene. Accordingly, other genes involved in bone and cartilage metabolism, including type I and II collagen genes [24,25] and the rat osteocalcin gene [26], have been found to be regulated by this factor. Functional analysis of the proximal promoter in the *Xenopus* A6 cell line did not confirm any direct involvement of the two most distal δEF1 motifs located between +2818 and +2852. However, the possibility exists that an *in vitro* cell system, such as the one used here, may not contain all the necessary nuclear factors that are functional during early development.

Evidence for developmentally regulated alternative promoter usage in the *X. laevis* MGP gene

During early development, *X. laevis* embryos ranging from stages 2 to 9 were found to contain only the shorter IB MGP mRNA, transcribed from the proximal promoter. This form was also found in the unfertilized egg, confirming its origin as maternally inherited and explaining why it is the only form detected until zygotic transcription takes place (stage 8), just before gastrulation. In contrast, the larger IA transcript, containing an additional 5′ exon, was only

amplified after mid-blastula transition, indicating that transcription of the zygotic MGP gene is directed by nuclear factors binding to the distal promoter. These results were further corroborated by the results obtained after radial microinjection into the marginal zone of four-cell *X. laevis* embryos of the two promoter constructs driving luciferase expression. These data clearly show that, after mid-blastula transition, only the distal promoter drives luciferase transcription, providing additional evidence for differential promoter usage *in vivo*. These findings indicate that transcription of the larger IA form is important for gastrulation, whereas the shorter IB form is likely to play a role during the initial embryonic divisions. During development, transcription from exon IA or IB may be regulated through binding of the transcription initiation complex in either promoter after interaction with specific DNA-binding proteins transcribed from either maternally inherited mRNAs or developmentally regulated genes, both mechanisms already documented in other genes [27]. Similar regulatory mechanisms have been described for genes, whose expression is linked to specific cell differentiation patterns during normal development or malignant transformation as well as in adult tissues [16,28].

The IA transcript was always detected in postgastrulation developmental stages as well as in isolated adult tissues, sites where the shorter IB transcript was not detected. Additional evidence confirming that transcription from the proximal promoter is either absent or very weak in *X. laevis* adult tissues was provided by work aiming to identify the start site of *Xl*MGP gene transcription. Primer extension analysis using mRNA purified from a pool of adult tissues or from the A6 cell line and a reverse primer located in exon IB only identified the larger transcript ([11] and our unpublished results). Alternatively, transcription from the proximal promoter may be present only at specific periods of cell differentiation not identified in our study.

The present demonstration that MGP IA and IB result from different promoter usage in the maternal germinal cells and in the zygote suggests that it is critical for early development to be able to differentially regulate the concentrations of available MGP protein. Indeed, the presence of a maternally inherited MGP transcript (IB) in the first stages of *Xenopus* development may indicate that the MGP protein is required shortly after fertilization. It has been previously suggested that MGP may modulate bone morphogenetic protein-2 (BMP-2)-induced cell differentiation by direct protein–protein interaction [29,30], a hypothesis further corroborated by the fact that MGP was originally

isolated as a complex with BMP-2 [31]. As BMP signaling plays a critical role in dorsoventral patterning and neural induction during early *Xenopus* development [32], the presence of MGP at these early stages suggests a role for this protein in embryonic cell differentiation. Furthermore, the localization of MGP mRNA in the olfactory placodes (Fig. 5, arrows) corroborates what has been previously found in the mouse model, i.e. MGP mRNA was consistently found in cells from the chondrocytic lineage and thus associated with cartilage formation and mineralization.

In conclusion, our data identifies for the first time, the presence of alternative promoter usage for the MGP gene and provides clear evidence for differential expression of this gene during the very early stages of embryonic development. This conclusion was based on the fact that (a) this proximal sequence drove reporter gene expression in A6 cells as efficiently as the previously reported distal promoter, (b) a shorter form of mRNA resulting from transcription initiating at exon IB was identified by RT-PCR during early development, and (c) only the distal promoter was found to be functional after mid-blastula transcription after microinjection of early embryo, providing further evidence for alternative promoter usage *in vivo*. It has previously been shown that MGP is important for cell differentiation in various tissues including development of normal bone and cartilage in chick limb [8] and ectopic differentiation of bone cells within the vascular system in calcifying arteries [33]. However, no information is at present available on the regulatory mechanisms responsible for changes in MGP gene expression between normal and abnormal cell differentiation. Although the presence of alternative promoters as a regulatory mechanism for MGP gene transcription has not previously been observed in mammalian species, the intriguing possibility that a similar situation may exist in mammals cannot be entirely dismissed and may represent an attractive alternative for understanding MGP gene transcription. Interestingly, at least one earlier report has shown the presence of two MGP messages in rat, very similar in size [34], but to our knowledge, these results were not further developed.

Experimental procedures

MGP promoter constructs

The plasmid −949LuC has been described previously [11]. The +2123/+3013LuC, +2733/+3013LuC, +2818/+3013LuC, +2831/+3013LuC, +2843/+3013LuC, and +2852/+3013LuC reporter constructs were generated by PCR amplification with the same antisense oligonucleotide

269

Table 1. Oligonucleotides used for PCR amplification and reporter gene constructs of *X. laevis* gene and ODC cDNA. Position numbers are relative to the transcription start codon of the *Xl*MGP gene and published sequence of ODC cDNA (accession number X56316). Sequences underlined in sense primers are *Xho*I sites, in antisense primers are *Hin*dIII sites.

Name	Sequence (5′ → 3′)	Position
Antisense *Xl*MGP-specific primers		
*Xl*MGPR1	CACGCAAGCTTGACTTCTTGCTGTTAGAGG	+3013
*Xl*MGPR2	GGGAAGTGACTGCAACATAGAGAC	+7964
Sense *Xl*MGP-specific primers		
*Xl*MGPF1	CCGGAGCTCATCAGACTGATAATCTGTG	+2123
*Xl*MGPF2	CCGGAGCTCAGCATCACTTATCAGATGC	+2733
*Xl*MGPF3	CCGGAGCTCGAGCCACCACCTAACTTCTAGATCG	+2818
XlMGPF4	CCGGAGCTCGAGTTCTAGATCGTACACCTTTGCC	+2831
*Xl*MGPF5	CCGGAGCTCGAGCACCTTTGCCCTCGGCTTCG	+2843
*Xl*MGPF6	CCGGAGCTCTTGCCCTCGGCTTCGGTTTTCT	+2852
*Xl*MGPF7	CCGGAGCTCCTACCAAATAGAGCCTCC	+1278
*Xl*MGPF8	ATCTCAAAGTTCCTTCATAGAG	+1
*Xl*MGPF9	ATGAAGACTCTTCCAGTTATTC	+3032
*Xl*MGPF10	CCGGAGCTCGAGCCACCAAAATAACTTCTAGATCGTAAAAATTTGCC	+2818
ODC-specific primers		
*ODC*F	CAGCTAGCTGTGGTGTGG	+674
*ODC*R	CAACATGGAAACTCACACC	+901

(*Xl*MGPR1; Table 1) and six different specific sense oligonucleotides (*Xl*MGPF1, *Xl*MGPF2, *Xl*MGPF3, *Xl*MGPF4, *Xl*MGPF5, and *Xl*MGPF6, respectively; Table 1). In each case, the sequence for a known restriction site was introduced within the primer and is underlined (Table 1). Point mutations were generated in the putative δEF1 by PCR amplification of the wild-type sequence with a forward primer (*Xl*MGP10; Table 1) containing a three-base pair mutation in each of the first two δEF1 motifs and the same specific reverse primer (*Xl*MGPR1; Table 1). All PCR fragments thus obtained were digested with *Xho*I and *Hin*dIII, and the resulting DNA fragments were gel purified and inserted into the promoterless pGL2 vector (Promega, Madison, WI, USA) previously digested with the same enzymes. The +1278/+2083LuC reporter construct was generated by PCR amplification with two specific oligonucleotides (*Xl*MGPF7 and *Xl*MGPR1; Table 1) and subsequent digestion with *Xho*I and *Hin*dIII. The resulting DNA fragment was inserted into the pGL2 vector as described above. Plasmids used for transfection studies were prepared using the plasmid Maxi Kit (Qiagen, Valencia, CA, USA). All constructs were verified by dsDNA sequencing. Transfection efficiencies were monitored using the control plasmid pTK-LUC.

Cell transfection and luciferase assays

The *X. laevis* A6 cell line (derived from kidney epithelial cells; ATCC No. CCL102) was cultured at 24 °C in 0.6 × L15 medium supplemented with 5% (v/v) fetal bovine serum and 1% (w/v) antibiotics (Invitrogen, Carlsbad, CA, USA). Cells were seeded at 60% confluence in six-well plates, and transient transfection assays were performed using the standard calcium phosphate coprecipitation technique [35] or Fugene (Roche Molecular Biochemicals, Indianapolis, IN, USA) as DNA carrier. Luciferase (LuC) activity was assayed as recommended by the manufacturer (Promega) in a TD-20/20 luminometer (Turner Designs, Fresno, CA, USA). Relative light units were normalized to protein concentration using the Coomassie dye binding assay (Pierce, Rockford, IL, USA). All experiments were repeated at least five times.

In luciferase assays performed directly in *X. laevis* embryos, embryos were injected radially in the marginal zone of the four-cell stage with a total of 200 pg pGL2-basic containing the appropriate promoter fragment and 25 pg pTK-Renilla luciferase. Embryos were scored at stage 11.5, lysed in 15 μL 1 × Passive Lysis Buffer per embryo, and centrifuged for 5 min at 8500 **g** to remove the pigment and yolk. Firefly and Renilla luciferase values were obtained by analyzing 15 μL lysate by the standard protocol provided in the Dual Luciferase Assay Kit (Promega) in a luminometer. All values are expressed as Relative Luciferase Units (firefly luciferase activity/Renilla luciferase activity). Each assay was performed in triplicate and repeated at least twice.

RNA preparation

Total RNA was prepared using the acid guanidinium thiocyanate procedure [36] or the Trizol reagent as recommended by the manufacturer (Invitrogen) from individual adult tissues, 5–10 million cells, or pools of randomly picked embryos, and then treated with RNase-free DNase I (Promega). The RNA integrity of each preparation was checked on 1% agarose/MOPS/formaldehyde gel stained with ethidium bromide [37].

RT-PCR amplification of MGP transcripts

From X. laevis embryos. First strand cDNA primed by random hexamers was synthesized with RevertAid™ H Minus M-MuLV Reverse Transcriptase (Fermentas, Hanover, MD, USA), and PCR was performed for 33 cycles (1 cycle: 30 s at 94 °C, 1 min at 60 °C, and 1 min at 68 °C) followed by a 10 min final extension at 68 °C, using as specific primers *Xl*MGPF8 or *Xl*MGPF9 combined with *Xl*MGPR2 (Table 1). As a control for the integrity of the RNA, *X. laevis* ornithine decarboxylase (ODC) was also amplified using specific oligonucleotides (*ODC*-F and *ODC*-R; Table 1) for 21 cycles under the conditions used for MGP amplification. For Southern blot analysis, PCR products were hybridized against a 315-bp (*Cla*I/*Xba*I) DNA probe containing the *Xl*MGP coding sequence (CDS).

From adult X. laevis tissues and cell line. cDNA amplifications were performed using RNA extracts from various *X. laevis* adult tissues including kidney, liver, bone, gonads, lung, intestine, muscle and heart and from A6 cells using the primers and procedures described above.

Whole mount *in situ* hybridization

Whole mount and hemi section *in situ* hybridization and probe preparation was carried out as previously described [12]. The plasmid containing *Xl*MGP CDS was linearized using *Xho*I and transcribed using T7 RNA polymerase to generate the antisense *in situ* hybridization probe. The sense *in situ* hybridization probe was obtained by digesting the above plasmid with *Xba*I and transcribing using T3 RNA polymerase. Stained embryos were bleached by illumination in solution containing 1% (v/v) H_2O_2, 4% (v/v) formamide and $0.5 \times$ NaCl/Cit, pH 7.0.

Acknowledgements

References

1 Cancela ML, Ohresser MCP, Reia JP, Viegas CSB, Williamson MK & Price PA (2001) Matrix Gla Protein in *Xenopus laevis*: molecular cloning, tissue distribution and evolutionary considerations. *J Bone Miner Res* **16**, 1611–1622.

2 Simes DC, Williamson MK, Ortiz-Delgado JB, Viegas CS, Price PA & Cancela ML (2003) Purification of matrix G1a protein from a marine teleost fish, *Argyrosomus regius*: calcified cartilage and not bone as the primary site of MGP accumulation in fish. *J Bone Miner Res* **18**, 244–259.

3 Fraser JD & Price PA (1988) Lung, heart, and kidney express high levels of mRNA for the vitamin K-dependent matrix gla protein. *J Biol Chem* **263**, 11033–11036.

4 Luo G, d'Souza R, Hougue D & Karsenty G (1995) The matrix gla protein is a marker of the chondrogenesis cell lineage during mouse development. *J Bone Miner Res* **10**, 325–334.

5 El-Maadawy S, Kaartinen MT, Schinke T, Murshed M, Karsenty G & McKee MD (2003) Cartilage formation and calcification in arteries of mice lacking matrix Gla protein. *Connect Tissue Res* **44** (Suppl. 1), 272–278.

6 Otawara Y & Price PA (1986) Developmental appearance of matrix GLA protein during calcification in the rat. *J Biol Chem* **261**, 10828–10832.

7 Luo G, Ducy P, McKee MD, Pinero GJ, Loyer E, Behringer RR & Karsenty G (1997) Spontaneous calcification of arteries and cartilage in mice lacking matrix Gla protein. *Nature* **386**, 78–81.

8 Yagami K, Suh J-Y, Enomoto-Iwamoto M, Koyama E, Abrams WR, Shapiro IM, Pacifici M & Iwamoto M (1999) Matrix Gla Protein is a developmental regulator of chondrocyte mineralization and, when constitutively expressed, blocks endochondral and intramembranous ossification in the limb. *J Cell Biol* **147**, 1097–1108.

9 Pinto JP, Conceição N, Gavaia PJ & Cancela ML (2003) Matrix Gla protein gene expression and protein accumulation colocalize with cartilage distribution during development of the teleost fish *Sparus aurata*. *Bone* **32**, 201–210.

10 Cancela L, Hsieh C-L, Francke U & Price PA (1990) Molecular structure, chromosome assignment and promoter organization of the human Matrix Gla protein gene. *J Biol Chem* **265**, 15040–15048.

11 Conceição N, Henriques NM, Ohresser MCP, Schule R & Cancela ML (2002) Molecular cloning of the Matrix Gla Protein gene from *Xenopus laevis*. Functional analysis of the promoter identifies a calcium sensitive region required for basal activity. *Eur J Biochem* **269**, 1947–1956.

12 Belo JA, Bouwmeester T, Leyns L, Kertesz N, Gallo M, Follettie M & De Robertis EM (1997) Cerberus-like is a secreted factor with neutralizing activity expressed in the anterior primitive endoderm of the mouse gastrula. *Mech Dev* **68**, 45–57.

13 Harada S, Sampath TK, Aubin JE & Rodan GA (1997) Osteogenic protein-1 up-regulation of the collagen X

promoter activity is mediated by a MEF-2-like sequence and requires an adjacent AP-1 sequence. *Mol Endocrinol* **11**, 1832–1845.

14 Borowsky B & Hoffman BJ (1998) Analysis of a gene encoding two glycine transporter variants reveals alternative promoter usage and a novel gene structure. *J Biol Chem* **273**, 29077–29085.

15 Kong RY, Kwan KM, Lau ET, Thomas JT, Boot-Handford RP, Grant ME & Cheah KS (1993) Intron-exon structure, alternative use of promoter and expression of the mouse collagen X gene, Col10a-1. *Eur J Biochem* **213**, 99–111.

16 Seth P, Mahajan VS & Chauhan SS (2003) Transcription of human cathepsin L mRNA species hCATL B from a novel alternative promoter in the first intron of its gene. *Gene* **321**, 83/91.

17 Joun H, Lanske B, Karperien M, Qian F, Defize L & Abou-Samra A (1997) Tissue-specific transcription start sites and alternative splicing of the parathyroid hormone (PTH) /PTH-related peptide (PTHrP) receptor gene: a new PTH/PTHrP receptor splice variant that lacks the signal peptide. *Endocrinology* **138**, 1742–1749.

18 Farzaneh-Far A, Davies JD, Braam LA, Spronk HM, Proudfoot D, Chan SW, O'Shaughnessy KM, Weissberg PL, Vermeer C & Shanahan CM (2001) A polymorphism of the human matrix gamma-carboxyglutamic acid protein promoter alters binding of an activating protein-1 complex and is associated with altered transcription and serum levels. *J Biol Chem* **276**, 32466–32473.

19 Fortini ME, Lai ZC & Rubin GM (1991) The *Drosophila zfh-1* and *zfh-2* genes encode novel proteins containing both zinc-finger and homeodomain motifs. *Mech Dev* **34**, 113–122.

20 Funahashi J, Kamachi Y, Goto K & Kondoh H (1991) Identification of nuclear factor δEF1 and its binding site essential for lens-specific activity of the δ1-crystallin enhancer. *Nucleic Acids Res* **19**, 3543–3547.

21 Funahashi J, Sekido R, Murai K, Kamachi Y & Kondoh H (1993) δ-Crystallin enhancer binding protein δEF1 is a zinc finger-homeodomain protein implicated in postgastrulation embryogenesis. *Development* **119**, 433–446.

22 Higashi Y, Moribe H, Takagi T, Sekido R, Kawakami K, Kikutani H & Kondoh H (1997) Impairment of T cell development in deltaEF1 mutant mice. *J Exp Med* **185**, 1467–1479.

23 Takagi T, Moribe H, Kondoh H & Higashi Y (1998) DeltaEF1, a zinc finger and homeodomain transcription factor, is required for skeleton patterning in multiple lineages. *Development* **125**, 21–31.

24 Terraz C, Toman D, Delauche M, Ronco P & Rossert J (2001) δEF1 binds to a far-upstream sequence of the mouse pro-1 (I) collagen gene and represses its expression in osteoblasts. *J Biol Chem* **276**, 37011–37019.

25 Murray D, Precht P, Balakir R & Horton WE Jr (2000) The transcription factor δEF1 is inversely expressed with type II collagen mRNA and can repress *Col2a1* promoter activity in transfected chondrocytes. *J Biol Chem* **275**, 3610–3618.

26 Sooy K & Demay MB (2002) Transcriptional repression of the rat osteocalcin gene by δEF1. *Endocrinology* **143**, 3370–3375.

27 Wessely O & De Robertis EM (2000) The *Xenopus* homologue of Bicaudal-C is a localized maternal mRNA that can induce endoderm formation. *Development* **127**, 2053–2062.

28 Bonham K, Ritchie SA, Dehm SM, Snyder K & Boyd FM (2000) An alternative, human SRC promoter and its regulation by hepatic nuclear factor-1alpha. *J Biol Chem* **275**, 37604–37611.

29 Bostrom K, Tsao D, Shen S, Wang Y & Demer LL (2001) Matrix GLA protein modulates differentiation induced by bone morphogenetic protein-2 in C3H10T1/2 cells. *J Biol Chem* **276**, 14044–14052.

30 Zebboudj AF, Shin V & Bostrom K (2003) Matrix GLA protein and BMP-2 regulate osteoinduction in calcifying vascular cells. *J Cell Biochem* **90**, 756–765.

31 Urist MR, Huo YK, Brownell AG, Hohl WM, Buyske J, Lietze A, Tempst P, Hunkapiller M & DeLange RJ (1984) Purification of bovine bone morphogenetic protein by hydroxyapatite chromatography. *Proc Natl Acad Sci USA* **81**, 371–375.

32 Munoz-Sanjuan I & Brivanlou AH (2002) Neural induction, the default model and embryonic stem cells. *Nat Rev Neurosci* **3**, 271–280.

33 Jono S, Ikari Y, Vermeer C, Dissel P, Hasegawa K, Shioi A, Taniwaki H, Kizu A, Nishizawa Y & Saito S (2004) Matrix Gla protein is associated with coronary artery calcification as assessed by electron-beam computed tomography. *Thromb Haemost* **91**, 790–794.

34 Barone LM, Owen TA, Tassinari MS, Bortell R, Stein GS & Lian JB (1991) Developmental expression and hormonal regulation of the rat matrix Gla protein (MGP) gene in chondrogenesis and osteogenesis. *J Cell Biochem* **46**, 351–365.

35 Pfitzner E, Becker P, Rolke A & Schüle R (1995) Functional antagonist between the retinoic acid receptor and the viral transactivator BZLF1 is mediated by protein–protein interactions. *Proc Natl Acad Sci USA* **92**, 12265–12269.

36 Chomczynski P & Sacci N (1987) Single step method of RNA isolation by acid guanidinium thiocyanate-phenol-chloroform extraction. *Anal Biochem* **162**, 156–159.

37 Sambrook J, Fritsch EF & Maniatis T (1989) *Molecular Cloning: a Laboratory Manual*, 2nd edn. Cold Spring Harbor Laboratory Press, Cold Spring Harbor, NY.

Cerberus is a feedback inhibitor of Nodal asymmetric signaling in the chick embryo

Ana Teresa Tavares[1],*, Sofia Andrade[1], Ana Cristina Silva[1,2] and José António Belo[1,2],*

The TGF-β-related molecule Nodal plays an essential and conserved role in left-right patterning of the vertebrate embryo. Previous reports have shown that the zebrafish and mouse Cerberus-related proteins Charon and Cerberus-like-2 (Cerl-2), respectively, act in the node region to prevent the Nodal signal from crossing to the right side, whereas chick Cerberus (cCer) has an unclear function in the left-side mesoderm. In this study, we investigate the transcriptional regulation and function of cCer in left-right development. By analyzing the enhancer activity of *cCer* 5′ genomic sequences in electroporated chick embryos, we identified a *cCer* left-side enhancer that contains two FoxH1 and one SMAD binding site. We show that these Nodal-responsive elements are necessary and sufficient for the activation of transcription in the left-side mesoderm. In transgenic mouse embryos, *cCer* regulatory sequences behave as in chick embryos, suggesting that the cis-regulatory sequences of *Cerberus*-related genes have diverged during vertebrate evolution. Moreover, our findings from *cCer* overexpression and knockdown experiments indicate that cCer is a negative-feedback regulator of Nodal asymmetric signaling. We propose that cCer and mouse Cerl-2 have evolved distinct regulatory mechanisms but retained a conserved function in left-right development, which is to restrict Nodal activity to the left side of the embryo.

KEY WORDS: Cerberus, FoxH1, Nodal signaling, Left-right asymmetry, Transcriptional regulation, Chick, Mouse

INTRODUCTION

Chick Cerberus (cCer; also known as Caronte) is a member of the Cerberus-Dan family of cysteine-knot-secreted proteins (Rodriguez Esteban et al., 1999; Yokouchi et al., 1999; Zhu et al., 1999). Cerberus-related proteins have been identified in other vertebrate species: the founding member *Xenopus* Cerberus (XCer) (Bouwmeester et al., 1996), zebrafish Charon (Hashimoto et al., 2004), mouse Cerberus-like (hereafter denominated Cerl-1) (Belo et al., 1997; Biben et al., 1998; Shawlot et al., 1998) and mouse Cerberus-like-2 (Cerl-2; also known as Dand5 or Dante) (Marques et al., 2004). *Xenopus XCer*, mouse *Cerl-1* and chick *Cer* genes are syntenic (www.metazome.net) and, at early stages, are expressed in equivalent embryonic structures, such as the anterior endomesoderm, anterior visceral endoderm and hypoblast, respectively (Bouwmeester et al., 1996; Belo et al., 1997; Foley et al., 2000). Mouse *Cerl-1* and chick *Cer* transcripts are also detected in the anterior definitive mesendoderm (Belo et al., 1997; Rodriguez Esteban et al., 1999). However, at later stages, *Cerberus*-related genes have very distinct patterns: *XCer* expression is no longer detected, mouse *Cerl-1* transcripts are found in nascent somites and presomitic mesoderm, zebrafish *charon* and mouse *Cerl-2* are expressed around the node region (*Cerl-2* expression levels are higher on the right side), and chick *Cer* is expressed in the left paraxial and lateral plate mesoderm (Bouwmeester et al., 1996; Belo et al., 1997; Rodriguez Esteban et al., 1999; Marques et al., 2004; Hashimoto et al., 2004). The understanding of how these different patterns of expression are generated may bring some insights into the evolution of *Cerberus*-related genes and their functions in the different vertebrate species.

[1]Instituto Gulbenkian de Ciência, 2781-901 Oeiras, Portugal. [2]Institute for Biotechnology and Bioengineering, Centro de Biomedicina Molecular e Estrutural, Universidade do Algarve, 8005-139 Faro, Portugal.

*Authors for correspondence (e-mails: atavares@igc.gulbenkian.pt; jbelo@ualg.pt)

A conserved regulator of vertebrate left-right patterning is *Nodal*, a member of the transforming growth factor-β (TGF-β) family of signaling molecules that is expressed in the node region and left lateral plate mesoderm (reviewed by Hamada et al., 2002; Schier, 2003). In the mouse embryo, Nodal activity is restricted to the left side by Cerl-2 (Marques et al., 2004), by the midline barrier and by *Lefty2*, a Nodal antagonist also expressed in the left lateral plate mesoderm (reviewed by Juan and Hamada, 2001). The left-side expression of *Nodal* and *Lefty2* is directly regulated by Nodal itself. Our present findings demonstrate that *cCer* asymmetric expression is also directly activated by Nodal signaling and suggest that the cis-regulatory sequences of *Cerberus*-related genes have diverged among vertebrates.

Zebrafish *charon*, mouse *Cerl-2* and chick *Cer* have all been implicated in the determination of the left-right axis, but their functions seem to differ: zebrafish *charon* and mouse *Cerl-2* have a role in preventing Nodal signals from crossing to the right side (Hashimoto et al., 2004; Marques et al., 2004), whereas chick *Cer* was reported to have a role in transferring the positional information from the node to the left lateral plate mesoderm (Rodriguez Esteban et al., 1999; Yokouchi et al., 1999). At the molecular level, Cerberus-related proteins behave as antagonists of members of the TGF-β family (Hsu et al., 1998; Rodriguez Esteban et al., 1999; Piccolo et al., 1999; Belo et al., 2000). During left-right patterning, zebrafish Charon and mouse Cerl-2 proteins were shown to act as Nodal antagonists (Hashimoto et al., 2004; Marques et al., 2004), whereas cCer has been proposed to act as a bone morphogenetic protein (BMP) antagonist (Rodriguez Esteban et al., 1999; Yokouchi et al., 1999). Chick Cer would allow the expression of *Nodal* in the left lateral plate mesoderm by inhibiting the repressive activity of BMPs on *Nodal* transcription. However, more recent reports have shown that BMP signaling is indeed essential for the activation of Nodal expression in the left lateral plate (Piedra and Ros, 2002; Schlange et al., 2002), leaving the role of cCer in left-right patterning unexplained. Our results from overexpression and knockdown experiments demonstrate that cCer acts as a negative regulator of

Nodal expression and prevents Nodal signaling from crossing to the right side. In conclusion, we propose that chick Cer, zebrafish Charon and mouse Cerl-2 evolved different regulatory mechanisms but retained a similar role in restricting Nodal activity to the left side.

MATERIALS AND METHODS

Isolation of a *cCer* genomic clone and sequence analysis

A *cCer* genomic clone (clone MPMGc125J2191Q3 from RZPD, Germany) was isolated by screening a chicken cosmid library (RZPD no. 125) with a *cCer* sequence probe (gift from J. C. Izpisúa Belmonte, The Salk Institute, La Jolla, CA). Shorter DNA fragments of this clone were introduced into pBluescriptIIKS (Stratagene), sequenced and identified as containing the 5′, cDNA, intronic and 3′ regions of the *cCer* gene.

To recognize possible binding sites for known transcription factors, *cCer* 5′ genomic sequences were analyzed using MatInspector Professional release 7.4 (Quandt et al., 1995).

To identify the transcription initiation site(s), 5′ rapid amplification of cDNA ends was performed using total RNA from HH3-9 chick embryos and the RLM-RACE kit (Ambion). PCR products were size-fractionated by agarose gel electrophoresis, purified using a gel extraction kit (Qiagen), cloned into the pGEM-T Easy vector (Promega) and sequenced.

DNA constructs and morpholinos

cCer 5′ genomic sequences were subcloned into an enhanced green fluorescence protein (EGFP) reporter vector containing the *EGFP* coding sequence and the SV40 early mRNA polyadenylation signals from pEGFP-N3 (Clontech). Deletions or point mutations of FoxH1- and SMAD-binding elements were designed according to the literature (Zhou et al., 1998; Mostert et al., 2001) and introduced into the *Cer0.36-EGFP* construct by PCR-based site-directed mutagenesis.

For the enhancer assays, *cCer* genomic sequences were either amplified by PCR (PCR1-5) or synthesized as complementary oligonucleotides, and subcloned into the p1229-*EGFP* enhancer-less vector. This vector carries the human β-globin minimal promoter and was generated by replacing the *lacZ* gene in the β-globinlacZ BGZA or p1229 vector (Yee and Rigby, 1993) with the *EGFP* coding sequence (Clontech).

Chick expression plasmids were based on a modified pCAGGS-MCS vector (gift from D. Henrique, Instituto de Medicina Molecular, Lisbon, Portugal) (Niwa et al., 1991). The coding sequence of *Xenopus Cerberus-short* (*XCerS*) was amplified by PCR from a pCS2-*XCerS* vector (gift from S. Piccolo) (Piccolo et al., 1999). The *cCer* coding sequence (cCerCDS) was isolated by reverse transcriptase (RT)-PCR according to the published sequence (GenBank accession no. AF179484) (Rodriguez Esteban et al., 1999) and subcloned into the *Xho*I and *Not*I sites of pCAGGS-MCS.

The pCAGGS-*RFP* vector (gift from D. Henrique), carrying the cDNA of monomeric red fluorescent protein (RFP; Clontech) (Campbell et al., 2002) under the control of the CAGGS promoter, was used to control the extent and efficiency of electroporation.

To generate the luciferase (luc) reporter constructs, *cCer* regulatory sequences were amplified by PCR (using *Cer-EGFP* plasmids as template) and subcloned into the pGL2-Basic vector (Promega).

Fluorescein-tagged antisense morpholino oligonucleotides (cCer MO: 5′-CATGGTCCTGCTGATGCTGTAGATC-3′; cCer CoMO: 5′-CATcGT-CgTGCTcATGaTGTAcATC-3′, mismatches in lowercase) were designed and produced by Gene Tools. The efficacy of cCer morpholinos to inhibit the translation of *Cer-Luc* reporter constructs was tested in a cell-free transcription/translation system (see Fig. S3 in the supplementary material) (Summerton et al., 1997).

Bead implantation and whole-mount in situ hybridization

Fertilized chicken eggs (Quinta da Freiria) were incubated at 37.5°C for the appropriate period. Embryos were staged according to Hamburger and Hamilton (HH) (Hamburger and Hamilton, 1951), explanted at HH stage 4-7 (HH4-7) together with the vitelline membrane and anchored to a metacrilate ring according to the protocol of New (New, 1955). Affigel-blue beads (Bio-Rad) were soaked in Shh protein [1 mg/ml in 0.1% bovine serum albumin (BSA)/phosphate-buffered saline (PBS); R&D Systems]; heparin acrylic beads (Sigma) were soaked in recombinant Nodal protein

(0.5 mg/ml; R&D Systems); and AG1-X2 anion-exchange beads (Bio-Rad) were soaked either in SU5402 [3 mM in dimethylsulfoxide (DMSO); Calbiochem] (Mohammadi et al., 1997) or in SB-431542 (10 mM in DMSO; Tocris) (Inman et al., 2002). Treated embryos were cultured at 37.5°C in a humid chamber, fixed in 4% paraformaldehyde and processed for whole-mount in situ hybridization.

Whole-mount in situ hybridization on chicken and mouse embryos was performed as described by Liguori et al. (Liguori et al., 2003). Detailed descriptions of the RNA probes used are available from the authors on request. Embryos were developed with BM purple (Roche) for purple color and with INT/BCIP (Roche) for orange.

Embryo electroporation

Embryos were processed for New culture (New, 1955) at HH3-5 and transferred into a silicon rubber pool containing a 2 mm-square cathode (CY700-1Y electrode; Nepa Gene). The ring was then covered with warmed Hank's buffer (GibcoBRL) and the embryo was injected with a DNA solution (0.5-3 mg/ml; 0.1% Fast Green; Sigma) using a pulled glass capillary and an IM-300 microinjector (Narishige). Electroporation was performed by placing a 2 mm-square anode (CY700-2 electrode; Nepa Gene) over the embryo and applying five pulses (10 V for 50 ms at 350 ms intervals) using a square wave electroporator (ECM830; BTX). The embryo was then placed on a 30 mm Petri dish with albumen (New, 1995), incubated for the appropriate period of time (7-48h), and observed under a fluorescence stereomicroscope (Leica MZ16FA).

Luciferase reporter assay

Capped sense mouse *Nodal* mRNA was synthesized using the mMessage mMachine kit (Ambion). Eggs were obtained from *Xenopus laevis* females, cultured and microinjected as previously described (Medina et al., 2000). Embryonic stages were determined according to Nieuwkoop and Faber (Nieuwkoop and Faber, 1967). *Xenopus* embryos were injected in each animal blastomere of the eight-cell stage with a total of 200 pg of reporter plasmid, with or without *Nodal* mRNA (50 pg), and 25 pg of pTK-Renilla luciferase. Animal caps were isolated from the blastula stage, cultured until sibling embryos reached stage 12 and lysed in 20 μL of passive lysis buffer per cap. Firefly and Renilla luciferase values were obtained by analyzing 20 μL lysate by the standard protocol provided in the Dual Luciferase Assay kit (Promega) in a luminometer (MicroLumatPlus, Berthold Technologies). Each assay was performed in triplicate and repeated independently at least twice.

Generation of transgenic mouse embryos

The transgenic mouse line *Cer2.5-EGFP* was generated by microinjection of linearized reporter construct DNA into the pronuclei of fertilized eggs from FVB mice, as described (Nagy et al., 2003). F1 embryos were collected from embryonic day (E)7.5 to E10.5, observed under a fluorescence stereomicroscope (Leica MZ16FA), fixed in 4% paraformaldehyde and processed for whole-mount in situ hybridization. For histological analyses, embryos were embedded in gelatin, cryosectioned and photographed under a fluorescence microscope (Leica DMRA2). In some slides, cell nuclei were labeled with DAPI (Molecular Probes).

RESULTS

Nodal signaling regulates *cCer* expression in the left-side mesoderm

In the chick embryo, sonic hedgehog (Shh) signaling positively regulates *Nodal* asymmetric expression (Pagán-Westphal and Tabin, 1998). In turn, Nodal was shown to induce the expression of *XCer* (Osada et al., 2000) and mouse *Cerl-1* (Waldrip et al., 1998; Brennan et al., 2001). Therefore, the induction of *cCer* expression by Shh (Rodriguez Esteban et al., 1999; Yokouchi et al., 1999; Zhu et al., 1999) might be mediated by Nodal. To test this hypothesis, beads soaked in recombinant mouse Nodal protein were implanted on the right side of HH6 chick embryos and *cCer* expression was examined by whole-mount in situ hybridization. Indeed, ectopic expression of *cCer* was observed in the right-side mesoderm of these embryos
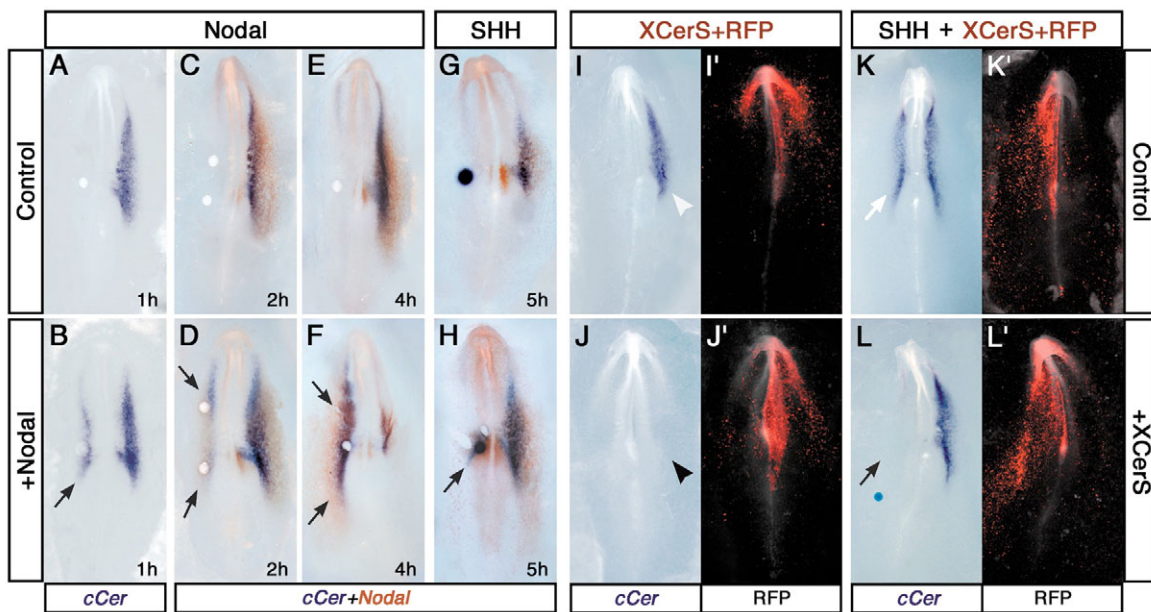
Fig. 1. Regulation of chick *Cer* and *Nodal* expression by Nodal and Shh signaling pathways. (A-H) Beads soaked in phosphate-buffered saline (PBS, control; A,C,E,G), Nodal protein (B,D,F) or Shh protein (H) were implanted on the right side at Hamburger and Hamilton stage 7 (HH7; A-F) or HH4 (G,H). Chick embryos were fixed after 1 hour (A,B), 2 hours (C,D), 4 hours (E,F) or 5 hours (G,H) and processed for single-label [chick *Cer* (*cCer*); A,B] or double-label (*cCer* and *Nodal*; C-H) whole-mount in situ hybridization (*cCer*, purple; *Nodal*, orange). Nodal protein induced the right-side expression of *cCer* transcripts in less than 1 hour (B; arrow), and *Nodal* transcripts in approximately 2 hours (D; arrows). After 4 hours, both *cCer* and *Nodal* expression levels were higher on the right than on the left side (F; arrows). On the other hand, Shh protein took approximately 5 hours to induce the transcription of both *cCer* and *Nodal* (H; arrow). **(I-L)** *cCer* transcripts detected by whole-mount in situ hybridization. **(I′,J′,K′,L′)** Merge of bright-field and RFP red fluorescence images. (I-J′) Effect of the Nodal antagonist *Xenopus* CerS (XCerS) on *cCer* expression. (J,J′) Chick embryos were electroporated with pCAGGS-XCerS on the left side of the node at HH4 (i.e. in the cells that express *Nodal*). pCAGGS-*RFP* was electroporated alone (control; I,I′) or with pCAGGS-XCerS (J,J′), and used to label the populations of electroporated cells. In contrast to the control electroporation (I; arrowhead), the inhibition of Nodal by XCerS suppressed the left-sided expression of *cCer* (J; arrowhead). (K-L′) Effect of the Nodal antagonist XCerS on Shh-induced *cCer* expression. HH4 chick embryos were electroporated with pCAGGS-*RFP* alone (control; K,K′) or co-electroporated with pCAGGS-*RFP* and pCAGGS-*XCerS* (L,L′), and grafted on the right side with beads soaked in Shh protein. Ectopic induction of *cCer* expression by Shh (K; arrow) was suppressed by the Nodal inhibitor XCerS (L; arrow). All embryos are viewed from the ventral side. *cCer*, chick *Cer*; RFP, red fluorescent protein; XCerS, *Xenopus* CerS.

(81%, *n*=33, Fig. 1A-F). *cCer* was also induced in embryos electroporated with a *Dorsalin-Nodal* expression construct (pCAGGS-*DcNodal*) (Bertocchini and Stern, 2002), but with less efficiency (35%, *n*=23, data not shown).

It has been suggested that Shh induces *Nodal* in the chick lateral plate mesoderm via a secondary signal (Pagán-Westphal and Tabin, 1998). In the mouse embryo, *Nodal* expression in the left lateral plate mesoderm is directly activated by Nodal protein produced in the node (Saijoh et al., 2003; Yamamoto et al., 2003). Accordingly, we observed that exogenous Nodal protein is able to activate *Nodal* expression in the right lateral plate mesoderm of chick embryos (68%, *n*=19, Fig. 1C-F). Nodal protein induced ectopic *cCer* expression in less than 1 hour (73%, *n*=11, Fig. 1B and data not shown) and *Nodal* expression in approximately 2 hours (71%, *n*=7, Fig. 1D), whereas beads soaked in Shh protein started to activate *cCer* and *Nodal* transcription no sooner than 4-5 hours after implantation (66%, *n*=6, Fig. 1H; 0% 2 hours after implantation, *n*=5, data not shown). Taken together, these observations suggest that the transcription of *cCer* and *Nodal* is directly regulated by Nodal.

To determine whether endogenous Nodal signaling is necessary for *cCer* expression, chick embryos were electroporated with a pCAGGS expression vector containing the Nodal-specific antagonist *Xenopus Cerberus-short* (*XCerS*) (Piccolo et al., 1999; Bertocchini and Stern, 2002). Embryos were co-electroporated with pCAGGS-red fluorescent protein (RFP) and initially scored for the co-localization of RFP fluorescence and *XCerS* mRNA (data not shown). As expected, the inhibition of Nodal by XCerS resulted in the downregulation of *cCer* (89%, *n*=9, Fig. 1J) and *Nodal* (85%, *n*=13, data not shown), whereas control electroporations had no effect (*n*=10, Fig. 1I). Similarly, *cCer* expression was also repressed by SB-431542, an inhibitor of Nodal receptors (88%, *n*=16, see Fig. S1 in the supplementary material). Therefore, we conclude that endogenous Nodal signaling is required for normal activation of *cCer* and *Nodal* expression in the left lateral plate mesoderm. In addition, ectopic induction of *cCer* by Shh protein was inhibited by XCerS (86%, *n*=7, Fig. 1L), which demonstrates that Nodal signaling is required for the activation of *cCer* expression by Shh.

Identification of the *cCer* left-side enhancer

To investigate further whether *cCer* is a direct target of Nodal signaling, we analyzed the regulatory sequences responsible for *cCer* transcription in the left-side mesoderm. For this, *cCer* 5′ genomic sequences of different lengths were subcloned into an enhanced green fluorescence protein (EGFP) reporter vector (*Cer-EGFP* constructs) and introduced into chick embryos by
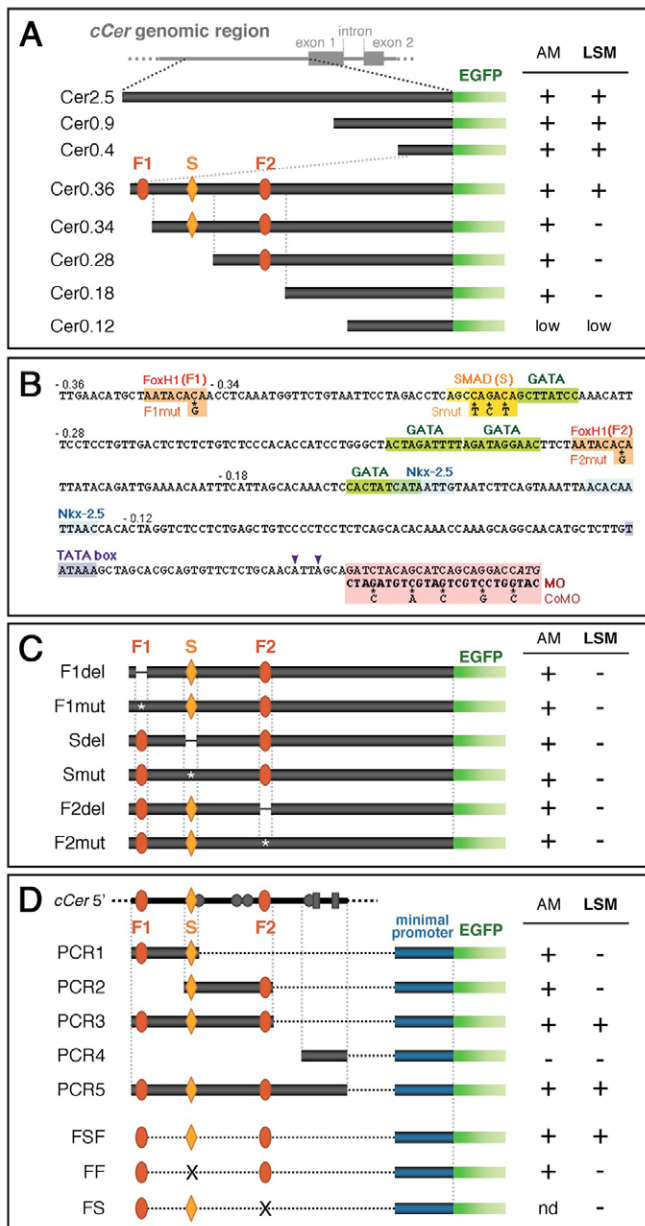
Fig. 2. Identification of the chick *Cer* left-side enhancer.
(**A**) Deletion analysis of chick *Cer* (*cCer*) cis-regulatory sequences. The genomic organization of *cCer* is depicted at the top. *cCer* 5′ sequences (black boxes) were fused to the reporter *EGFP* gene (green boxes) to determine the activity of each DNA fragment. The FoxH1 elements (red; F1 and F2) and the SMAD element (orange; S) are depicted in the reporter constructs. The presence (+) or absence (−) of *EGFP* expression in the anterior mesendoderm and its derivatives (AM) and in the left-side mesoderm (LSM) from electroporated chick embryos is listed on the right. Each result is representative of at least 12 embryos. LSM expression was disrupted in embryos electroporated with *Cer0.34* or shorter constructs. *Cer0.12-EGFP* expression was very weak and ubiquitous (low). (**B**) Nucleotide sequence of the 5′-flanking region of *cCer*. Binding sites for the transcription factors FoxH1 (F1 and F2; orange), SMAD (S; yellow), GATA (green) and Nkx-2.5 (light blue), and a putative TATA box (purple), are outlined. Two transcription initiation sites were identified by RLM-RACE at positions −26 and −29 upstream of the ATG (arrowheads). Point mutations were introduced into the F1, S and F2 sites, as indicated. The morpholino antisense oligo sequence (MO) and its control oligo with five mismatches (CoMO) are outlined in pink. (**C**) Site-directed mutagenesis analysis of FoxH1- and SMAD-binding elements. LSM expression was specifically abolished in embryos transfected with constructs carrying deletions or mutations (*) in the FoxH1 (F1del, F1mut, F2del and F2mut) or SMAD (Sdel and Smut) elements. (**D**) Enhancer analysis of potential regulatory sequences of *cCer*. Fragments of the *cCer* 5′ region (PCR1-5) and sequences of the FoxH1 and SMAD elements (FSF, FF and FS) were subcloned into an enhancer-less vector carrying the human beta-globin minimal promoter (blue boxes) upstream of the *EGFP* coding sequence. LSM expression was detected in embryos electroporated with the PCR3, PCR5 and FSF constructs (which contained all of the F1, F2 and S elements), but not in those electroporated with the PCR1, PCR2, PCR4, FF and FS constructs (which lacked at least one of those sites). EGFP fluorescence was observed in the AM of embryos electroporated with each of the EGFP reporter constructs tested, with the exception of PCR4. FS-EGFP expression was not tested in the AM cells (nd). +/−, presence/absence of *EGFP* expression; AM, anterior mesendoderm and its derivatives; CoMo, control morpholino oligo sequence; EGFP, enhanced green fluorescence protein; F1/F2, FoxH1-binding sites; LSM, left-side mesoderm; MO, morpholino antisense oligo sequence; nd, not tested. S, SMAD-binding site.

microinjection and electroporation in New culture (New, 1955). A representation of these constructs and their electroporation results are summarized in Fig. 2A.

Our initial results showed that a 2.5 kb DNA fragment upstream of the ATG of *cCer* (Cer2.5) was able to drive the expression of *EGFP* into the cell populations that express *cCer* (i.e. the anterior mesendoderm and left paraxial and lateral plate mesoderm) (Rodriguez Esteban et al., 1999; Yokouchi et al., 1999; Zhu et al., 1999). Fluorescent cells are later detected in the foregut and heart (data not shown), which are derivatives of the chick anterior mesendoderm. The subsequent analysis of *EGFP* expression driven by shorter fragments (Cer0.9, Cer0.4 and Cer0.36) revealed a similar pattern (Fig. 3A,C, and data not shown). However, left-side expression was specifically disrupted in embryos electroporated with *Cer0.34-EGFP* and shorter constructs (data not shown). These

observations indicate that the *cCer* left-side enhancer is located in the 360 bp 5′ region and that the −360 to −340 sequence contains an essential regulatory element.

FoxH1 and SMAD elements are essential for *cCer* enhancer activity in the left-side mesoderm

To confirm that *cCer* left-side expression is directly activated by Nodal, we first analyzed the *cCer* left-side enhancer sequence and looked for the presence of FoxH1- and SMAD-binding sites. These transcription factors are nuclear effectors of the Nodal signaling pathway (reviewed in Schier and Shen, 2000) and were shown to directly regulate the asymmetric expression of the *Nodal*, *Lefty2* and *Pitx2* genes (Saijoh et al., 2000; Osada et al., 2000; Yashiro et al., 2000; Shiratori et al., 2001). Sequence analysis of the *cCer* 360 bp 5′ region (Cer0.36) using MatInspector software (Professional

release 7.4) revealed the presence of a possible TATA box at –60, and consensus binding sites for several putative regulators of *cCer* transcription, including two FoxH1 and one SMAD element (Fig. 2B).

To determine whether the FoxH1 elements (F1 and F2) or the SMAD element (S) are necessary for the regulation of *cCer* asymmetric expression, we constructed *Cer0.36-EGFP* reporter vectors containing deletions (del) or mutations (mut) in each one of those sites that were previously shown to disrupt their activity (F1del, F1mut, F2del, F2mut, Sdel and Smut) (Zhou et al., 1998; Mostert et al., 2001) (indicated in Fig. 2B). Each of the F1del, F1mut, F2del, F2mut, Sdel and Smut constructs was electroporated into chick embryos, and EGFP fluorescence was analyzed both in the anterior mesendoderm and in the left-side mesoderm (results are summarized in Fig. 2C). All constructs were able to drive *EGFP* expression in the anterior mesendoderm (Fig. 3B and data not shown), but left-side expression was specifically abolished (Fig. 3D and data not shown). These observations demonstrate that the FoxH1 and SMAD sites in *Cer0.36* are essential for the induction or maintenance of left-side transcription.

In addition, the functions of the FoxH1 and SMAD elements in the *cCer* left-side enhancer were quantified in luciferase reporter assays with *Xenopus* animal caps. The *Cer0.36* reporter construct was clearly activated in the presence of Nodal (Fig. 3I). However, luciferase activity was reduced with the introduction of mutations in one of the FoxH1 or SMAD elements (F1mut, Smut and F2mut constructs; Fig. 3I). Taken together, our results indicate that the *cCer* left-side enhancer is directly activated by the Nodal-FoxH1/SMAD signaling pathway.

FoxH1 and SMAD elements are sufficient to activate the *cCer* left-side enhancer

We next investigated whether the FoxH1 and SMAD elements in the *cCer* left-side enhancer are sufficient to induce left-side expression. For this, potential regulatory sequences were subcloned into enhancer-less vectors that contain the human beta-globin minimal promoter upstream of either the *EGFP* or the luciferase reporter gene. The potential enhancer sequences tested were either shorter fragments of *Cer0.36* (PCR1-5) or combinations of individual FoxH1 (F) and SMAD (S) elements (FSF, FF and FS; results are summarized in Fig. 2D). Embryos electroporated with PCR1, PCR2, PCR4, FF or FS did not display *EGFP* expression in the left-side mesoderm (Fig. 3F,H, and data not shown). By contrast, asymmetric expression was detected in embryos electroporated with the PCR3, PCR5 or FSF constructs (Fig. 3E,G, and data not shown). Accordingly, luciferase activities of the reporter constructs that lack one of the FoxH1 or SMAD elements (PCR1, PCR2, FS and FF) were severely reduced when compared with those of PCR3 or FSF (Fig. 3J). These observations indicate that the FSF module in the *cCer* left-side enhancer is sufficient to activate asymmetric expression.

Regulation of the *cCer* left-side enhancer by Nodal signaling

Asymmetric expression of *cCer* is induced by Shh on the left side and repressed by fibroblast growth factor 8 (FGF8) on the right side (Rodriguez Esteban et al., 1999; Yokouchi et al., 1999; Zhu et al., 1999). To investigate whether the *cCer* enhancer region is also regulated by these signaling molecules, chick embryos were electroporated with *Cer0.4-EGFP* and grafted on the right side of the node with beads soaked either in Shh protein or in the FGF receptor-1 inhibitor SU5402. In addition to the expected left-side pattern, *EGFP* expression was activated on the right side both by the
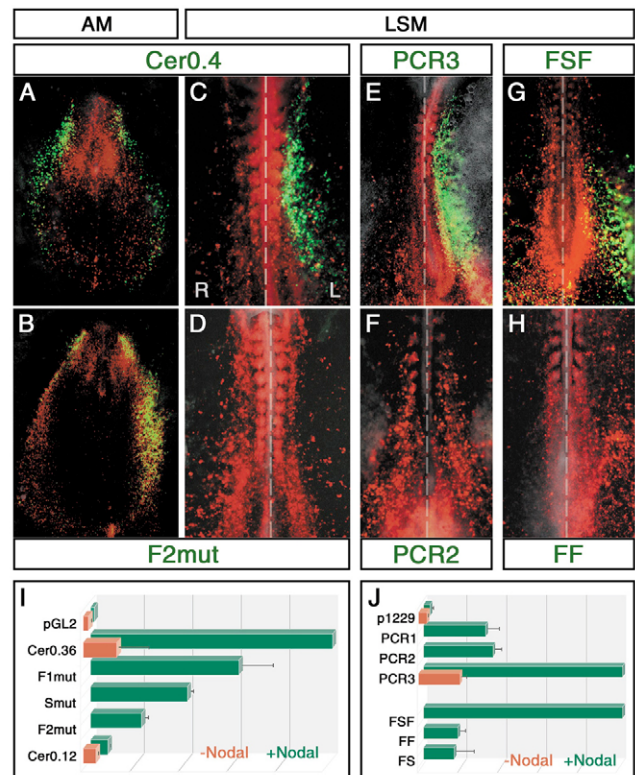
Fig. 3. Expression analysis of *Cer-EGFP* reporter constructs. (A-H) *Cer-EGFP* reporter expression in electroporated chick embryos. Different embryos were co-transfected with one *Cer-EGFP* reporter construct (green fluorescence) and the pCAGGS-*RFP* construct (positive control; red fluorescence). (A,C) Cer0.4-EGFP; (B,D) F2mut; (E) PCR3; (F) PCR2; (G) FSF; (H) FF (see Fig. 2 for construct details). (A,B) EGFP fluorescence was observed in the anterior mesendoderm (AM) of embryos electroporated with Cer0.4 (A) and F2mut (B) reporter constructs. Embryos were electroporated at Hamburger and Hamilton stage 3 (HH3) and fixed at HH6. (C-H) Asymmetric *EGFP* expression was detected in the left-side mesoderm (LSM) of embryos electroporated with Cer0.4 (C), PCR3 (E) and FSF (G), but not in those electroporated with the F2mut (D), PCR2 (F) or FF (H) reporter constructs. Embryos were electroporated at HH4-5 and fixed at HH8-9. Dashed line separates the right and left sides of the embryos. (**I,J**) *Cer-Luc* reporter activity in *Xenopus* animal cap luciferase assays. Luciferase reporter plasmids containing the indicated wild-type or mutant fragments of chick *Cer* (*cCer*) regulatory sequences were injected into *Xenopus* embryos in the absence (orange) or presence (green) of *Nodal* mRNA. Data are relative to the highest luciferase activity values (Cer0.36+Nodal in I; PCR3+Nodal and FSF+Nodal in J). The activities of reporter constructs that either lack one of the FoxH1 elements (F1mut, F2mut, PCR1, PCR2 or FS) or lack the SMAD element (Smut and FF) were reduced. AM, anterior mesendoderm; L, left; LSM, left-side mesoderm; R, right.

Shh protein (100%, $n=10$, Fig. 4C) and by SU5402 (62%, $n=13$, Fig. 4D). These observations demonstrate that the *cCer* left-side enhancer is regulated by Shh and FGF signaling in the same way as *cCer* expression.

To confirm that *cCer* enhancer activity is regulated by Nodal, embryos were electroporated with the *Cer0.4-EGFP* reporter construct and grafted with beads soaked in Nodal protein. As expected, Nodal was able to ectopically induce *EGFP* expression in the right-side mesoderm (100%, $n=11$, Fig. 4B; compare with
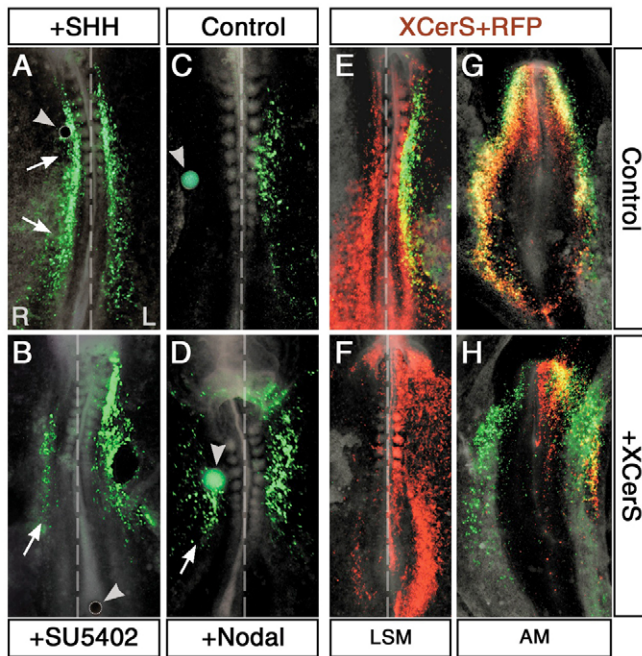
Fig. 4. Regulation of the chick *Cer* left-side enhancer by Shh, FGF and Nodal signaling pathways. (A-F) Analysis of *Cer-EGFP* expression in the left-side mesoderm (LSM) of embryos electroporated at HH4-5 and fixed at HH8-9. (G,H) Analysis of *Cer-EGFP* expression in the anterior mesendoderm (AM) of embryos electroporated at HH3 and fixed at HH6. (A-D) Chick embryos were electroporated with *Cer0.4-EGFP* and grafted with beads (arrowheads) soaked in Shh protein (A), the FgfR1 inhibitor SU5402 (B), phosphate-buffered saline (PBS, control; C) or Nodal protein (D). *EGFP* expression was ectopically induced on the right side by Shh, SU5402 and Nodal (arrows). (E-H) Effect of the Nodal antagonist *Xenopus* CerS (XCerS) on chick *Cer* (*cCer*) left-side enhancer activity. Chick embryos were electroporated either with pCAGGS-*RFP* and *PCR5-EGFP* (control; E,G) or with these plus pCAGGS-*XCerS* (F,H). XCerS repressed the transcription of *PCR5-EGFP* in the LSM (E,F), whereas it had no effect on AM expression (G,H). AM, anterior mesendoderm; LSM, left-side mesoderm; XCerS, *Xenopus* CerS.

control, *n*=5, Fig. 4A). Conversely, when embryos were co-electroporated with the *PCR5-EGFP* reporter construct and the Nodal antagonist *XCerS* (pCAGGS-*XCerS*), *cCer* enhancer activity was specifically repressed in the left-side mesoderm (64%, *n*=11, Fig. 4F; compare with control, *n*=4, Fig. 4E). XCerS did not have an effect on anterior mesendoderm expression (*n*=4, Fig. 4G,H). These observations indicate that Nodal signaling is required for the regulation of *cCer* transcription in the left-side mesoderm.

cCer regulatory region is active in the left-side mesoderm of transgenic mouse embryos

Chick and mouse *Cerberus*-related genes have both coincident and distinct domains of expression during embryonic development. At early stages, chick *Cer* and mouse *Cerl-1* are both expressed in equivalent embryonic structures, such as the anterior mesendoderm (Rodriguez Esteban et al., 1999; Belo et al., 1997). However, at later stages, chick *Cer* is expressed in the left-side mesoderm (Rodriguez Esteban et al., 1999; Yokouchi et al., 1999; Zhu et al., 1999) (see also Fig. 1A), whereas mouse *Cerl-1* expression is found in the rostral domain of the nascent somites and presomitic mesoderm (Belo et al., 1997) and mouse *Cerl-2* is expressed in the node region

(Marques et al., 2004). In order to determine whether the upstream regulators of *cCer* expression are conserved in mouse, we generated a transgenic line carrying the *cCer* regulatory region (*Cer2.5-EGFP*) and analyzed reporter gene expression in mouse embryos at different stages. At E7.5, EGFP fluorescence was detected in the anterior mesendoderm (data not shown), an expression domain common to chick *Cer* and mouse *Cerl-1* genes. However, at E8.5, *EGFP* was expressed in the left lateral plate mesoderm (Fig. 5A,B), which is a *cCer*-specific pattern. As in *Cer-EGFP*-electroporated chick embryos, fluorescent cells were also found in the foregut and heart of E8.5 transgenic embryos (Fig. 5Aa,B). These results indicate that the upstream regulators of *cCer* expression are present not only in tissues that express both *cCer* and mouse *Cerl-1* (i.e. anterior mesendoderm), but also in the mouse left-side mesoderm, a region that expresses *cCer* but not the mouse Cerl genes.

In the mouse embryo, the asymmetric expression of both *Nodal* and *Lefty2* is directly regulated by Nodal signaling (Saijoh et al., 2000; Saijoh et al., 2003; Yamamoto et al., 2003). In *Cer2.5-EGFP* mouse embryos, *EGFP* mRNA expression is exclusively detected in the left lateral plate mesoderm at E8.25, and coincides with the expression patterns of *Nodal* (Fig. 5C,C') and *Lefty2* (Fig. 5D,D'), which reinforces the hypothesis that *cCer* regulatory sequences are directly regulated by Nodal.

Nodal signaling is negatively regulated by cCer

In the chick embryo, *Lefty* is expressed in the midline (as is mouse *Lefty1*) and in a small posterior domain of the left lateral plate mesoderm at late stages, whereas the *cCer* expression pattern is much more similar to that of mouse *Lefty2* in the left-side mesoderm (Rodriguez Esteban et al., 1999; Ishimaru et al., 2000). Like Lefty proteins, Cerberus-related molecules were shown to act as Nodal antagonists in zebrafish (Hashimoto et al., 2004), *Xenopus* (Hsu et al., 1998; Piccolo et al., 1999), chick (Bertocchini and Stern, 2002) and mouse (Belo et al., 2000; Marques et al., 2004) embryos. Therefore, we proposed that cCer has taken the role of mouse Lefty2 in the left-side mesoderm, and acts to restrict the range of Nodal signaling. To test this hypothesis, we have performed *cCer* overexpression and knockdown experiments in chick embryos. Because *Nodal* transcription is autoregulated, *Nodal* expression was analyzed as a readout of Nodal signaling.
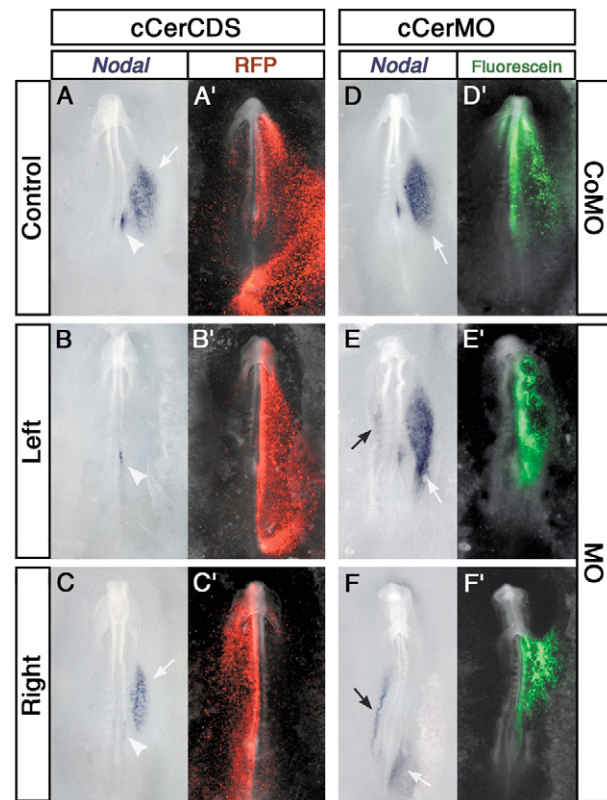
Chick embryos electroporated on the left side with a pCAGGS expression vector containing the *cCer* coding sequence (pCAGGS-*cCerCDS*) showed a dramatic reduction or absence of *Nodal* expression in the left lateral plate mesoderm, but not in the node region (95%, *n*=20, Fig. 6B; compare with control, *n*=4, Fig. 6A). On the other hand, when *cCer* was misexpressed on the right side, *Nodal* was never ectopically induced (*n*=18, Fig. 6C) and was downregulated only in one embryo (6%, *n*=18, data not shown). In this embryo, it is possible that the cCer protein had traveled from the right to the left side, where it inhibited the Nodal signal. In addition, the expression of the Nodal target gene *Pitx2* was downregulated by cCer on the left side (56%, *n*=16, data not shown), whereas it was never induced on the right side (*n*=11, data not shown). At older stages, chick embryos showed reversed heart looping when *cCer* was overexpressed on the left side (47%, *n*=15, data not shown), but not when *cCer* was misexpressed on the right side (*n*=7) nor in control electroporations (*n*=4). Taken together, these observations suggest that cCer may act as a negative regulator of Nodal signaling.

To investigate the effect of cCer downregulation on *Nodal* expression, fluorescein-tagged morpholino oligonucleotides against *cCer* (MO) or against a related sequence (five mismatches; CoMO; see Fig. 2B) were electroporated into the future left-side mesoderm
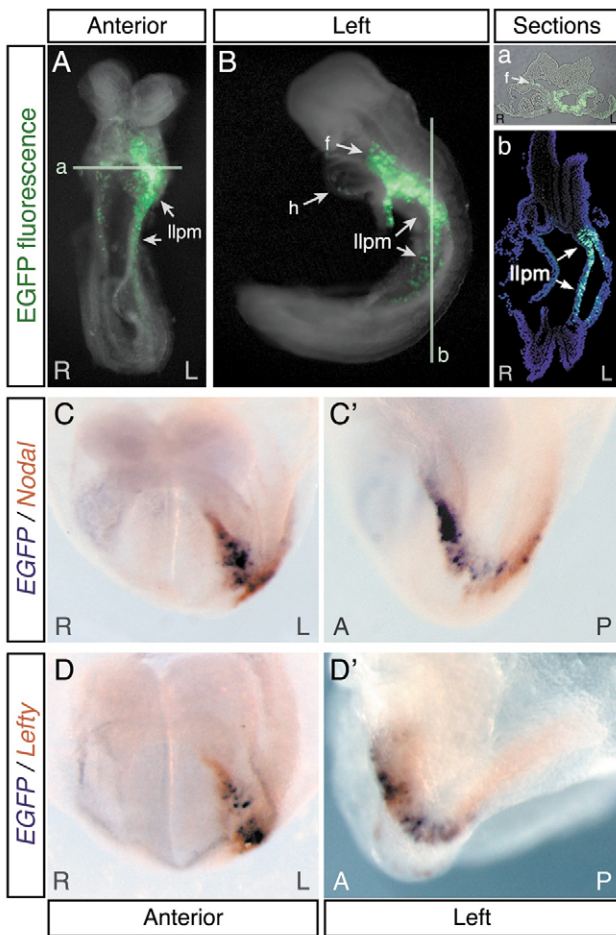
Fig. 5. Chick *Cer* regulatory regions are able to drive *EGFP* expression in the left lateral plate mesoderm of mouse embryos. (**A**,**B**) E8.5 *Cer2.5-EGFP* transgenic mouse embryos in ventral (A) and left-side (B) views. (**Aa**) Transverse section of embryo in A (line). (**Bb**) Longitudinal section of embryo in B (line). Cell nuclei are labeled with DAPI (blue). Green fluorescence was asymmetrically detected in the left lateral plate mesoderm (llpm; A,B), both in the splanchnopleure and in the somatopleure (Aa,Bb). Fluorescent cells were also found in the foregut (f) and heart (h; B,Aa). (**C-D'**) Expression patterns of *EGFP* (purple) and *Nodal* (orange; C,C') or *Lefty1,2* (orange; D,D') in E8.25 transgenic mouse embryos detected by double whole-mount in situ hybridization. (C,D) Anterior views. (C',D') Left-side views. The expression domain of *EGFP* overlapped with *Nodal* and *Lefty2* in the left lateral plate mesoderm. A, anterior; f, foregut; h, heart; L, left; llpm, left lateral plate mesoderm; P, posterior; R, right.

Fig. 6. Regulation of *Nodal* expression by chick Cer. (**A-C'**) Effect of chick *Cer* (*cCer*) overexpression. Chick embryos were electroporated with pCAGGS-cCerCDS (coding sequence) on the left (A-B') or right (C,C') side at Hamburger and Hamilton stage 4 (HH4) and fixed at HH8. pCAGGS-RFP was electroporated alone (control; A,A') or with pCAGGS-cCerCDS (B-C'). (A-C) *Nodal* transcripts detected by whole-mount in situ hybridization. (A',B',C') Merge of bright-field and RFP fluorescence images. *cCer* overexpression on the left side suppressed *Nodal* expression (A) in the left lateral plate mesoderm (B; arrow in A), whereas *cCer* misexpression on the right side had no effect (C; arrow). *Nodal* transcripts were always detected in the node (A-C; arrowheads). (**D-F'**) Effect of *cCer* knockdown. HH4-6 chick embryos were electroporated on the left side with fluorescein-tagged morpholinos (MO) and fixed at HH8-11. (D-F) *Nodal* transcripts detected by whole-mount in situ hybridization. (D',E',F') Merge of bright-field and fluorescein green fluorescence images. (E,F) *Nodal* expression was ectopically induced by *cCer* MO in the right lateral plate mesoderm (black arrows), whereas it was normal in the left side (white arrows). Electroporation of a control morpholino (CoMo) did not perturb *Nodal* left-side expression (D; white arrow). *cCer*, chick *Cer*; cCerCDS, chick *Cer* coding sequence.

of HH4-6 chick embryos. At HH8-11, *Nodal* transcription was ectopically induced on the right side of cCer morphant embryos (MO: 51%, *n*=37, Fig. 6E,F versus CoMo: 7%, *n*=27, Fig. 6D). In nine HH10-11 morphant embryos, *Nodal* expression on the right was higher than on the left side (Fig. 6F). This observation can be explained by a right-side-biased amplification of Nodal signaling, as predicted by the self-enhancement and lateral inhibition (SELI) model in the absence of Nodal inhibitors (Nakaguchi et al., 2006). The *Lefty* midline expression domain was normal in cCer MO-treated embryos (*n*=26, see Fig. S2 in the supplementary material), suggesting that the midline barrier was not affected. At older stages,

cCer knockdown resulted in the inversion of heart looping (43%, *n*=7 versus CoMO: 0%, *n*=5, data not shown). These results indicate that the main function of cCer in the left-side mesoderm is to prevent Nodal signaling from crossing to the right side.

DISCUSSION
cCer asymmetric expression is regulated by Nodal
We have demonstrated that Nodal is sufficient and necessary for the induction of *cCer* expression (Fig. 1). However, previous studies have reported that Nodal is unable to activate *cCer* expression in the right lateral plate mesoderm (Rodriguez Esteban et al., 1999;
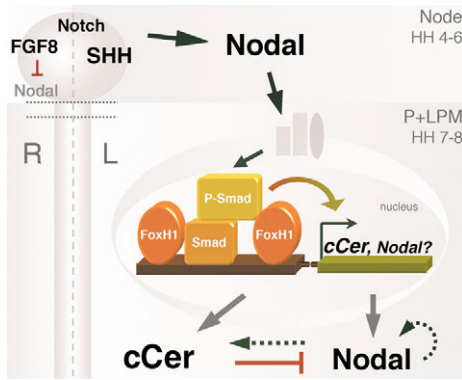
Fig. 7. Proposed model of the regulation and function of chick Cer in the left-side mesoderm. At Hamburger and Hamilton stage 5-6 (HH5-6), the early expression of *Nodal* in the node is activated on the left side by Notch and Shh signaling pathways, and is repressed on the right side by Fgf8. At HH7, the Nodal protein released by the node directly activates chick *Cer* (*cCer*) and *Nodal* expression in the adjacent left paraxial and lateral plate mesoderm (P+LPM). Nodal signal is transduced into the phosphorylation of SMAD2 and/or SMAD3, which then bind SMAD4, translocate into the nucleus and synergize with the FoxH1 transcription factor in the activation of *cCer* transcription. At HH8, Nodal protein produced by the P+LPM cells upregulates *cCer* and *Nodal* expression throughout the left lateral plate mesoderm (broken arrows). cCer protein is then required to downregulate the Nodal signal in the left lateral plate mesoderm and prevent it from crossing to the right side of the chick embryo. L, left; R, right.

Yokouchi et al., 1999; Zhu et al., 1999). The inconsistency between these and our results may be a consequence of the usage of different Nodal overexpression methods: we grafted beads soaked in active Nodal protein (mature form; R&D Systems), whereas others used retroviral vectors carrying a Bmp4-Nodal fusion protein that were introduced either by direct injection (Rodriguez Esteban et al., 1999) or by implantation of expressing cell pellets (Yokouchi et al., 1999; Zhu et al., 1999). In fact, induction of ectopic *cCer* expression was much less efficient when we used a Dorsalin-Nodal fusion construct (34%, versus 81% with Nodal protein beads) and was never detected when we overexpressed chick Nodal complete cDNA (*n*=10, data not shown). Therefore, it is possible that the proprotein convertase required for Nodal maturation is present at low levels in the right side of the chick embryo (Constam and Robertson, 2000), or that the Nodal protein encoded by these constructs is less stable than the recombinant protein (Le Good et al., 2005).

In zebrafish, *Xenopus* and mouse embryos, *Nodal* expression in the left lateral plate mesoderm is directly induced by Nodal protein released by the node (Long et al., 2003; Osada et al., 2000; Saijoh et al., 2003; Yamamoto et al., 2003). Accordingly, our results indicate that Nodal signaling positively regulates *Nodal* expression in the left lateral plate in the chick embryo (Fig. 1). This observation supports the hypothesis that Nodal itself is the intermediary signal that transfers the asymmetric information from the node to the lateral plate (Pagán-Westphal and Tabin, 1998).

cCer left-side enhancer is regulated by Nodal signaling via FoxH1 and SMAD elements

Here we have provided evidence that the FoxH1 and SMAD elements present in the *cCer* left-side enhancer are essential and sufficient for the activation of asymmetric expression (Figs 2, 3).

FoxH1 and SMAD transcription factors are nuclear mediators of Nodal signaling (reviewed by Schier and Shen, 2000). As expected, Nodal is necessary and sufficient to activate the *cCer* left-side enhancer (Fig. 4). These observations, together with the evidence that *cCer* asymmetric expression is activated by Nodal (Fig. 1), indicate that Nodal signaling directly regulates *cCer* transcription in the left-side mesoderm via the activity of FoxH1 and SMAD factors. In the future, the isolation of chick FoxH1 and the investigation of its direct binding and activation of the FoxH1 elements present in the *cCer* left-side enhancer may bring additional support to these results.

cCer restricts the range of Nodal signaling to the left side

Previous reports have proposed that cCer is able to induce ectopic *Nodal* expression on the right side by antagonizing the repressive activity of BMPs on *Nodal* transcription (Rodriguez Esteban et al., 1999; Yokouchi et al., 1999). However, BMPs can have opposite effects on *Nodal* expression: Bmp4 is a negative regulator of Nodal in the right side of the chick node at early stages (HH5-6) (Monsoro-Burq and Le Douarin, 2001), whereas Bmp2 positively regulates Nodal signaling in the lateral plate mesoderm at later stages (HH7-8) (Piedra and Ros, 2002; Schlange et al., 2002). Because cCer was introduced at early stages (HH6) on the right side of the node (Rodriguez Esteban et al., 1999; Yokouchi et al., 1999), it might be inducing *Nodal* expression by blocking the inhibitory function of Bmp4 in the node region. In fact, when *cCer*-expressing cells were implanted at later stages (HH7-8) in the lateral plate, *Nodal* expression was not affected (Zhu et al., 1999).

In our hands, *cCer* misexpression in the node region (*n*=7, data not shown) or right lateral plate (Fig. 6C) was never able to induce *Nodal*, whereas *cCer* overexpression on the left side actually repressed *Nodal* (Fig. 6B). Conversely, Nodal was ectopically expressed on the right side of *cCer*-knockdown embryos (Fig. 6E,F). These findings revealed that *cCer* acts as a negative regulator of Nodal signaling. Similar results have been obtained with the Nodal antagonist Lefty: Nodal activity was repressed by the ectopic expression of chick Lefty (Rodriguez Esteban et al., 1999) or mouse Lefty1 or Lefty2 (Yoshioka et al., 1998) in the chick embryo, whereas it was upregulated on the right side of Lefty2 mutant mice (Meno et al., 2001). Given the similarities between the expression patterns and functions of chick *Cer* and mouse *Lefty2* (reviewed by Juan and Hamada, 2001), we propose that cCer has taken the role of mouse Lefty2 in left-right patterning, and acts in addition to the midline barrier to confine Nodal signaling to the left side.

Feedback model of cCer and Nodal regulation

Taken together, our findings suggest a feedback mechanism by which Nodal signaling is restricted in the left lateral plate mesoderm of the chick embryo (Fig. 7). During the establishment of the left-right axis, *Nodal* expression is first activated in the left perinodal region by the Notch and Shh signaling pathways (reviewed by Raya and Izpisua-Belmonte, 2004). This initial Nodal signal directly induces *cCer* expression via the activation of the *cCer* left-side enhancer by FoxH1 and SMAD transcription factors. We hypothesize that SMAD2 and/or SMAD3 regulate *cCer* transcription, because they are thought to transduce Nodal signal in the left-side mesoderm (reviewed by Schier, 2003) and phospho-SMAD2 has been detected in the chick lateral plate mesoderm (Faure et al., 2002). Additionally, we propose that, as in the mouse embryo (reviewed in Hamada et al., 2002), Nodal also activates its own transcription, leading to the amplification of *Nodal* and *cCer*

expression throughout the left lateral plate. The partial overlap of the *Nodal* and *cCer* expression domains is possibly determined by functional differences in their regulatory regions and/or in Nodal and cCer diffusion rates, as proposed for the mouse Nodal and Lefty2 proteins (Nakaguchi et al., 2006). Together with the midline barrier, cCer has a key role in preventing the Nodal signal from crossing to the right side. Ultimately, the negative-feedback regulation of Nodal signaling by cCer results in the downregulation of *Nodal* and *cCer* expression in the left lateral plate mesoderm. Further support for this model may come from the analysis of chick *Nodal* transcriptional regulation as well as from the investigation of the diffusion rates and stability of Nodal and cCer proteins.

Evolution of *Cerberus*-related genes: divergence of gene regulation but conservation of function in left-right patterning

Unlike other known *Cerberus*-related genes, *cCer* is expressed on the left side of the paraxial and lateral plate mesoderm. Variations in the expression patterns of orthologous genes may arise either from the presence of particular cis-regulatory elements in their genomic sequence, or from the existence of differences in the localization and activation status of their upstream regulators, or both. Cross-species studies of cis-regulatory sequences are likely to help distinguish between these two hypotheses. In our study, the analysis of *Cer-EGFP* transgenic mouse embryos revealed that the upstream regulators of the *cCer* left-side enhancer (i.e. Nodal) are present in the mouse left lateral plate mesoderm, and suggested that the regulatory regions of *Cerberus*-related genes have diverged in chick and mouse. In agreement with this, the comparison between the *cCer* left-side enhancer and non-coding sequences of human, mouse, *Xenopus* and *Fugu Cerberus*-related genes using ConSite and VISTA programs was unable to detect any conserved FoxH1-binding sites or other common regulatory elements. FoxH1- and SMAD-binding sites are indeed present in the asymmetric enhancers of several left-side-specific genes, such as the ascidian, *Xenopus*, mouse and human *Nodal* genes, mouse and human *Lefty2* genes, and mouse and *Xenopus Pitx2* genes (Saijoh et al., 2000; Osada et al., 2000; Yashiro et al., 2000; Shiratori et al., 2001). Our findings add *cCer* to this list, and underscore the essential role of evolutionarily conserved FoxH1-SMAD modules in the transcriptional regulation of asymmetric gene expression (Osada et al., 2000).

Although chick *Cer*, zebrafish *charon* and mouse *Cerl-2* have different expression patterns, the Cerberus-related proteins encoded by these genes seem to have a conserved function in left-right development, which is to restrict Nodal signaling to the left side of the embryo. *Nodal* expression in the node region also differs among vertebrate species: it is bilateral in zebrafish and in early mouse embryos, whereas it is restricted to the left side in the chick embryo (reviewed in Raya and Izpisua-Belmonte, 2004). This difference may justify the need for a Nodal antagonist in the node of zebrafish and mouse embryos, which is not required in the chick node.

The divergence in gene regulation between chick, *Xenopus* and mouse *Cerberus* homologues, here demonstrated by the presence of a FoxH1-SMAD module in the *cCer* regulatory region, has conveyed a novel scenery for the activity of cCer and enabled it to take the role of Lefty2 as a negative-feedback regulator of Nodal signaling in the left lateral plate. In the future, the analysis of novel Cerberus-related molecules involved in the left-right development of other vertebrate species (such as *Xenopus* and rabbit) should provide further insight into the evolution of *Cerberus* gene regulation and function.

References
Belo, J. A., Bouwmeester, T., Leyns, L., Kertesz, N., Gallo, M., Follettie, M. and De Robertis, E. M. (1997). Cerberus-like is a secreted factor with neutralizing activity expressed in the anterior primitive endoderm of the mouse gastrula. *Mech. Dev.* **68**, 45-57.
Belo, J. A., Bachiller, D., Agius, E., Kemp, C., Borges, A. C., Marques, S., Piccolo, S. and De Robertis, E. M. (2000). Cerberus-like is a secreted BMP and Nodal antagonist not essential for mouse development. *Genesis* **26**, 265-270.
Bertocchini, F. and Stern, C. D. (2002). The hypoblast of the chick embryo positions the primitive streak by antagonizing nodal signaling. *Dev. Cell* **3**, 735-744.
Biben, C., Stanley, E., Fabri, L., Kotecha, S., Rhinn, M., Drinkwater, C., Lah, M., Wang, C. C., Nash, A., Hilton, D. et al. (1998). Murine Cerberus homologue mCer-1: a candidate anterior patterning molecule. *Dev. Biol.* **194**, 135-151.
Bouwmeester, T., Kim, S., Sasai, Y., Lu, B. and De Robertis, E. M. (1996). Cerberus is a head-inducing secreted factor expressed in the anterior endoderm of Spemann's organizer. *Nature* **382**, 595-601.
Brennan, J., Lu, C. C., Norris, D. P., Rodriguez, T. A., Beddington, R. S. and Robertson, E. J. (2001). Nodal signaling in the epiblast patterns the early mouse embryo. *Nature* **411**, 965-969.
Campbell, R. E., Tour, O., Palmer, A. E., Steinbach, P. A., Baird, G. S., Zacharias, D. A. and Tsien, R. Y. (2002). A monomeric red fluorescent protein. *Proc. Natl. Acad. Sci. USA* **99**, 7877-7882.
Constam, D. B. and Robertson, E. J. (2000). SPC4/PACE4 regulates a TGFbeta signaling network during axis formation. *Genes Dev.* **14**, 1146-1155.
Faure, S., de Santa Barbara, P., Roberts, D. J. and Whitman, M. (2002). Endogenous patterns of BMP signaling during early chick development. *Dev. Biol.* **244**, 44-65.
Foley, A. C., Skromne, I. S. and Stern, C. D. (2000). Reconciling different models of forebrain induction and patterning: a dual role for the hypoblast. *Development* **127**, 3839-3854.
Hamada, H., Meno, C., Watanabe, D. and Saijoh, Y. (2002). Establishment of vertebrate left-right asymmetry. *Nat. Rev. Genet.* **3**, 103-113.
Hamburger, V. and Hamilton, H. L. (1951). A series of normal stages in the development of the chick embryo. *J. Morphol.* **88**, 49-92.
Hashimoto, H., Rebagliati, M., Ahmad, N., Muraoka, O., Kurokawa, T., Hibi, M. and Suzuki, T. (2004). The Cerberus/Dan-family protein Charon is a negative regulator of Nodal signalling during left-right patterning in zebrafish. *Development* **131**, 1741-1753.
Hsu, D. R., Economides, A. N., Wang, X., Eimon, P. M. and Harland, R. M. (1998). The Xenopus dorsalizing factor Gremlin identifies a novel family of secreted proteins that antagonize BMP activities. *Mol. Cell* **1**, 673-683.
Inman, G. J., Nicolas, F. J., Callahan, J. F., Harling, J. D., Gaster, L. M., Reith, A. D., Laping, N. J. and Hill, C. S. (2002). SB-431542 is a potent and specific inhibitor of transforming growth factor-beta superfamily type I activin receptor-like kinase (ALK) receptors ALK4, ALK5, and ALK7. *Mol. Pharmacol.* **62**, 65-74.
Ishimaru, Y., Yoshioka, H., Tao, H., Thisse, B., Thisse, C., Wright, C. V. E., Hamada, H., Ohuchi, H. and Noji, S. (2000). Asymmetric expression of antivin/lefty1 in the early chick embryo. *Mech. Dev.* **90**, 115-118.
Juan, H. and Hamada, H. (2001). Roles of nodal-lefty regulatory loops in embryonic patterning of vertebrates. *Genes Cells* **6**, 923-930.
Le Good, J. A., Joubin, K., Giraldez, A. J., Ben-Haim, N., Beck, S., Chen, Y., Schier, A. F. and Constam, D. B. (2005). Nodal stability determines signaling range. *Curr. Biol.* **15**, 31-36.
Liguori, G. L., Echevarria, D., Improta, R., Signore, M., Adamson, E., Martinez, S. and Persico, M. G. (2003). Anterior neural plate regionalization in cripto null mutant mouse embryos in the absence of node and primitive streak. *Dev. Biol.* **264**, 537-549.
Long, S., Ahmad, N. and Rebagliati, M. (2003). The zebrafish nodal-related gene southpaw is required for visceral and diencephalic left-right asymmetry. *Development* **130**, 2303-2316.
Marques, S., Borges, A. C., Silva, A. C., Freitas, S., Cordenonsi, M. and Belo, J. A. (2004). The activity of the Nodal antagonist Cerl-2 in the mouse node is required for correct L/R body axis. *Genes Dev.* **18**, 2342-2347.

Medina, A., Reintsch, W. and Steinbeisser, H. (2000). Xenopus frizzled 7 can act in canonical and non-canonical Wnt signaling pathways: implications on early patterning and morphogenesis. *Mech. Dev.* **92**, 227-237.

Meno, C., Takeuchi, J., Sakuma, R., Koshiba-Takeuchi, K., Ohishi, S., Saijoh, Y., Miyazaki, J., ten Dijke, P., Ogura, T. and Hamada, H. (2001). Diffusion of nodal signaling activity in the absence of the feedback inhibitor Lefty2. *Dev. Cell* **1**, 127-38.

Mohammadi, M., McMahon, G., Sun, L., Tang, C., Hirth, P., Yeh, B. K., Hubbard, S. R. and Schlessinger, J. (1997). Structures of the tyrosine kinase domain of fibroblast growth factor receptor in complex with inhibitors. *Science* **276**, 955-960.

Monsoro-Burq, A. H. and Le Douarin, N. M. (2001). Bmp4 plays a key role in left-right patterning in chick embryos by maintaining Sonic Hedgehog asymmetry. *Mol. Cell* **7**, 789-799.

Mostert, V., Sandra, W., Dreher, I., Köhrle, J. and Abel, J. (2001). Identification of an element within the promoter of human selenoprotein P responsive to transforming growth factor-beta. *Eur. J. Biochem.* **268**, 6176-6181.

Nagy, A., Gertsenstein, M., Vintersten, K. and Behringer, R. (2003). *Manipulating the Mouse Embryo: A Laboratory Manual.* New York: Cold Spring Harbor Laboratory Press.

Nakaguchi, E., Mochizuki, A., Yamamoto, M., Yashiro, K., Meno, C. and Hamada, H. (2006). Generation of robust left-right asymmetry in the mouse embryo requires a self-enhancement and lateral-inhibition system. *Dev. Cell* **11**, 495-504.

New, D. A. T. (1955). A new technique for the cultivation of the chick embryo in vitro. *J. Embryol. Exp. Morphol.* **3**, 326-331.

Nieuwkoop, P. D. and Faber J. (1967). *Normal Table of Xenopus laevis (Daudin).* Amsterdam: North-Holland.

Niwa, H., Yamamura, K. and Miyazaki, J. (1991). Efficient selection for high-expression transfectants with a novel eukaryotic vector. *Gene* **108**, 193-200.

Osada, S. I., Saijoh, Y., Frisch, A., Yeo, C. Y., Adachi, H., Watanabe, M., Whitman, M., Hamada, H. and Wright, C. V. (2000). Activin/Nodal responsiveness and asymmetric expression of a Xenopus nodal-related gene converge on a FAST-regulated module in intron 1. *Development* **127**, 2503-2514.

Pagán-Westphal, S. M. and Tabin, C. J. (1998). The transfer of left-right positional information during chick embryogenesis. *Cell* **93**, 25-35.

Piccolo, S., Agius, E., Leyns, L., Bhattacharyya, S., Grunz, H., Bouwmeester, T. and De Robertis, E. M. (1999). The head inducer Cerberus is a multifunctional antagonist of Nodal, BMP and Wnt signals. *Nature* **397**, 707-710.

Piedra, M. E. and Ros, M. A. (2002). BMP signaling positively regulates Nodal expression during left right specification in the chick embryo. *Development* **129**, 3431-3440.

Quandt, K., Frech, K., Karas, H., Wingender, E. and Werner, T. (1995). MatInd and MatInspector – New fast and versatile tools for detection of consensus matches in nucleotide sequence data. *Nucleic Acids Res.* **23**, 4878-4884. (http://www.genomatix.de/).

Raya, A. and Izpisua-Belmonte, J. C. (2004). Unveiling the establishment of left–right asymmetry in the chick embryo. *Mech. Dev.* **121**, 1043-1054.

Rodriguez Esteban, C., Capdevila, J., Economides, A. N., Pascual, J., Ortiz, A. and Izpisua Belmonte, J. C. (1999). The novel Cer-like protein Caronte mediates the establishment of embryonic left-right asymmetry. *Nature* **401**, 243-251.

Saijoh, Y., Adachi, H., Sakuma, R., Yeo, C. Y., Yashiro, K., Watanabe, M., Hashiguchi, H., Mochida, K., Ohishi, S., Kawabata, M. et al. (2000). Left–right asymmetric expression of lefty2 and nodal is induced by a signaling pathway that includes the transcription factor FAST2. *Mol. Cell* **5**, 35-47.

Saijoh, Y., Oki, S., Ohishi, S. and Hamada, H. (2003). Left–right patterning of the mouse lateral plate requires nodal produced in the node. *Dev. Biol.* **256**, 160-172.

Schier, A. (2003). Nodal signaling in vertebrate development. *Annu. Rev. Cell Dev. Biol.* **19**, 589-621.

Schier, A. F. and Shen, M. M. (2000). Nodal signalling in vertebrate development. *Nature* **403**, 385-389.

Schlange, T., Arnold, H.-H. and Brand, T. (2002). BMP2 is a positive regulator of Nodal signaling during left-right axis formation in the chicken embryo. *Development* **129**, 3421-3429.

Shawlot, W., Deng, J. M. and Behringer, R. R. (1998). Expression of the mouse cerberus-related gene, Cerr1, suggests a role in anterior neural induction and somitogenesis. *Proc. Natl. Acad. Sci. USA* **95**, 6198-6203.

Shiratori, H., Sakuma, R., Watanabe, M., Hashiguchi, H., Mochida, K., Sakai, Y., Nishino, J., Saijoh, Y., Whitman, M. and Hamada, H. (2001). Two-step regulation of left–right asymmetric expression of Pitx2: initiation by nodal signaling and maintenance by Nkx2. *Mol. Cell* **7**, 137-149.

Summerton, J., Stein, D., Huang, S. B., Matthews, P., Weller, D. and Partridge, M. (1997). Morpholino and phosphorothioate antisense oligomers compared in cell-free and in-cell systems. *Antisense Nucleic Acid Drug Dev.* **7**, 63-70.

Waldrip, W. R., Bikoff, E. K., Hoodless, P. A., Wrana, J. L. and Robertson, E. J. (1998). Smad2 signalling in extraembryonic tissues determines anterior-posterior polarity of the early mouse embryo. *Cell* **92**, 797-808.

Yamamoto, M., Mine, N., Mochida, K., Sakai, Y., Saijoh, Y., Meno, C. and Hamada, H. (2003). Nodal signaling induces the midline barrier by activating Nodal expression in the lateral plate. *Development* **130**, 1795-1804.

Yashiro, K., Saijoh, Y., Sakuma, R., Tada, M., Tomita, N., Amano, K., Matsuda, Y., Monden, M., Okada, S. and Hamada, H. (2000). Distinct transcriptional regulation and phylogenetic diversity of human LEFTY genes. *Genes Cells* **5**, 343-357.

Yee, S. P. and Rigby, P. W. (1993). The regulation of myogenin gene expression during the embryonic development of the mouse. *Genes Dev.* **7**, 1277-1289.

Yokouchi, Y., Vogan, K. J., Pearse, R. V., 2nd and Tabin, C. J. (1999). Antagonistic signaling by Caronte, a novel Cerberus-related gene, establishes left-right asymmetric gene expression. *Cell* **98**, 573-583.

Yoshioka, H., Meno, C., Koshiba, K., Sugihara, M., Itoh, H., Ishimaru, Y., Inoue, T., Ohuchi, H., Semina, E. V., Murray, J. C. et al. (1998). Pitx2, a bicoid type homeobox gene, is involved in a Lefty-signaling pathway in determination of left–right asymmetry. *Cell* **94**, 299-305.

Zhou, S., Zawel, L., Lengauer, C., Kinzler, K. W. and Vogelstein, B. (1998). Characterization of human FAST-1, a TGFbeta and activin signal transducer. *Mol. Cell* **2**, 121-127.

Zhu, L., Marvin, M. J., Gardiner, A., Lassar, A. B., Mercola, M., Stern, C. D. and Levin, M. (1999). Cerberus regulates left-right asymmetry of the embryonic head and heart. *Curr. Biol.* **9**, 931-938.